

AD-A062 019

NAVAL AIR DEVELOPMENT CENTER WARMINSTER PA SENSORS A--ETC F/6 20/1  
PLRAY - A RAY PROPAGATION LOSS PROGRAM.(U)  
OCT 78 C L BARTBERGER  
NADC-77296-30

UNCLASSIFIED

NL

1 OF 3  
AD  
A062 019



ADA062019

DDC FILE COPY

REPORT NO. NADC-77296-30



**LEVEL**

**PLRAY - A RAY PROPAGATION LOSS PROGRAM**

Charles Bartberger  
Sensors and Avionics Technology Directorate  
NAVAL AIR DEVELOPMENT CENTER  
Warminster, Pennsylvania 18974

26 October 1978

PHASE REPORT  
AIRTASK NO. A5335330/001D/8W04800000  
Work Unit No. WO 480

**APPROVED FOR PUBLIC RELEASE; DISTRIBUTION UNLIMITED**

Prepared for  
NAVAL AIR SYSTEMS COMMAND  
Department of the Navy  
Washington, D.C. 20361

78 12 04.075



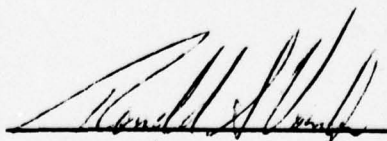
## NOTICES

**REPORT NUMBERING SYSTEM** - The numbering of technical project reports issued by the Naval Air Development Center is arranged for specific identification purposes. Each number consists of the Center acronym, the calendar year in which the number was assigned, the sequence number of the report within the specific calendar year, and the official 2-digit correspondence code of the Command Office or the Functional Directorate responsible for the report. For example: Report No. NADC-78015-20 indicates the fifteenth Center report for the year 1978, and prepared by the Systems Directorate. The numerical codes are as follows:

| CODE | OFFICE OR DIRECTORATE                             |
|------|---|
| 00   | Commander, Naval Air Development Center           |
| 01   | Technical Director, Naval Air Development Center  |
| 02   | Comptroller                                       |
| 10   | Directorate Command Projects                      |
| 20   | Systems Directorate                               |
| 30   | Sensors & Avionics Technology Directorate         |
| 40   | Communication & Navigation Technology Directorate |
| 50   | Software Computer Directorate                     |
| 60   | Aircraft & Crew Systems Technology Directorate    |
| 70   | Planning Assessment Resources                     |
| 80   | Engineering Support Group                         |

**PRODUCT ENDORSEMENT** - The discussion or instructions concerning commercial products herein do not constitute an endorsement by the Government nor do they convey or imply the license or right to use such products.

APPROVED BY:

  
Ronald S. Vaughn

DATE: 26 October 1978

UNCLASSIFIED

SECURITY CLASSIFICATION OF THIS PAGE (When Data Entered)

| REPORT DOCUMENTATION PAGE   |   | READ INSTRUCTIONS<br>BEFORE COMPLETING FORM |
|---|---|---|
| 1. REPORT NUMBER<br>NADC-77296-30   | 2. GOVT ACCESSION NO.   | 3. RECIPIENT'S CATALOG NUMBER               |
| 4. TITLE (and Subtitle)<br>PLRAY - A RAY PROPAGATION LOSS PROGRAM,  | 5. TYPE OF REPORT & PERIOD COVERED<br>Phase Report,   | 6. PERFORMING ORG. REPORT NUMBER            |
| 7. AUTHOR(s)<br>Charles L. Bartberger   | 8. CONTRACT OR GRANT NUMBER(s)  |   |
| 9. PERFORMING ORGANIZATION NAME AND ADDRESS<br>Sensors & Avionics Technology Directorate<br>Naval Air Development Center<br>Warminster, Pennsylvania 18974  | 10. PROGRAM ELEMENT, PROJECT, TASK<br>AREA & WORK UNIT NUMBERS<br>A5335330/001D/8W04800000<br>Work Unit No. W0480 |   |
| 11. CONTROLLING OFFICE NAME AND ADDRESS<br>Naval Air Systems Command<br>Department of the Navy<br>Washington, D. C. 20361   | 12. REPORT DATE<br>26 October 1978  |   |
| 14. MONITORING AGENCY NAME & ADDRESS (if different from Controlling Office)<br>12 238p.   | 13. NUMBER OF PAGES<br>237  |   |
| 16. DISTRIBUTION STATEMENT (of this Report)<br>APPROVED FOR PUBLIC RELEASE; DISTRIBUTION UNLIMITED  | 15. SECURITY CLASS. (of this report)<br>Unclassified  |   |
|   | 15a. DECLASSIFICATION/DOWNGRADING<br>SCHEDULE   |   |
| 17. DISTRIBUTION STATEMENT (of the abstract entered in Block 20, if different from Report)  | 16 W0480  |   |
| 18. SUPPLEMENTARY NOTES<br>APPENDICES A, B, C, D, E, F, G, H, I, J, K, L  | 17 W04800000  |   |
| 19. KEY WORDS (Continue on reverse side if necessary and identify by block number)<br>Computer programs<br>Propagation loss<br>Underwater acoustics   |   |   |
| 20. ABSTRACT (Continue on reverse side if necessary and identify by block number)<br>PLRAY is a ray propagation loss program similar in many respects to FACT. It computes propagation loss as a function of range at constant depth in a horizontally stratified ocean with a flat bottom. It does this by computing a family of rays and interpolating between them to obtain the intensities of the various multipath arrivals at the specified receiver locations. Like FACT, PLRAY provides the option of incoherent or semicoherent ray addition. It contains wave corrections for smooth caustics but not for cusped caustics. |   |   |

DD FORM 1 JAN 73 1473

EDITION OF 1 NOV 65 IS OBSOLETE  
S/N 0102-LF-014-6601

UNCLASSIFIED

SECURITY CLASSIFICATION OF THIS PAGE (When Data Entered)

393 537

LB

UNCLASSIFIED

SECURITY CLASSIFICATION OF THIS PAGE (When Data Entered)

The cusped caustic errors are minimized by separating the source and receiver slightly in depth. It also contains a surface duct model which replaces ray computations for propagation in a surface duct. PLRAY incorporates two features not included in FACT; it permits the user to insert his own bottom loss curves in place of the internally contained curves and it makes provision for insertion of a beam pattern. Although occasionally significant differences in output are observed, PLRAY and FACT generally yield comparable results.

|                                 |                                     |
|---------------------------------|-------------------------------------|
| NTIS                            | <input checked="" type="checkbox"/> |
| DDC                             | <input type="checkbox"/>            |
| UNANNOUNCED                     | <input type="checkbox"/>            |
| JUSTIFICATION                   |                                     |
| BY                              |                                     |
| DISTRIBUTION/AVAILABILITY CODES |                                     |
| Dist.                           | and/or SPECIAL                      |
| A                               |                                     |

S/N 0102- LF-014-6601

UNCLASSIFIED

SECURITY CLASSIFICATION OF THIS PAGE (When Data Entered)



## TABLE OF CONTENTS

|  | Page |
|--|------|
| LIST OF FIGURES . . . . .  | 3    |
| SUMMARY . . . . .  | 6    |
| CONCLUSIONS . . . . .  | 9    |
| INTRODUCTION. . . . .  | 10   |
| GENERAL DESCRIPTION OF THE PROGRAM. . . . .  | 12   |
| Inputs . . . . .   | 12   |
| Curve-Fitting (SUBROUTINES CURFIT, PARAB, FIT, BRIDGE) . . . . .                         | 12   |
| Receiver Depth Loop. . . . .   | 13   |
| Augmentation of Profile (SUBROUTINE INSERT). . . . .                                     | 13   |
| Sectors (SUBROUTINE SECLIM). . . . .   | 13   |
| Ray Sub-Families (SUBROUTINE DIVSEC) . . . . .   | 13   |
| Ray Computations (SUBROUTINE INCR) . . . . .   | 14   |
| Arrival Orders . . . . .   | 14   |
| Processing of Multiple Frequencies . . . . .   | 14   |
| Caustics (SUBROUTINE RCAUST) . . . . .   | 14   |
| Ray Intensity Computations (SUBROUTINE RAYSUM) . . . . .                                 | 15   |
| Coherence Computations (SUBROUTINE RAYSUM) . . . . .                                     | 15   |
| Surface Duct Propagation (SUBROUTINE SDUCT). . . . .                                     | 16   |
| Propagation Loss (PROGRAM PLRAY) . . . . .   | 16   |
| Plot Routine (SUBROUTINE PLPLOT) . . . . .   | 16   |
| Core Requirement . . . . .   | 16   |
| Running Time . . . . .   | 16   |
| DETAILED DESCRIPTION OF THE PROGRAM . . . . .  | 17   |
| Data Input Section . . . . .   | 17   |
| Receiver Depth Loop. . . . .   | 19   |
| SUBROUTINE INSERT . . . . .  | 20   |
| PROGRAM PLRAY (Continued). . . . .   | 20   |
| SUBROUTINE SECLIM. . . . .   | 21   |
| PROGRAM PLRAY (Continued). . . . .   | 22   |
| Sector Loop. . . . .   | 22   |
| Multipath Ray Types. . . . .   | 22   |
| SUBROUTINE DIVSEC(IL). . . . .   | 23   |
| PROGRAM PLRAY (Continued). . . . .   | 27   |
| SUBROUTINE INCR(ITH) - Computation of Range and Range Derivative<br>Increments . . . . . | 27   |
| SUBROUTINE BOTTOM(THBD). . . . .   | 28   |
| PROGRAM PLRAY (Continued). . . . .   | 29   |
| Zero Order Arrivals. . . . .   | 29   |
| SUBROUTINE RAYSUM(IL). . . . .   | 29   |
| SUBROUTINE RCAUST(KTH,J) . . . . .   | 32   |
| SUBROUTINE RAYSUM(IL) (Continued). . . . .   | 33   |
| PROGRAM PLRAY (Continued). . . . .   | 41   |



## TABLE OF CONTENTS (Continued)

|  | Page |
|--|------|
| SUBROUTINE SDUCT . . . . .                                       | 42   |
| FUNCTION DEPFN(Z). . . . .                                       | 43   |
| SUBROUTINE BEAM(L) . . . . .                                     | 43   |
| COMPARISON WITH OTHER MODELS. . . . .                            | 45   |
| Profile 1. . . . .   | 46   |
| Profile 2. . . . .   | 59   |
| Profile 3. . . . .   | 64   |
| Profile 4. . . . .   | 72   |
| Profile 5. . . . .   | 80   |
| Profile 6. . . . .   | 80   |
| Profile 7. . . . .   | 87   |
| Profile 8. . . . .   | 93   |
| Cusped Caustics. . . . .   | 98   |
| DISCUSSION. . . . .  | 103  |
| Incoherent Runs. . . . .   | 103  |
| Semicoherent Runs - Bottom-Bounce Interference Patterns. . . . . | 104  |
| Convergence Zones. . . . .                                       | 106  |
| Direct Zones . . . . .   | 107  |
| Cusped Caustics. . . . .   | 108  |
| REFERENCES. . . . .  | 109  |

## TABLE

|   |  |    |
|---|--|----|
| I | FORTTRAN and Algebraic Symbols in DEPFN. . . . . | 44 |
|---|--|----|

## APPENDIXES

|   |   |     |
|---|---|-----|
| A | Listing of FORTRAN Source Deck. . . . .         | A-1 |
| B | Glossary of Principal FORTRAN Symbols . . . . . | B-1 |
| C | Brief Description of Subroutines. . . . .       | C-1 |
| D | Input Data Deck . . . . .                       | D-1 |
| E | Earth Curvature Correction. . . . .             | E-1 |
| F | Steep Angle Approximation . . . . .             | F-1 |
| G | Ray Ranges and Range Derivatives. . . . .       | G-1 |
| H | Intensity in the Vicinity of a Caustic. . . . . | H-1 |
| I | Ray Spreading Loss Factor . . . . .             | I-1 |
| J | Coherence Computations. . . . .                 | J-1 |
| K | Surface Duct Model. . . . .                     | K-1 |
| L | The AP2 Normal Mode Program . . . . .           | L-1 |

## LIST OF FIGURES

| Figure | Title  | Page |
|--------|--|------|
| 1a     | Multipath Ray Types for Zero Order Arrivals, ICASE = 1. . . .  | 24   |
| 1b     | Multipath Ray Types for Zero Order Arrivals, ICASE = 2. . . .  | 24   |
| 2a     | Multipath Ray Types for First Order Arrivals, ICASE = 1. . . .   | 25   |
| 2b     | Multipath Ray Types for First Order Arrivals, ICASE = 2. . . .   | 25   |
| 3a     | Multipath Ray Types, Zero Order Arrivals, ICASE = 2. . . . .   | 26   |
| 3b     | Multipath Ray Types, Zero Order Arrivals, ICASE = 1. . . . .   | 26   |
| 3c     | Multipath Ray Types, Zero Order Arrivals, ICASE = 1<br>(First Sector, Special Case). . . . .                         | 26   |
| 4      | Example of a Double-Caustic Curve . . . . .  | 31   |
| 5      | Illustration of Index JJ. . . . .  | 35   |
| 6      | Profile 1 . . . . .  | 47   |
| 7      | Profile 2 . . . . .  | 48   |
| 8      | Profile 3 . . . . .  | 49   |
| 9      | Profile 4 . . . . .  | 50   |
| 10     | Profile 5 . . . . .  | 51   |
| 11     | Profile 6 . . . . .  | 52   |
| 12     | Profile 7 . . . . .  | 53   |
| 13     | Profile 8 . . . . .  | 54   |
| 14     | Bottom Loss, Profile 1. . . . .  | 55   |
| 15     | Bottom Loss, Profile 2. . . . .  | 55   |
| 16     | Bottom Loss, Profiles 3, 5, and 7 . . . . .  | 56   |
| 17     | Bottom Loss, Profile 4. . . . .  | 56   |
| 18     | Bottom Loss, Profile 6. . . . .  | 57   |
| 19     | Bottom Loss, Profile 8. . . . .  | 57   |
| 20     | Semicoherent Propagation Loss, Profile 1; Frequency 105<br>Hz, Source Depth 80 Ft, Receiver Depth 100 Ft . . . . .   | 58   |
| 21     | Incoherent Propagation Loss, Profile 1; Frequency 105 Hz,<br>Source Depth 80 Ft, Receiver Depth 100 Ft . . . . .     | 60   |
| 22     | Semicoherent Propagation Loss, Profile 2; Frequency 100<br>Hz, Source Depth 300 Ft, Receiver Depth 60 Ft . . . . .   | 61   |
| 23     | Incoherent Propagation Loss, Profile 2; Frequency 100 Hz,<br>Source Depth 300 Ft, Receiver Depth 60 Ft . . . . .     | 62   |
| 24     | Semicoherent Propagation Loss, Profile 2; Frequency 100<br>Hz, Source Depth 300 Ft, Receiver Depth 200 Ft. . . . .   | 63   |
| 25     | Incoherent Propagation Loss, Profile 2; Frequency 100 Hz,<br>Source Depth 300 Ft, Receiver Depth 200 Ft. . . . .     | 65   |
| 26     | Semicoherent Propagation Loss, Profile 3; Frequency 100<br>Hz, Source Depth 300 Ft, Receiver Depth 60 Ft . . . . .   | 66   |
| 27     | Incoherent Propagation Loss, Profile 3; Frequency 100 Hz,<br>Source Depth 300 Ft, Receiver Depth 60 Ft . . . . .     | 67   |
| 28     | Semicoherent Propagation Loss, Profile 3; Frequency 100<br>Hz, Source Depth 300 Ft, Receiver Depth 1000 Ft . . . . . | 68   |
| 29     | Incoherent Propagation Loss, Profile 3; Frequency 100 Hz,<br>Source Depth 300 Ft, Receiver Depth 1000 Ft . . . . .   | 70   |
| 30     | Semicoherent Propagation Loss, Profile 3; Frequency 300<br>Hz, Source Depth 300 Ft, Receiver Depth 1000 Ft . . . . . | 71   |
| 31     | Incoherent Propagation Loss, Profile 3; Frequency 300 Hz,<br>Source Depth 300 Ft, Receiver Depth 1000 Ft . . . . .   | 73   |

## LIST OF FIGURES (Continued)

| Figure | Title   | Page |
|--------|---|------|
| 32     | Semicoherent Propagation Loss, Profile 4; Frequency 150 Hz, Source Depth 200 Ft, Receiver Depth 60 Ft . . . . .   | 74   |
| 33     | Incoherent Propagation Loss, Profile 4; Frequency 150 Hz, Source Depth 200 Ft, Receiver Depth 60 Ft . . . . .     | 76   |
| 34     | Semicoherent Propagation Loss, Profile 4; Frequency 150 Hz, Source Depth 200 Ft, Receiver Depth 300 Ft. . . . .   | 77   |
| 35     | Incoherent Propagation Loss, Profile 4; Frequency 150 Hz, Source Depth 200 Ft, Receiver Depth 300 Ft. . . . .     | 78   |
| 36     | Semicoherent Propagation Loss, Profile 4; Frequency 150 Hz, Source Depth 200 Ft, Receiver Depth 1000 Ft . . . . . | 79   |
| 37     | Incoherent Propagation Loss, Profile 4; Frequency 150 Hz, Source Depth 200 Ft, Receiver Depth 1000 Ft . . . . .   | 81   |
| 38     | Semicoherent Propagation Loss, Profile 5; Frequency 100 Hz, Source Depth 300 Ft, Receiver Depth 100 Ft. . . . .   | 82   |
| 39     | Incoherent Propagation Loss, Profile 5; Frequency 100 Hz, Source Depth 300 Ft, Receiver Depth 100 Ft. . . . .     | 83   |
| 40     | Semicoherent Propagation Loss, Profile 5; Frequency 100 Hz, Source Depth 300 Ft, Receiver Depth 1000 Ft . . . . . | 84   |
| 41     | Incoherent Propagation Loss, Profile 5; Frequency 100 Hz, Source Depth 300 Ft, Receiver Depth 1000 Ft . . . . .   | 85   |
| 42     | Semicoherent Propagation Loss, Profile 6; Frequency 50 Hz, Source Depth 300 Ft, Receiver Depth 1000 Ft . . . . .  | 86   |
| 43     | Incoherent Propagation Loss, Profile 6; Frequency 50 Hz, Source Depth 300 Ft, Receiver Depth 1000 Ft . . . . .    | 88   |
| 44     | Semicoherent Propagation Loss, Profile 7; Frequency 100 Hz, Source Depth 300 Ft, Receiver Depth 100 Ft. . . . .   | 89   |
| 45     | Incoherent Propagation Loss, Profile 7; Frequency 100 Hz, Source Depth 300 Ft, Receiver Depth 100 Ft. . . . .     | 90   |
| 46     | Semicoherent Propagation Loss, Profile 7; Frequency 100 Hz, Source Depth 300 Ft, Receiver Depth 1000 Ft . . . . . | 91   |
| 47     | Incoherent Propagation Loss, Profile 7; Frequency 100 Hz, Source Depth 300 Ft, Receiver Depth 1000 Ft . . . . .   | 92   |
| 48     | Semicoherent Propagation Loss, Profile 8; Frequency 50 Hz, Source Depth 250 Ft, Receiver Depth 150 Ft. . . . .    | 94   |
| 49     | Semicoherent Propagation Loss, Profile 8; Frequency 100 Hz, Source Depth 250 Ft, Receiver Depth 150 Ft. . . . .   | 95   |
| 50     | Semicoherent Propagation Loss, Profile 8; Frequency 200 Hz, Source Depth 250 Ft, Receiver Depth 150 Ft. . . . .   | 96   |
| 51     | Semicoherent Propagation Loss, Profile 8; Frequency 50 Hz, Source Depth 250 Ft, Receiver Depth 450 Ft. . . . .    | 97   |
| 52     | Semicoherent Propagation Loss, Profile 8; Frequency 100 Hz, Source Depth 250 Ft, Receiver Depth 450 Ft. . . . .   | 99   |
| 53     | Semicoherent Propagation Loss, Profile 8; Frequency 200 Hz, Source Depth 250 Ft, Receiver Depth 450 Ft. . . . .   | 100  |
| 54     | Semicoherent Propagation Loss, Profile 3, Showing Effect of Cusped Caustic; Frequency 100 Hz . . . . .            | 101  |
| 55     | Height of Convergence Zone Peak as a Function of Receiver Depth, Profile 3; Frequency 100 Hz. . . . .             | 102  |



## LIST OF FIGURES (Continued)

| Figure | Title  | Page |
|--------|--|------|
| J1     | Multipath Ray Types, Zero Order Arrivals. . . . .  | J-3  |
| J2     | Multipath Ray Types, First Order Arrivals . . . . .  | J-4  |
| J3     | Approximate Coherence Model . . . . .  | J-6  |
| J4     | Attenuation Factor as a Function of the Number of Range<br>Points Per Cycle of Ray Interference Pattern. . . . . | J-10 |
| K1     | Cut-Off Frequency as a Function of Duct Depth . . . . .  | K-12 |



## S U M M A R Y

PLRAY (Ray Propagation Loss) is a locally generated acoustic ray program similar to the FACT (Fast Asymptotic Coherent Transmission) model. It is designed to compute propagation loss as a function of receiver range at constant depth in a horizontally stratified ocean with a flat bottom. Since the propagation loss is derived from the resultant intensity of the multipath propagation, it is necessary to compute the intensities of the individual contributing rays which arrive at each receiver location. As in FACT, this is done by computing a family of rays, specified by their source angles, and interpolating between them to determine the intensities of those rays which, if they had been computed, would have arrived at the desired receiver location. PLRAY, like FACT, offers the option of either incoherent or semicoherent ray addition. In the incoherent mode of summation, the individual ray intensities are added directly without regard to phase. In the semicoherent mode the group of rays in each arrival order, such as the four single bottom-bounce rays, are treated coherently, their relative phases being computed in a simple approximate manner. The resultant coherent intensities of the various arrival orders are then added incoherently.

PLRAY is similar to FACT in its basic structure. It processes only one source/receiver depth combination at a time, but computations may be made simultaneously at up to six frequencies. The maximum number of receiver range points is 251 in PLRAY and 250 in FACT. The choice between incoherent and semicoherent ray addition may be made separately for each frequency.

PLRAY incorporates wave corrections for smooth caustics similarly to FACT but lacks a correction for cusped caustics. Although the absence of the cusped caustic correction leads to excessively large errors when the source and receiver are at the same depth, reasonable results are obtained when the source and receiver depths differ by only a few feet. When the source and receiver are specified at or very near the same depth, the program automatically shifts them by an amount necessary to maintain a difference of two feet.

PLRAY contains a surface duct model, similar in some respects to that of FACT, which is activated in place of ray computations for propagation in a surface duct. The surface duct model is used when both the source and receiver are located in the duct or when one is in the duct and the other is below the duct but not deeper than 1.8 times the duct depth.

PLRAY differs from FACT in the manner of interpolating between the points of the input velocity profile table. FACT uses linear segments to connect the points, while PLRAY uses curvilinear segments in which the square of the index of refraction (or  $1/c^2$ ) is parabolic. The segments are joined with continuity of slope. PLRAY also differs from FACT in the method of computing ray intensities. The key factor in the intensity computations is the derivative of the range with respect to the ray source angle (or some monotonic function of ray source angle). PLRAY computes the derivative from analytical formulas. FACT fits the curve of range vs (a function of) source angle with a parabola fitted to three points. Such a procedure appears to be advantageous for the caustic correction procedure when caustics occur, but it is subject to inaccuracies in the computation of ordinary ray intensities.

PLRAY also differs from FACT with respect to bottom loss curves. Both programs contain internally the sets of FNWC (Fleet Numerical Weather Central) curves. FACT contains an updated set of nine curves for the frequency 3500 Hz, which have not been inserted into PLRAY. The programs differ in the manner of implementing the curves at frequencies other than the specific frequencies for which they were originally devised. PLRAY interpolates linearly between the pair of curves on either side of the frequency of interest. FACT does not interpolate but divides the spectrum into frequency intervals, such that the bottom loss is constant throughout each interval and jumps discontinuously from one interval to the next. With PLRAY the user is not limited to the internally contained FNWC curves, but is permitted to read in his own bottom loss curves in their stead.

PLRAY also incorporates a provision for reading in a beam pattern. The pattern is applied at the source.

PLRAY has been compared with FACT in 21 cases involving eight different velocity profiles. In most of the cases runs were made both semicoherently and incoherently. As a check on the accuracy of both programs, the outputs of the semicoherent runs were compared with the output of a locally generated normal mode program called AP2. To facilitate comparison with the ray program outputs, the normal mode curves were smoothed by application of a weighted sliding window which removed most of the fine structure.

The interference patterns generated by PLRAY and FACT in the semicoherent runs are observed chiefly in the bottom-bounce regions. In most of the runs, computations were carried out sufficiently far in range to cover the first bottom-bounce region and a portion of the second. In general, both ray programs were able to duplicate in remarkable detail the features of the AP2 normal mode interference pattern in the first bottom-bounce region. The best agreement was observed for the steeper rays at short ranges. The agreement with AP2 was observed to deteriorate with increasing range, increasing receiver (or source) depth, and increasing frequency. With a few exceptions the agreement was rather poor in the second bottom-bounce region. Generally poor agreement was also observed in the two cases in which both source and receiver were located within a depressed sound channel, where presumably the propagation of energy in the channel tended to overshadow the bottom-bounce propagation.

In many of the runs it was observed that while the three programs agreed quite well on the relative locations and the db levels of the individual features of the interference pattern, there was a discrepancy in the absolute ranges appearing as an expansion or contraction of the range scale. The distortions are usually quite small at short ranges but tend to become serious at longer ranges. A number of possible causes of the scale distortion have been examined, but no completely satisfactory explanation has as yet been found.

Both PLRAY and FACT contain algorithms for cutting down the amplitude of the interference oscillations in cases where the number of receiver range points per cycle of the oscillations is insufficient to provide adequate sampling. The coherence factor which generates the oscillations is multiplied by an attenuation coefficient which varies with the number of points per cycle from a full value of 1 when the sampling is adequate to 0 when the sampling is totally inadequate. PLRAY and FACT differ in the manner in which the number



of points per cycle is computed. PLRAY computes an instantaneous value based on an analytical formula, while FACT computes an average value over the entire range interval covered by the family of rays involved. Since the period of the oscillations tends to vary strongly with range in the first bottom-bounce region, cases have been encountered in which the PLRAY and FACT propagation loss curves differ greatly in appearance; with the PLRAY curves showing a steady increase in amplitude with range, and the FACT curves showing a constant amplitude, with oscillations exhibiting a very choppy appearance at the shorter ranges due to inadequate sampling. However, comparison of the FACT curves with the normal mode oscillations indicates that adequate sampling can be obtained with somewhat fewer points per cycle than are called for in the algorithm. Further investigation of the sampling problem is needed with a view to redefining the parameters.

Except for the manner in which the sampling problem is handled, PLRAY and FACT yield generally comparable results in the semicoherent runs and neither shows any clear advantage over the other.

In the incoherent runs PLRAY and FACT show excellent agreement throughout the bottom-bounce regions except for the difference in the ways in which the internally contained bottom loss curves are applied.

With regard to the prediction of convergence zones, PLRAY and FACT agree with AP2 on the locations of the zones, but differ widely in the shapes of the zones and the heights of the peaks. However, even though the caustic corrections do not perform as well as might be desired, they are a highly significant improvement over unmodified ray theory.

Runs were made with three velocity profiles containing surface ducts of appreciable thickness. In those runs in which both the source and receiver were located within the duct PLRAY generally agreed closely with the normal mode predictions in the range interval dominated by the surface duct propagation. The results of FACT were somewhat more variable, showing good agreement in some runs and less satisfactory agreement in others. In those runs in which the source was in the duct and the receiver slightly below, both ray programs gave variable results.

In the runs on two of the eight velocity profiles FACT produced results of questionable validity. One of the two profiles contains a shallow SOFAR channel with a double minimum. The source and receiver were located on opposite sides of the first minimum. The convergence zones predicted by FACT have a strange shape consisting on the near side of a long gradual rise covering about 20 kyd, followed on the far side by a steep drop. The other profile contains a large surface duct. PLRAY and AP2 agreed well on the interference pattern in the first bottom-bounce region. FACT, while predicting roughly the correct average levels, generated an entirely different interference pattern. When the receiver was placed slightly below the bottom of the duct, the FACT program failed to generate any interference pattern at all and produced virtually identical curves at frequencies of 50 and 100 Hz. Aside from the cusped caustic problem, PLRAY experienced no difficulties of comparable magnitude in any of the runs.

# C O N C L U S I O N S

1. PLRAY and FACT in general yield comparable performance in runs in deep water at frequencies below 1 kHz. (No comparisons were made at high frequencies.)
2. The interference patterns generated by both PLRAY and FACT in the semicoherent runs show good agreement in the first bottom-bounce region with the corresponding patterns generated by normal mode theory. The quality of the agreement tends to deteriorate with increasing range, increasing receiver (or source) depth, and increasing frequency.
3. Distortions of the interference patterns, which appear as expansions or contractions of the range scale, are frequently observed in the comparisons of PLRAY, FACT, and the normal mode program. These distortions do not normally affect the locations of convergence zones.
4. Although both ray programs usually agree on the locations of convergence zones, neither PLRAY nor FACT appears capable of accurately predicting the shapes of the zones and the heights of the zone peaks as generated by normal mode theory. However, both programs offer a great improvement over conventional ray theory, which predicts highly erroneous spikes at caustics.
5. Except for differences in the shapes of convergence zones, PLRAY and FACT, when using the same bottom loss curves, produce virtually identical results in the incoherent mode of ray addition. The programs differ, however, in the manner of interpolating with respect to frequency between the internally contained FNWC bottom loss curves. (FACT does not interpolate.)
6. The parameters in the algorithm which reduces the amplitude of the oscillations of the interference pattern in cases of inadequate range sampling are not properly chosen. Further investigation is needed with a view to selecting optimum values. This conclusion applies to both PLRAY and FACT.
7. The surface duct model of PLRAY yields somewhat more accurate results than that of FACT when the source and receiver are both located in the duct. Neither program, however, proved highly accurate when the source was in the duct and the receiver was slightly below.
8. The absence of a cusped caustic correction in PLRAY leads to a gross error when the source and receiver are at the same depth. However, the error is reduced to an acceptable magnitude with negligible effect on the computations at other ranges simply by separating the source and receiver by a few feet in depth.



## INTRODUCTION

Approximately 10 years ago a computer program (reference (a)) was developed at the Naval Air Development Center for the prediction of acoustic propagation loss in a horizontally stratified ocean. This program has been extensively used over the past decade not only at NAVAIRDEVCEEN, but also by various other naval activities and private contractors, and has proved to be a very valuable tool. However, as has long been recognized, it suffers from a number of limitations, chief among which are the following :

1. Being based strictly on ray theory, it is subject to the limitations of ray theory. In particular, it predicts infinite intensity at caustics (ray focal points), and it fails to account for leakage of energy by diffraction out of sound channels. The most commonly encountered example of the leakage problem occurs when both the source and receiver are located within a surface duct. In such cases the predictions generated by the program may be grossly in error, particularly at low frequencies.

2. Among the various modes of operation available to the user of the old NAVAIRDEVCEEN program, the so-called CLC option was designed for the routine computation of propagation loss as a function of range. In this mode of operation, the program computes a large family of rays and interpolates between these rays to compute the propagation loss at the specified ranges. The CLC option has two limitations. First, in computing the multipath propagation, only incoherent ray summation is available; that is, the individual ray intensities are added directly and no provision is made for including the effects of phase interference. Secondly, the structure of the program and the size of the arrays in the computer are such that rays cannot be traced beyond the range at which they have passed 15 vertices (7-1/2 complete ray cycles). Beyond this point the rays are lost.

3. Coherent ray summation is available when the target ray (eigenray) option is used. In this mode of operation each specified receiver location is treated as a separate case, and a search and iteration procedure is employed to find each individual ray which propagates to that location. The principal limitation of the target ray option is the long computer running time required. An additional limitation, which has proved troublesome in a few isolated runs, is the restriction of the number of target rays to 30.

Although the second and third of the above limitations could be removed by re-structuring the program, the first is basic because it is inherent in the ray approximation to wave propagation. Considerable work has been done over the past decade in developing wave corrections to ray theory and in the application of these corrections to practical ray programs. The best known and most widely used of these programs is the FACT model (reference (b)), developed by the former AESD (Acoustic Environmental Support Detachment), Office of Naval Research. This model incorporates a number of new features, the most important of which are caustic corrections and an approximate method of computing phase interference effects near the ocean surface. The FACT program also includes a surface duct model which was originally developed for the FNWC, Monterey, California (reference (c)), and a wave correction for rays propagating in a depressed sound channel when the source and receiver are both located near the channel axis.

The FACT program has been made available to the Naval Air Development Center and is currently operational on the NAVAIRDEVCON CDC 6600 computer. However, after an examination of FACT and a brief period of testing it, a decision was made to develop a somewhat similar program locally. One consideration in this decision was a desire to retain some of the more desirable features of the old NAVAIRDEVCON program, especially the fitting of the input velocity profile points with curvilinear segments and the attendant procedure for calculating ray paths and intensities. The FACT program, even though it represents a significant advance over conventional ray programs with respect to its excellent novel features, leaves much to be desired in those portions where standard ray theory is applied. Instead of fitting the velocity profile with curvilinear segments, which provide continuity of slope, it employs the old method of straight lines; then in the computation of ray intensities it uses an approximate method of questionable accuracy. The key parameter entering the computation is the derivative of the ray range with respect to the ray source angle (or some monotonic function of the source angle). Instead of computing the derivative from an analytical formula, the FACT program fits a parabola to three points and calculates the derivative from the slope of the parabola. Cases have been found where this method leads to significant errors.

Another consideration in the development of a local program is the ease with which the program may be modified to meet special requirements which continually arise in the laboratory's work. It is far simpler (and safer) to make internal changes in a home-grown program whose details are thoroughly understood than to dig through the intricacies of an externally prepared program such as FACT.

The resulting program, called PLRAY, is similar to FACT in its basic structure and requires essentially the same computer running time. In any one run it computes the propagation loss as a function of range for a single source/receiver depth combination, while up to six frequencies may be processed simultaneously. It has a basically similar coherence feature, so that the propagation loss may be computed either incoherently or semicoherently. (Both programs have a third option labeled "coherent," but this is not truly coherent in either program and appears to be of little practical value.) PLRAY incorporates corrections for smooth caustics but lacks the cusped caustic correction feature of FACT. The presence of cusped caustics leads to large errors when the source and receiver are at the same depth. In PLRAY the errors are reduced to acceptable proportions by moving the source and receiver depths slightly apart. PLRAY also lacks the wave correction for depressed sound channel propagation, but it contains a locally generated surface duct model broadly similar to the surface duct model of FACT. Finally, PLRAY contains a provision for inserting a set of beam patterns.

## GENERAL DESCRIPTION OF THE PROGRAM

PLRAY computes propagation loss as a function of range at constant depth in an ideal horizontally stratified ocean whose acoustic structure is specified by a single velocity profile. It does this by computing a family of rays and interpolating between these rays to obtain the intensities at the various specified receiver locations. The intensity at any one receiver location is the result of the contributions of a number of rays which propagate over different paths. The program offers the option of selecting either of two different methods of computing the resultant multipath intensity: (1) incoherent summation, in which the individual ray intensities are added without regard to phase interference, and (2) semicoherent summation, in which the group of rays associated with each arrival order (e.g., the four single bottom-bounce rays) are added coherently and the resultant intensities of the various arrival orders are added incoherently.

The program is written in FORTRAN V3.0-P380 for the CDC 6600 computer.

## INPUTS

The first data card contains a set of integers, including the number of frequencies, the number of receiver depths, and several other parameters which are discussed in the detailed description of the program. This is followed by a set of environmental input cards. These inputs consist of the sea state, bottom parameter, velocity profile, and, if desired, a set of bottom loss curves which the user may wish to substitute for the internally contained curves. The environmental inputs are followed by a set of up to six frequencies, a single source depth, a set of up to eight receiver depths, and a range card which contains the minimum range, range increment, and maximum range. The minimum range (not included in FACT) permits the user to begin the computations at any range desired. The maximum number of range points allowed is 251. Finally, if desired, a set of beam patterns may be inserted as tables of pressure ratio (relative to the beam axis) vs ray source angle, one table for each of the frequencies specified. Beam inputs are read and pattern computations are performed in SUBROUTINE BEAM.\*

## CURVE-FITTING (SUBROUTINES CURFIT, PARAB, FIT, BRIDGE)

Before curve-fitting, corrections for the curvature of the earth are applied to the depths and sound speeds of the velocity profile. The curve-fitting routine, which fits curvilinear segments which join with continuous slope, is taken directly from reference (a) and will not be described further in this report.

---

\* Experience has shown that the above method of specifying the beam patterns is cumbersome. It is included in the current description because it is perfectly general and does not contain any classified information. For any given application it is usually preferable to specify the physical parameters of the beam hardware and let the computer program calculate the beam response. This is readily accomplished simply by rewriting the BEAM subroutine without affecting the rest of the program.



## RECEIVER DEPTH LOOP

At this point a loop over receiver depths is entered, which extends to the end of the program. All operations from this point on must be carried out separately for each different receiver depth. At the beginning of the loop the source and receiver depths are compared to determine whether they differ by at least 2 feet. If not, they are automatically shifted to maintain this separation.

## AUGMENTATION OF PROFILE (SUBROUTINE INSERT)

Before proceeding with the ray computations, a new velocity profile table is set up by inserting the source and receiver depths into the original profile. The sound speeds at the source and receiver depths are calculated from the parameters of the respective curvilinear segments in which they lie. At this point the source and receiver are redefined for the purpose of the subsequent computations. The sound speeds at source and receiver are compared, and the depth with the larger sound speed is treated as though it were the source, while the depth with the smaller sound speed is treated as though it were the receiver. In what follows, the original pair of points will be labeled the true source and true receiver, and the new pair will be labeled the ray source and ray receiver, or simply the source and receiver.

## SECTORS (SUBROUTINE SECLIM)

The family of rays computed actually consists of a group of sub-families of rays of different types. The sub-families are bounded by limiting rays. For example, the limiting ray to the ocean bottom separates the RSR rays from the bottom-bounce rays. In order that the interpolations may be performed, it is necessary to separate the sub-families and work with each of them one at a time.

For this purpose it is convenient to specify the rays in terms of the absolute values of their source angles. Each sub-family is then confined to a sector in the angular space from 0 to 90 degrees, the sectors being bounded by the appropriate limiting ray source angles. The sectors are processed one at a time in order of increasing source angles. The outermost sector is terminated at 30 degrees. No rays are computed at steeper angles. Instead, the intensities are computed by a simplified approximate formula.

## RAY SUB-FAMILIES (SUBROUTINE DIVSEC)

The number and spacing of the rays of each sub-family are automatically determined by an algorithm in the program. The spacing is extremely close near the inner edge of the sector and increases in a geometric progression until it reaches a constant limiting value. Normally the constant spacing is continued until the outer edge is reached. However, if the sector is bounded at its outer edge by a limiting ray to a local maximum of the velocity profile (as distinguished from a limiting ray to the surface or bottom), the spacing is decreased, on approaching the boundary, in a manner symmetric to the spacing at the inner edge.



## RAY COMPUTATIONS (SUBROUTINE INCR)

Three basic horizontal range intervals are computed for each ray of the sub-family: the range interval from source depth to receiver depth, the range interval corresponding to one complete ray cycle, and the range interval corresponding to the upper portion of a cycle above the receiver depth. These three quantities supply all the information necessary to compute the ray ranges. At the same time the corresponding three intervals are computed for the range derivatives, which are required for intensity computations. In PLRAY, the derivatives are taken with respect to the tangent of the source angle.

## ARRIVAL ORDERS

Although applicable to sources and receivers at any depth, the structure of both FACT and PLRAY with respect to arrival orders is most easily explained when the source and receiver are located in the upper portion of the ocean. In this case the bulk of the ray cycle consists of the portion which passes through the deep ocean, and the direct and surface-reflected (or upper-refracted) rays are relatively close together.

The arrival order number is defined as the number of passages through the deep ocean, that is, the number of bottom bounces or deep refractions. The zero order arrival consists of the two rays which propagate directly to the receiver without going deep. The first and subsequent arrival orders each consist of four rays. If the source and receiver are shallow, all the rays in a given arrival order propagate over similar paths and may be expected to exhibit some degree of coherence. If the source is deep and the receiver shallow, coherence is to be expected only at the receiver end, in which case the four rays are treated as two pairs, one pair leaving the source in a downward direction and the other pair in an upward direction. Reciprocal considerations apply to the case where the source is shallow and the receiver is deep. Within each sector the arrival orders are processed sequentially, beginning with order zero.

The individual ray types (such as down-up, up-down-up, down-up-down, and up-down-up-down) which comprise the multipath system of any given arrival order will be termed the multipath ray types.

## PROCESSING OF MULTIPLE FREQUENCIES

All operations up to this point have been independent of frequency and the results thus far apply equally to all frequencies which have been specified. However, from this point on the factors which enter the computation of intensities are frequency dependent. In order that all the frequencies of interest may be processed simultaneously, arrays are provided as necessary in the program for the frequency-dependent variables and frequency DO loops are provided as necessary for the computations. It is to be understood that the description which follows applies to each of the frequencies which are being simultaneously processed.

## CAUSTICS (SUBROUTINE RCAUST)

Before ray intensities are computed for any given arrival order within any sector, a search is conducted (in SUBROUTINE RAYSUM) to determine whether any

caustics exist. The range vs source angle curve for each multipath type is examined to see whether a minimum or maximum occurs within the sector. Since by ray theory the intensity is inversely proportional to the range derivative, the predicted intensity becomes infinite at a minimum or maximum of the range curve. This is the location of a caustic.

If a caustic is found, caustic-correction intensities based on the Airy function  $Ai$  are computed over a range interval extending from a predetermined limit on the shadow-zone side of the caustic to a predetermined limit on the illuminated side. If a beam has been specified, the intensities at all receiver range points in this range interval are multiplied by the square of the beam pressure ratio, evaluated at the source angle of the ray to the caustic. The range interval is then marked with a flag so that it may be excluded from the subsequent ray intensity computations.

#### RAY INTENSITY COMPUTATIONS (SUBROUTINE RAYSUM)

After the caustic-correction intensities have been computed in the prescribed range interval, ray intensities are computed at the remaining receiver locations covered by the rays of the sector. If a beam has been specified, the ray intensities are multiplied by the squares of the respective beam pressure ratios. At each receiver location the sum of the intensities of the contributing multipath ray types is calculated, yielding the resultant incoherent intensity for the current arrival order. If incoherent ray summation has been called for, this resultant value is added to whatever value is already present in the pertinent range-frequency bin of the resultant intensity array.

#### COHERENCE COMPUTATIONS (SUBROUTINE RAYSUM)

If semi-coherent addition is called for, it is necessary to calculate a coherence factor by which the incoherent intensity sum is multiplied before being stored in the resultant intensity array. (There are special cases in which the above procedure is slightly modified; see detailed description of the program.) It should be mentioned at the outset that coherence is calculated only for those rays which strike the surface.

The coherence factor is computed in a simple approximate manner. Consider a pair of rays which leave the source at approximately the same angle, one going upward to be reflected at the surface and the other going directly downward. After the surface reflection, both of these rays travel along essentially the same path and arrive together at the receiver. The reflected ray may be considered to have originated at an image source at a point above the surface, located symmetrically with respect to the actual source. The assumption is made that in the vicinity of the source these two rays are parallel straight lines and that their difference in phase is simply the result of the difference in path length, plus a 180-degree phase shift resulting from the surface reflection. A similar effect occurs at the receiver end. These effects are formulated mathematically in a coherence factor which multiplies the incoherent intensity sum. As the range to the receiver varies, the phase differences also vary, leading to an oscillatory interference pattern.

Two limitations are placed on the coherence factor. First, if the oscillations of the interference pattern occur rapidly in range, there may be a

sampling problem. The parameter of interest here is the number of specified receiver range points per cycle of oscillation of the pattern. If the number of points per cycle is too small, then when the propagation loss is plotted against range the resulting curve will not adequately represent the situation. This problem is treated in a somewhat arbitrary way by simply reducing the amplitude of the oscillations. An attenuation factor is introduced, which is a function of the number of points per cycle.

The second limitation is concerned with the tendency for the coherence to deteriorate when the two interfering rays are separated too far in range. This situation may be expected to occur when the source or receiver is deep and will tend to be aggravated at shallow angles, where the assumption of straight-line propagation becomes less valid. The problem is handled by arbitrarily assuming that coherence occurs only when the horizontal separation between the two interfering rays at the source depth (for interference at the source end) or at the receiver depth (for interference at the receiver end) is less than a pre-determined limiting value.

#### SURFACE DUCT PROPAGATION (SUBROUTINE SDUCT)

If the source and receiver are located within a surface duct, the use of ray theory to calculate the propagation loss does not in general lead to satisfactory results. The greatest source of error in shallow ducts and/or at low frequencies is the leakage of energy out of the duct. Leakage is not accounted for in ray theory. In addition, even in good ducts, early experience with PLRAY has indicated that the caustic correction procedure cannot adequately handle the many near-horizontal caustics occurring in the ducts. For these reasons PLRAY incorporates a surface duct model which calculates the propagation loss designed to approximate the predictions of normal mode theory for propagation within and immediately below the duct.

#### PROPAGATION LOSS (PROGRAM PLRAY)

After all intensities have been calculated they are converted to propagation loss and stored again in the same array.

#### PLOT ROUTINE (SUBROUTINE PLPLOT)

The program contains a plot routine for the purpose of plotting the propagation loss vs range on a Houston COMLOT, Model DP-1.

#### CORE REQUIREMENT

Without the software for the Houston plotter PLRAY requires slightly less than 21000 (decimal) words on the CDC 6600 computer. The Houston plotter adds approximately 1600 words.

#### RUNNING TIME

PLRAY and FACT require essentially the same running time. For example, in one of the typical runs made for this report the time was 12.46 sec for PLRAY and 11.66 sec for FACT.



## DETAILED DESCRIPTION OF THE PROGRAM

As an aid in understanding the following detailed description, the reader is referred to the FORTRAN listing of the program in appendix A and to the glossary of the principal FORTRAN symbols presented in appendix B. A thumbnail description of the various subroutines and functions is given in appendix C. A detailed description of the input data deck for a run of PLRAY will be found in appendix D.

## DATA INPUT SECTION

The first portion of PLRAY is devoted principally to reading and printing the input data, applying corrections for the earth's curvature to depths and sound speeds, and fitting the velocity profile with curvilinear segments.

Card 1 contains 7 integers. NF is the number of frequencies for which computations are to be run, not to exceed 6. It also performs the additional function of serving as a code to stop the run. The program is written in the form of a huge loop. After the computations have been completed for a set of input data, the program returns to the first READ statement and checks the variable NF. If NF has a nonzero value, a new set of input data is read in and processed. However, if NF is zero, the program stops; thus, a blank card may be used to stop.

NREC is the number of receiver depths, limited to 8.

Iprof is a code parameter governing the environmental inputs, namely, the velocity profile and the externally specified bottom loss curves. A value of zero is selected for normal operation. If Iprof is set to 1, the READ statements for the velocity profile table and the bottom loss tables are bypassed. This value is selected when it is desired to run an additional set of computations using the same environmental inputs (for example, an additional source depth or frequency or a different set of ranges). When Iprof is set to 2, only the velocity profile inputs are bypassed, and when set to 3, only the bottom loss inputs are bypassed. (It should be pointed out that the bottom loss inputs are bypassed also for all values of the bottom parameter IBP except 6.)

The integer IUNIT is required when the velocity profile is specified in terms of temperatures and salinities instead of sound speeds. If IUNIT = 0, it is assumed that the temperatures are in °F; if IUNIT = 1, they are in °C.

IPLOT is the plot control parameter. If IPLOT is assigned a value of 1, a plot is called for.

IPR is a print control parameter. For normal output, IPR is set to zero (or left blank). A value of 1 causes the program to print a certain amount of diagnostic information which is useful in analyzing the details of the run. A value of 2 produces more detailed diagnostic information.

IBEAM is the beam control parameter. The default value 0 signifies that there is no beam pattern. If IBEAM = 1, a set of NF beam patterns is to be read in. If an additional run is to be made using the same beam patterns,

IBEAM is set to 2. In this case the beam inputs are bypassed and the previously inserted beam patterns apply.

Card 2 is the environmental input header card. The first variable, ISP, is the sea state. It is used in computing the surface reflection loss. IBP is the bottom parameter. Values from 1 through 5 call for application of the internally contained FNWC bottom loss curves, types 1 through 5. The external bottom loss input statements are bypassed. A value of 6 signifies that external bottom loss data are to be read in. LAT is the latitude of the velocity profile, a real (decimal) number. The latitude is required for the computation of sound speed from temperature and salinity. The default value is 45 degrees. When the sound speeds are read in directly, LAT serves only for identification. IDR is a letter N or S and serves only for identification. IDBT is a run identification parameter consisting of up to 40 alphanumeric characters.

Card set 3 is a set of cards on which the external bottom loss curves are specified. These cards are needed only when IBP = 6 and IPROF = 0 or 2. The first of these, card 3a, contains the variables NFR, the number of frequencies for which curves are to be provided, and FR(J), the values of these frequencies in Hz. The FR(J) must be arranged in a monotonically increasing order. The bottom loss values in db for each frequency are specified on a pair of cards 3b. Fifteen points are required. The last value specified must correspond to 90 degrees. If less than 15 points are required to specify the curve, the remaining 10-column fields may be left blank. The corresponding grazing angles in degrees are specified on a pair of cards 3c. The cards are stacked in the order 3b, 3c for the first frequency, 3b, 3c for the second frequency, etc.

Card set 4 is the set of cards containing the velocity profile, one card for each point. Each card contains fields for the depth ZB, sound speed CB, temperature T, and salinity S. If sound speeds are to be read in, the temperature and salinity are not required. If temperature and salinity are to be read in, the sound speed field must be left blank (or zero). The integer NDCD is a code variable which terminates the read-in. A nonzero value must be inserted for NDCD on the last card. These cards must be stacked in order of increasing depth.

The profile variables may be specified in either English units (ft, ft/sec, °F) or metric units (m, m/sec, °C). If sound speeds are read in, the program automatically distinguishes between the two systems of units. If temperatures are read in, IUNIT must be 0 for the English system and 1 for the metric system. When the inputs are temperatures and salinities, the sound speeds are calculated from Wilson's equation (reference (d)) in FUNCTION VELOC.

As each depth and sound speed are read in (or calculated), corrections are applied for the curvature of the earth (see appendix E). Upon completion of the profile input, SUBROUTINE CURFIT is called for the purpose of fitting the profile with curvilinear segments. CURFIT and its associated subroutines PARAB, FIT, and BRIDGE are taken directly from the old NAVAIRDEVCE program and are described in reference (a).

After the curve fit a test is made for the presence of a surface duct. A search is made for the largest sound speed in the first 1000 feet below the surface of the ocean, and a test is made to determine if this largest value

occurs at a local maximum point of the profile. If so, the value of the index IB at this depth is stored as the duct parameter IDUCT. The purpose of the test is to determine the duct depth for use in the surface duct model. If the maximum sound speed occurs at the surface, there is of course no surface duct, and IDUCT = 1. If a duct is observed but is found to be deeper than 1000 ft, IDUCT is set to 1 and the surface duct model is not implemented.

Card 5 contains the NF frequencies F(IF) and the corresponding NF values of the coherence parameter JCOH(IF), which controls the method of ray energy summation. A value of 0 calls for incoherent summation, while a value of 1 calls for semicoherent summation. The program also permits a value of 2 to be specified, in which case the semicoherent mode of summation is selected, but without the attenuation factor which cuts down the amplitude of the phase interference oscillations when the range sampling is insufficient. Use of JCOH(IF) = 2 is not recommended.

Card 6 contains the source depth ZS0 in the first field and the NREC receiver depths ZR0(I) in the subsequent fields. These depths must be expressed in feet. Neither the source nor the receiver may be located within 0.1 foot of the surface or bottom.

Card 7 contains RMIN, the minimum range, DR, the range increment, and RMAX, the maximum range, all in yards. The number of range points is not permitted to exceed 251. If the specified inputs result in more than this number, RMAX is automatically truncated to the maximum allowable value. The value of the parameter KMAX, which represents the total number of specified range points, is evaluated at this time.

If IBEAM = 1, the beam patterns are inserted at this point by calling BEAM(0). The READ statements are in SUBROUTINE BEAM(L). The patterns are read in as tables of pressure ratio (relative to the beam axis) vs ray source angle (degree), beginning at -90 degrees (downward) and extending to +90 degrees (upward). NF patterns are read in, one for each frequency. The first card, 8a, contains the integers NBF(IF) indicating the number of points (up to a maximum of 100) required to specify each of the patterns. This is followed by card sets 8b and 8c for the first frequency, card sets 8b and 8c for the second, and so on. Card set 8b contains the grazing angles THETA(I) and card set 8c contains the corresponding beam pressure ratios BM(I,IF). The beam patterns are applied to the source depth ZS0 (referred to subsequently as the true source depth).

This portion of PLRAY concludes with a few miscellaneous calculations. The volume attenuation coefficient of the water ALPHA(IF) is calculated from Therp's formula (reference (e)) for each of the frequencies. SUBROUTINE SURF is called to compute the surface reflection loss SLOSS(IF). Except for name changes, this routine is identical to the surface loss routine of reference (a). Finally, the earth curvature correction is applied to the source depth, the corrected value being labeled ZS.

#### RECEIVER DEPTH LOOP

The remainder of the program is enclosed within a receiver depth DO loop. Since only one receiver depth can be processed at a time, it is necessary to



carry out the complete set of calculations for one depth before starting on the next. At the beginning of the loop the earth curvature correction is applied to the current receiver depth, the corrected value being labeled ZR. Since PLRAY is subject to large errors when the source and receiver are at the same depth, ZS and ZR are compared to determine whether they differ by at least 2 feet. If not, ZS is automatically shifted upward and ZR downward by a sufficient amount to assure a 2-foot separation. The next step is the setting up of a new augmented velocity profile by inserting the source and receiver depths into the old one. This is done in SUBROUTINE INSERT.

#### SUBROUTINE INSERT

The depths and sound speeds of the original profile are designated ZB(IB) and CB(IB), the index being IB. The principal function of INSERT is to set up a new table of ZA(IA) and CA(IA) which includes the source and receiver depths. If the source depth happens to coincide with one of the ZB(IB), it is not necessary to add a new point. Otherwise, the sound speed CS is calculated at depth ZS from the appropriate curvilinear segment parameters and this point is inserted into the IA table at the proper place. The indices IA of subsequent points are increased by 1. A similar procedure is followed for the receiver depth ZR. The sound speed at the receiver depth is designated CR.

Since no new table is established for the segment parameters CSP(IB), GP(IB), and ZP(IB), it will be necessary later to be able to identify the value of IB which corresponds to any given value of IA. The identification is accomplished by setting up an array IDF(IA) such that

IDF(IA)

INSERT also redefines the source and receiver locations for use in the subsequent ray computations. Let ZAA and CAA be the depth and sound speed of the redefined source and ZBB and CBB the depth and sound speed of the redefined receiver. Then CAA is defined as the larger of CS and CR, and CBB is defined as the smaller. Thus, in the ray computations the source will always have a larger sound speed than the receiver. To avoid confusion in terminology, the original source and receiver will henceforth be referred to as the true source and true receiver. Since the beam pattern is always applied to the true source, it will be necessary to ascertain whether this is ZAA or ZBB. The identification parameter is SN. It is assigned a value of 1 if ZAA is the true source and -1 if ZBB is the true source.

At the end of INSERT is a test to determine whether the surface duct model is to be implemented. The first requirement is that IDUCT have a value other than 1, that is, that a duct exist. Secondly, it is required that the source be located within the duct and the receiver be at a depth not in excess of 1.8 times the duct depth, or vice versa. If these conditions are met, the parameter IAD is set to the value of the index IA at the bottom of the duct (equivalent to IDUCT for the index IB), and the flag ISD, which is normally zero, is set to 1.

#### PROGRAM PLRAY (CONTINUED)

Following the return from INSERT, a value of 1 or 2 is assigned to the parameter ICASE. A value of 1 applies if the source depth ZAA is greater than

the receiver depth ZBB; otherwise ICASE = 2. This parameter is required because of the difference in the characteristics of the multipath ray types, depending upon whether the source is above or below the receiver.

#### SUBROUTINE SECLIM

At this point SECLIM is called for the purpose of setting up the ray source angle sectors. The sectors are bounded by limiting rays which separate rays of one type from rays of another. The boundaries of the sectors are defined in terms of the limiting sound speeds CL(IL), which are the vertex velocities of the limiting rays. If the vertex depth of the limiting ray to any sector boundary occurs at an interior maximum point of the velocity profile, as distinguished from the top or bottom, the corresponding value of CL(IL) is flagged with a minus sign.

The sound speed CL(1), representing the inner boundary of the first sector, is the vertex velocity of the shallowest ray which reaches the receiver depth. Since the sound speed at the source is by definition greater than (or equal to) the sound speed at the receiver, this ray is normally the zero degree ray and CL(IL) is equal to CAA. However, if in the velocity profile there exists between the source and receiver depths a local maximum at which the sound speed exceeds CAA, CL(1) is set to the negative of the sound speed at this maximum. The index IA of the depth at which CL(1) is defined is identified by the symbol ILT.

Beginning at the index ILT, a search is made simultaneously both upward and downward along the velocity profile for the limiting depths which define the CL(IL) at the sector boundaries. In order that any given depth ZA(IA) may qualify as a suitable limiting depth, it is necessary first of all that the sound speed CA(IA) exceed the absolute value of the previous limiting sound speed CL(IL-1). In addition, one of the following two requirements must be met: (1) CA(IA) must occur at a maximum of the profile, that is, if IA = 1, CA(1) must exceed CA(2), if IA = NA, CA(NA) must exceed CA(NA-1), and otherwise CA(IA) must exceed both CA(IA-1) and CA(IA+1). If the maximum occurs at the surface or bottom, CL(IL) is given a positive algebraic sign; otherwise it is given a negative sign. (2) If the above condition is not met, tests are run on the sound speed gradient G(IA), which is calculated at the beginning of the subroutine. If G(IA) is an internal maximum or minimum value (that is, not occurring at the surface or bottom), CL(IL) is set equal to the negative of CA(IA).

Strictly speaking, the ray to a segment boundary at which the gradient is an extremum (a maximum or minimum) is not a true limiting ray and does not form a boundary between families of rays of different types. However, experience has shown that the presence of such extrema frequently gives rise to extrema in the ray range, i.e., to caustics. If the gradient criterion is not included, the large sector formed by true limiting rays sometimes exhibits multiple caustics, which cannot be handled by the PLRAY caustic correction procedure. The gradient criterion has been inserted to divide the larger sector into two smaller ones, thereby alleviating the problem.

After all the values of CL(IL) associated with the velocity profile have been determined, a final value is arbitrarily assigned, corresponding to a ray

which leaves the source at 30 degrees. This ray forms the outer boundary of the last sector in which rays are computed. Beyond 30 degrees the ray intensities are computed from an approximate formula (appendix F).

#### PROGRAM PLRAY (CONTINUED)

Following the sector determination, PLRAY initializes several variables prior to the ray computations. The  $H(K,IF)$  array and the parameters ISURF and IBOT are set to zero.  $H(K,IF)$  is a large array in which the various ray, caustic-correction and surface duct intensities are stored as a function of range (K) and frequency (IF).

Before entering the sector loop, PLRAY tests the values of the  $CL(IL)$  to determine which sectors, if any, contain rays which propagate within a surface duct and assigns to the variable ILD the value of IL at the outer boundary of the highest order sector of this type. If there is no surface duct, the value of IAD is 1.

#### SECTOR LOOP

The program now enters a sector DO loop (index IL) in which the complete set of computations are carried out in each sector, one at a time, beginning with the innermost. At the beginning of the loop the angle TH2 is computed. TH1 and TH2 normally represent the angles at the inner and outer boundaries of the sector. However, on the first transit through the loop ( $IL = 1$ ), which serves only to initialize TH1, the value assigned to TH2 is the angle of the inner boundary of the first sector. The program then jumps to the end of the loop where TH1 is updated by setting it equal to TH2. The steady state is reached on the second transit ( $IL = 2$ ), where TH1 and TH2 have been assigned the proper values corresponding to the first sector. Thus, each sector is identified by the value of IL at its outer boundary.

Immediately following the computation of TH2, the index IL is tested to determine whether ray computations in the surface duct (if any) are to be suppressed. If IL has a value less than or equal to ILD and the source and receiver are both located within the duct, the program skips to the end of the loop and updates TH1 in preparation for the next sector.

Assuming the computations in the sector are not to be suppressed, ISURF is set equal to 1 if the rays in the sector strike the surface and IBOT is set to 1 if the rays in the sector strike the bottom.

The next step is to set the parameter MJ. MJ is a flag used to identify a special case associated with the first sector ( $IL = 2$ ). Before explaining the function of MJ it will be instructive to discuss the way in which the various multipath ray types corresponding to any given ray source angle are normally defined.

#### MULTIPATH RAY TYPES

The bounding angles TH1 and TH2 of a sector are normally defined as positive numbers and the individual ray source angles within the sector are normally defined in SUBROUTINE DIVSEC as positive numbers. However, the multipath ray



types associated with a particular source angle include (where applicable) both up-going and down-going rays. The ray configurations are shown schematically in figures 1a and 1b for zero order arrivals and in figures 2a and 2b for first order arrivals. The ray configurations for the second and higher orders are the same as for the first, the only difference being that additional ray cycles are added to the four existing rays.

In the subsequent description of the program, the different multipath ray types will be identified by the index  $J$ . As may be seen from figures 1a and 1b, there are normally two multipath ray types for the zero order arrivals. The ray  $SR_1$ , which propagates directly from the source to the receiver with no intervening vertex, is identified by  $J = 1$ . The second ray  $SR_2$ , which experiences one upper vertex, is identified by  $J = 2$ . In the case of the first and subsequent orders there are normally four multipath ray types. In figures 2a and 2b the down-up ray  $SR_1$  is identified by  $J = 1$ , the up-down-up ray  $SR_2$  by  $J = 2$ , the down-up-down ray  $SR_3$  by  $J = 3$ , and the up-down-up-down ray  $SR_4$  by  $J = 4$ .

A more realistic portrayal of the zero order rays, exhibiting the refraction resulting from the profile gradients, is shown in figures 3a, 3b, and 3c. Figure 3a is a typical example of  $ICASE = 2$ . It will be observed that in this case the rays  $SR_1$  and  $SR_2$  are of different types; considered as a function of the source angle, they belong to different families. Figure 3b is an example of  $ICASE = 1$  in which there is a local maximum of the profile between the source and receiver depths. Here again the rays  $SR_1$  and  $SR_2$  belong to separate families. There is no continuity between the two families because of the blank sector formed by the rays which are trapped in the surface duct and never reach the receiver depth.

Consider now figure 3c. In this case, as the source angle is reduced to zero, the two rays  $SR_1$  and  $SR_2$  become coincident. Thus, the up-going rays and down-going rays both belong to one family. Therefore in this case the boundaries of the first sector are redefined so as to include both negative and positive source angles. The lower bounding angle  $TH1$  is set equal to the negative of the upper bounding angle  $TH2$ , and there is now only one multipath ray type ( $J = 1$ ) in the zero order arrivals. In the first and higher order, arrivals the number of multipath ray types is reduced from 4 to 2. The parameter  $MJ$  indicates the number of multipath ray types in the zero order arrivals of the first sector, two normally, and one in the above special case.

#### SUBROUTINE DIVSEC(IL)

SUBROUTINE DIVSEC computes the source angles of all rays to be computed in the sector. To avoid computations in the immediate vicinity of limiting rays, a small dead zone of width  $DELO = 0.00001$  radian is inserted at each of the two boundaries of the sector, so that the source angle of the first ray computed in the sector is  $TH1 + DELO$ . The angular spacing  $DEL$  between successive rays is variable. Beginning at a value  $5 * DELO$ , it is successively doubled until a limiting value  $DELM$  is reached. The value of  $DELM$  is 0.01 radian in all sectors but the last, and 0.04 radian in the last sector. The reason for the larger value is that the last sector consists of the steeper, less profile-dependent bottom-bounce rays, for which the range vs source angle curves are well-behaved.

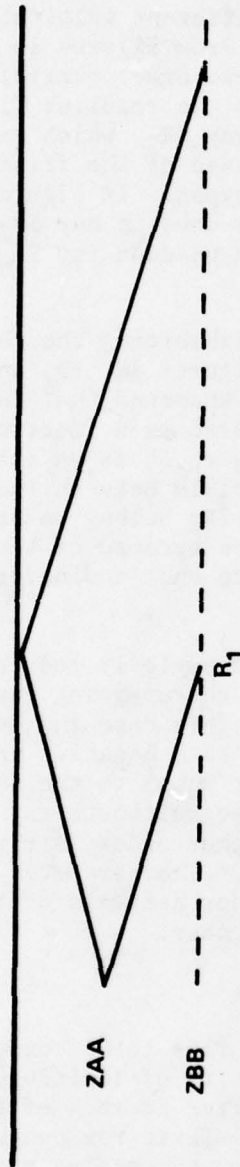


FIGURE 1a - Multipath Ray Types for Zero Order Arrivals, ICASE = 1

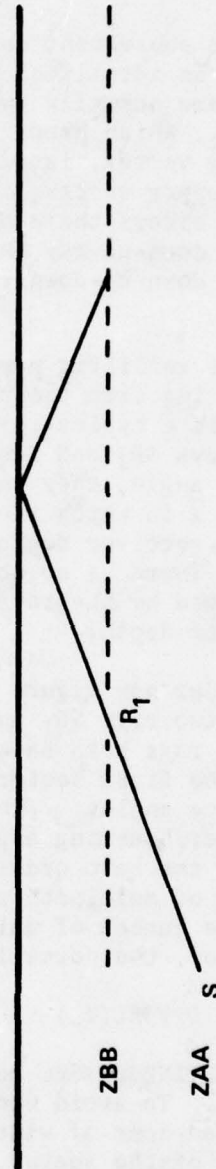


FIGURE 1b - Multipath Ray Types for Zero Order Arrivals, ICASE = 2

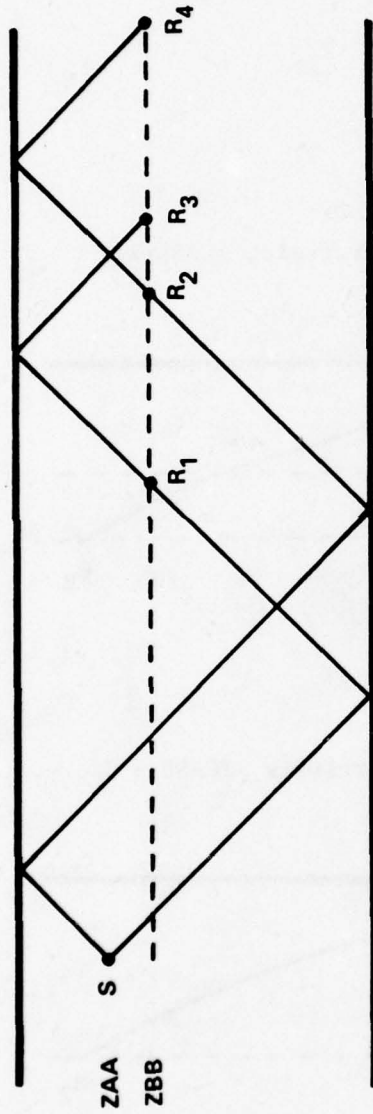


FIGURE 2a - Multipath Ray Types for First Order Arrivals, ICASE = 1

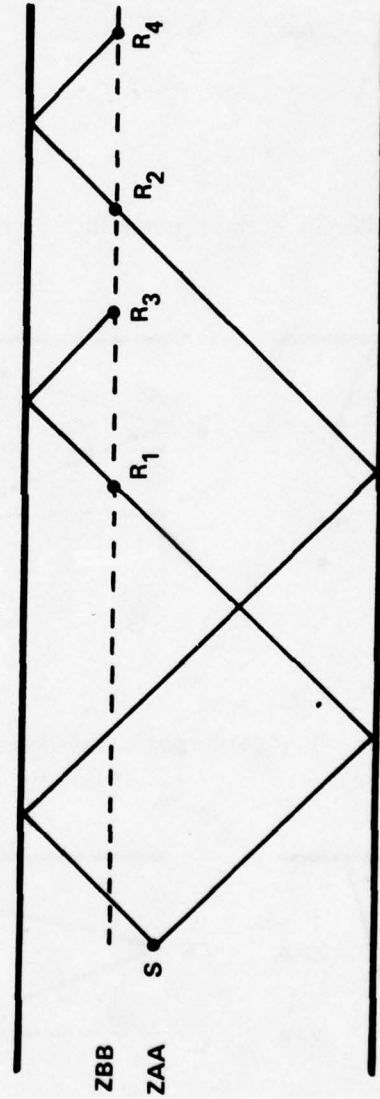


FIGURE 2b - Multipath Ray Types for First Order Arrivals, ICASE = 2



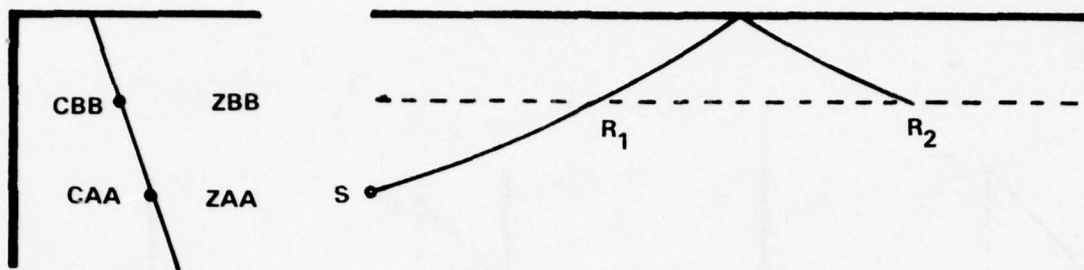


FIGURE 3a - Multipath Ray Types, Zero Order Arrivals, ICASE = 2

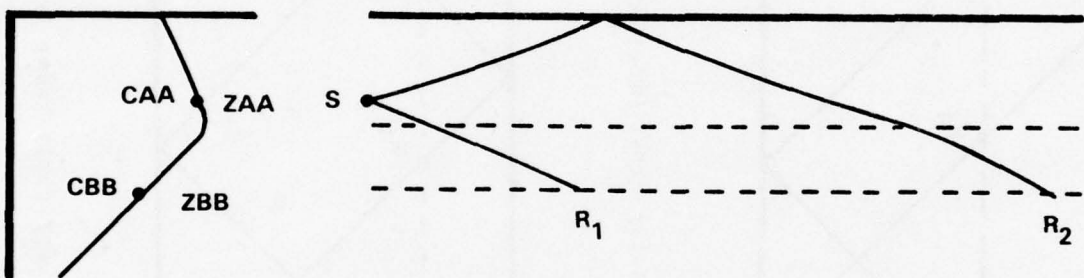


FIGURE 3b - Multipath Ray Types, Zero Order Arrivals, ICASE = 1

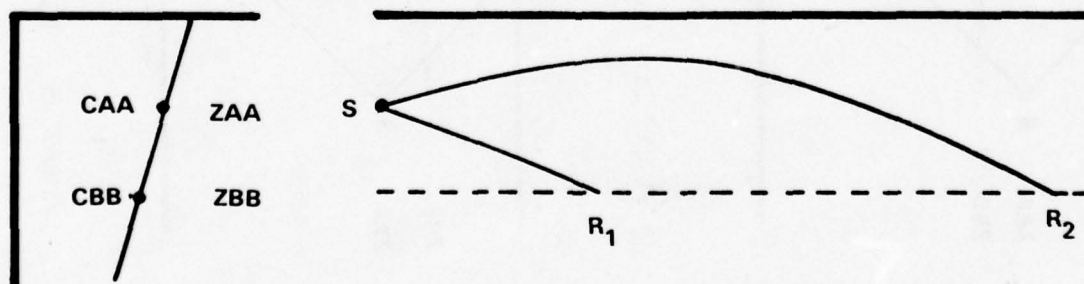


FIGURE 3c - Multipath Ray Types, Zero Order Arrivals, ICASE = 1  
(First Sector, Special Case)

If the limiting sound speed  $CL(IL)$  at the outer boundary of the sector is positive, the uniform spacing of the rays is continued throughout the remainder of the sector. However, a negative value of  $CL(IL)$  signifies that the outer boundary is formed by a limiting ray to an internal maximum of the profile. In this case, as the outer edge of the sector is approached, the ray range approaches infinity, resulting in extremely nonlinear behavior. Such behavior requires the rays to be more closely spaced. In the subroutine this is accomplished by applying in reverse the algorithm used in the vicinity of the inner boundary.

In the event  $CL(IL)$  is negative, the ray source angles in the sector are defined in the following way. Every time a source angle  $TH(I)$  is set up, a corresponding temporary angle  $THT(I)$  is also set up at a corresponding distance from the outer boundary. As the process continues, with  $TH(I)$  becoming larger and  $THT(I)$  becoming smaller, eventually the two angles overlap. As soon as the overlap occurs, the process is stopped and the angles  $THT$  are transferred in an appropriate manner to the  $TH$  array. The total number of rays in the sector is  $NTH$ .

#### PROGRAM PLRAY (CONTINUED)

The basic building blocks from which the ranges and range derivatives are constructed are calculated in a sector angle  $(ITH)$  DO loop. Before calling SUBROUTINE INCR for this purpose, PLRAY computes for each ray in the sector the vertex velocity  $CV$  and the tangent of the ray source angle  $VA(ITH)$ .  $VA$  serves as the independent variable for the range derivatives, in lieu of the source angle itself.

#### SUBROUTINE INCR(ITH) - COMPUTATION OF RANGE AND RANGE DERIVATIVE INCREMENTS

In the first portion of INCR the increments of the range,  $DX(IA)$ , and the derivative of range with respect to  $VA$ ,  $DXP(IA)$ , are computed in each of the applicable layers of the velocity profile. Then these individual increments are added up to yield the three basic building blocks, namely, (1) the range increment  $RSR(ITH)$  and range derivative increment  $RPSR(ITH)$  corresponding to the portion of the ray path between the source and receiver; (2) the respective increments  $RUP(ITH)$  and  $RPUP(ITH)$  corresponding to the portion of a ray cycle which lies above the receiver depth; (3) the respective increments  $RCYC(ITH)$  and  $RPCYC(ITH)$  corresponding to a complete ray cycle. The formulas from which  $DX(IA)$  and  $DXP(IA)$  are computed are derived in appendix G.

Before beginning the computations it is necessary to determine the upper and lower vertex depths. To determine the upper vertex depth, a search is made through all the layers from the source depth to the surface to find the first layer boundary  $IA$  at which the sound speed  $CA(IA)$  exceeds the vertex velocity of the ray. If no such boundary exists, the upper vertex occurs at the surface. However, if the boundary is found, the values of  $ZA(IA)$  and  $CA(IA)$  are stored temporarily as  $ZUT$  and  $CUT$ ,  $CA(IA)$  is replaced with the vertex velocity  $CV$ , and  $ZA(IA)$  is replaced with the vertex depth, which is the depth on the velocity profile corresponding to the sound speed  $CV$ . This depth is computed by solving the parabolic formula of the particular profile segment in which  $CV$  lies.

A similar procedure is followed in finding the lower vertex depth by searching downward through the profile layers from the source depth to the bottom. If a layer boundary IA is found at which CA(IA) exceeds CV, the values of ZA(IA) and CA(IA) are stored temporarily as ZDT and CDT and are replaced with the lower vertex depth and the vertex velocity.

The increments DX(IA) and DXP(IA) are computed in a DO loop in which the index IA runs from a minimum value IUP determined by the upper vertex depth to a maximum value IDN determined by the lower vertex depth. In each layer, V1 and V2 represent the tangents of the ray angles at the top and bottom of the layer and VV1 and VV2 are their respective reciprocals. If the ray has a refractive upper vertex, that is, if the ray does not reach the surface, V1 and VV1 are both set to zero. If the ray has a refractive lower vertex (does not reach the bottom), V2 and VV2 are set to zero. At the end of the loop the temporarily stored values of ZA and CA are replaced.

The increments RSR(ITH), RUP(ITH), and RCYC(ITH) and their respective derivatives are then computed in appropriate DO loops.

Before returning to PLRAY, INCR checks IBOT to determine whether the ray hits the bottom. If so, the ray angle at the bottom, THBD (degrees) is calculated and SUBROUTINE BOTTOM is called for the computation of the bottom loss BOTL(IF) for the specified frequencies. These values are then stored in a two-dimensional source angle-frequency array BLOSS(ITH,IF).

#### SUBROUTINE BOTTOM(THBD)

This subroutine computes the bottom loss (db) as a function of grazing angle THBD and frequency F(IF). The bottom loss is obtained by interpolating between values given in either of two sets of tables, either the internally stored tables based on the FNWC bottom loss curves, or the external tables supplied by the user in the input data deck. If the bottom parameter IBP is assigned a value between 1 and 5, the FNWC curves are used, the value of IBP indicating which of the five FNWC bottom classes is to be selected. If IBP = 6, the bottom loss is computed from the externally supplied curves. In addition to the above, two other options are available. If IBP = 0, the bottom loss is set to zero. If IBP is negative, the bottom loss is arbitrarily set to 100 db. The remainder of this section is concerned with values of IBP between 1 and 6.

The grazing angles and corresponding bottom losses of the tables are DG(I,IBP,J) and DB(I,IBP,J), where the index I refers to the point number along the particular bottom loss curve, and the index J identifies the frequency to which the curve applies. The actual values of the frequencies of the bottom loss curves are FR(J). The frequencies at which the propagation loss is to be computed are F(IF). The interpolations are carried out for one frequency at a time (FF = F(IF)) in a frequency DO loop.

In the general case a two-way interpolation is required. First, the two bottom loss curve frequencies FR(J) and FR(J+1) are selected such that FF lies between them, and interpolations with respect to grazing angle are carried out to obtain the two bottom loss values corresponding to THBD. Then an interpolation with respect to frequency is made between these two values to obtain the



bottom loss corresponding to FF. In the event FF coincides with one of the FR(J), only a single interpolation with respect to grazing angle is required.

If the frequency FF is less than FR(1), it is assumed that the bottom loss curve for FR(1) applies. Similarly, if the frequency FF is larger than FR(NFR), it is assumed that the bottom loss curve for FR(NFR) applies. As stated previously, the frequencies FR(J) must be arranged in a monotonically increasing order.

#### PROGRAM PLRAY (CONTINUED)

Having calculated the basic increments of range and range derivative for the rays of the sector, the program is now ready to compute the ray intensities and their multipath sums. The computations are performed first for the zero order arrivals, following which a loop is entered for the first and subsequent order arrivals. The variable indicating the order of the arrivals is NCYC. The number of multipath ray types involved is NJ. For the zero order arrivals  $NJ = MJ$ ; for the higher orders  $NJ = 2 * MJ$ .

#### ZERO ORDER ARRIVALS

The ranges R(ITH,J) and range derivatives RP(ITH,J) are computed from the basic increments generated by INCR, and the NJ values of the parameter SIGN(J) are determined. SIGN(J) is the algebraic sign of the angle of the Jth multipath ray type at the true source. When a beam pattern is specified, these signs are needed to distinguish between up-going and down-going rays at the true source, where the beam pattern is applied. The remainder of the computations are carried out in RAYSUM and RCAUST. Since these two subroutines are designed to process all arrivals, regardless of the order, the following description will include the higher orders in addition to the zeroth.

When the surface duct model is used in lieu of ray theory to calculate the propagation within a surface duct, it has been found necessary to suppress not only the ducted rays, but also the contributions of the zero order arrivals of all rays. Comparison with the predictions of normal mode theory shows that inclusion of the contributions of the steeper rays in the direct propagation zone leads to erroneously high intensities at short ranges. Although originally overlooked in the development of PLRAY, this result is reasonable, since the surface duct model is designed to cover the complete propagation in the duct, even at short ranges. The computation of the zero order arrivals is therefore bypassed for all sectors.

#### SUBROUTINE RAYSUM(IL)

##### Brief Overview

RAYSUM processes a single arrival order of the rays in a single sector. After determining the minimum and maximum ranges covered by these rays, it searches for the presence of caustics. When a caustic is found, RAYSUM calls RCAUST for the computation of caustic-correction intensities over an interval of ranges on either side of the caustic. Except for a small overlap region where both caustic and ray intensities are computed and compared for the purpose of providing a smooth transition between the two regions, RAYSUM bypasses

the caustic-correction region and computes ray intensities over the remainder of the range interval covered by the rays. It then sums the intensities of the multipath ray types at each range. If semicoherent summation is requested, RAYSUM computes a coherence factor by which the summed intensity at each range is multiplied.

#### Minimum and Maximum Ranges

RAYSUM searches through the ranges of all the rays of each multipath type in the sector and picks out the minimum and maximum range RMNJ and RMXJ of each multipath type and the overall minimum and maximum range RMN and RMX among all ray types. These ranges are then converted to values of the range index K, namely, KMNJ(J) and KMXJ(J) for each individual ray type and KMN and KMX for the composite of all ray types. Neither KMX nor KMXJ(J) may exceed the limiting value KMAX, corresponding to the maximum specified range.

#### Search for Caustics

The search is carried out separately for each multipath ray type (each value of J). A caustic occurs at a point where the range vs VA (tangent of the source angle) curve passes through a minimum or a maximum. In the original version of the program the procedure consisted simply of a search for one or the other. Experience has shown, however, that sometimes these curves are not simply parabola-like, but may exhibit more complicated behavior. Although it has proved impossible to take care of all eventualities, an algorithm has been inserted to deal with one of the more common complications.

Figure 4 shows a range curve exhibiting both a maximum and a minimum. Although it may be possible to include two caustic corrections in one interval, the complications in the program become severe. Fortunately, in most cases examined, one of the two extrema has been found to be a relatively small dip or rise at one end of the curve. As currently written, the program searches for the more important of the two extrema and ignores the other. The price paid for neglecting the other extremum is an occasional caustic spike in the resultant propagation loss curve.

Referring to figure 4, RMXJ and RMNJ are the largest and smallest ranges in the sector. RU and RD are the larger and smaller of the ranges of the first and last rays computed in the sector. The significance of the range differences DRUP and DRDN is apparent in the figure. If there is no extremum in the curve, DRUP and DRDN are both zero. If there is only a maximum, DRDN is zero. If there is only a minimum, DRUP is zero. When both extrema occur, DRUP and DRDN are compared and the extremum associated with the smaller of the two is ignored. In the example shown in figure 4 the minimum is ignored and the correction is applied only to the maximum.

The parameter ICAUST(J) is a flag indicating whether the Jth multipath ray type in the sector experiences a caustic and, if so, whether it is a minimum-range or maximum-range caustic. A value of 0 signifies no caustic, 1 a minimum-range caustic, and -1 a maximum-range caustic. If a caustic is found, the value of the index ITH, such that the ray to the caustic lies between ITH-1 and ITH, is stored as ICTH(J). When a caustic is present, SUBROUTINE RCAUST is called. The parameter KTH in the call is equivalent to ICTH(J).

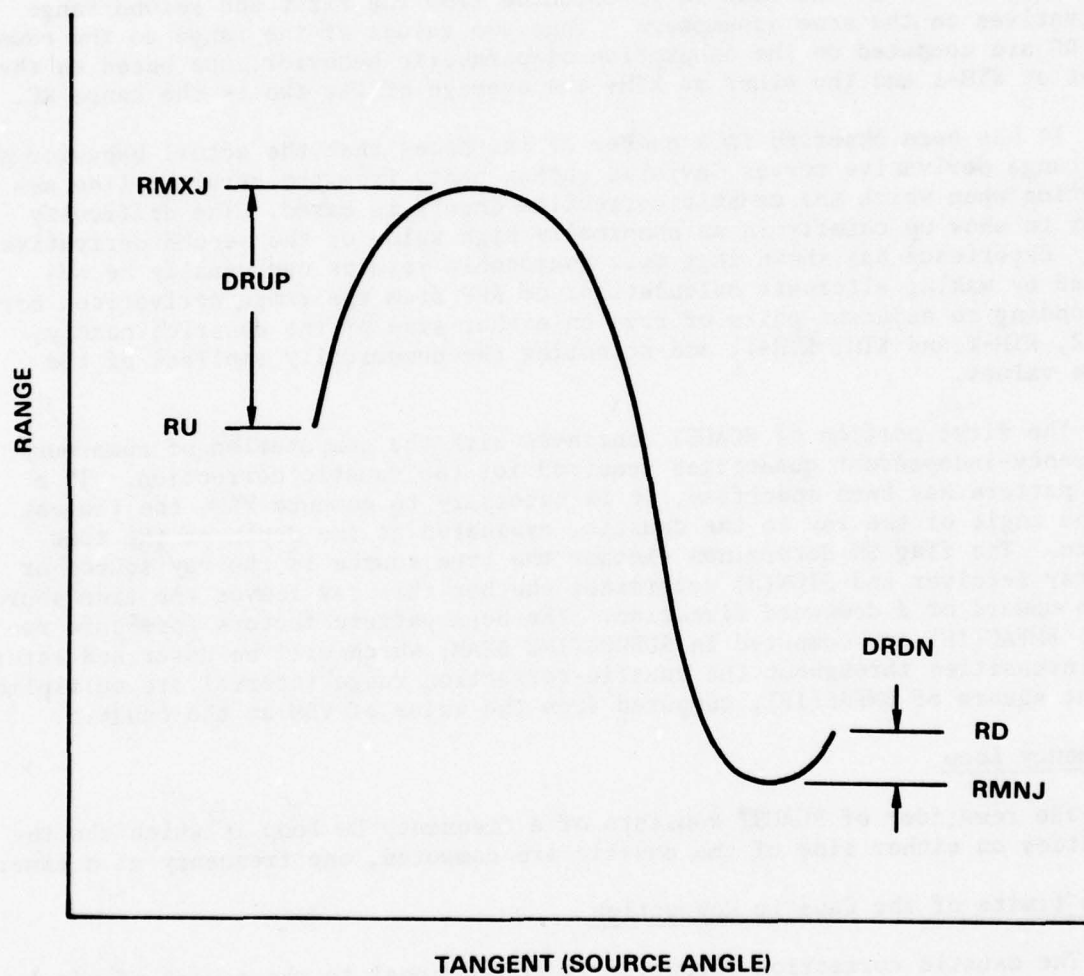


FIGURE 4 - Example of a Double-Caustic Curve



## SUBROUTINE RCAUST(KTH,J)

A derivation of the caustic correction formulas will be found in appendix H. The key parameter determining the intensity at a caustic is the second derivative of the range, RPP. In this program the derivative is taken with respect to VA. A tentative value of RPP is computed from the average slope of the first derivative between the points KTH-1 and KTH on either side of the caustic, the assumption being that in the vicinity of the caustic the range curve is parabolic and the first derivative linear. The value VAC of the tangent function VA at the caustic is computed from the first and second range derivatives on the same assumption. Then two values of the range to the caustic RC are computed on the assumption of parabolic behavior, one based on the point at KTH-1 and the other at KTH; the average of the two is the range RC.

It has been observed in a number of instances that the actual behavior of the range derivative curves deviates rather badly from the straight-line assumption upon which the caustic correction theory is based. The difficulty tends to show up chiefly in an abnormally high value of the second derivative RPP. Experience has shown that more reasonable results can usually be obtained by making alternate calculations of RPP from the range derivatives corresponding to adjacent pairs of rays on either side of the caustic, namely, KTH-2, KTH-1, and KTH, KTH+1, and selecting the numerically smallest of the three values.

The first portion of RCAUST continues with the computation of numerous frequency-independent quantities required for the caustic correction. If a beam pattern has been specified, it is necessary to compute VBM, the tangent of the angle of the ray to the caustic, evaluated at the depth of the true source. The flag SN determines whether the true source is the ray source or the ray receiver and SIGN(J) determines whether this ray leaves the true source in an upward or a downward direction. The beam pattern factors (pressure ratios) BMFAC(IF) are computed in SUBROUTINE BEAM, which will be described later. The intensities throughout the caustic-correction range interval are multiplied by the square of BMFAC(IF), computed from the value of VBM at the caustic.

Frequency Loop

The remainder of RCAUST consists of a frequency DO loop in which the intensities on either side of the caustic are computed, one frequency at a time.

Range Limits of the Caustic Correction

The caustic correction intensity is proportional to the square of the Airy function  $Ai(x)$ , the constant of proportionality being COEF2, a coefficient which varies inversely with the  $2/3$  power of RPP. The argument  $x$  of the Airy function is proportional to the horizontal distance from the caustic at the receiver depth. The constant of proportionality, COEF1, varies inversely with the  $1/3$  power of RPP. On the shadow side of the caustic, where  $x$  is positive,  $Ai(x)$  decays exponentially. An arbitrary limit of 3.5 is imposed on  $x$  as the point where the intensity has decayed to a negligible value. The range corresponding to this limiting value of  $x$  is RC1. For a minimum range caustic RC1 is less than RC. For a maximum range caustic it is greater.

On the illuminated side of the caustic, where  $x$  is negative, the Airy function is oscillatory. On this side, two limiting values are assigned to  $x$ . The first limit,  $x = -1.77$ , corresponds (in an ideal case of a parabolic range curve) to a point beyond the first maximum where the intensity is equal to the incoherent sum of the two rays which form the caustic. Ideally, termination of the caustic corrections at this limit assures continuity with the adjacent ray intensities. In working with actual velocity profiles, however, conditions are never ideal, and a discontinuity is usually found, with the caustic-correction intensity too high relative to the ray intensity. To smooth the discontinuity, the caustic-correction computations are extended out to a second limit,  $x = -2.2$ , which is close to the first zero of the Airy function. The sum of the two ray intensities is also computed in the overlap interval from  $-1.77$  to  $-2.2$  and continuity is assured by selecting the larger of the two intensities at each range point in the interval. The range corresponding to the first limit  $-1.77$  is RC2 and the range corresponding to the second limit  $-2.2$  is RC3. For a minimum range caustic RC2 and RC3 are larger than RC, and for a maximum range caustic they are smaller.

Range indices K1, K2, and K3 corresponding to RC1, RC2, and RC3 respectively are established such that the set of values of K from K1 to K2 inclusive contains all the range points between RC1 and RC2, and the set of values from (but not including) K2 to and including K3 contains all the range points between RC2 and RC3. As a minor refinement to the above, the value of K3 is altered, if necessary, so that the difference between K2 and K3 does not exceed 15.

### Intensities

The caustic-correction intensity, identified by the symbol TRM, consists of two factors, HK and FAC. HK is associated with the caustic itself and corresponds to the spreading loss factor in the ray intensity. FAC is an attenuation factor which includes the volume attenuation of the water, the bottom and surface losses, and the beam deviation loss. The beam loss is expressed in the form of an intensity ratio, which is the square of the pressure ratio BMFAC(IF). The intensities computed in the interval between K1 and K2 are added directly to the H(K,IF) array. The intensities computed in the overlap interval from K2 to K3 are stored temporarily in an array HC(KC,J,IF) for later comparison with ray intensities in the same interval. KC is a relative range index which begins at K2+1 for a minimum range caustic and at K3 for a maximum range caustic.

Since the limits K2 and K3 are needed in RAYSUM to define the interval over which the intensity comparisons are to be made, they are transmitted in COMMON through the variables KA(J,IF) respectively.

SUBROUTINE RAYSUM(IL) (CONTINUED)

### Parameters for Simplified Computations at Steep Angles

Upon the return from RCAUST a check is made to determine whether the current sector is the final one (IL = NL). If so, the parameters A0(J) and A1(J) are evaluated for each value of J. These parameters are required for the steep angle computations.

### Range Loop

The remainder of RAYSUM is contained within a range loop in which the index K runs from a lower limit K1 to the already determined upper limit KMX. In all sectors but the last, K1 has the normal value KMN. The last sector contains the steepest rays, extending out to 30 degrees. The minimum value of K for these rays is of course KMN. However, provision is made in the final sector for the computation by a simplified approximate method (appendix F) of the intensities at shorter ranges, where K runs from 1 to KMN-1. For this reason K1 is assigned a value of 1.

### The Index JJ

The presence of a minimum or maximum in the range curve leads to an additional complication besides the problem of caustics. The complication arises from the existence of two branches on the range curve, so that there are now two rays with different source angles propagating to the same range point. This situation is illustrated in figure 5, which shows a range curve containing a minimum. The shaded area surrounding the minimum point is the region unconditionally covered by the caustic correction. Above this is a second shaded area in which both caustic and ray intensities are computed. The unshaded area at the top is the region covered by ray computations only. For the purpose of the ray intensity computations the two branches of the curve are identified by different values of the index JJ. On the left branch, which has a negative slope, JJ is assigned a value 1, while on the right branch, which has a positive slope, the value is 2.

The presence of the two branches requires the setting up of three new arrays, VAKK(J,JJ) for the tangent function, RPKK(J,JJ) for the range derivative, and HTRM(J,JJ,IF) for the ray intensity. The VAKK and HTRM arrays are set to zero for each value of K at the beginning of the range loop.

### Ray Intensities

The ray intensity computations are performed within a DO loop over the ray type index J. At each specified range point the intensities are computed sequentially for each multipath ray type. Before continuing with a description of the program details, it will be useful to present a brief overview of the manner in which the ray intensities are computed.

The formula for the ray intensity consists of the product of a spreading loss factor and an attenuation factor which includes the losses due to surface and bottom reflections, volume attenuation of the water, and (where applicable) the beam pattern. The formula for the spreading loss factor is discussed in appendix I.

The range-dependent variables which enter into the formula for the intensity include VAK, the tangent of the source angle of the ray which propagates to the range K, VBK, the tangent of the angle at the receiver, RPK, the range derivative (actually RPKA, its magnitude), CVK, the ray vertex velocity (actually CVK2, its square), and BLK, the bottom loss. The primary variables are VAK, RPK, and BLK; CVK and VBK are derived from VAK. The letter K appearing in these variable names signifies that they pertain to the ray which propagates



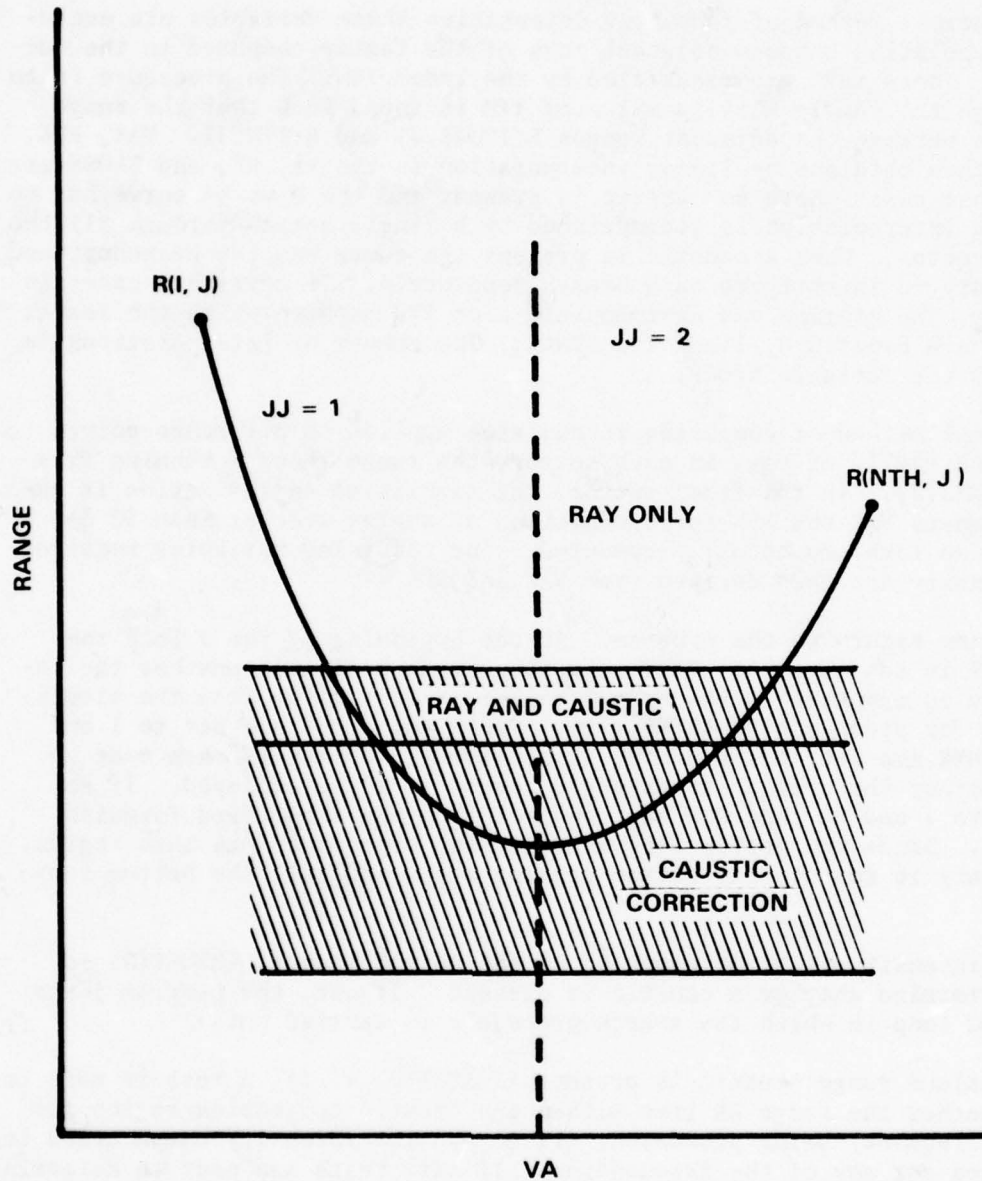


FIGURE 5 - Illustration of Index JJ

to the range point with index K, identified as RK. Since the ray has not actually been computed, it is necessary to evaluate the primary variables from the information at hand.

In the normal method of computing intensities these variables are evaluated by interpolating between adjacent rays of the family computed in the current sector. These rays are identified by the index ITH. The procedure is to search through the family until a value of ITH is found such that the range point RK lies between the adjacent ranges  $R(ITH-1, J)$  and  $R(ITH, J)$ . VAK, RPK, and BLK are then obtained by linear interpolation in the VA, RP, and BLOSS arrays. In those cases where no caustic is present and the R vs VA curve has no extremum, the interpolation is accomplished by a single search through all the rays of the sector. When a caustic is present the curve has two branches, and it is necessary to investigate each branch separately. To cover all cases in a single loop, the minimum and maximum values of ITH between which the search is conducted are denoted by ITHMN and ITHMX. The number of interpolations is controlled by the variable NLOOP.

The normal method of computing intensities applies to all range points covered by the family of rays in each sector, the range index K running from KMNJ(J) to KMXJ(J). In the final sector, the simplified approximation is employed to compute VAK and RPK for propagation at angles steeper than 30 degrees, where no rays are actually computed. The remaining variables required for the intensity are then derived from VAK and RPK.

Let us now return to the program. At the beginning of the J loop the variable KTYP is set to zero. KTYP is a flag which indicates whether the intensity is to be computed in the normal manner ( $KTYP = 0$ ) or from the simplified formula for steep angles ( $KTYP = 1$ ). ILOOP and NLOOP are set to 1 and ITHMN and ITHMX are set to 1 and NTH, respectively. A test is then made to determine whether the special steep-angle method is to be employed. If so, KTYP is set to 1 and VA and RPK are computed from the simplified formulas (appendix F). Since the bottom loss has not been precomputed in this region, it is necessary to compute the bottom grazing angle and call the bottom subroutine.

If the intensity is to be computed in the normal manner, ICAUST(J) is tested to determine whether a caustic is present. If not, the program jumps to the JTH DO loop in which the search procedure is carried out.

If a maximum range caustic is present ( $ICAUST(J) = -1$ ), a test is made to determine whether the range RK lies within the caustic correction region for the highest frequency being processed. If so, no ray intensity computation is to be computed for any of the frequencies. If not, tests are made to determine whether the range RK lies within either or both of the two branches of the range-VA curve. The branches will be labeled left and right on the assumption that the index ITH increases from 1 at the extreme left to NTH at the extreme right.

If RK lies only on the left branch, ITHMX is set to ICTH(J), the index of the ray adjacent to the caustic. ILOOP and NLOOP retain their original values of 1. If RK lies only on the right branch, ITHMN is set to ICTH(J) and ILOOP and NLOOP are both changed to 2 (indicating the second branch). If RK lies on

both branches, NLOOP is changed to 2 while ILOOP remains at 1, thereby signifying that there will be two searches and interpolations. ITHMX is set to ICTH(J) in preparation for the first search, which occurs on the left branch.

When a minimum range caustic is present, ICAUST(J) being positive, a similar procedure is followed, with appropriate interchanging of the "greater than" and "less than" symbols.

The search procedure is carried out in the JTH DO loop. When no caustic is present the rays are examined in increasing order from 1 to NTH. When a caustic is present, the search begins at ICTH(J) and proceeds outward toward the edges. After the proper value of ITH has been determined, the interpolations for VAK and RPK are performed.

The procedure from this point on applies to both the normal case and the special steep-angle case. The algebraic sign of the range derivative RPK is tested and the appropriate value of the parameter JJ is assigned, 1 if RPK is negative and 2 if positive. The value of VAK is stored in the appropriate bin of the VAKK(J,JJ) array and the absolute value RPKA is computed and stored in the RPKK(J,JJ) array. Finally, the spreading loss factor HK of the ray intensity is computed.

It now remains to compute the frequency-dependent factors. First, if a beam has been specified, the beam pressure ratios BMFAC(IF) are obtained by calling BEAM(1). The angular input from which these functions are computed is VBM, the tangent of the ray angle at the true source. VBM is obtained from VAK if the true source is located at the ray source (SN = +1.) and from VBK if the true source is located at the ray receiver (SN = -1.). SIGN(J) indicates whether the ray is up-going (+) or down-going (-). The values of BMFAC(IF) are stored in the BMF(J,JJ,IF) array for future use in the coherence computations. If no beam has been specified, these steps are bypassed.

The remainder of the intensity calculations are performed in a frequency DO loop. Before proceeding further it is necessary to ascertain whether the intensity corresponding to this particular range and frequency has already been calculated in SUBROUTINE RCAUST. A partial exclusion has already been made by comparing the range index K with the caustic correction limit KA(J,IFMAX) for the highest frequency. At lower frequencies the extent in range of the caustic-correction region increases. K is now compared with KA(J,IF) for the current frequency. If the test shows that the present range-frequency point has not been covered in RCAUST, the attenuation factor FAC is calculated. FAC is composed of the beam intensity ratio, which is the square of BMFAC(IF), and the antilogs of the bottom loss BLK, surface loss SLK, and the volume attenuation loss. If the special steep-angle method has been used (KTYP = 1), the bottom loss has already been computed. Otherwise (KTYP = 0) it is necessary to interpolate between the appropriate pair of rays in the BLOSS array. The resulting intensity is stored in the HTRM(J,JJ,IF) array.

At the conclusion of the intensity calculations a test of ILOOP is made to ascertain whether the procedure must be repeated for the other branch (if any) of the range-VA curve.



There remains yet one more item of business before completion of this section of RAYSUM - comparison of the ray intensities with the caustic-correction intensities in the overlap region. The comparison is made separately for each frequency. At the outset a test is made to ascertain whether the current range-frequency point lies within the transition region. If so, the intensities of the rays on the two branches,  $HTRM(J,1,IF)$  and  $HTRM(J,2,IF)$  are added to yield TRM and TRM is compared with the caustic intensity  $HC(KC,J,IF)$ . If  $HC(KC,J,IF)$  is the larger, it is added to the  $H(K,IF)$  array and both  $HTRM(J,1,IF)$  and  $HTRM(J,2,IF)$  are set to zero. If TRM is the larger, nothing is added to the  $H(K,IF)$  array at this point. Instead, the two HTRM values are retained for use in the final summation.

#### Ray Summation

The remainder of SUBROUTINE RAYSUM is devoted to the summation of the multipath ray intensities and computation of coherence factors. Since it is assumed that there is no coherence between rays belonging to different branches of the range-VA curve, rays corresponding to the two different values of JJ may be processed separately. For this reason the ray summation and coherence computations are made in a DO loop over JJ which extends to the end of the subroutine. Nested inside the JJ loop is a frequency loop which also extends to the end.

At the outset the coherence parameter ICOH and the variable TRM are initialized to zero. A zero value of ICOH signifies that no coherence exists at either end of the rays. It will later be set to 1 if coherence occurs only at the source end, to 2 if only at the receiver end, and to 3 if at both ends. The variable TRM will denote the resultant intensity of the current arrival order, ultimately to be added to the appropriate bin of the  $H(K,IF)$  array.

The intensities of the individual rays are then summed in a loop over the multipath index J to yield the resultant incoherent intensity HK of the arrival order. In the same loop are computed the number of contributing rays, ISUM, and the code parameter IND, which indicates exactly which rays are contributing. The J values of the contributing rays are arranged in IND in increasing order from left to right. It should be noted that it is not necessarily true that all of the NJ rays contribute to the multipath sum. It is possible that the receiver location may be reached by some of the rays but lie in a shadow zone of others. It is also possible that one or more of the rays may lie in a range interval covered by a caustic correction and therefore be excluded from the ray intensity computation.

At this point if ISUM is zero, the program jumps to the end of the frequency loop, since there are no contributions to the intensity. If incoherent summation has been requested ( $JCOH(IF) = 1$ ) or if the rays do not reach the surface ( $ISURF = 0$ ) or if there is only one contributing ray ( $ISUM = 1$ ), no further computations are necessary and the value of TRM (zero in this case) is augmented by HK in preparation for insertion into the final  $H(K,KF)$  array. If ISUM has a value of 2, 3, or 4, the program proceeds to ascertain whether coherence occurs and, if so, to compute the coherence factors.

### Coherence Computations

A discussion of the background of the coherence feature of PLRAY and a derivation of the formulas for the coherence factors is given in appendix J. Coherence factors are computed either for pairs or rays or for all four rays. In the case of two rays ( $ISUM = 2$ ), a test is made to determine whether  $ICOH$  is 0, 1, or 2. If it is zero there is no coherence and the resultant intensity is simply the incoherent sum. If  $ICOH = 1$ , the coherence factor is computed at the ray source end. If it is 2, the coherence factor is computed at the ray receiver end. If  $ISUM = 3$ , one pair of rays is selected and processed as in the two-ray case, and the third is added incoherently. If  $ISUM = 4$ ,  $ICOH$  may have a value of 0, 1, 2, or 3. If  $ICOH = 0$ , the resultant intensity is just the incoherent sum. If 1 or 2, the four rays are split into two pairs and each pair is processed as in the two-ray case. If  $ICOH = 3$ , the coherence factors are computed for the combined interference of all four rays. When two pairs of rays are to be processed, the loop in which the processing is done must be traversed twice. The parameter which controls the number of transits through the loop is  $NLOOP$ .

Consider now the case of two rays. If  $ISUM = 2$ , a check is made to see if the contributing rays are 1 and 4 or 2 and 3, in which case coherence is assumed not to occur. Otherwise, the average value of  $VAK$  for the two rays is computed, and from this the average vertex velocity  $CVK$  and the average tangent of the ray angle at the surface,  $V0$ . It is necessary at this point to determine whether the coherence is to be considered at the source or receiver end. The source end is selected for zero order arrivals if  $ZAA < ZBB$  and for first and higher order arrivals if the contributing rays are 1 and 2 or 3 and 4. Otherwise the receiver end is selected. The horizontal separation of the rays  $ZRCOH$  is computed from equation (J-1) of appendix J and computed with the threshold value  $RCOH$ . If the threshold is exceeded,  $ICOH$  remains zero and the incoherent sum applies. Otherwise  $ICOH$  is set to 1 if the coherence is at the source end and to  $ICOH + 2$  if the coherence is at the receiver end.  $NLOOP$  is set to 1.

The phase angle is now computed from equation (J-3), using  $ZAA$  or  $ZBB$  for the depth, according to the value of  $ICOH$ , and the coefficient

$$FRACTS = 2g_a g_b / (g_a^2 + g_b^2)$$

is also computed, where  $g_a$  and  $g_b$  are the beam pattern functions (pressure ratios) of the two rays, their FORTRAN equivalents being  $BMF1$  and  $BMF2$ . If no beam has been specified,  $FRACTS$  is given the value of 1. If "full" coherence ( $JCOH = 2$ ) has been requested, the coherence factor  $COFACS$  (second factor in equation (J-5)) is computed and multiplied by the incoherent sum  $HK$  to yield the resultant coherent intensity. However, the "full" coherence option is not recommended for normal use. If the semicoherent option ( $JCOH = 0$ ) has been specified, it is necessary to consider the sampling problem. The attenuation factor  $FRACTB$  ( $F$  in appendix J) is computed from equation (J-15) and compared with  $FRACTA$ , the absolute value of  $FRACTS$ . If  $FRACTB$  is smaller,  $FRACTS$  is replaced by  $FRACTB$  with the algebraic sign of  $FRACTS$  appended.

Consider next the case of three rays. If ISUM = 3, one of the three rays is treated incoherently and the other two rays are handled as in the two-ray case. The rules for selecting the rays are given in table J-I of appendix J. Prior to processing the pair of rays the intensity of the single ray must be subtracted from the three-ray sum and included instead in the variable TRM.

Consider finally the case of four rays. To determine the value of ICOH, the average of all four values of VAK is computed and, from this, the average CVK and V0. The average separation ZRCOH of the two pairs of rays at the source end is computed. If ZRCOH is less than the threshold value RCOH, ICOH is set to 1. Then the average separation of the two pairs of rays at the receiver end is similarly tested and if it is found to be less than RCOH, ICOH is increased by 2.

If coherence occurs only at one end or the other, there will be two pairs of rays to be processed, and NLOOP is set to 2. The first pair selected is 1 and 2 if ICOH = 1, and 1 and 3 if ICOH = 2. The average value of VAK and the consequent values of CVK and V0 are computed for these two rays, and the coherence factor and resultant coherent intensity are computed and added to TRM as in the two-ray case.

The second pair of rays is now selected, rays 3 and 4 if ICOH = 1 and rays 2 and 4 if ICOH = 2. These rays are processed in the same manner as the first pair and the resultant intensity is added to TRM, which now contains the combined intensity of all four rays.

When ICOH = 3, the resultant intensity is computed in accordance with equation (J-11) or (J-14). These formulas are identical except for an interchange of  $\phi_A$  and  $\phi_B$  (PHIA and PHIB) and for the method of calculating  $g_+$  and  $g_-$ . The parameter which controls the selection is SN. If SN = +1, the true source is located at the ray source and equation (J-11) applies. If SN = -1, the true source is located at the ray receiver and equation (J-14) applies. The first factor in these equations is computed and limited, if necessary, by the attenuation factor FRACTS in the same manner as in the two-ray case. The second factor is treated in a similar manner except that the coefficient involving the g functions is not present.

In all the cases considered the resultant intensity is stored in the variable TRM. At the end of the frequency loop, TRM is added to the contents of the appropriate range-frequency bin of the H(K,IF) array.

#### Termination of Computations Within the Sector

The criteria for limiting the number of ray cycles (NCYC) to be computed in a sector are contained in PLRAY and will be discussed below. One of the criteria provides for termination when the intensities of all the ray arrivals in the sector are less than  $10^{-13}$ , corresponding to a propagation loss greater than 130 db. The intensity test is performed in RAYSUM. The maximum intensity is denoted by the variable HLIM. Prior to the beginning of the big range loop HLIM is set to 0. Then as each intensity HTRM(J,JJ,IF) is computed, it is tested against HLIM and if it is larger, the value of HLIM is appropriately increased. At the end of the range loop HLIM contains the largest intensity of all the ray contributions in the sector. If HLIM is less than  $10^{-13}$  and



the current sector is the final one ( $IL = NL$ ), the cycle counter NCYC is set to 999.

PROGRAM PLRAY (CONTINUED)

#### Initialization of Ranges and Range Derivatives for First and Higher Order Arrivals

After completion of the processing of the zero order arrivals, initial values of  $R(ITH,J)$  and  $RP(ITH,J)$  are computed such that the proper values for the first and subsequent arrival orders may be obtained by successively adding the full cycle increments  $RCYC(ITH)$  and  $RPCYC(ITH)$ . Two different sets of formulas are required, depending upon the value of MJ. If  $MJ = 1$ , only two multipath ray types are involved; if  $MJ = 2$ , all four are present.

#### Arrival Order Loop; Termination of Computations in Sector

After initialization; the program enters an arrival order loop, the arrival order number being indicated by NCYC. At the beginning of the loop the ray ranges  $R(ITH,J)$  and range derivatives  $RP(ITH,J)$  are updated by adding the ray cycle terms  $RCYC(ITH)$  and  $RPCYC(ITH)$ . Before calling RAYSUM to process the current arrival order, a test is made to determine whether the computations should be terminated.

There are two criteria for terminating the computations. First, in all sectors except the last, no further computations are required if all of the ranges  $R(ITH,J)$  exceed the maximum receiver range RMAX. This criterion does not apply to the final sector, which includes bottom bounce propagation at steep angles beyond the sector boundary at 30 degrees. The criterion applied in the final sector is based on intensity.

During the updating of the ranges, the variable RM is set equal to the smallest of all the  $R(ITH,J)$ . If RM exceeds RMAX and the current sector is not the final one, the program jumps to the end of the sector loop, updates TH1, and begins to work on the next sector. On the other hand, if RM is less than RMAX or if this is the final sector, the algebraic signs  $SIGN(J)$  are evaluated and RAYSUM is called.

As mentioned previously, RAYSUM computes the maximum intensity HLIM of all the arrivals in the sector, and if HLIM is less than  $10^{-13}$  and the current sector is the final one, NCYC is set to 999. Upon the return from RAYSUM, PLRAY tests NCYC and if its value is 999, the computations are terminated and the program jumps out of the sector loop. Otherwise TH1 is updated and the processing of the next sector is begun.

#### Invocation of the Surface Duct Model

After the last sector has been processed, the flag ISD is checked. A nonzero value signifies that the surface duct model is required and SUBROUTINE SDUCT is called. A description of SDUCT is given below.

Propagation Loss

At the conclusion of the computations in RAYSUM, RCAUST, and SDUCT, the H(K,IF) array contains the resultant intensities at all the ranges and frequencies. If any of the range-frequency bins is empty, due to the absence of any rays propagating there, it is arbitrarily assigned a value HMIN, equivalent to a propagation loss of 999 db. The intensities in all bins are then converted to propagation loss and printed.

Propagation Loss Plot

The plot routine SUBROUTINE PLPLOT is called if IPLOT has been assigned a value of 1. This routine plots the propagation loss as a function of range.

## SUBROUTINE SDUCT

This subroutine, together with the auxiliary routine FUNCTION DEPFN, contains the surface duct model described in appendix K. The surface duct model actually consists of two models, a poor duct model and a good duct model. The poor duct model is applicable to ducts in which only the first mode of a normal mode solution contributes significantly to the propagation. The good duct model applies to ducts in which two or more modes must be considered.

At the beginning of SDUCT is a short section in which the beam pattern (if any) is computed. The beam pattern function is based on the source angle of the limiting ray to the bottom of the duct. Next, the cut-off frequency FMIN is computed. The cut-off frequency is a somewhat arbitrarily selected value such that at frequencies less than FMIN the duct is so leaky that it can be ignored. The remainder of the subroutine is enclosed within a frequency DO loop. All that follows, therefore, applies separately to each individual frequency.

At the beginning of the loop the frequency (denoted by FR in SDUCT) is tested against FMIN. If FR is less than FMIN, the program jumps to the end of the loop. If not, the next step is to compute the number of trapped modes EN (designated by the symbol  $n$  in appendix K), the leakage and surface scattering attenuation coefficients ALPH1 and ALPHS ( $\alpha_1$  and  $\alpha_S$ ), and the parameter V0 ( $\Delta c_0$ ). These quantities are needed for both the poor duct model and the good duct model. Then EN is tested against the limiting value of 1.5 to determine which of the two models is to be invoked.

Poor Duct Model

The first step is the computation of the depth functions US and UR. These are computed in FUNCTION DEPFN, described below. Their product is the complete depth function U. The remainder of this portion of the subroutine is a range loop (index K) in which the intensities are computed from two different formulas. HK is computed from the portion of the normal mode formula (K-16) exclusive of the attenuation factor, and HKK is computed from the spherical spreading formula (K-42), exclusive of the same attenuation factor. HK and HKK are compared and the larger of the two is chosen and multiplied by the attenuation and beam pattern factors. If the resulting intensity is greater than the lower limit HM, corresponding to 130 db propagation loss, it is added into the proper

bin of the H(K,IF) array. If it is less than HM, computations are terminated and the program jumps to the end of the range loop.

#### Good Duct Model

This portion of the subroutine begins with the computation of various range-independent quantities, including the attenuation coefficient ALPH2 ( $\alpha_2$  in appendix K), the constants CR and CS ( $K_R$  and  $K_S$ ), and several other constant factors involved in the intensity formulas. As in the case of the poor duct model, the intensities are computed as a function of range in a DO loop over the index K. The intensity HK is the portion of  $H_1$  exclusive of the sine factors in the cylindrical spreading formula (K-44); similarly, HKK is the portion of  $H_2$  exclusive of the same sine factors in the spherical spreading formula (K-45). HK and HKK are compared and the larger is selected and multiplied by the sine factors. If there is a beam pattern, the beam intensity factor, the square of BMFAC(IF), is also included. The resulting intensity is then checked against HM and this portion of the routine closes in the same manner as the poor duct portion.

#### FUNCTION DEPFN(Z)

Except for the difference in symbols, the coding of this routine is a straightforward application of the formulas developed in appendix K. To aid in correlating the FORTRAN with the algebra, several of the symbols are listed in table I.

#### SUBROUTINE BEAM(L)

This subroutine is divided into two parts. The first part, which is activated when BEAM is called from PLRAY with L = 0, calls for reading the beam inputs and printing them. The second part, which is activated when BEAM is called from RAYSUM, RCAUST, or SDUCT with L = 1, computes the beam pressure ratios BMFAC(IF) corresponding to the current value of the ray tangent VBM.

The first data card of part 1 contains a set of integers (NBF(IF), IF = 1, NF). NBF(IF) is the number of data points required to specify the beam pattern for the frequency F(IF), the maximum permissible number being 100. This is followed by two sets of cards for the first frequency, then two sets for the second frequency, and so on. The first set of cards contains the beam angles THETA(I) in increasing order from -90 degrees (downward) to +90 degrees (upward), 10 values per card. The second set contains the corresponding beam pressure ratios BM(I,IF) (pressure at angle  $\theta$  divided by pressure along beam axis). The pressure ratio must be a real number, positive if the pressure is in phase with the pressure along the axis, and negative if 180 degrees out of phase. There is no provision for complex ratios corresponding to phases other than 0 and 180 degrees. After the angles and beam functions for each frequency are read in, they are printed. Then the sines of the angles are computed and stored in an array SINE(I,IF).

The second portion of BEAM begins with the conversion of the input tangent function VBM to a sine function SBM. The output beam pressure ratios BMFAC(IF) are then computed in a frequency DO loop by interpolating in the SINE(I,IF) and BM(I,IF) tables.



T A B L E I  
 FORTRAN AND ALGEBRAIC SYMBOLS IN DEPFN

| <u>FORTRAN</u> | <u>Algebraic</u> |
|----------------|------------------|
| B1             | $a_{11}$         |
| C1             | $a_{21}$         |
| C2             | $a_{22}$         |
| C3             | $a_{23}$         |
| D1             | $a_{31}$         |
| D2             | $a_{32}$         |
| F              | $f$              |
| FF             | $f'$             |
| THETA          | $\phi(z)$        |
| UFAC           | $A$              |
| V              | $\Delta c$       |
| V0             | $\Delta c_0$     |
| V1             | $\Delta c_1$     |
| VZ             | $1 - z/z_T$      |
| ZA             | $z_a$            |
| ZAA            | $z_a'$           |
| Z1             | $z_1$            |
| Z2             | $z_2$            |

## COMPARISON WITH OTHER MODELS

To compare the performance of PLRAY with that of FACT, runs were made on both programs for a variety of environmental inputs. Runs were made both semicoherently and incoherently. As a check on the semicoherent runs of both programs, comparison runs were made also on a locally generated normal mode program called AP2 (appendix L), which is capable of accepting the same velocity profile and bottom loss inputs as the two ray programs.

The principal limitation of a normal mode solution in deep water is the large number of modes which must be computed. The number of modes required for a complete solution (in the practical sense) is approximately equal to the number of half wavelengths in the ocean depth. For example, if the ocean is 15,000 feet deep, the number of modes required at 100 Hz is approximately 600. Since AP2 is dimensioned only for 500 modes, there was a shortage of modes in several of the runs made to check PLRAY and FACT. Failure to compute the higher order modes is equivalent in ray theory to failure to compute the steeper rays. From the phase velocity of the highest order mode computed it is possible to compute the angle of the steepest equivalent ray, and from this the minimum range at which reliable bottom-bounce propagation is computed. In presenting the AP2 results the portion of each curve below the minimum reliable range has been omitted. It should be noted, however, that in the direct propagation zone at very short ranges, where according to ray theory the dominant contribution to the resultant intensity comes from shallow-angle rays which propagate directly from the source to the receiver, the absence of the higher order modes does not introduce appreciable error. For this reason, in many of the runs which suffer from a deficiency of modes there is a short interval (not shown in the plots) at the beginning of the range scale where reliable results are obtained, the extent of the interval depending upon the nature of the velocity profile and upon the source and receiver depths. The existence of this interval has proved helpful in a few instances in checking the performance of PLRAY and FACT.

To facilitate comparison with the semicoherent predictions of the two ray programs it is desirable to smooth out the rapid oscillations of the fully coherent normal mode curves. The smoothing was accomplished by means of a weighted sliding window containing nine terms. The losses were first converted to intensities. Then the average intensity  $\bar{I}_i$  at the  $i$ th range was computed from the formula

$$\bar{I}_i = (I_{i-4} + 2I_{i-3} + 3I_{i-2} + 4I_{i-1} + 5I_i + 4I_{i+1} + 3I_{i+2} + 2I_{i+3} + I_{i+4})/25$$

The average intensities were then converted back to db.\*

---

\* The actual procedure included one additional refinement. To compensate for the distortion introduced by inverse square spreading at short ranges, the intensities were multiplied by the squares of the respective ranges before averaging. The resulting average was then divided by the square of the central range of the window before conversion to db.

The results for the semicoherent runs are presented in the form of three plots. The PLRAY plot is shown at the top of the page, the FACT plot is in the center, and at the bottom the smoothed AP2 curve is superimposed on the plot of the original AP2 output.

Both semicoherent and incoherent runs were made with eight different deep-water velocity profiles selected from a number of different ocean areas. The eight profiles are shown in figures 6 through 13. The bottom loss curves associated with these profiles are shown in figures 14 through 19. The curves of profiles 1 and 6 (figures 14 and 18) are based on NAVAIRDEVCEC experimental measurements; the remainder are FNWC curves. It will be noted that the curves of figure 16 apply to profiles 3, 5, and 7.

The runs on the first seven profiles were carried out to a range of 100 kyd. The runs on profile 8 were limited to a range of 50 kyd.

The propagation loss plots for most of the runs can be divided into range intervals dominated by one or another of three different types of propagation. At short ranges is the direct propagation zone, dominated by rays which propagate directly from the source to the receiver either with no intervening vertices or with a single surface bounce or upper refractive vertex. These are the zero order arrivals. Included in this category also is surface duct propagation out to the range at which the ducted intensity drops to the level of the bottom-reflected intensity. In the second category are the convergence zones, formed by rays which are refracted in the deep ocean without striking the bottom. Most of the profiles lead to a single zone within the range interval of the computations. In the third category is the bottom-bounce region. To be precise, this category should be broken down into a series of regions, the first dominated by single bottom-bounce rays, the second by double bottom-bounce rays, and so on. In most of the runs the major portion of the plot consists of the first bottom-bounce region extending out to the convergence zone, with a small portion of the second region appearing beyond the zone.

#### PROFILE 1

The semicoherent predictions of PLRAY and FACT for Profile 1 are compared with AP2 in figure 20. The frequency is 105 Hz and the source and receiver depths are 80 and 100 feet. It will be noted that there is remarkably good agreement among all three models at all ranges. All the features of the interference pattern in the first bottom-bounce region out to 70 kyd are present. The agreement between PLRAY and AP2 here and in the relatively featureless second bottom-bounce region is excellent. FACT also agrees very well except for a discrepancy in the ranges at which the scallops appear in the first bottom-bounce region. The FACT range scale appears to be compressed by about 7 percent. This is a phenomenon which has been observed in many of the runs. Sometimes the compression (or expansion) relative to AP2 occurs with one of the ray models, sometimes with the other, sometimes with both. The cause of the scale distortion is not understood. A number of possible explanations have been examined but none have proved adequate. The problem will be discussed in a later section.

One curious feature of figure 20 is the appearance of a convergence zone at about 76 kyd in both the PLRAY and FACT curves, whereas there is not even a



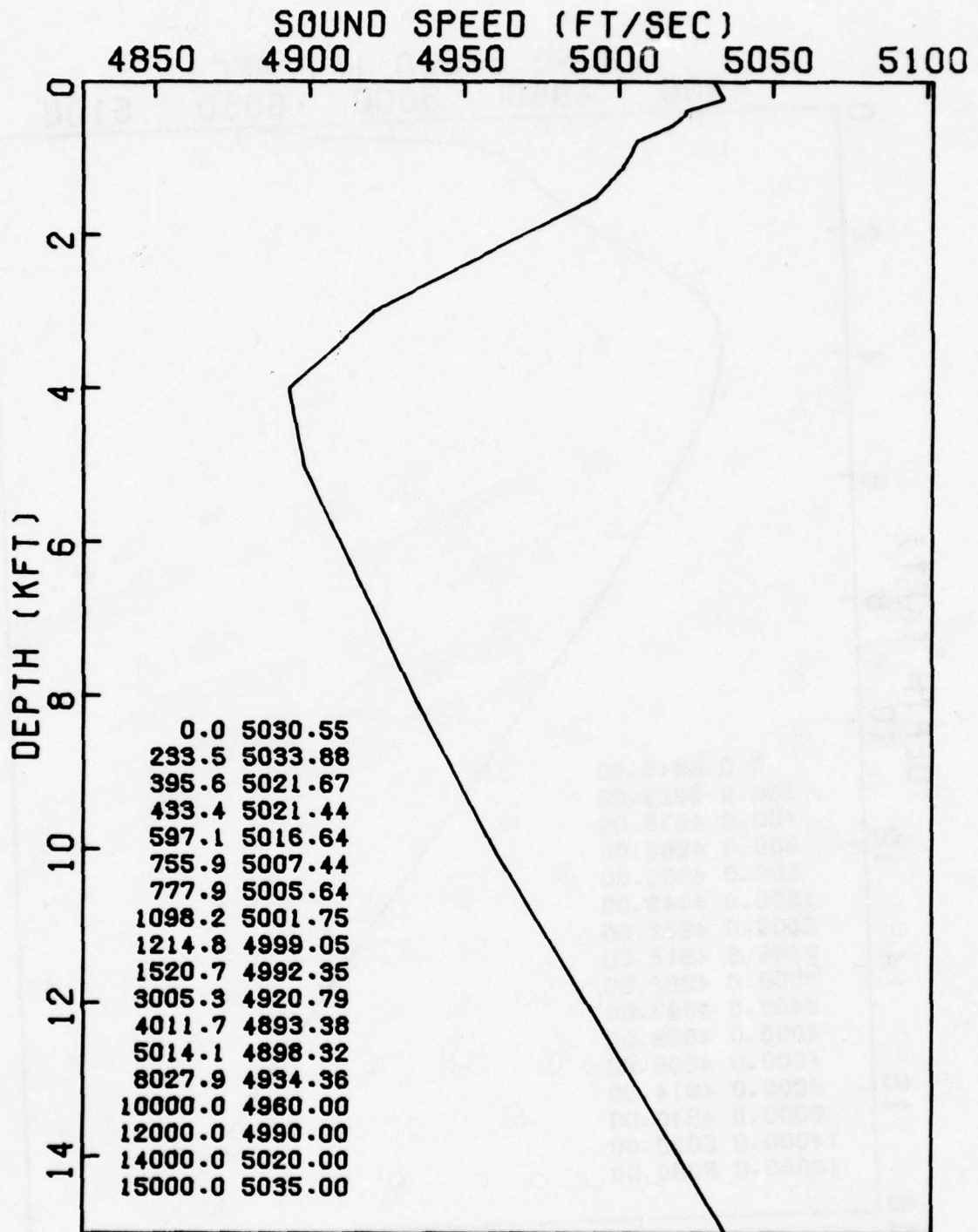


FIGURE 6 - Profile 1

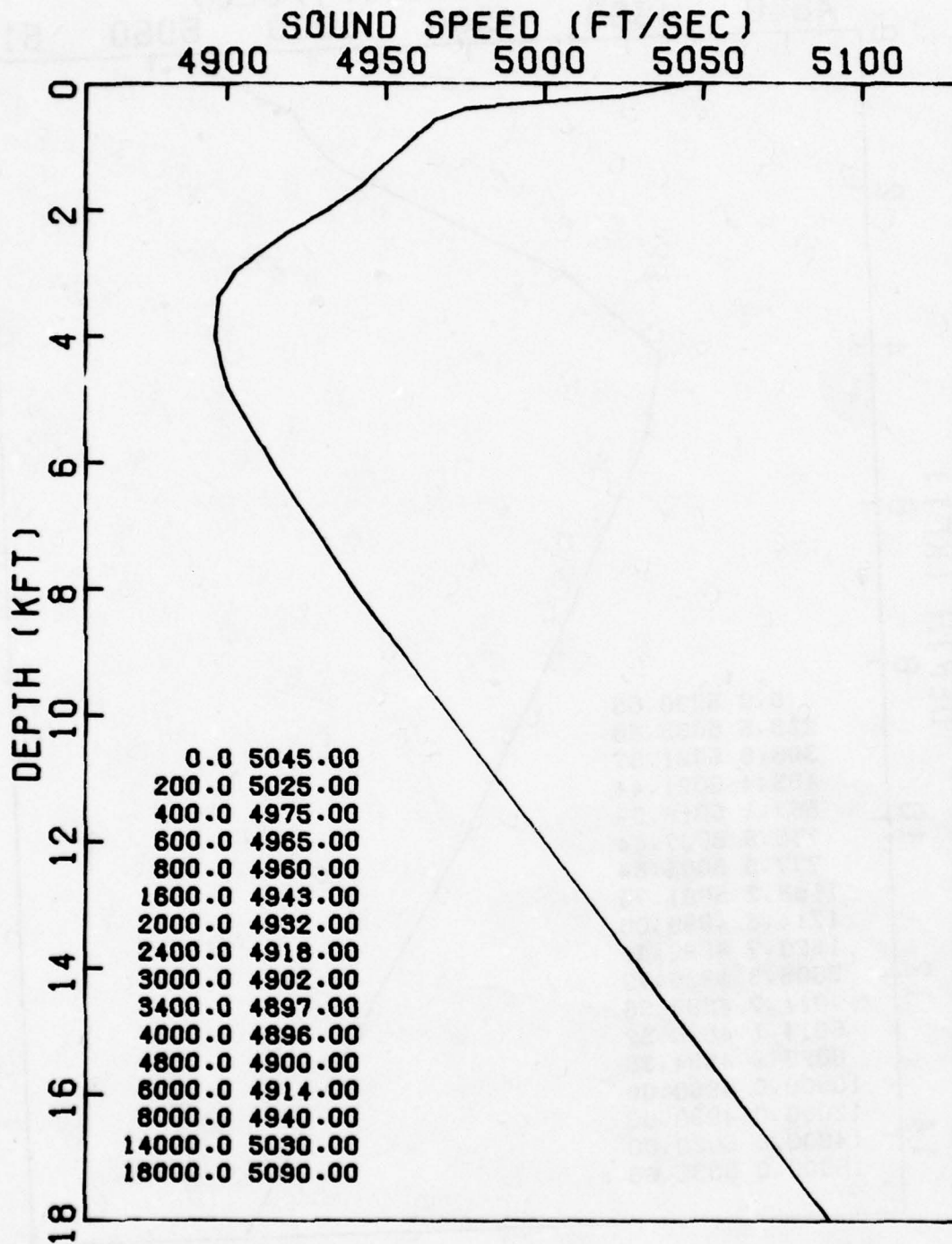


FIGURE 7 - Profile 2

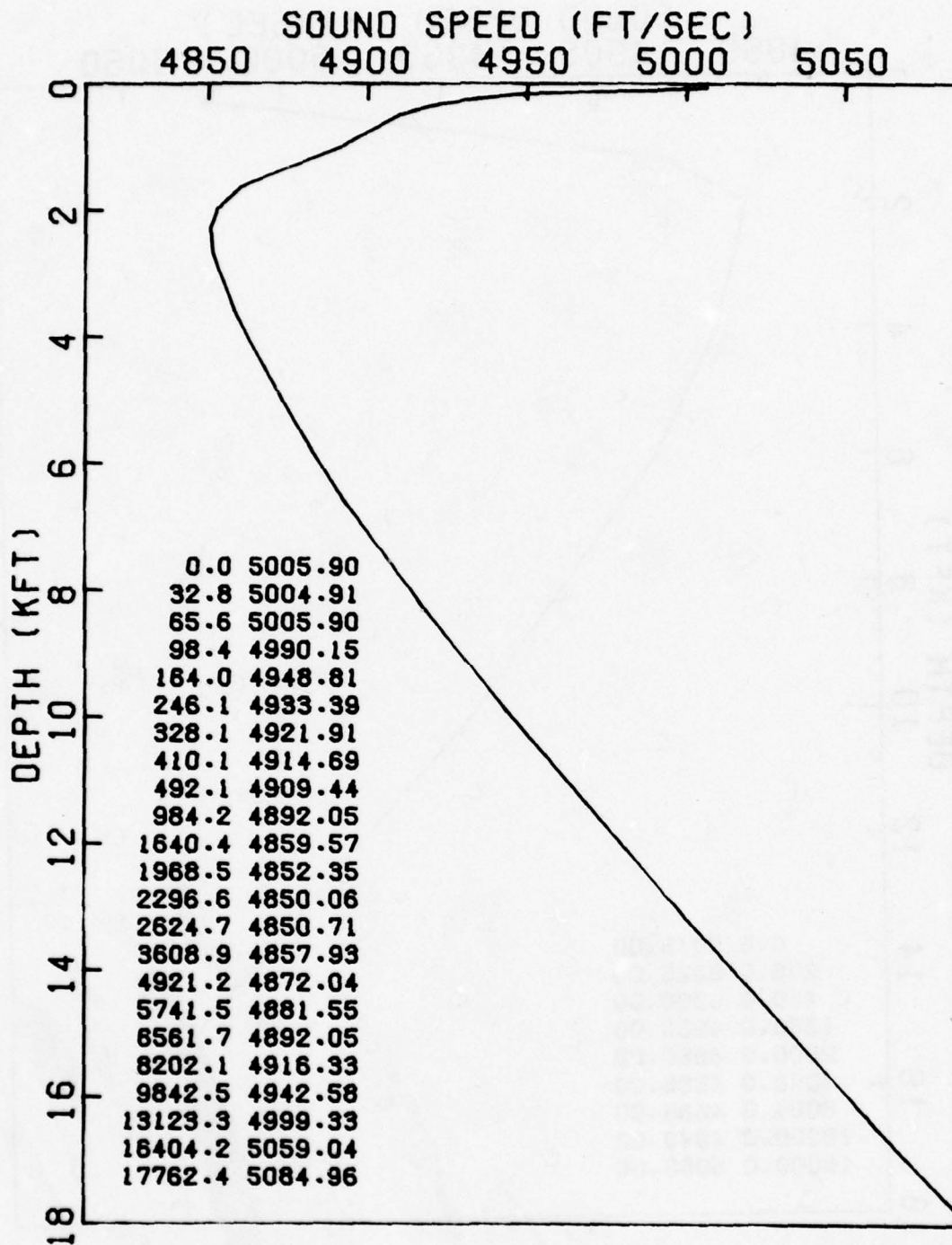


FIGURE 8 - Profile 3



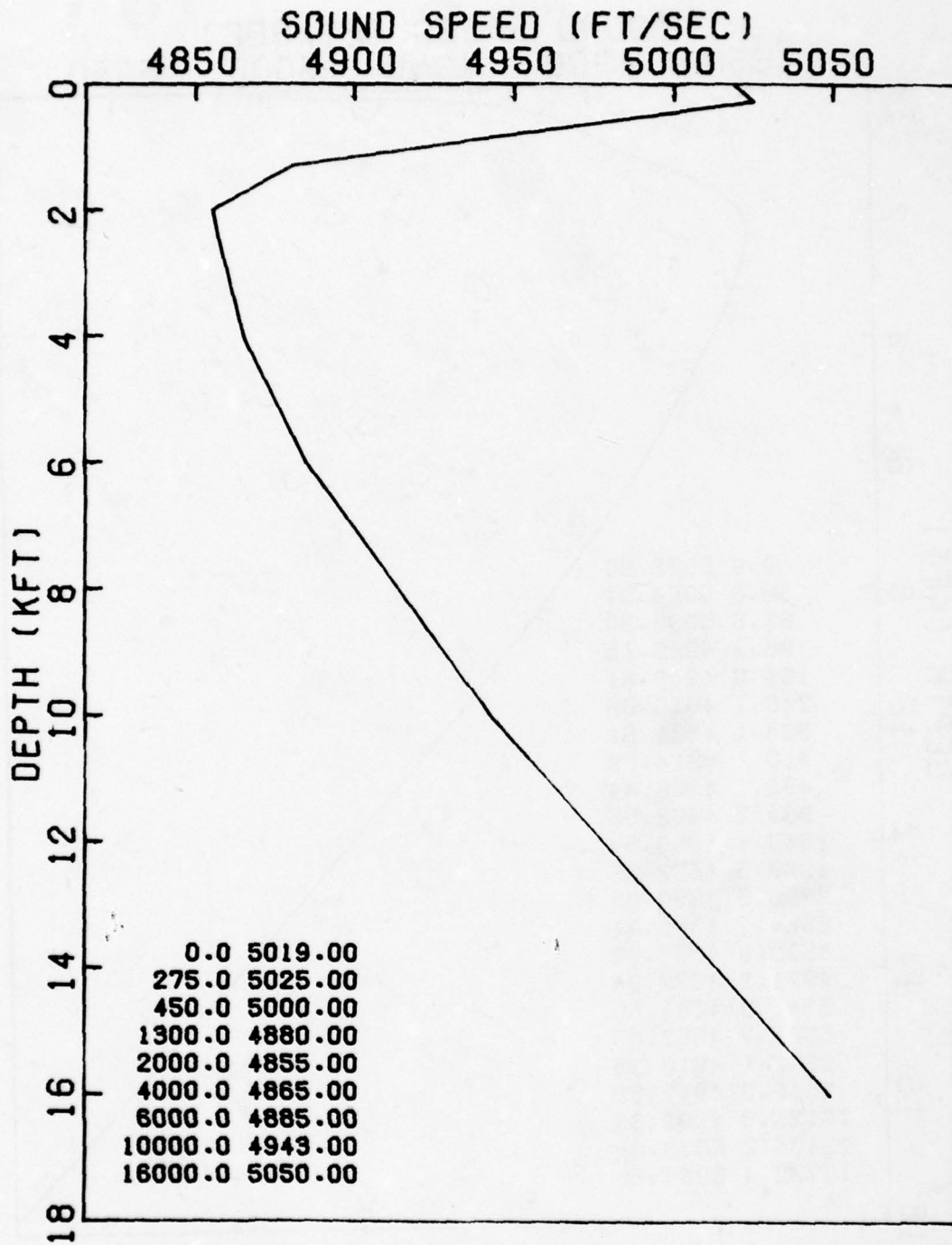


FIGURE 9 - Profile 4

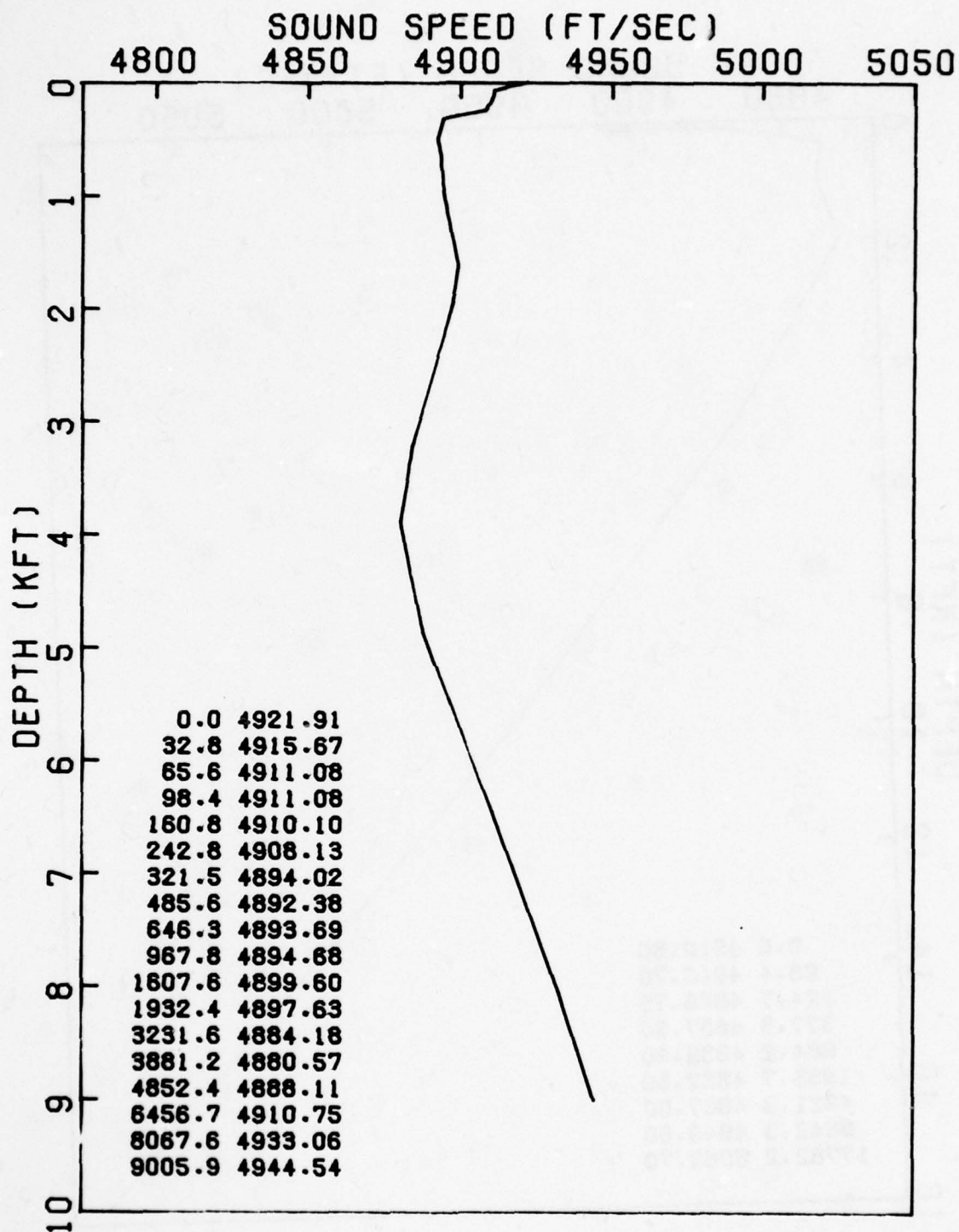


FIGURE 10 - Profile 5

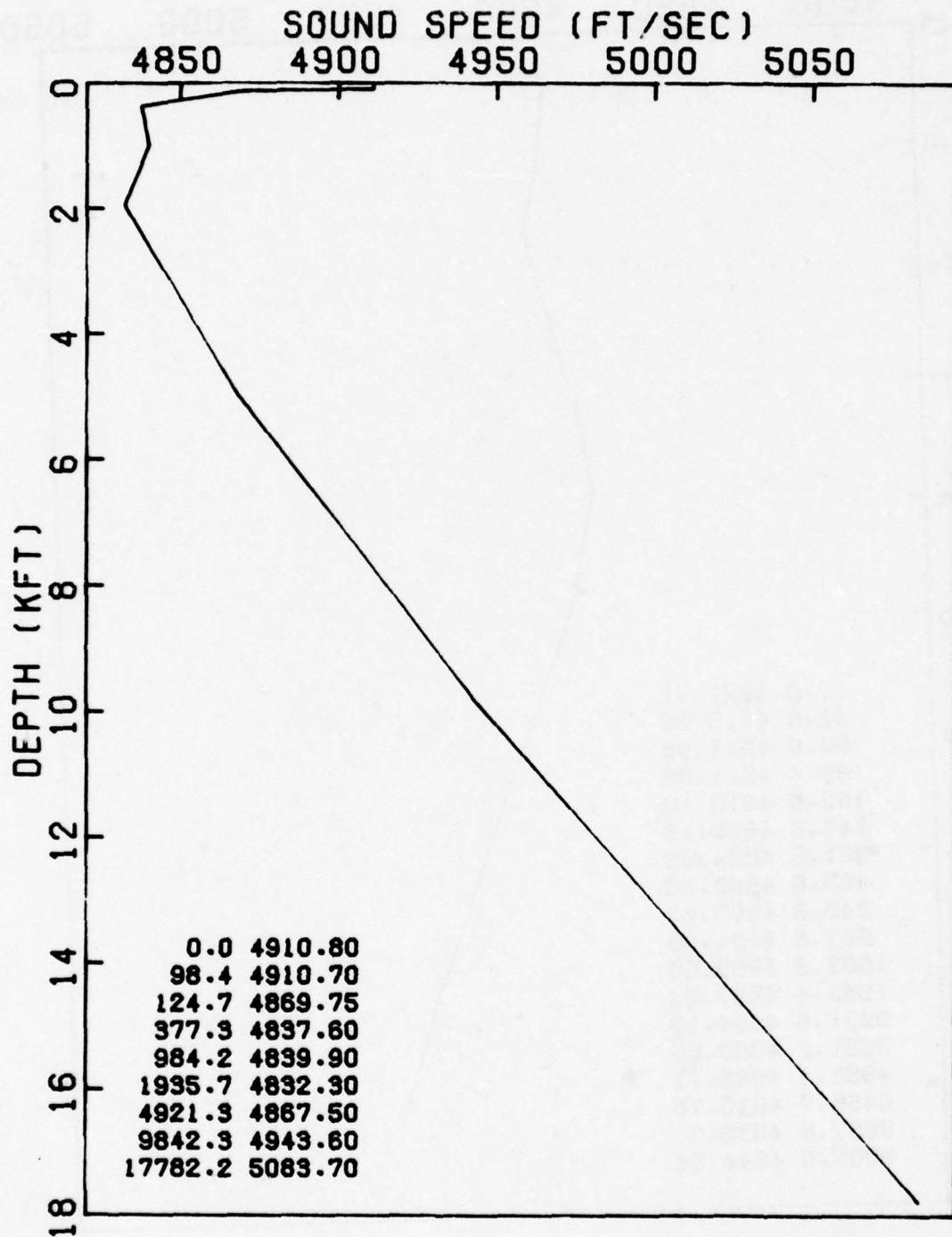


FIGURE 11 - Profile 6



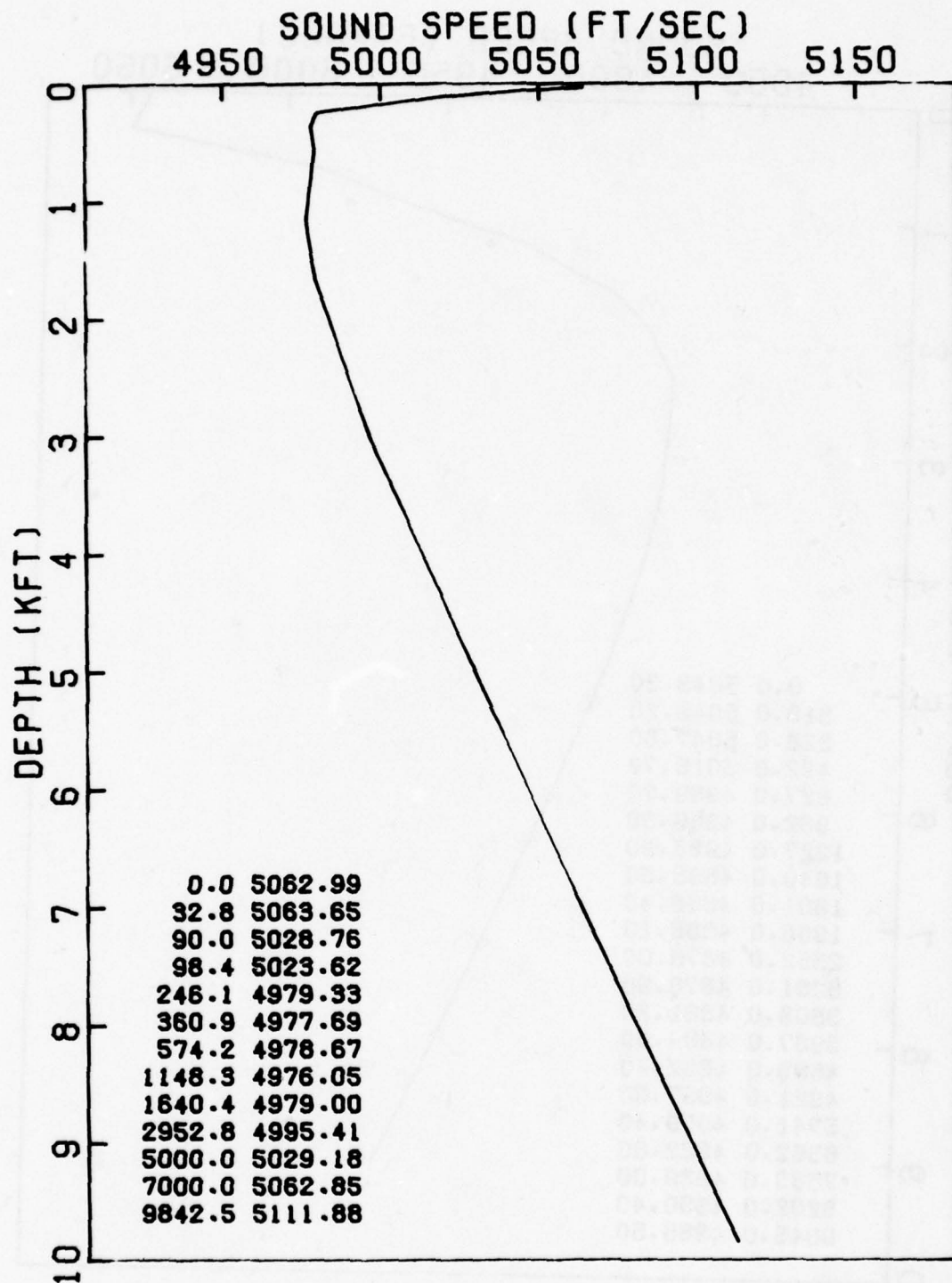


FIGURE 12 - Profile 7

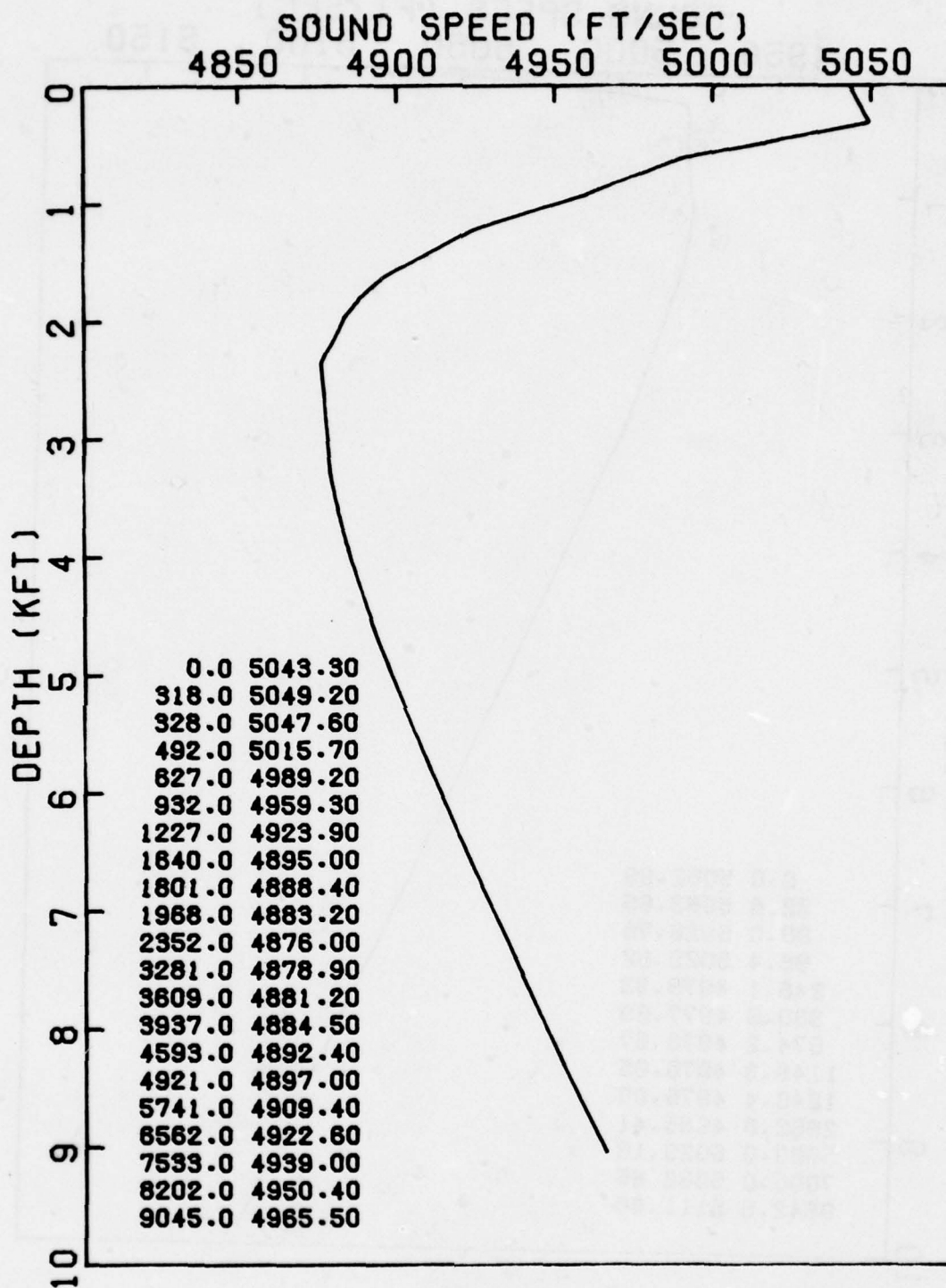


FIGURE 13 - Profile 8

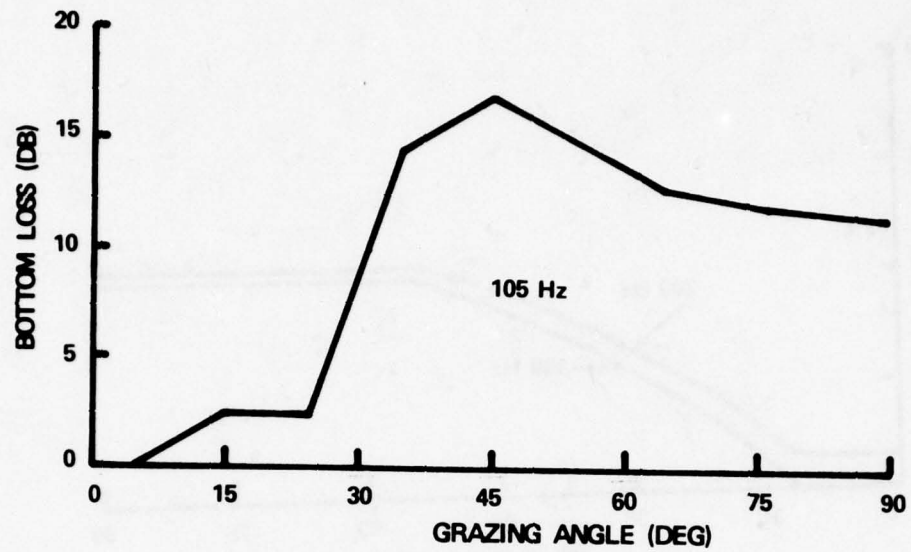


FIGURE 14 - Bottom Loss, Profile 1

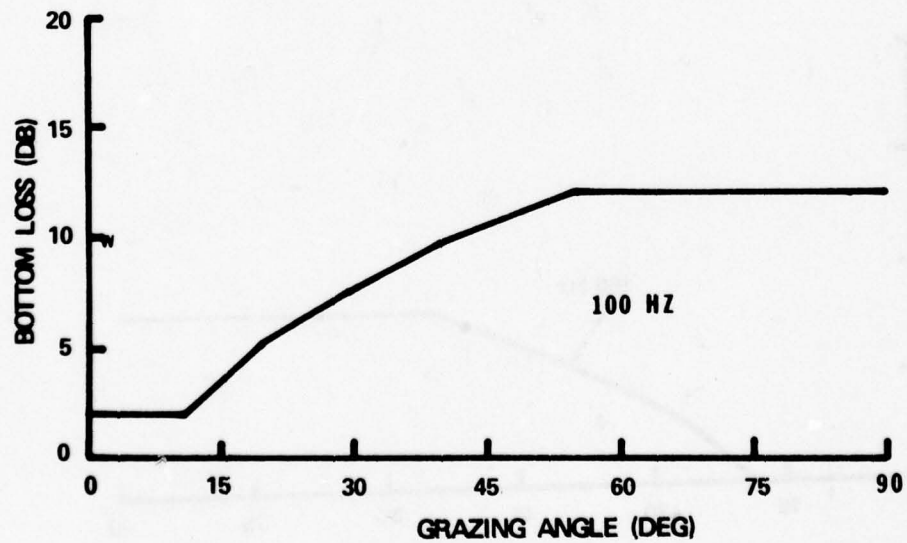


FIGURE 15 - Bottom Loss, Profile 2



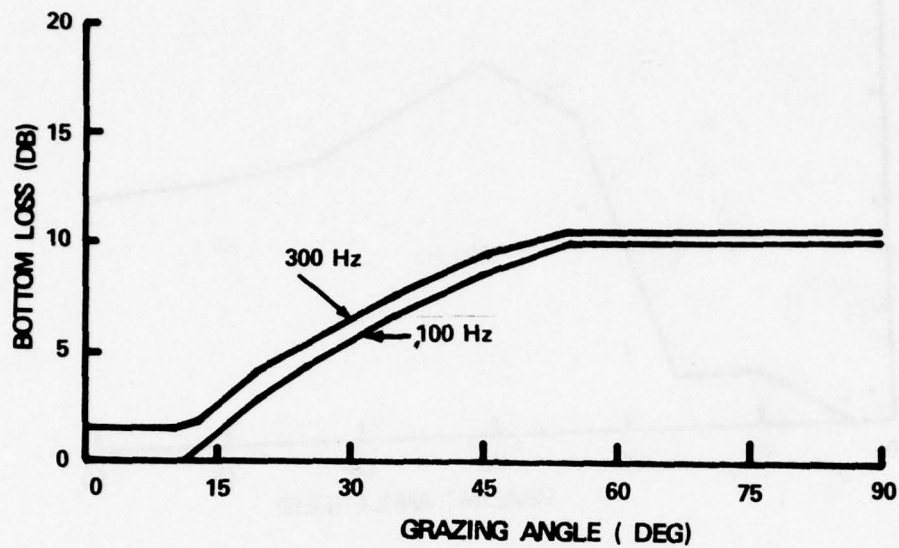


FIGURE 16 - Bottom Loss, Profiles 3, 5, and 7

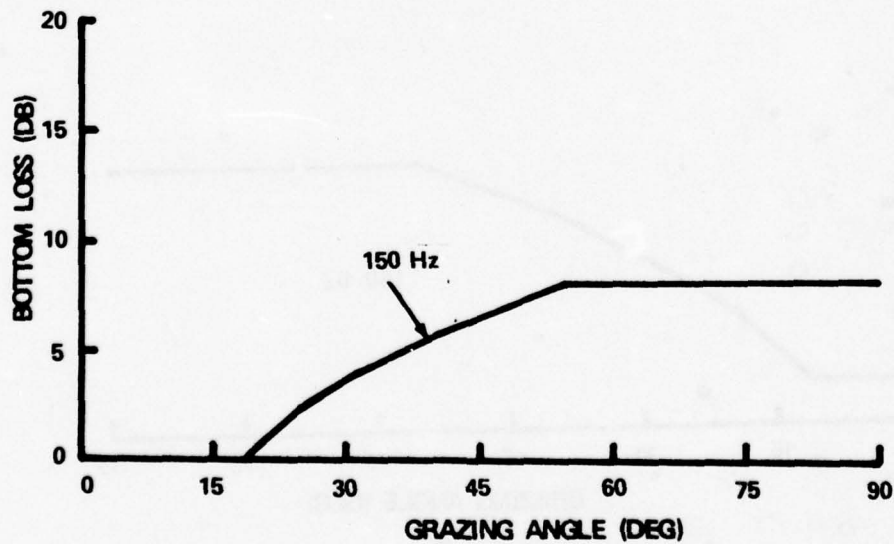


FIGURE 17 - Bottom Loss, Profile 4

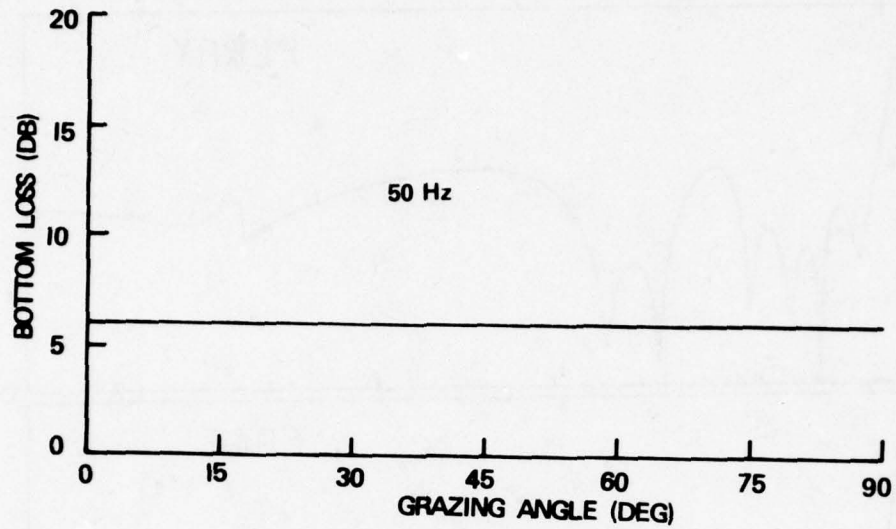


FIGURE 18 - Bottom Loss, Profile 6

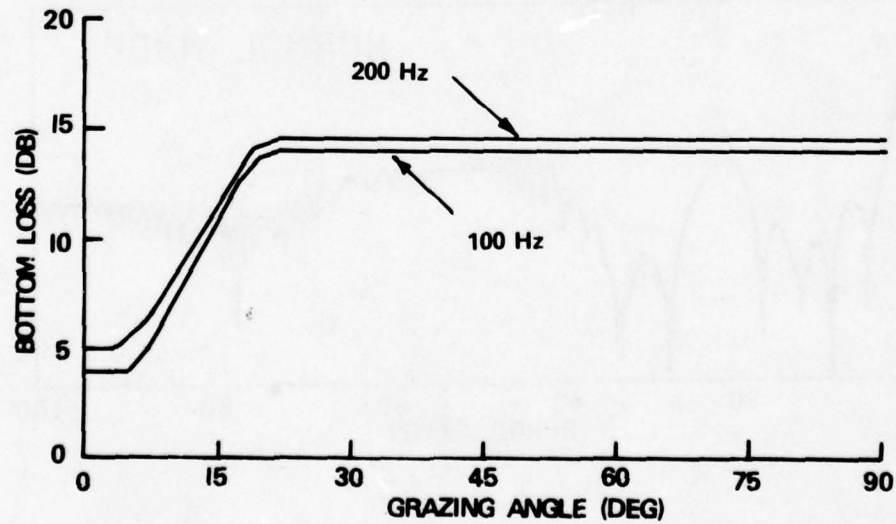


FIGURE 19 - Bottom Loss, Profile 8

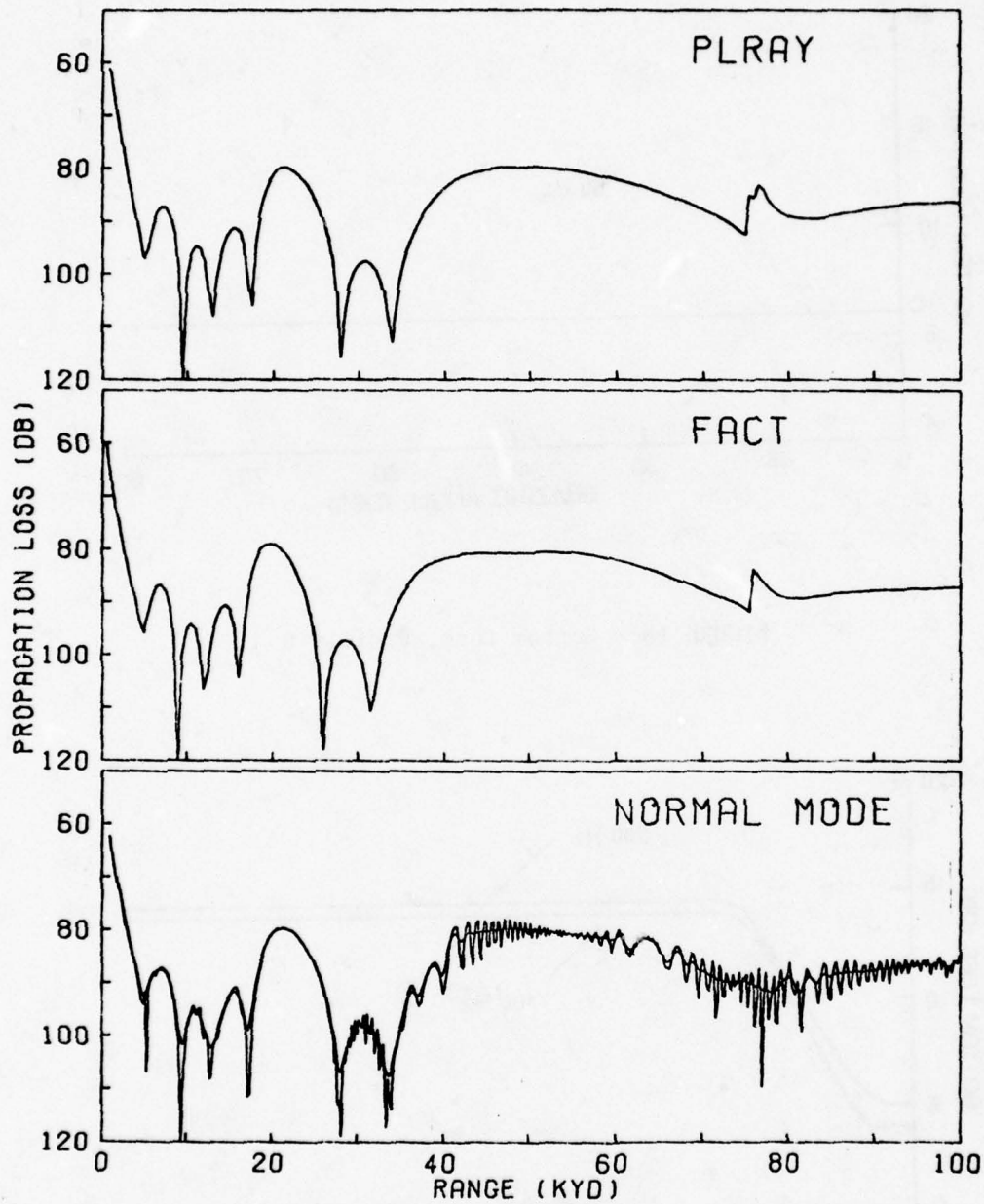


FIGURE 20 - Semicoherent Propagation Loss, Profile 1; Frequency 105 Hz, Source Depth 80 Ft, Receiver Depth 100 Ft



suggestion of such a phenomenon in the AP2 curve. The presence of the zone in the ray program outputs is an example of a fundamental error of ray theory and will be discussed later.

The incoherent predictions of PLRAY and FACT are shown in figure 21. Except for a minor difference in the convergence zone, the two curves are virtually identical. The difference in the convergence zones is immaterial since normal mode theory predicts that no zone exists. The dip in both curves at about 10 kyd is due to the sharp rise in the bottom loss curve around 30 degrees (figure 14). The compression of the FACT range scale relative to PLRAY, noted previously, is also visible in the vicinity of the dip.

## PROFILE 2

Two sets of runs were made on Profile 2, both at a frequency of 100 Hz and a source depth of 300 feet. The semicoherent results for the first set of runs, in which the receiver was located at a depth of 60 feet, are shown in figure 22. In this case the features of the interference pattern in both bottom-bounce regions are reproduced in all three plots, but the agreement is not as close as in the run on Profile 1. Here the range scales of both PLRAY and FACT are altered relative to AP2, the scale of PLRAY being slightly compressed and the scale of FACT expanded. The differences in range become very large in the second bottom-bounce region.

All three models predict a convergence zone with two peaks. The agreement on the second peak is fairly good, PLRAY being about 2 db too high and FACT about 2 db too low. However, the agreement on the first peak is poor, the normal mode curve being some 6 to 7 db below both ray curves.

In the direct propagation zone PLRAY and FACT agree extremely well with each other, but both deviate from AP2, which shows a considerably more rapid increase in loss in the interval between 1 and 2 kyd.\*

The incoherent predictions of PLRAY and FACT, plotted in figure 23, are almost identical everywhere except in the convergence zone. It is curious that while there is little difference in the PLRAY convergence zone between the semicoherent and incoherent runs, there is considerable difference in the FACT runs. The first peak is higher and the dip between the two peaks is completely filled.

The second set of semicoherent runs, made for a receiver depth of 200 feet, are plotted in figure 24. Here the agreement among the three models is slightly better than in the runs at 60 feet. In the bottom-bounce regions PLRAY and FACT yield roughly comparable results relative to AP2, except that the large dip just before the convergence zone is absent in the FACT curve and the heights of some of the peaks do not agree as well. FACT shows better

---

\* This is one of the runs for which the number of modes required (approximately 725) is in excess of the available 500. The AP2 output is not plotted in figure 22 at ranges less than the minimum reliable range of 12 kyd. However, examination of the original computer output indicates that reliable results are obtained in the direct zone out to approximately 2 kyd.

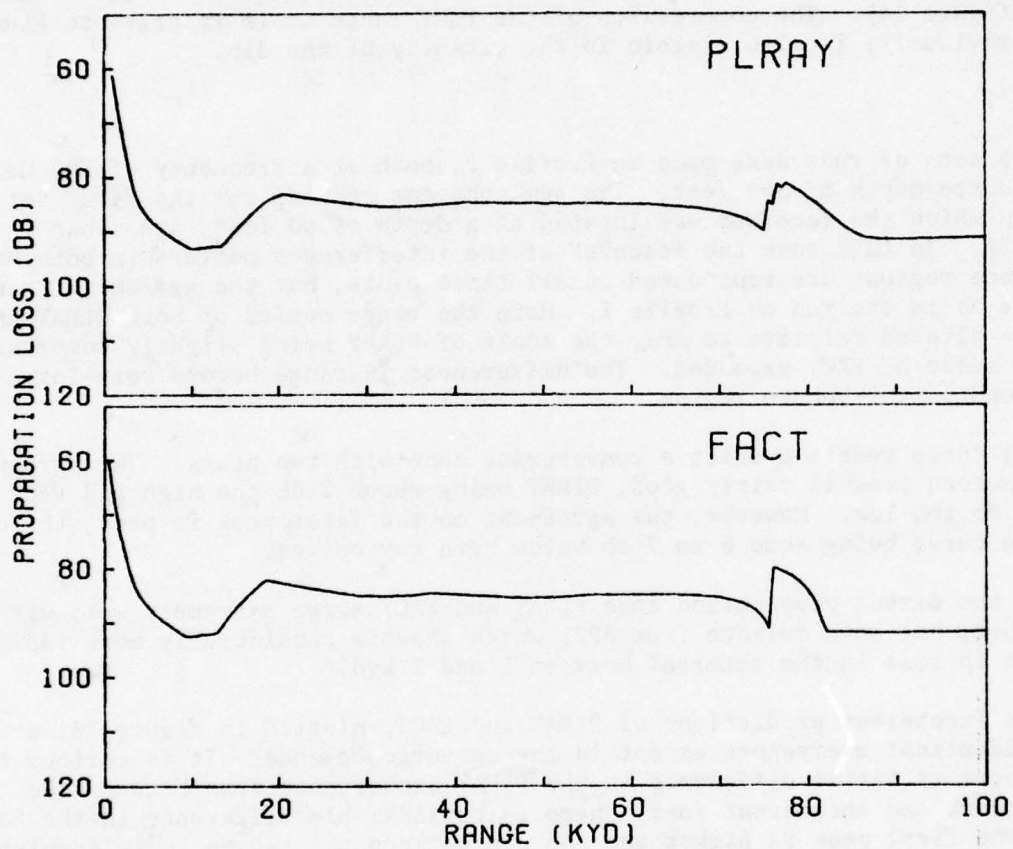


FIGURE 21 - Incoherent Propagation Loss, Profile 1; Frequency 105 Hz, Source Depth 80 Ft, Receiver Depth 100 Ft

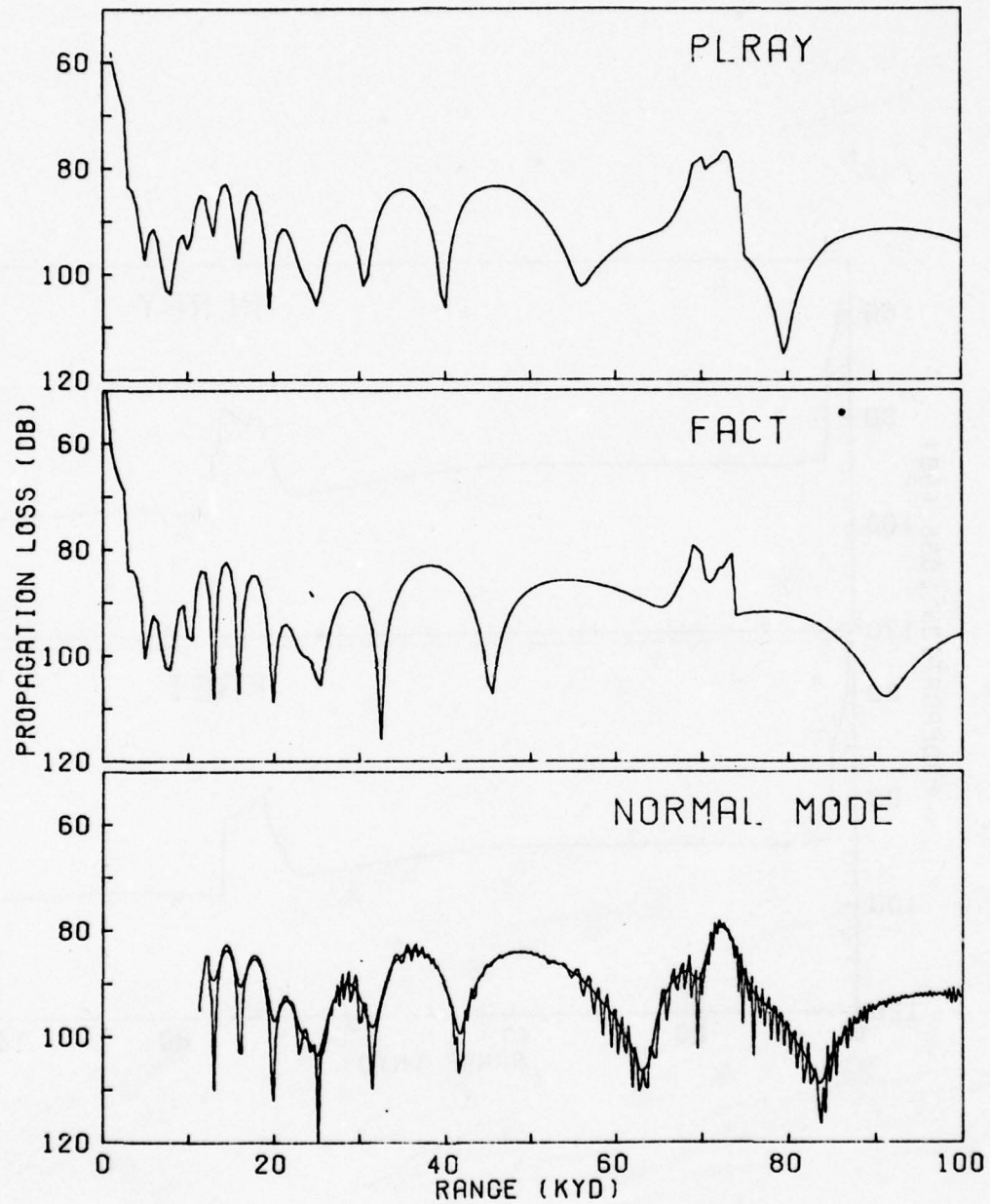


FIGURE 22 - Semicoherent Propagation Loss, Profile 2; Frequency 100 Hz, Source Depth 300 Ft, Receiver Depth 60 Ft



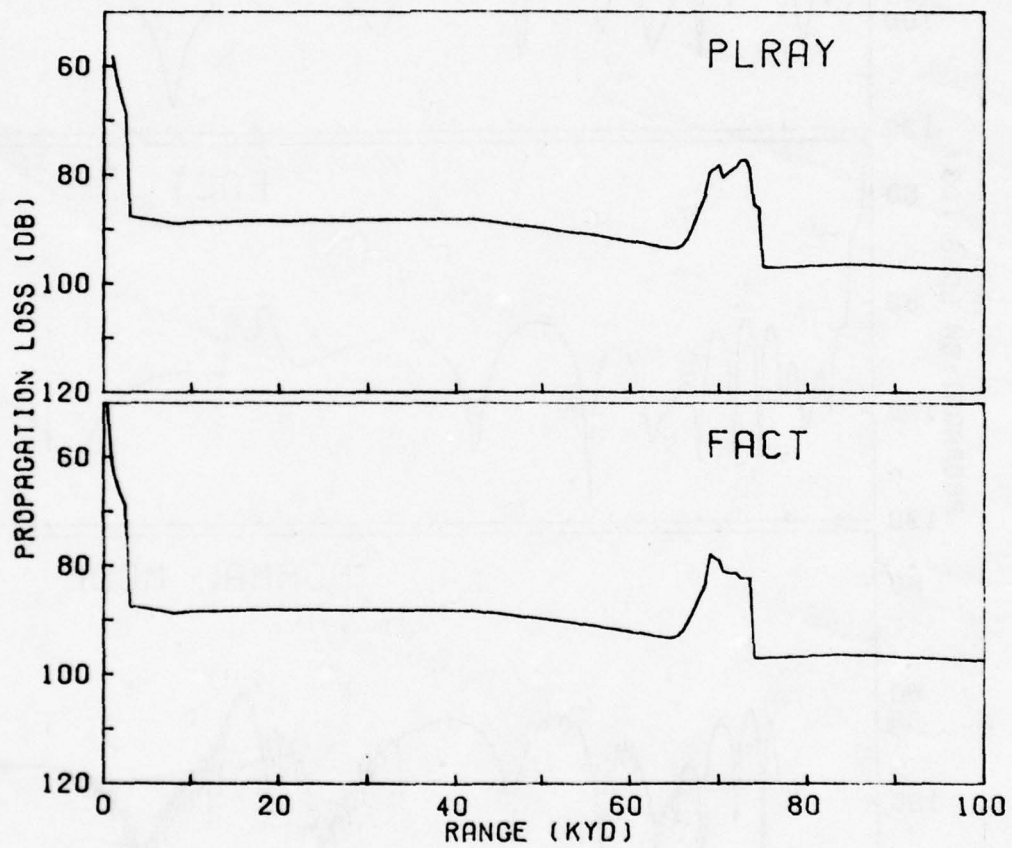


FIGURE 23 - Incoherent Propagation Loss, Profile 2; Frequency 100 Hz, Source Depth 300 Ft, Receiver Depth 60 Ft

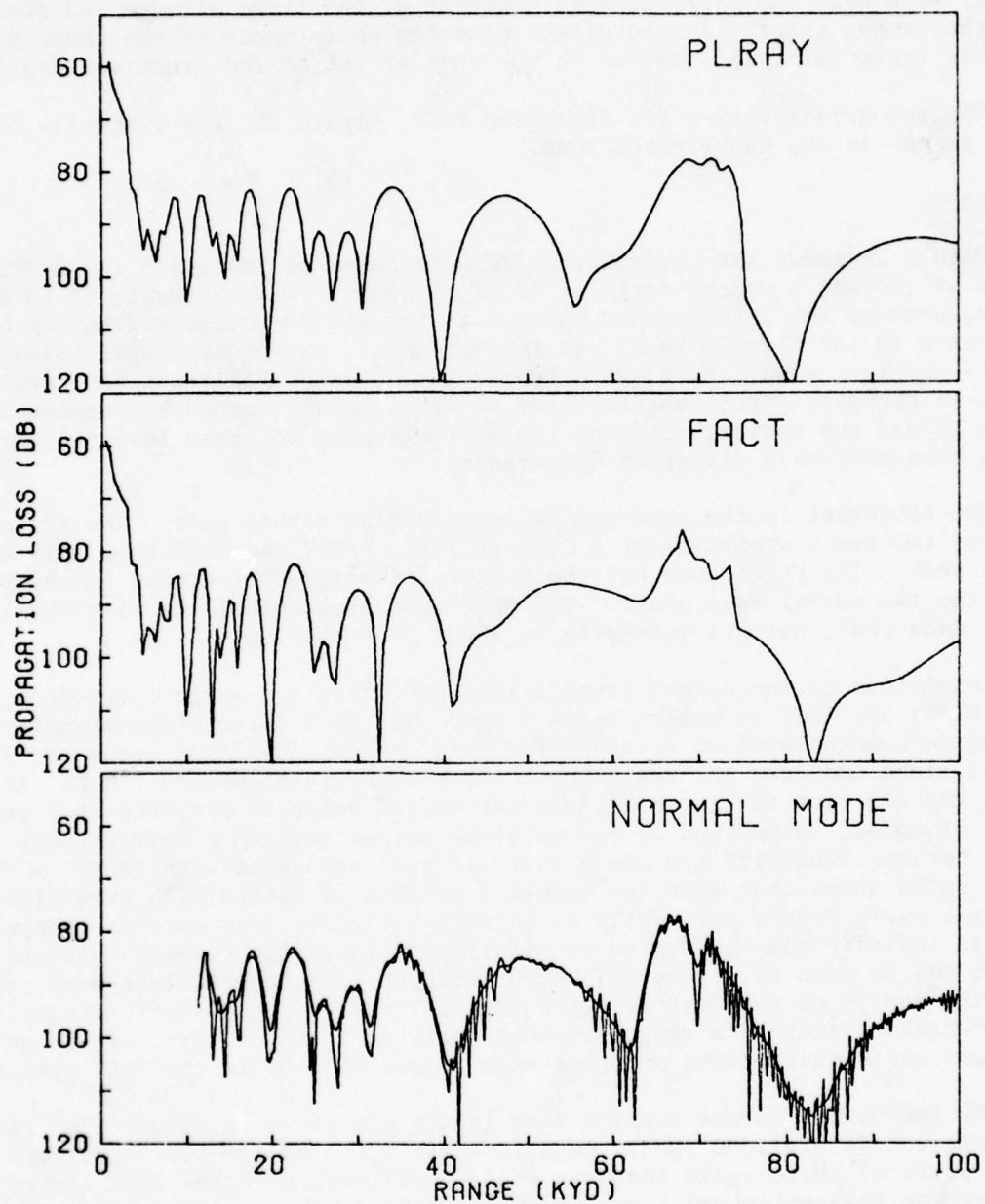


FIGURE 24 - Semicoherent Propagation Loss, Profile 2; Frequency 100 Hz, Source Depth 300 Ft, Receiver Depth 200 Ft

agreement in the second bottom-bounce region than PLRAY. The range scale distortions of the interference patterns are in the same direction as in figure 22, though somewhat smaller in magnitude. In the zone itself FACT agrees closely with AP2; the PLRAY zone is centered at too large a range and does not have the proper shape. In the direct zone the performance of the three programs is essentially the same as in the runs at the 60-foot receiver depth.

The incoherent curves for PLRAY and FACT, figure 25, are virtually identical except in the convergence zone.

### PROFILE 3

Figure 26 shows the semicoherent results based on Profile 3 for a frequency of 100 Hz, a source depth of 300 feet, and a receiver depth of 60 feet. The features of the interference pattern in the bottom-bounce region can be recognized in all three curves, but the agreement, except at ranges below 20 kyd, is not very good. Here again the range scales of PLRAY and FACT are distorted in opposite directions relative to AP2. In the second bottom-bounce region beyond the convergence zone the distortion is so great that the three curves have radically different appearances.

The agreement in the convergence zone is also rather poor. The AP2 zone exhibits two peaks separated by a deep valley. PLRAY and FACT show only a single peak. The PLRAY zone has the proper intensity, but occurs midway between the two normal mode peaks. The FACT zone lies coincident with the second normal mode peak, but its intensity is about 3 db too low.

Inspection of the direct propagation zone reveals a large discrepancy between PLRAY and FACT at ranges below 7 kyd. The FACT curve drops abruptly to the bottom-bounce level at a range of 2 kyd, whereas the PLRAY curve has a gradual slope and does not reach the bottom-bounce level before 7 kyd. Although the AP2 plot of figure 26 does not extend below 12 kyd, due to a deficiency of modes, inspection of the original output reveals a narrow range interval between 1 and 1.5 kyd where there is good agreement with FACT. A check of ray paths shows that when the velocity profile is fitted with curvilinear segments, as in PLRAY, the family of surface-reflected rays extends theoretically to infinity and the region of significant intensity extends to about 7 kyd, as may be seen in figure 26. When straight-line segments are used, as in FACT, the family of surface-reflected rays is confined to a finite range interval which extends to a range somewhere between 5 and 5.5 kyd. It is not clear why the contributions of these rays do not show up in the FACT output.

The incoherent curves for the same inputs are shown in figure 27. As has been observed in previous runs, the agreement in the bottom-bounce regions is almost perfect. Here again there is a large difference in the FACT convergence zone between the semicoherent run and the incoherent run. In the incoherent run the zone begins at a shorter range, the first peak is higher, and the second peak has disappeared. In PLRAY the zones are virtually identical. In the direct propagation zone the discrepancy noted above is clearly visible.

A second set of runs on Profile 3 was made at a receiver depth of 1000 feet, the semicoherent runs being plotted in figure 28. There is fair agreement among the three curves at short ranges, but the agreement deteriorates



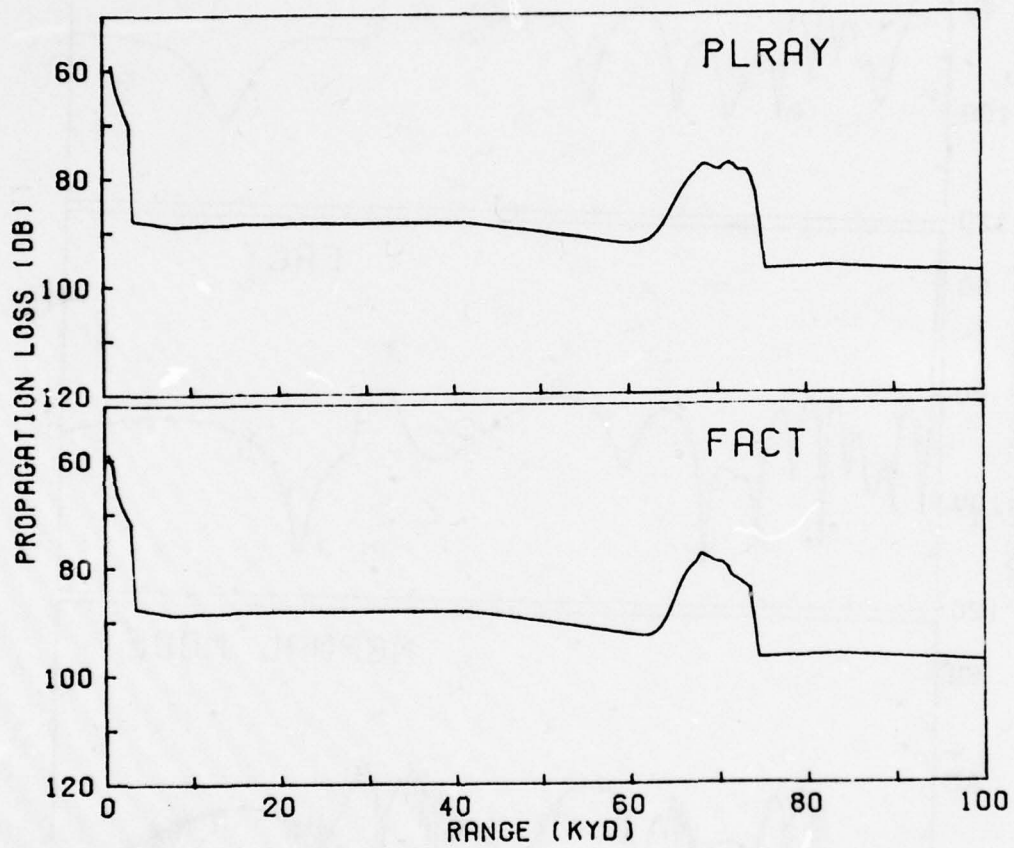


FIGURE 25 - Incoherent Propagation Loss, Profile 2; Frequency 100 Hz, Source Depth 300 Ft, Receiver Depth 200 Ft

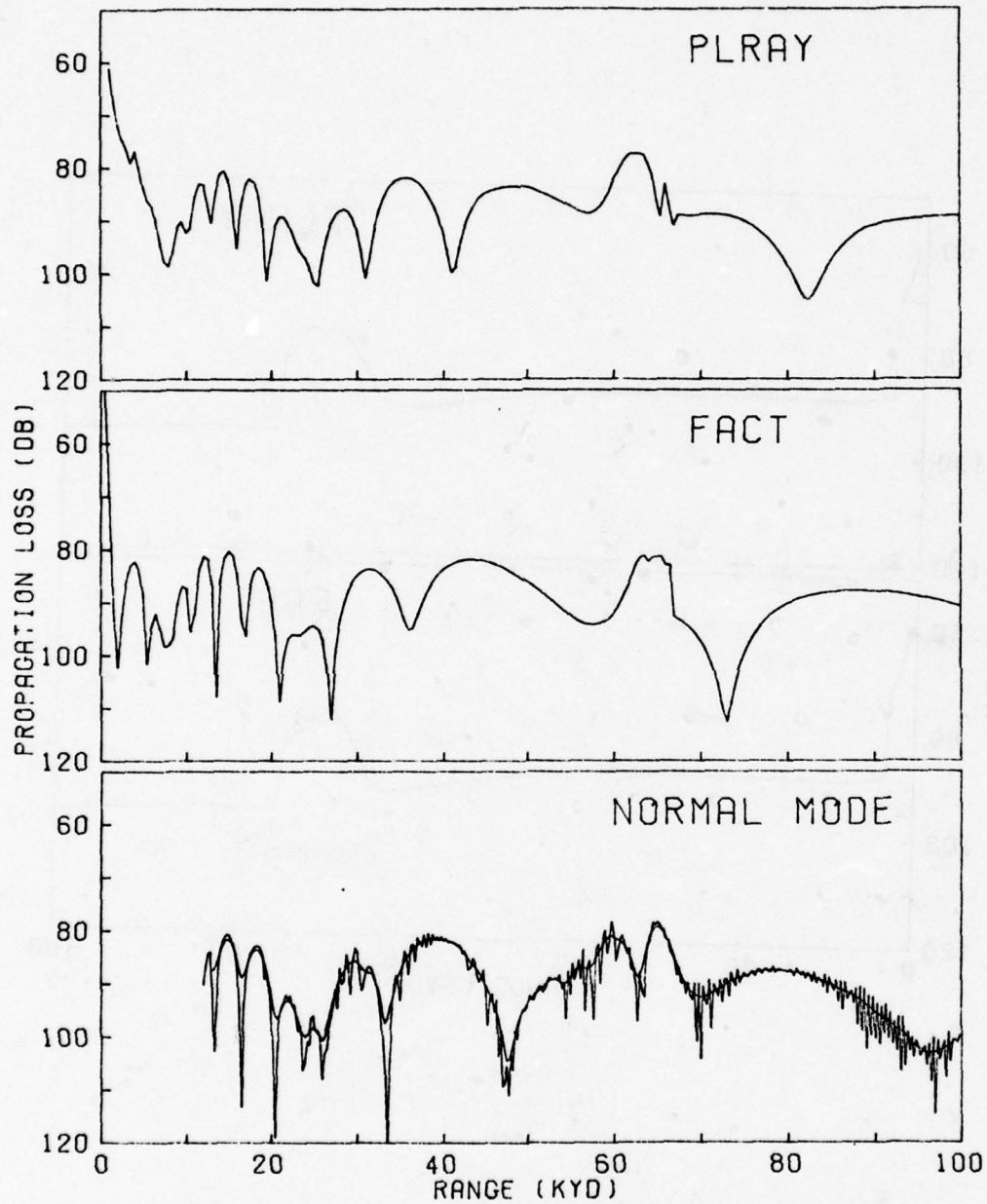


FIGURE 26 - Semicoherent Propagation Loss, Profile 3; Frequency 100 Hz, Source Depth 300 Ft, Receiver Depth 60 Ft

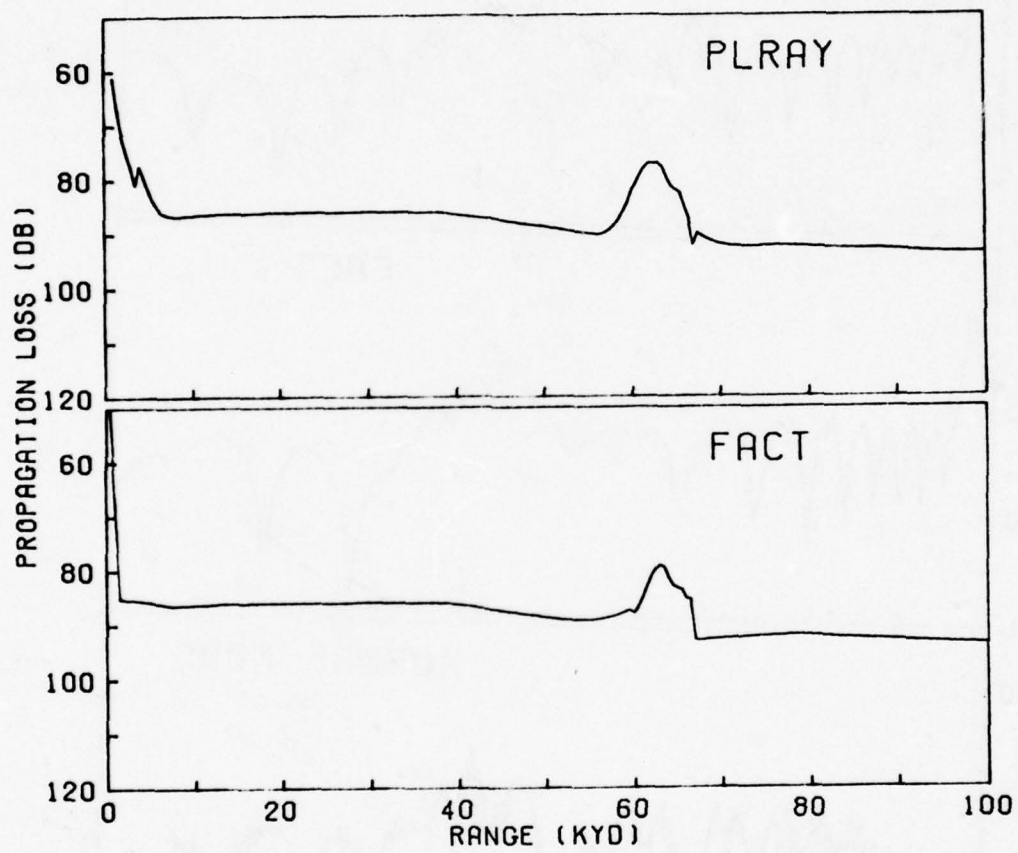


FIGURE 27 - Incoherent Propagation Loss, Profile 3; Frequency 100 Hz,  
Source Depth 300 Ft, Receiver Depth 60 Ft



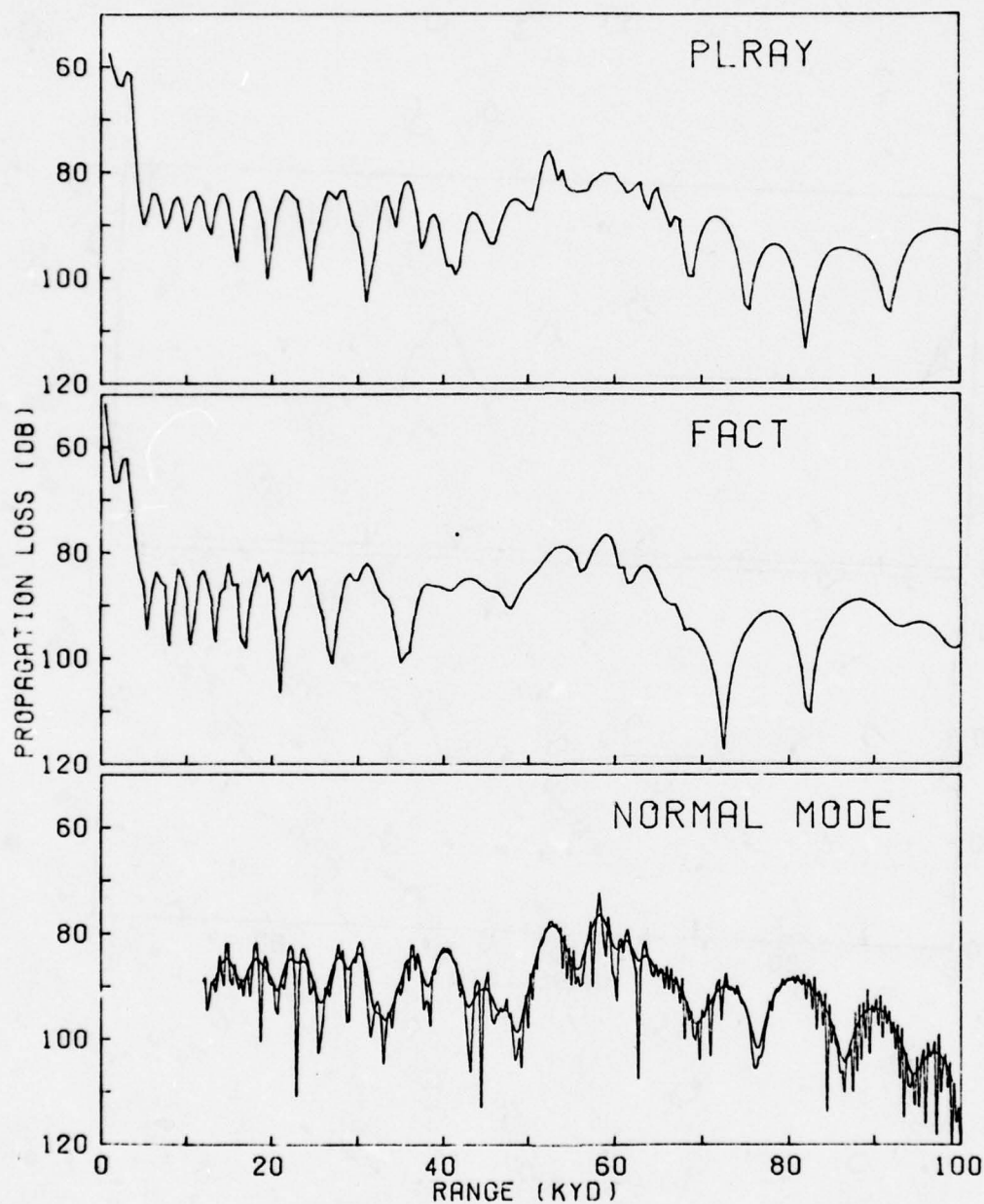


FIGURE 28 - Semicoherent Propagation Loss, Profile 3; Frequency 100 Hz, Source Depth 300 Ft, Receiver Depth 1000 Ft

with increasing range. It will be observed that the oscillations of the PLRAY interference pattern decrease in amplitude and become smooth at short ranges. The FACT oscillations, on the other hand, retain their amplitude and choppy nature and are in relatively good agreement, at least at the shorter ranges, with the normal mode oscillations. The discrepancy between the two ray models is the result of a difference in the method of implementing the amplitude reduction technique in cases of inadequate range sampling and will be discussed in more detail later. According to reference (b) FACT is supposed to begin cutting down on the amplitude when the number of range points per cycle of the oscillations falls below 6. At the shorter ranges of figure 28 the number of points per cycle is less than 6, but the amplitude is not being appropriately reduced. The fact that in spite of the failure to conform to the stated algorithm, the FACT curve appears to give good results suggests that the choice of constants in the algorithm is too conservative. It would probably be better to begin the amplitude reduction at a value less than 6 points per cycle.

Returning to figure 28, it will be noted that neither ray model reproduces the normal mode convergence zone accurately. PLRAY agrees well with the first peak but scarcely shows the second peak at all. FACT shows both peaks but neither the shapes nor the heights agree well. Both programs are in good agreement with AP2 on the trailing edge of the zone.

In the direct zone out to 4 kyd all three programs agree closely. In the original AP2 output (not shown in figure 28) there is a large dip at 2 kyd which is more nearly reproduced by FACT than by PLRAY.

The incoherent curves for the same case are plotted in figure 29. Except in the convergence zone, where both are essentially the same as their semicoherent counterparts, the two models yield virtually identical results.

Figure 30 is a plot of the semicoherent output of PLRAY and FACT for a frequency of 300 Hz, the source and receiver depths being 300 and 1000 feet. AP2 was not run at this frequency because of the excessively large number of modes required. The feature of primary interest here is the behavior in the bottom-bounce region between 5 and 45 kyd. It will be observed that the oscillations of PLRAY start with essentially zero amplitude and gradually increase to a very large amplitude. The FACT oscillations, on the other hand, retain an essentially constant amplitude throughout. These curves illustrate dramatically the difference between the two models in their method of handling the range sampling problem. Both models employ essentially the same formula for the amplitude reduction as a function of the number of points per cycle. PLRAY uses the solid curve of figure J4 (appendix J), and FACT uses the dashed curve. The difference between the two programs is in the method of computing the number of range points per cycle. PLRAY computes the instantaneous value at each range point, based on an analytical formula. As may be seen in figure 30, the frequency of the oscillations increases drastically as the range decreases from 45 to 5 kyd. Strict application of the curve of figure J4 results in the behavior shown.

FACT, on the other hand, computes an average number of points per cycle over the entire range interval covered by the family of rays in the sector. Careful measurement of the oscillations has shown that at ranges below 12 kyd the number of points per cycle is less than 2, so that if the algorithm were

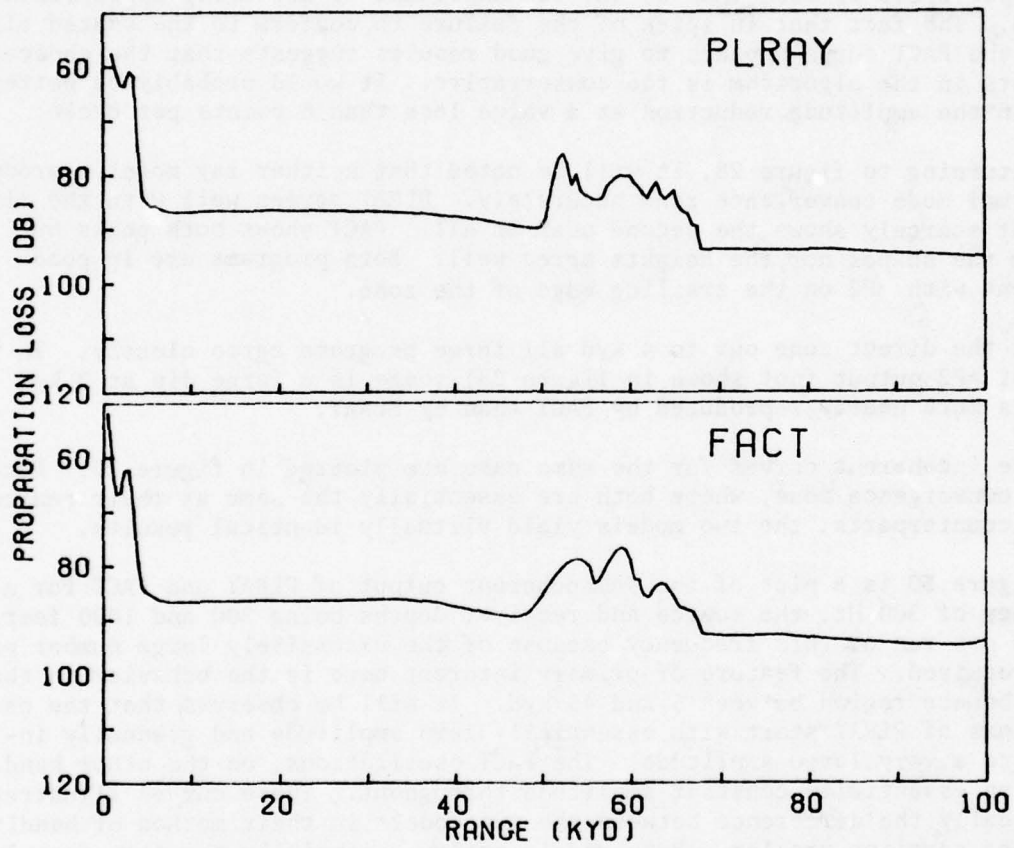


FIGURE 29 - Incoherent Propagation Loss, Profile 3; Frequency 100 Hz,  
Source Depth 300 Ft, Receiver Depth 1000 Ft



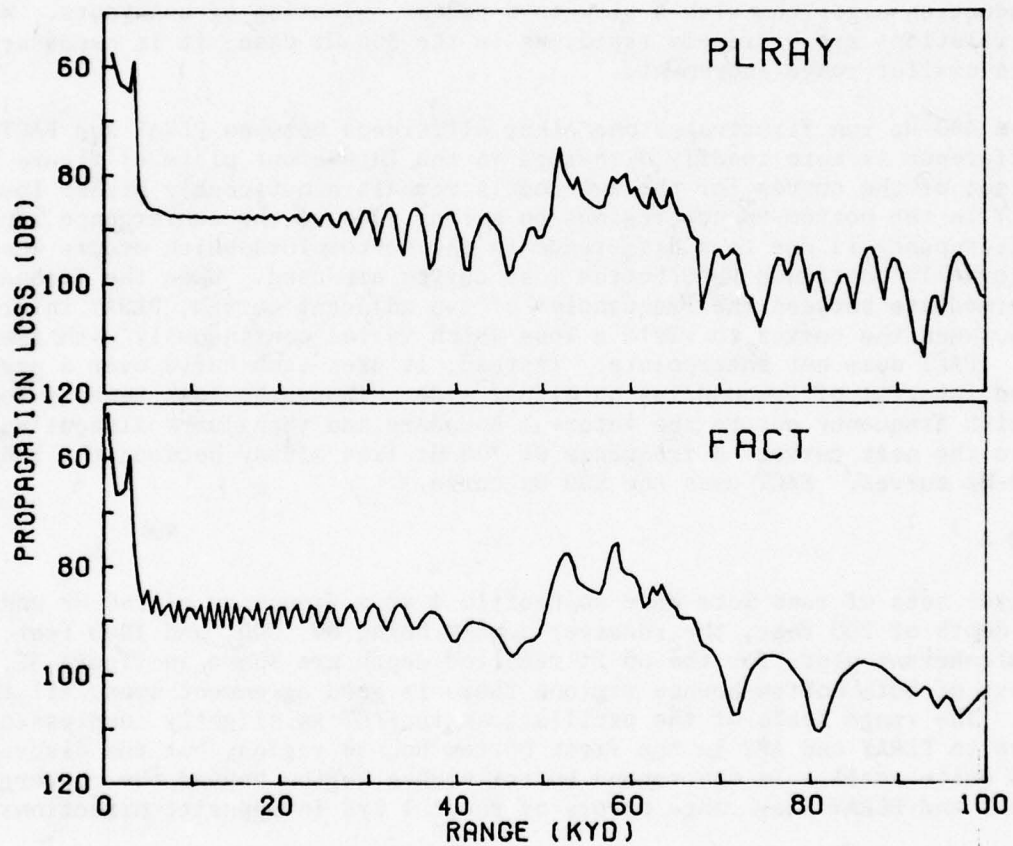


FIGURE 30 - Semicoherent Propagation Loss, Profile 3; Frequency 300 Hz, Source Depth 300 Ft, Receiver Depth 1000 Ft

correctly implemented, the amplitude of the oscillations would be reduced to zero. On the other hand, in the vicinity of 40 kyd the number of points per cycle is well above the limiting value of 6, where no reduction in amplitude should be called for.

It appears that neither of the two curves is really satisfactory. The PLRAY curve, even though it faithfully follows the rules, looks decidedly unreasonable. The FACT curve looks more reasonable, but runs into sampling problems at the shorter ranges. Fortunately, very few runs have been encountered in which this problem has proved severely troublesome. On the basis of the 100 Hz case described above, it would be desirable to re-examine the amplitude reduction algorithm with a view to a better selection of constants. Where the oscillations are extremely rapid, as in the 300 Hz case, it is necessary to use a smaller range increment.

The 300-Hz run illustrates one other difference between PLRAY and FACT. The difference is more readily discerned in the incoherent plots of figure 31. Comparison of the curves for the two models reveals a noticeably higher loss for FACT in the bottom-bounce regions on either side of the convergence zone. This discrepancy is due to a difference in the bottom loss which occurs when the internally contained FNWC bottom loss curves are used. When the frequency is intermediate between the frequencies of two adjacent curves, PLRAY interpolates between the curves to yield a loss which varies continuously with frequency. FACT does not interpolate. Instead, it uses each curve over a predetermined interval of frequencies on either side. Thus, the loss remains constant with frequency out to the interval boundary and then jumps discontinuously to the next curve. A frequency of 300 Hz lies midway between the 100- and 500-Hz curves. FACT uses the 500 Hz curve.

#### PROFILE 4

Three sets of runs were made on Profile 4 at a frequency of 150 Hz and a source depth of 200 feet, the receiver depths being 60, 300, and 1000 feet. The semicoherent plots for the 60 ft receiver depth are shown in figure 32. Over most of both bottom-bounce regions there is good agreement among all three models. The range scale of the oscillations in FACT is slightly compressed relative to PLRAY and AP2 in the first bottom-bounce region, but the discrepancy is quite small. In the second bottom-bounce region beyond the convergence zone FACT and PLRAY show range errors of about 1 kyd in opposite directions.

The normal mode convergence zone exhibits two peaks, the second being about 4 db higher than the first. Only the first peak shows up in the two ray programs, and this peak is 4 db too high. The gradual tapering off on the PLRAY curve on the far side of the zone is in considerably better agreement with AP2 than the FACT curve, which drops sharply.

In the direct zone AP2 has been found to give useful results out to a range of about 7 kyd. The agreement between PLRAY and AP2 in this region is good. FACT also agrees well out to 4 kyd but begins to deviate slightly on the low loss side at ranges beyond 4 kyd. It should be noted that the surface duct models of PLRAY and FACT come into play in this run since the source and receiver both lie within the 275 ft surface duct of Profile 4. The difference

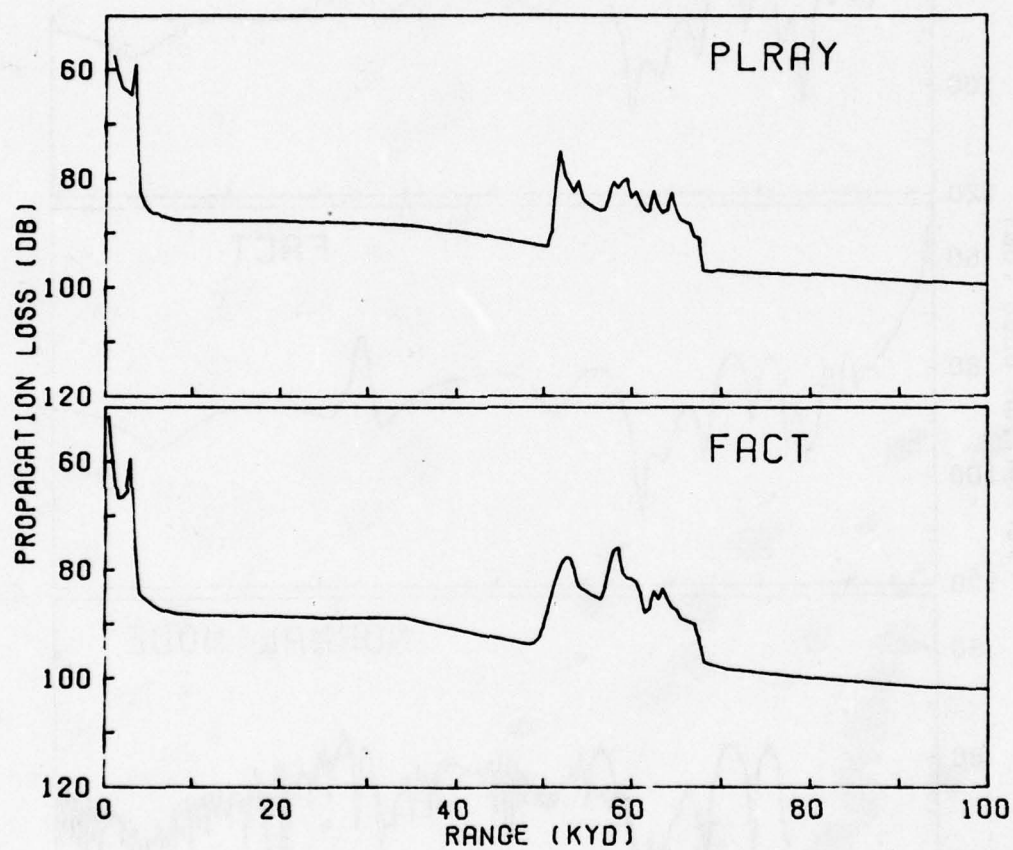


FIGURE 31 - Incoherent Propagation Loss, Profile 3; Frequency 300 Hz,  
Source Depth 300 Ft, Receiver Depth 1000 Ft



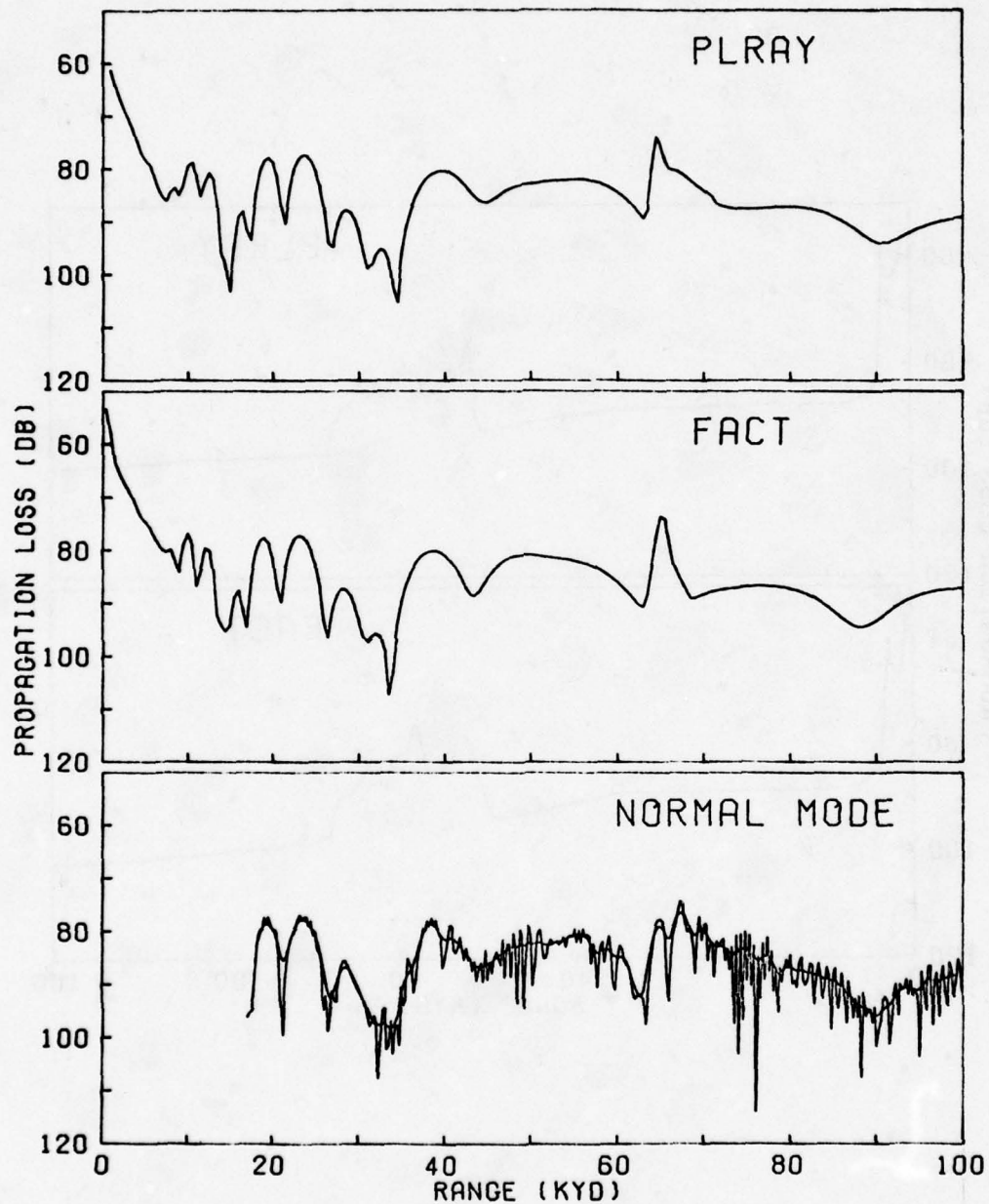


FIGURE 32 - Semicoherent Propagation Loss, Profile 4; Frequency 150 Hz, Source Depth 200 Ft, Receiver Depth 60 Ft

in behavior of the two ray programs is probably due to a difference in the respective surface duct models.

The corresponding incoherent curves for this case are plotted in figure 33. Except for the discrepancies noted above, PLRAY and FACT are in good agreement.

The semicoherent results for the 300 ft receiver depth are shown in figure 34. Here, except for small distortions of the range scales, there is good agreement among the three programs in the first bottom-bounce region. The agreement in the second bottom-bounce region is considerably poorer, both ray programs exhibiting too high a loss immediately beyond the convergence zone. The reduction of the amplitude of the PLRAY oscillations at ranges below 20 kyd is due to the range sampling effect discussed previously. In the convergence zone itself the two peaks of PLRAY agree with the corresponding peaks of AP2 within about 2 db. The second peak of FACT occurs at too large a range and between the two peaks there is an excessively deep minimum.

In the direct propagation zone there is fairly good agreement between PLRAY and AP2 (not shown in figure 34). FACT, on the other hand, shows a significantly different trend, dropping to the bottom-bounce level at about 4 kyd as compared with 7 kyd for PLRAY. The error in this case is much larger and in the opposite direction from that observed at the 60 ft receiver depth. At 300 feet the receiver, though slightly below the bottom of the surface duct, is within the range of depths covered by the surface duct models. Although the PLRAY and FACT runs have not been analyzed to determine the sources of the major contributions to the intensity, it is possible that the discrepancy between the two outputs may be caused in part by a difference in the surface duct models.

The incoherent results for this case are plotted in figure 35. Here again we see excellent agreement in the bottom-bounce regions.

Figure 36 shows the semicoherent plots for the 1000 ft receiver depth. Here the agreement among the three curves has deteriorated somewhat. Both PLRAY and FACT show the major features of the interference pattern reasonably well out to a range of 50 kyd. The reduction in amplitude of the PLRAY oscillations at short ranges is due to the attenuation introduced by the range sampling algorithm. The smooth nature of the oscillations below 30 kyd indicates that only the single bottom-bounce rays are contributing to the interference pattern; the oscillations caused by the double bottom-bounce rays, which have a higher frequency, are completely attenuated. At ranges beyond 30 kyd the double bottom-bounce rays begin to contribute, producing the minor oscillations superimposed on the basic interference pattern. Comparison with AP2 shows a certain amount of correlation in the secondary oscillations. The FACT curve exhibits only smooth oscillations of uniform amplitude in this region. Apparently the average number of points per cycle computed by FACT for the single bottom-bounce rays has resulted in a partial attenuation, while the average number of points per cycle for the double bottom-bounce rays is such as to eliminate the secondary oscillations completely.

Beyond 50 kyd, there is qualitative agreement between PLRAY and AP2. The average levels agree quite well, but there is no one-to-one correspondence in

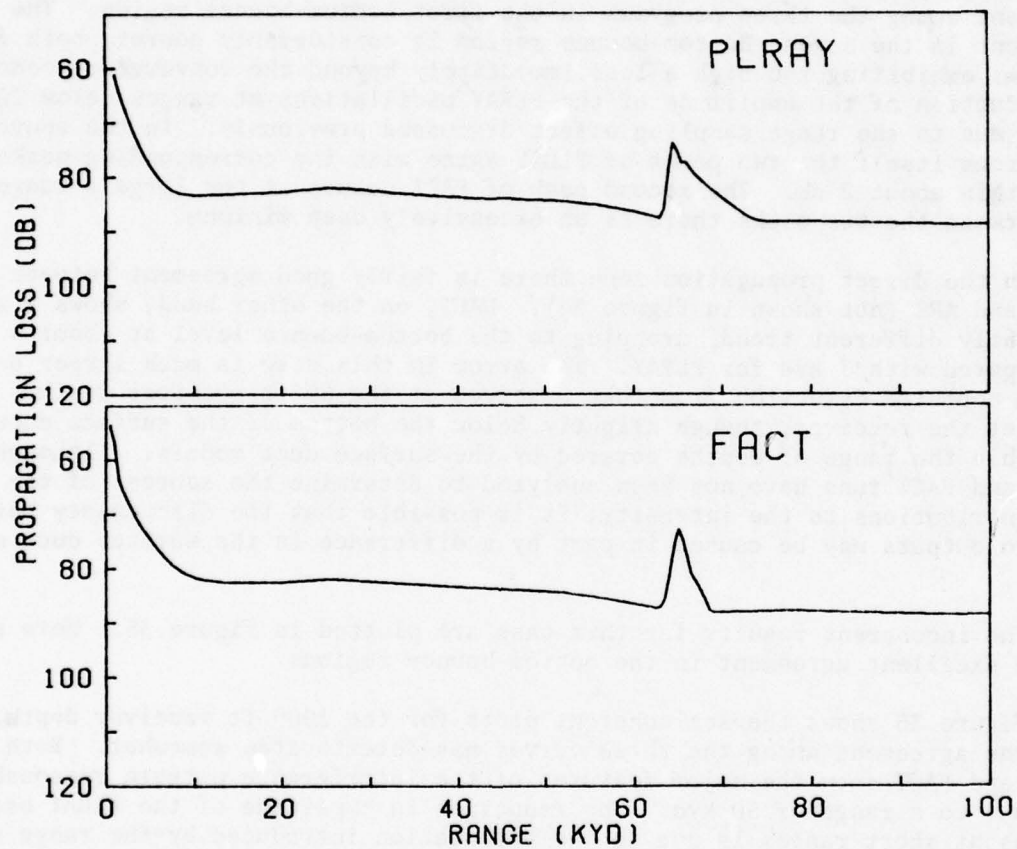


FIGURE 33 - Incoherent Propagation Loss, Profile 4; Frequency 150 Hz,  
Source Depth 200 Ft, Receiver Depth 60 Ft



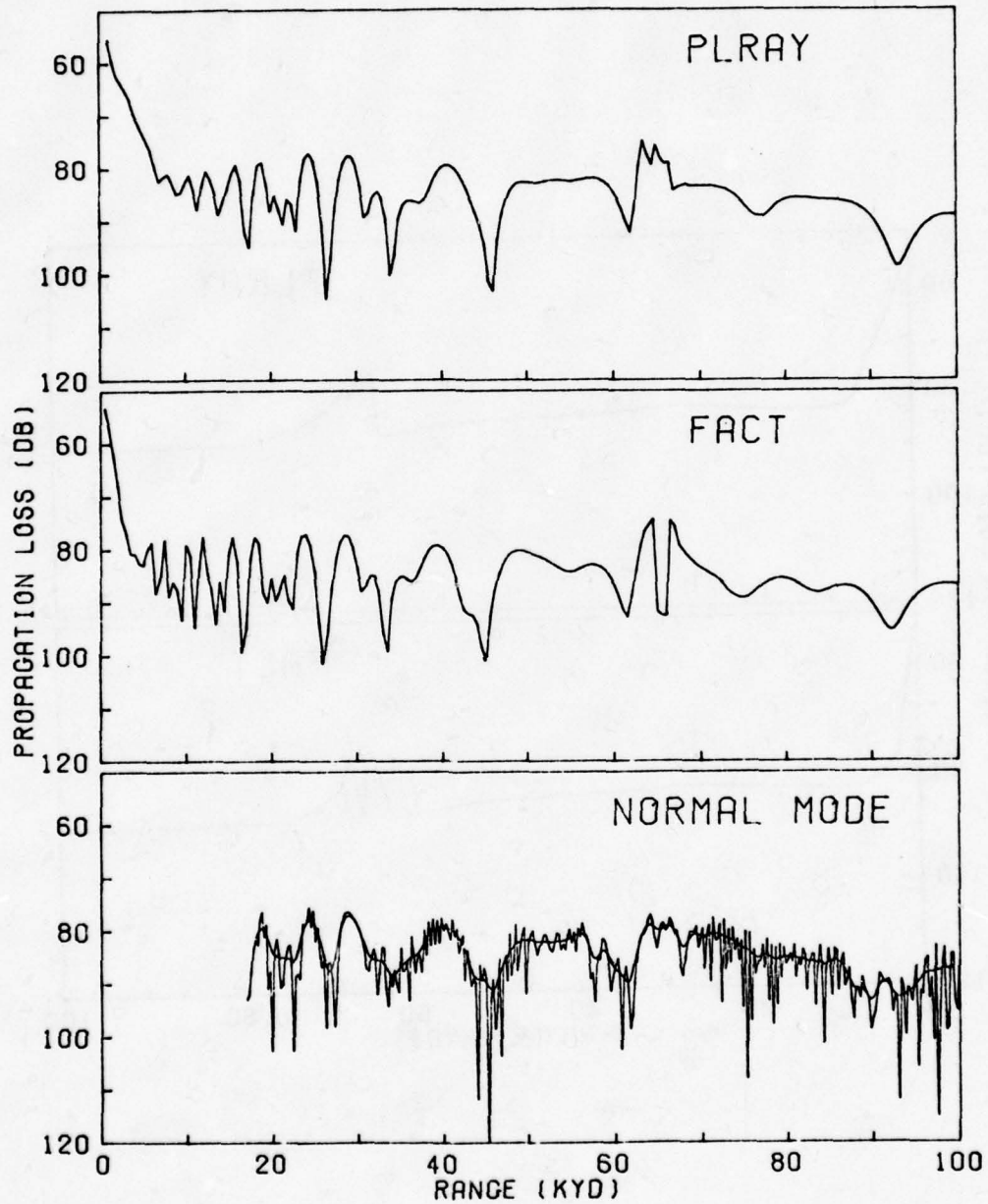


FIGURE 34 - Semicoherent Propagation Loss, Profile 4; Frequency 150 Hz, Source Depth 200 Ft, Receiver Depth 300 Ft

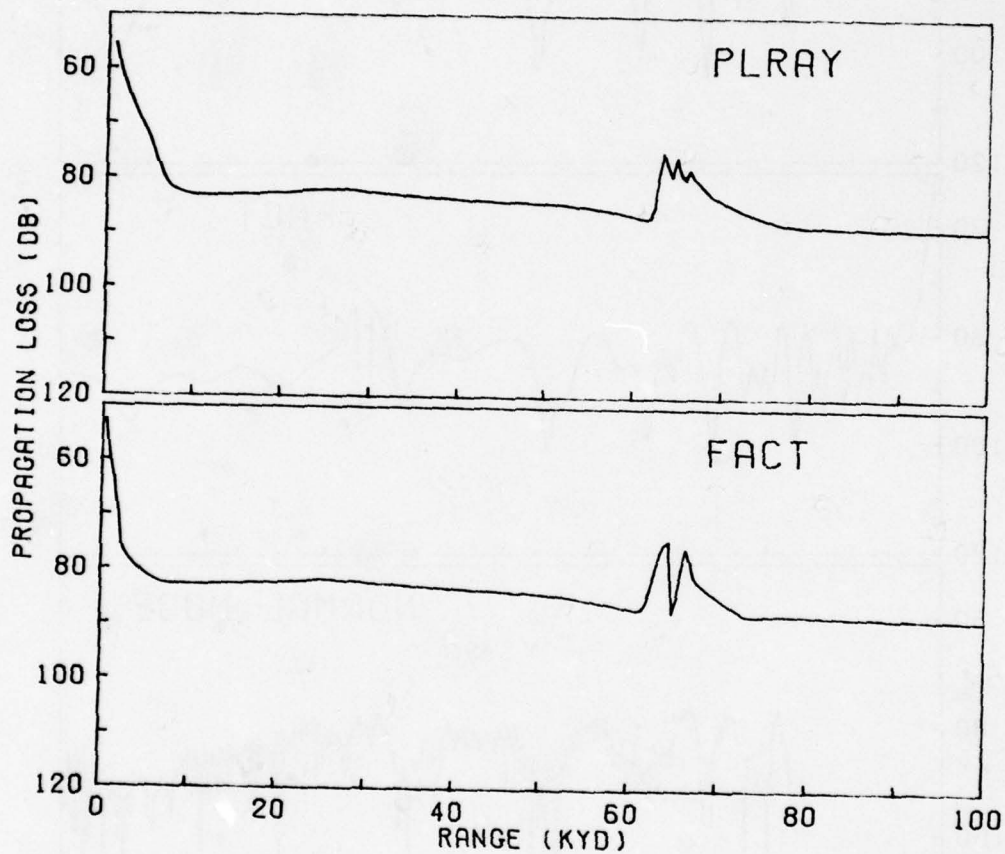


FIGURE 35 - Incoherent Propagation Loss, Profile 4; Frequency 150 Hz,  
Source Depth 200 Ft, Receiver Depth 300 Ft

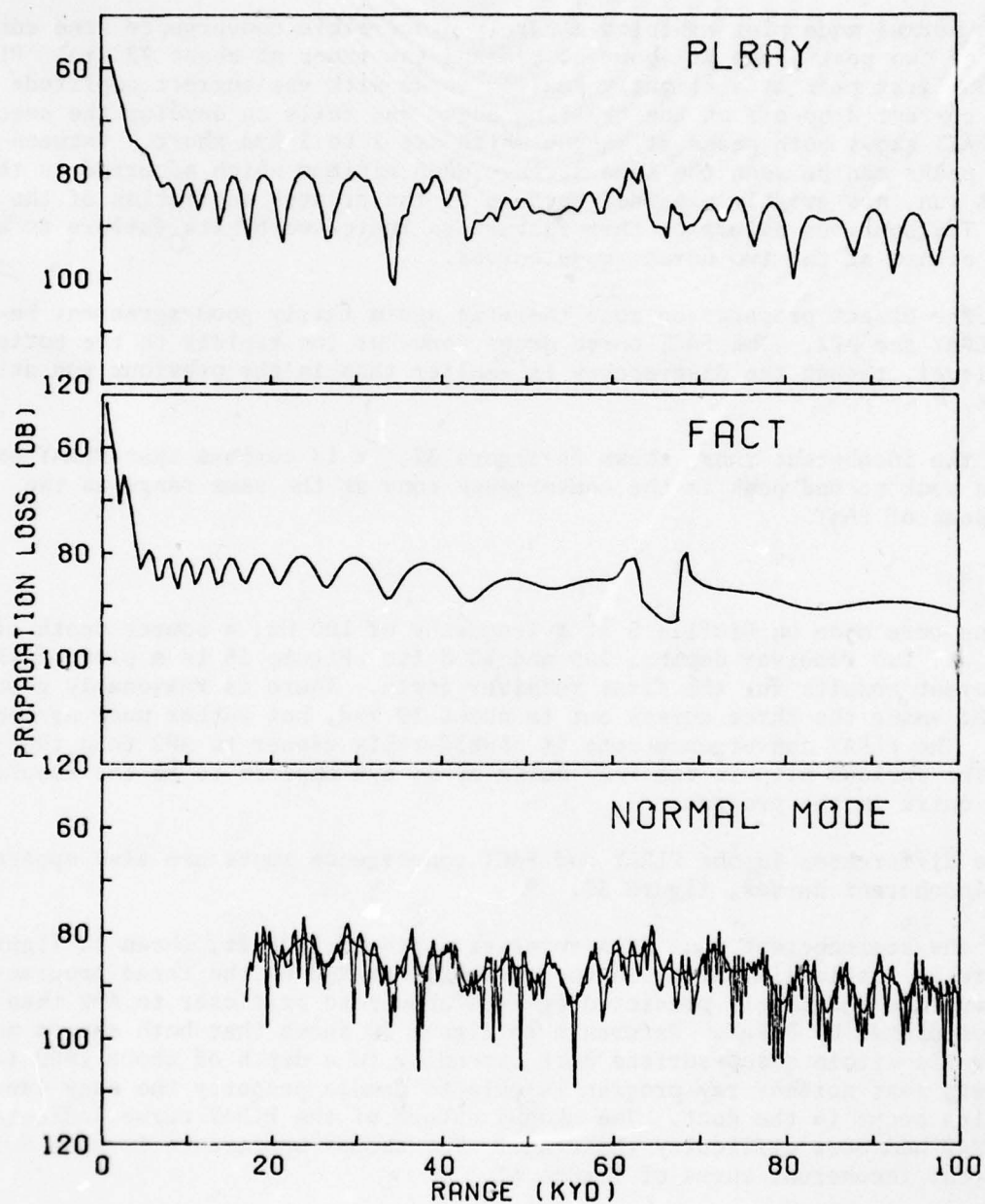


FIGURE 36 - Semicoherent Propagation Loss, Profile 4; Frequency 150 Hz, Source Depth 200 Ft, Receiver Depth 1000 Ft



the individual oscillations. In the FACT output beyond 50 kyd the oscillations have died out except for a set of gentle undulations of very low amplitude and long period.

The normal mode plot exhibits a barely discernible convergence zone consisting of two peaks, one at about 64 kyd and the other at about 72 kyd. PLRAY shows the first peak at a slightly smaller range with the correct amplitude and the correct drop-off on the trailing edge, but fails to develop the second peak. FACT shows both peaks at ranges which are 2 to 3 kyd short. Between the two peaks can be seen the same strange deep minimum which occurred in the previous run, now greatly expanded because of the greater separation of the peaks. The spurious nature of this feature is indicated by its failure to appear in either of the two normal mode curves.

In the direct propagation zone there is again fairly good agreement between PLRAY and AP2. The FACT curve drops somewhat too rapidly to the bottom-bounce level, though the discrepancy is smaller than in the previous run at 300 feet.

In the incoherent runs, shown in figure 37, it is curious that PLRAY exhibits a weak second peak in the convergence zone at the same range as the second peak of FACT.

#### PROFILE 5

Runs were made on Profile 5 at a frequency of 100 Hz, a source depth of 300 ft, and two receiver depths, 100 and 1000 ft. Figure 38 is a plot of the semicoherent results for the first receiver depth. There is reasonably good agreement among the three curves out to about 30 kyd, but rather poor agreement beyond. The PLRAY convergence zone is considerably closer to AP2 than that of FACT. The curious blip in the FACT curve at 66 kyd appears to be the result of some quirk in the program.

The differences in the PLRAY and FACT convergence zones are also apparent in the incoherent curves, figure 39.

In the semicoherent runs at a receiver depth of 1000 ft, shown in figure 40, there is little similarity in the curves generated by the three programs. On the average the levels predicted by FACT appear to be closer to AP2 than the levels predicted by PLRAY. Reference to figure 10 shows that both source and receiver lie within a sub-surface duct extending to a depth of about 1900 feet. It appears that neither ray program is able to handle properly the many caustics which occur in the duct. The choppy nature of the PLRAY curve indicates that PLRAY had more difficulty than FACT. The choppy appearance is also evident in the incoherent curve of figure 41.

#### PROFILE 6

Figure 42 shows the semicoherent run on Profile 6, the frequency being 50 Hz and the source and receiver depths 300 and 1000 feet respectively. Except for a range scale compression of about 7 percent, PLRAY shows fair agreement with AP2 out to the second peak of the first convergence zone at about 45 kyd. Although at longer ranges the agreement is rather poor, there is a good match

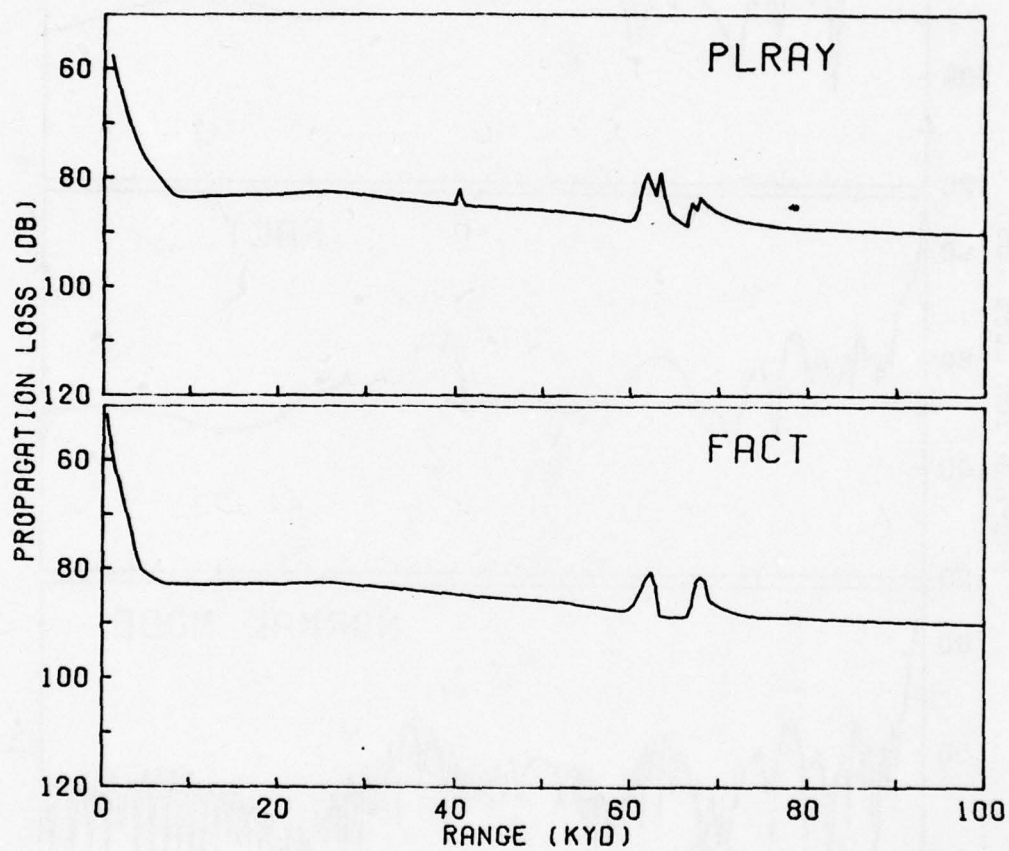


FIGURE 37 - Incoherent Propagation Loss, Profile 4; Frequency 150 Hz,  
Source Depth 200 Ft, Receiver Depth 1000 Ft

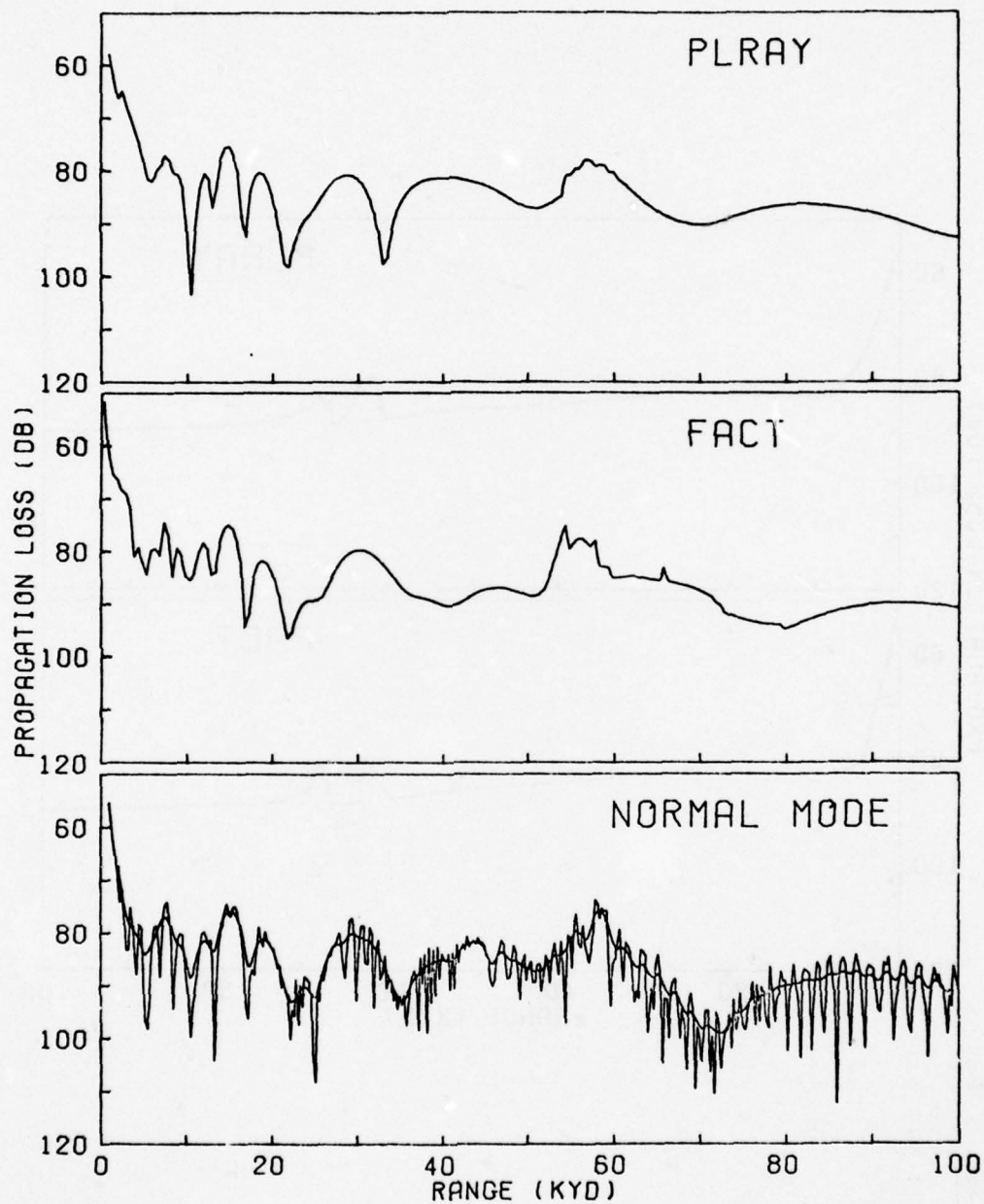


FIGURE 38 - Semicoherent Propagation Loss, Profile 5; Frequency 100 Hz, Source Depth 300 Ft, Receiver Depth 100 Ft



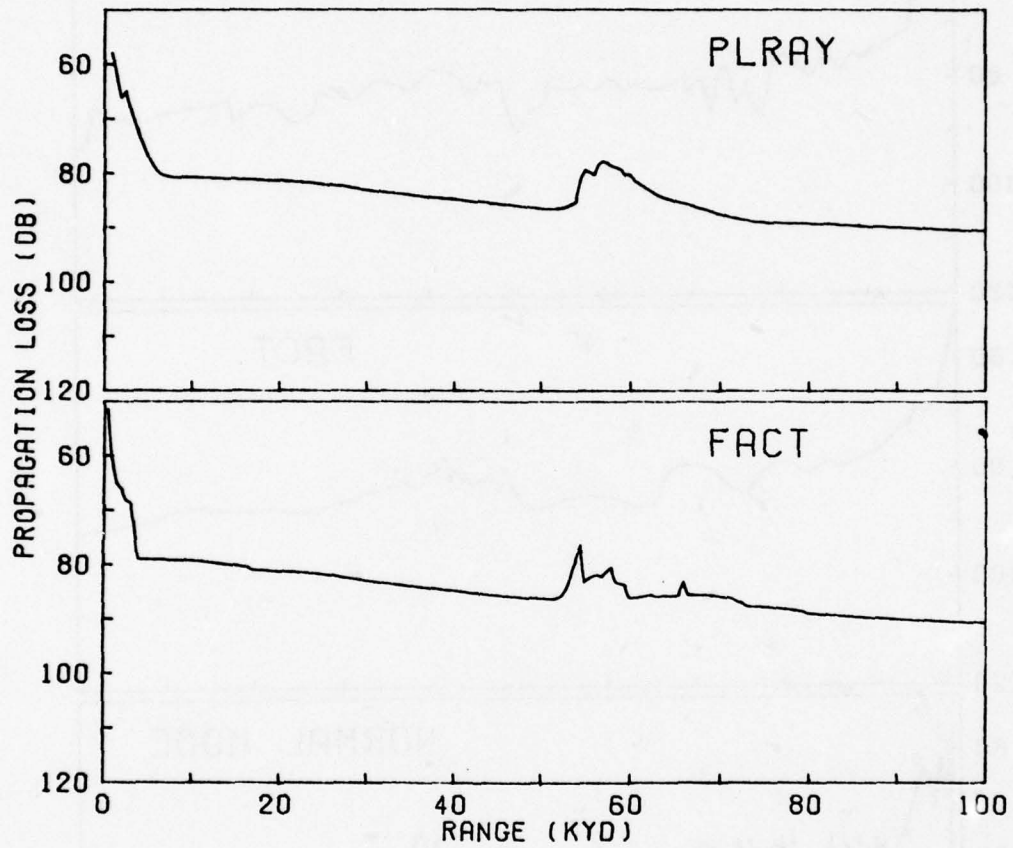


FIGURE 39 - Incoherent Propagation Loss, Profile 5; Frequency 100 Hz,  
Source Depth 300 Ft, Receiver Depth 100 Ft

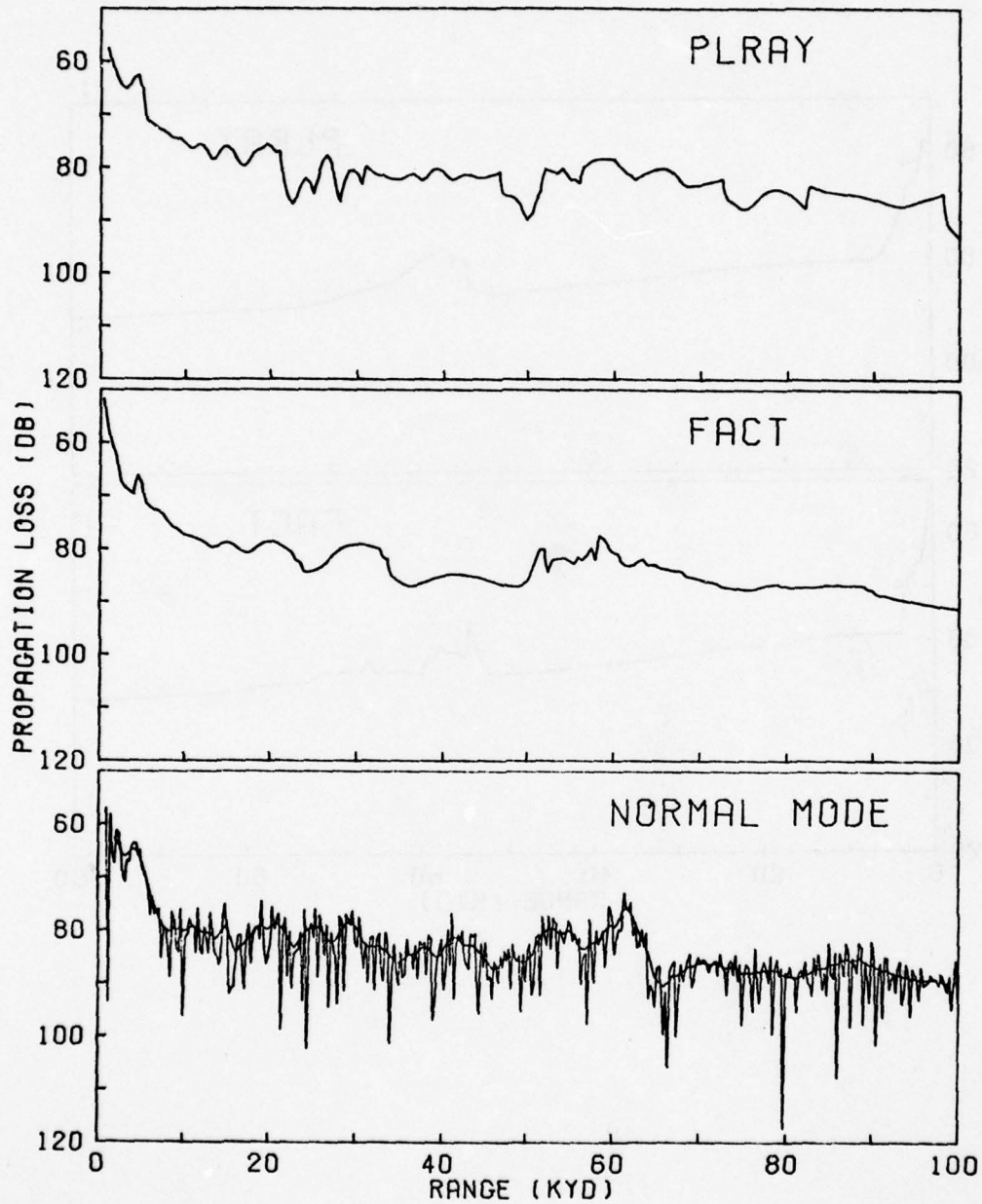


FIGURE 40 - Semicoherent propagation Loss, Profile 5; Frequency 100 Hz, Source Depth 300 Ft, Receiver Depth 1000 Ft

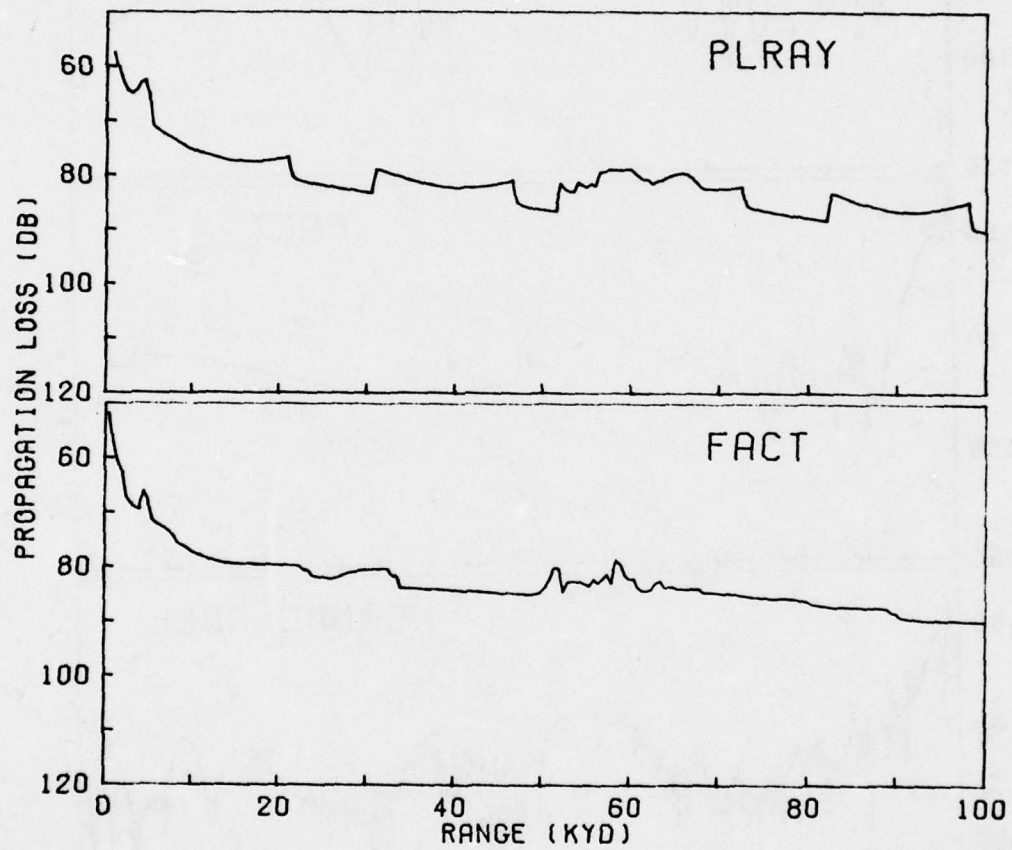


FIGURE 41 - Incoherent Propagation Loss, Profile 5; Frequency 100 Hz,  
Source Depth 300 Ft, Receiver Depth 1000 Ft



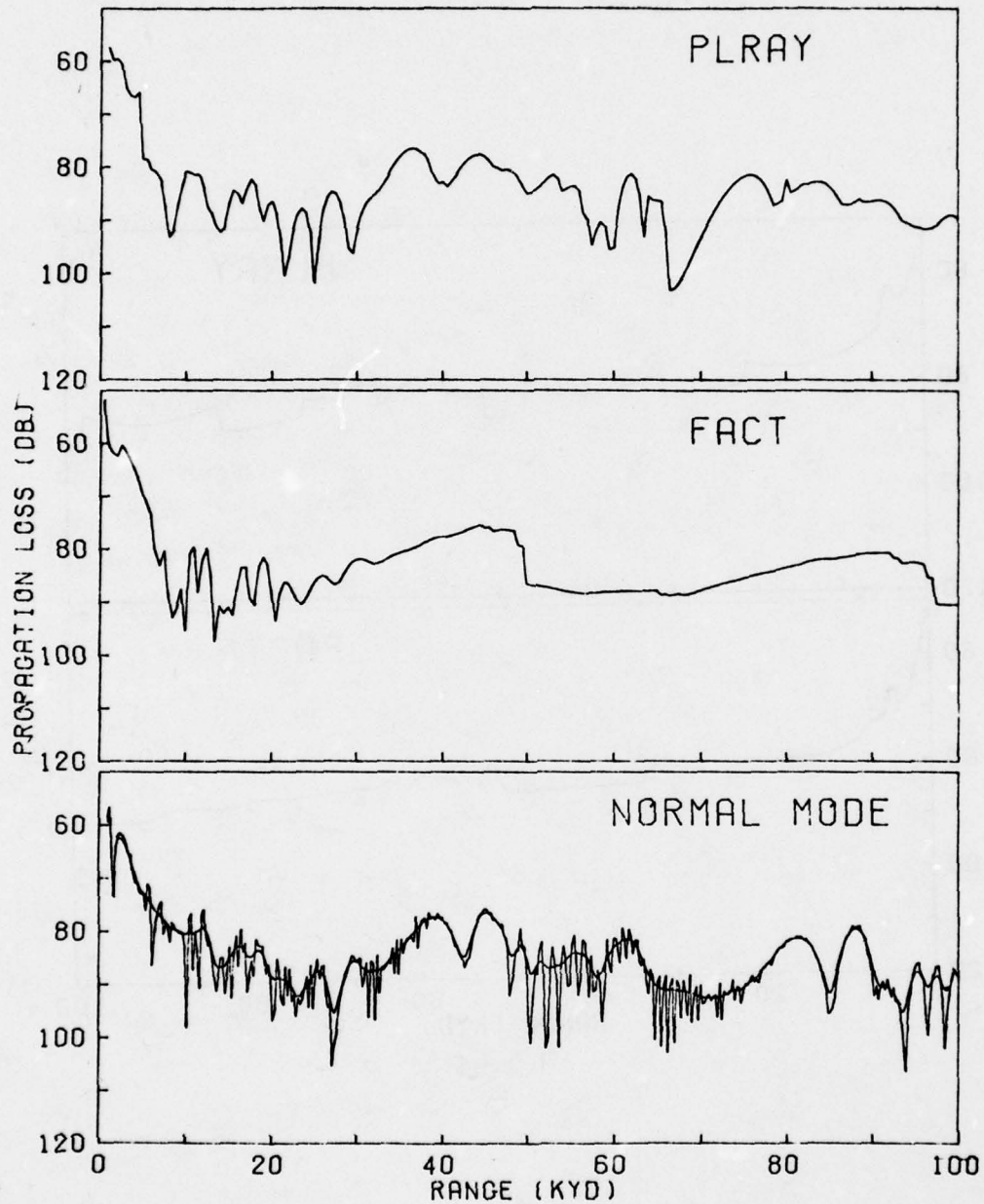


FIGURE 42 - Semicoherent Propagation Loss, Profile 6; Frequency 50 Hz,  
Source Depth 300 Ft, Receiver Depth 1000 Ft

at the first peak of the second convergence zone. FACT, on the other hand, shows reasonable agreement only out to about 20 kyd. Examination of the convergence zones reveals very peculiar behavior, with a slow rise to the maximum followed by a precipitous drop. Such behavior suggests that FACT may have encountered a gross error in applying the caustic corrections at the convergence zones. The same peculiarity is clearly evident in the incoherent run, figure 43, indicating that coherence has nothing to do with the problem.

#### PROFILE 7

The runs on Profile 7 were made at a frequency of 100 Hz for a source depth of 300 ft and receiver depths of 100 and 1000 ft. The semicoherent propagation loss for the 100 ft depth is plotted in figure 44. Except at ranges below 20 kyd neither of the ray programs agrees very well with AP2. However, at these shorter ranges FACT exhibits quite good agreement. Both curves show the same set of oscillations, although the FACT scale is expanded relative to AP2 and some of the oscillations have different peak values. In the PLRAY curve the rapid oscillations have been greatly smoothed at ranges below 10 kyd. The smoothing results from the attenuation introduced by the range sampling algorithm. If the FACT model had actually behaved in accordance with the dashed curve of figure J4, its oscillations would also have been greatly smoothed, since the average number of range points per cycle in the five cycles below 10 kyd is only about 3. This case is another example of the previous observation (figure 30) that adequate sampling is obtainable when the number of points per cycle is considerably less than 6.

Both ray curves agree roughly with the normal mode curve in the vicinity of the first convergence zone. However, the large dip in the normal mode curve at 46 kyd does not appear in either ray curve. The second peak at 49 kyd is present in PLRAY, but the level of the peak is 3 db too high. Beyond the first convergence zone neither curve shows much similarity to AP2, although in the vicinity of the second zone around 80 kyd PLRAY behaves somewhat better than FACT.

In the incoherent runs, figure 45, PLRAY and FACT agree very closely except in the second convergence zone, where discrepancies up to 3 db occur.

Figure 46 shows the semicoherent results for a receiver depth of 1000 feet. All three curves are relatively featureless. Except for the fact that the average levels are reasonably similar, there is little agreement among the three curves. At very short ranges the PLRAY curve drops much too rapidly. Between 10 and 30 kyd it agrees reasonably well with AP2, if allowance is made for the compression of the range scale. It fails to predict the large peak at 35 kyd and shows too high a loss between 33 and 45 kyd. FACT also exhibits numerous discrepancies, although on the whole it appears to agree with AP2 somewhat better than PLRAY.

As may be seen from the incoherent curves, figure 47, PLRAY tends to predict somewhat higher losses than FACT. The largest discrepancy occurs at short ranges.

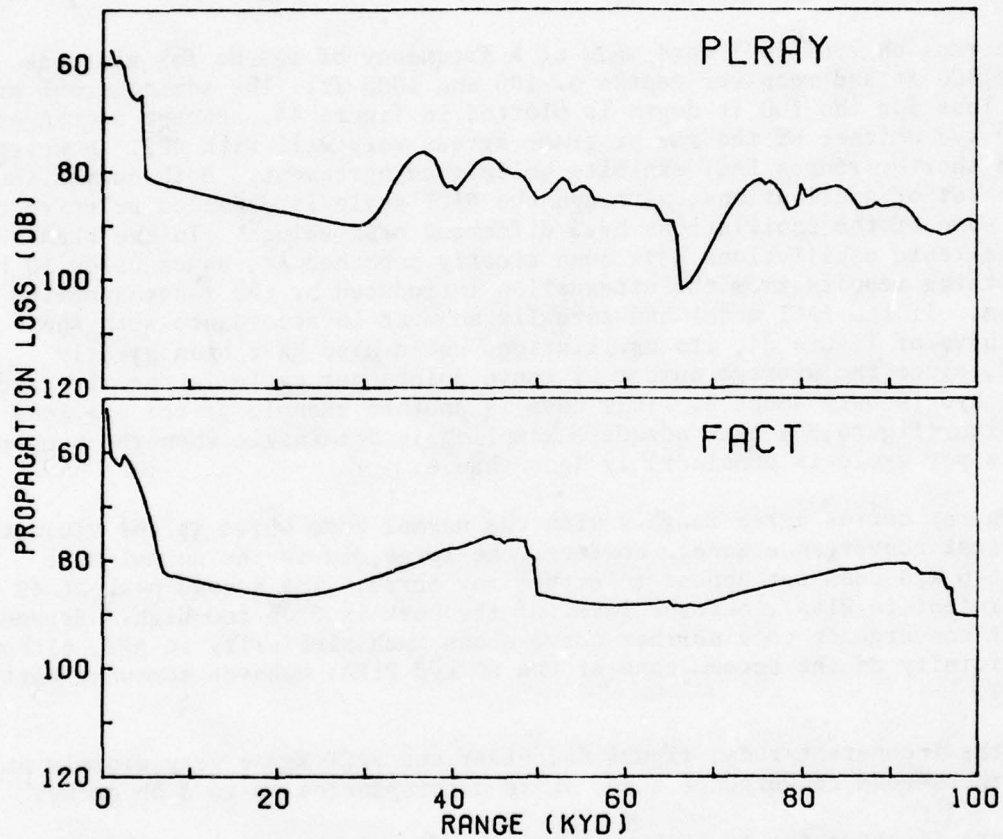


FIGURE 43 - Incoherent Propagation Loss, Profile 6; Frequency 50 Hz,  
Source Depth 300 Ft, Receiver Depth 1000 Ft



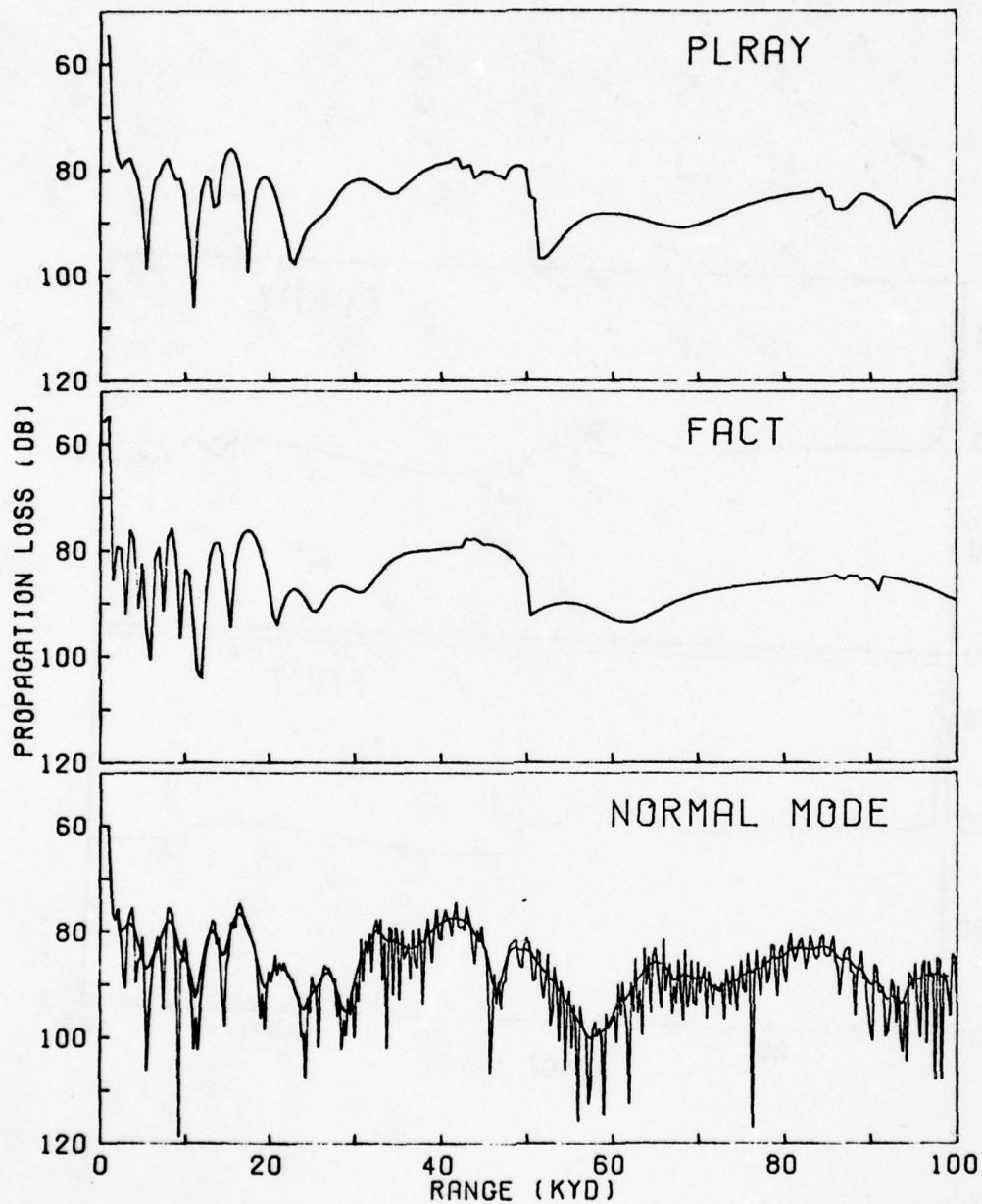


FIGURE 44 - Semicoherent Propagation Loss, Profile 7; Frequency 100 Hz, Source Depth 300 Ft, Receiver Depth 100 Ft

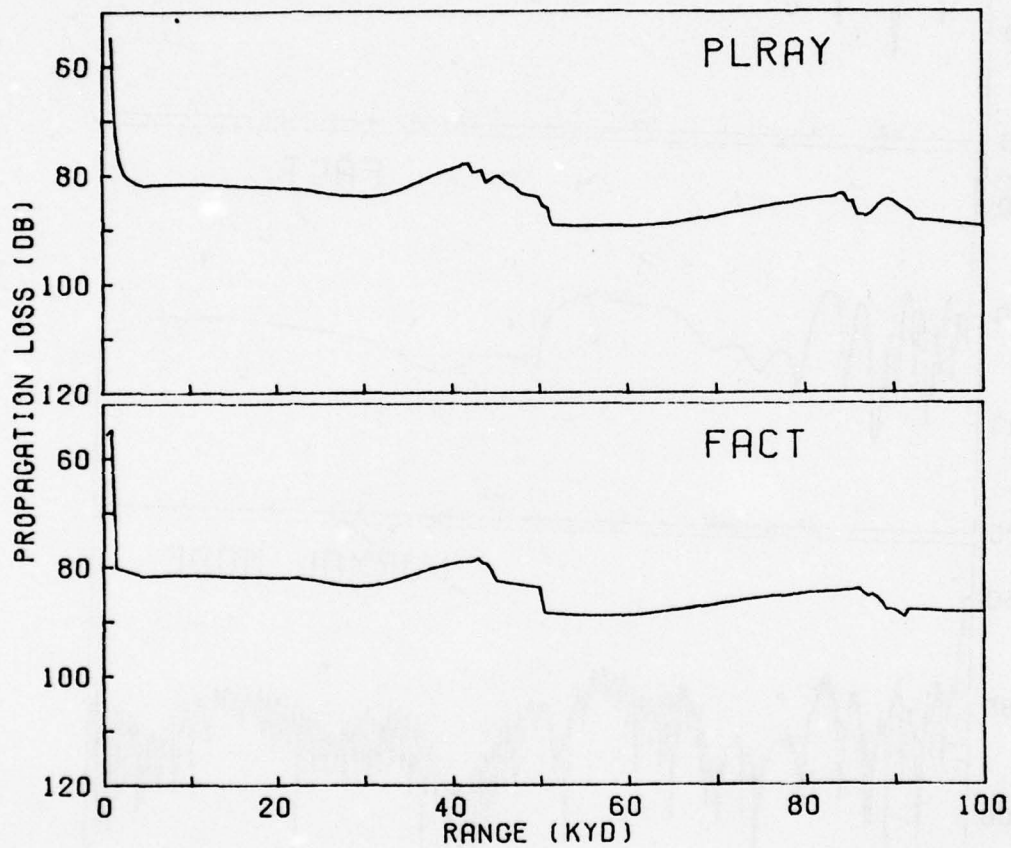


FIGURE 45 - Incoherent Propagation Loss, Profile 7; Frequency 100 Hz,  
Source Depth 300 Ft, Receiver Depth 100 Ft

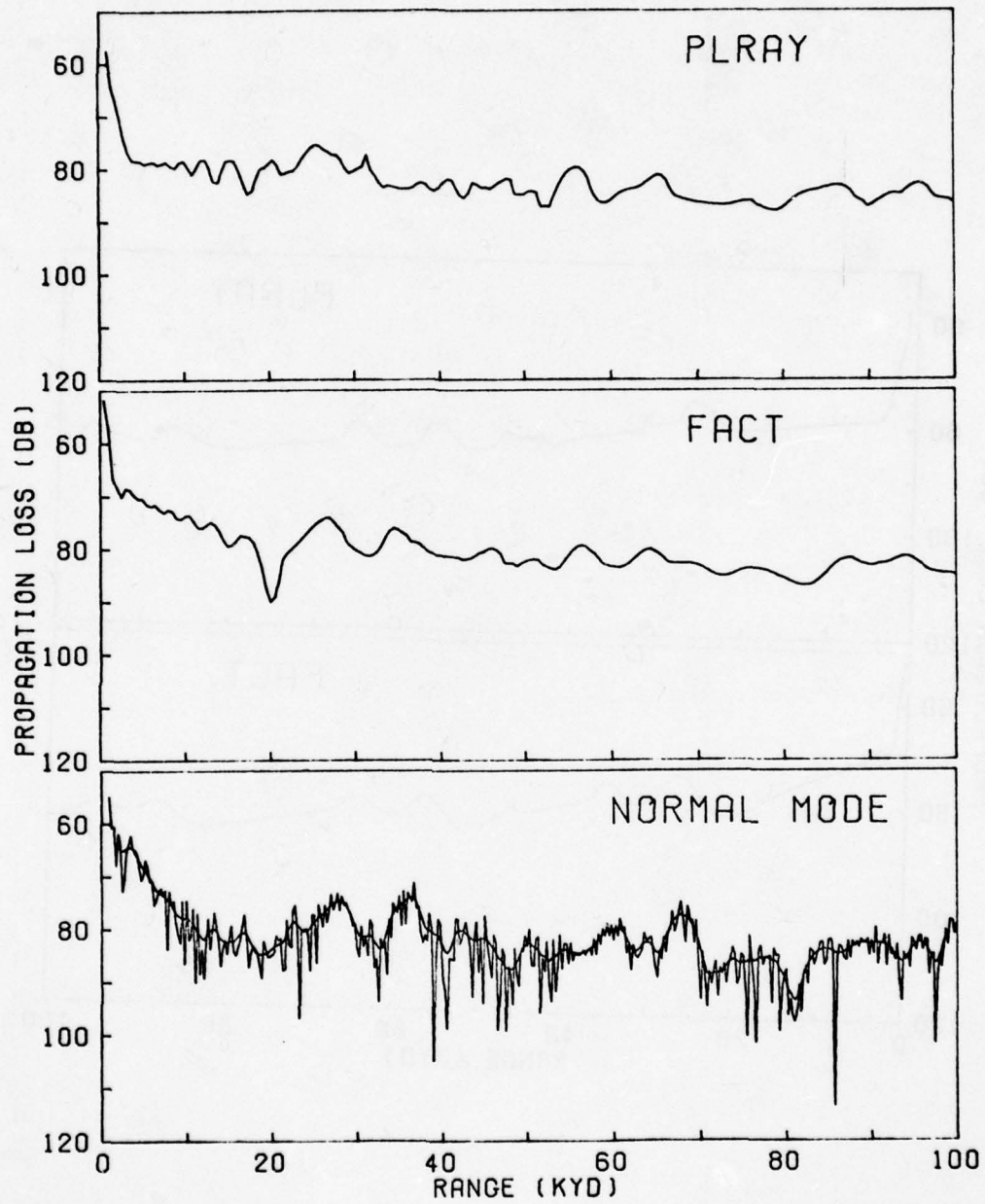


FIGURE 46 - Semicoherent Propagation Loss, Profile 7; Frequency 100 Hz, Source Depth 300 Ft, Receiver Depth 1000 Ft



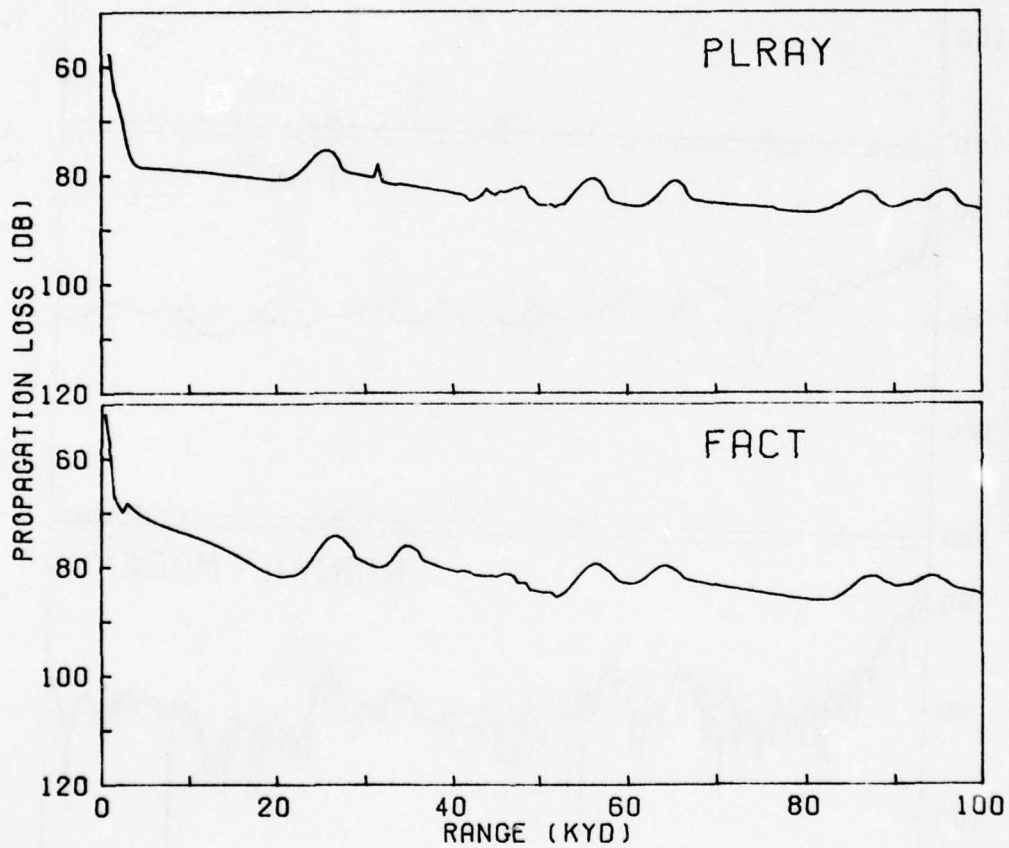


FIGURE 47 - Incoherent Propagation Loss, Profile 7; Frequency 100 Hz, Source Depth 300 Ft, Receiver Depth 1000 Ft

AD-A062 019

NAVAL AIR DEVELOPMENT CENTER WARMINSTER PA SENSORS A--ETC F/6 20/1  
PLRAY - A RAY PROPAGATION LOSS PROGRAM.(U)  
OCT 78 C L BARTBERGER

UNCLASSIFIED

NADC-77296-30

NL

2 OF 3  
AD  
A062 019



## PROFILE 8

Profile 8 was selected as a test case for the surface duct models of PLRAY and FACT, since it contains a 318-foot surface duct. To emphasize the effect of the duct, a high bottom loss (FNWC Type 5) was arbitrarily selected. Furthermore, all rays which penetrate the duct are bottom limited, so that there are no convergence zones. The source was located at a depth of 250 feet. Two receiver depths were selected, one at 150 feet, near the center of the duct, and the other at 450 feet, below the duct but within the depth interval covered by the PLRAY surface duct model. For each receiver depth semicoherent runs were made at three frequencies, 50, 100, and 200 Hz, corresponding to duct depths of approximately 3, 6, and 12 wavelengths respectively.

The plots at 50 Hz for the shallow receiver depth are shown in figure 48. At 50 Hz the duct is so leaky that the intensity drops to the level of the bottom-bounce propagation within the first 5 kyd. Within this region it is seen that PLRAY agrees closely with AP2, while the FACT curve drops somewhat too rapidly. In the range interval between 5 and 25 kyd the agreement between PLRAY and AP2 is excellent. Beyond 25 kyd the two curves separate widely until they merge again at about 43 kyd. The reason for the wide divergence is not obvious, though it appears to occur near the transition interval between the first and second bottom-bounce regions. The behavior of FACT beyond 5 kyd, however, bears little resemblance to PLRAY and AP2.

The results at 100 Hz are shown in figure 49. Here the duct is more efficient at trapping energy and the level of the bottom-bounce propagation is not reached until about 10 kyd. Except for a slight distortion of the range scale between 20 and 30 kyd and an interval of too high intensity between 32 and 38 kyd, PLRAY agrees well with AP2 throughout the entire plot. FACT, on the other hand, shows a radically different behavior. In the ducted region the loss predicted by FACT is too high, though the discrepancy is less than at 50 Hz. Throughout the bottom-bounce region, although the average levels are reasonable, the interference pattern has an entirely different character from that of the other two programs.

At 200 Hz, figure 50, the effect of the duct is visible out to a range of at least 20 kyd. Throughout this range interval both PLRAY and FACT show higher losses than AP2, though below about 8 kyd the divergence of PLRAY is somewhat smaller. The behavior of the AP2 curve at ranges below 5 kyd appears to be questionable, due to a shortage of modes. From 15 to 30 kyd PLRAY shows the same major features as AP2, though the losses tend to be 3 db too high. Beyond 30 kyd there is a wide divergence, with the PLRAY curve continuing to drop in large irregular oscillations and the AP2 curve leveling out at values between 85 and 90 db. FACT shows none of the features of the other two programs, though the average level appears to follow the same trend as PLRAY.

The 50-Hz curves for the 450 ft receiver depth are plotted in figure 51. At very short ranges below about 3 kyd both ray programs agree fairly well with AP2. From 3 to 8 kyd PLRAY and FACT agree with each other, but both curves depart widely from AP2, which drops much more steeply with increasing range. In the bottom-bounce region out as far as 28 kyd PLRAY closely follows the normal mode curve. The two curves diverge widely in the interval between 28 and 45 kyd, but come together again between 45 and 50 kyd. The behavior of



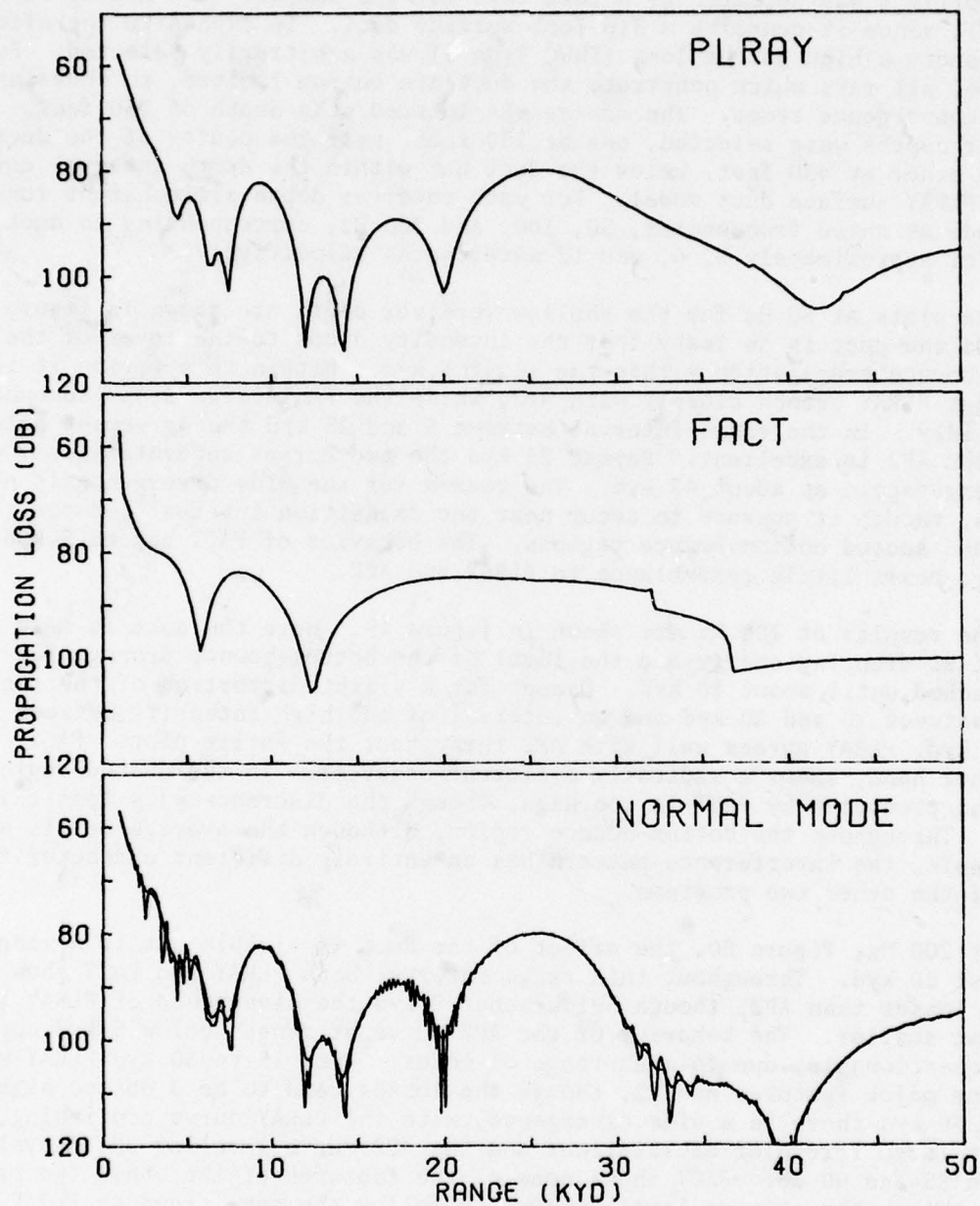


FIGURE 48 - Semicoherent Propagation Loss, Profile 8; Frequency 50 Hz, Source Depth 250 Ft, Receiver Depth 150 Ft

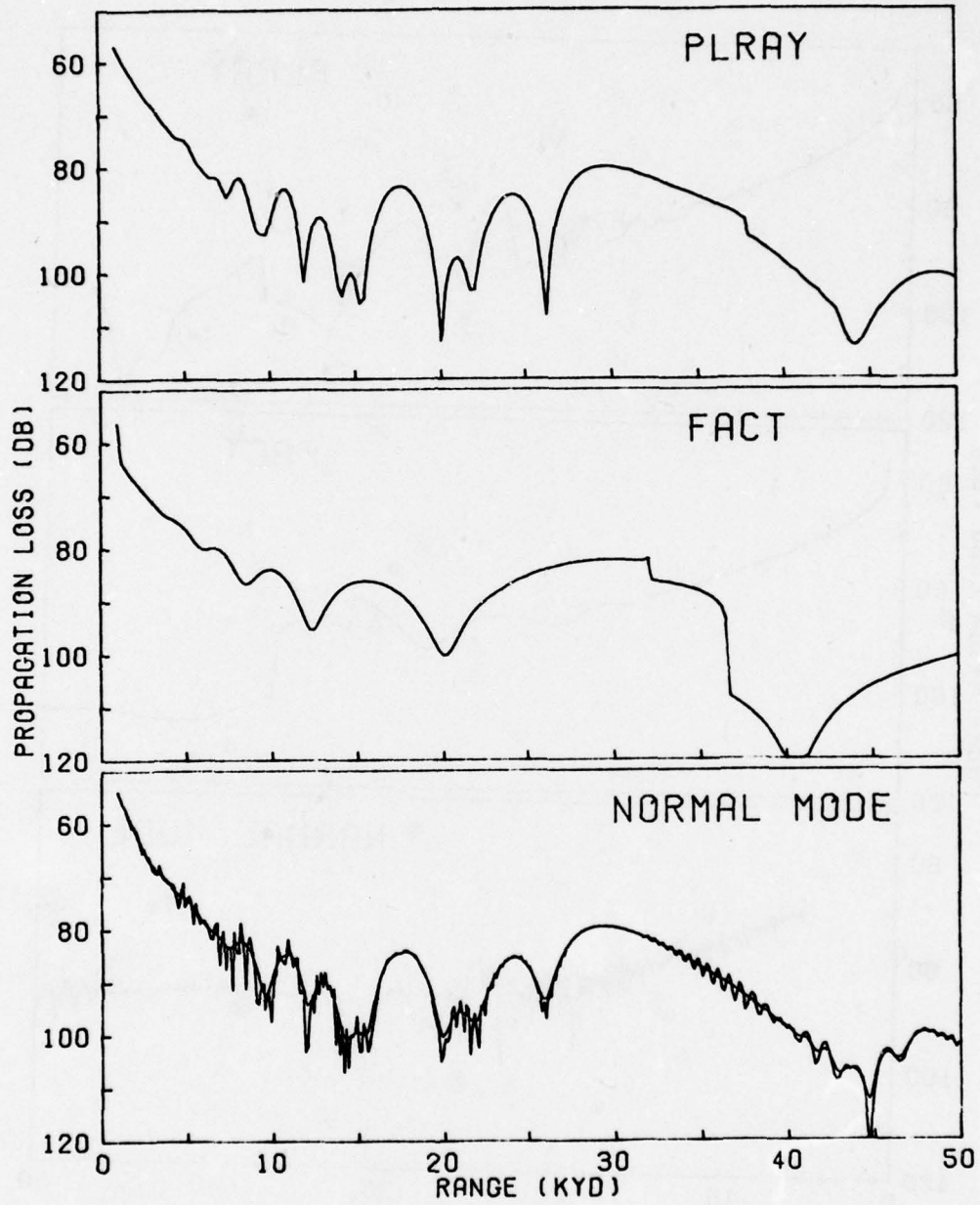


FIGURE 49 - Semicoherent Propagation Loss, Profile 8; Frequency 100 Hz, Source Depth 250 Ft, Receiver Depth 150 Ft

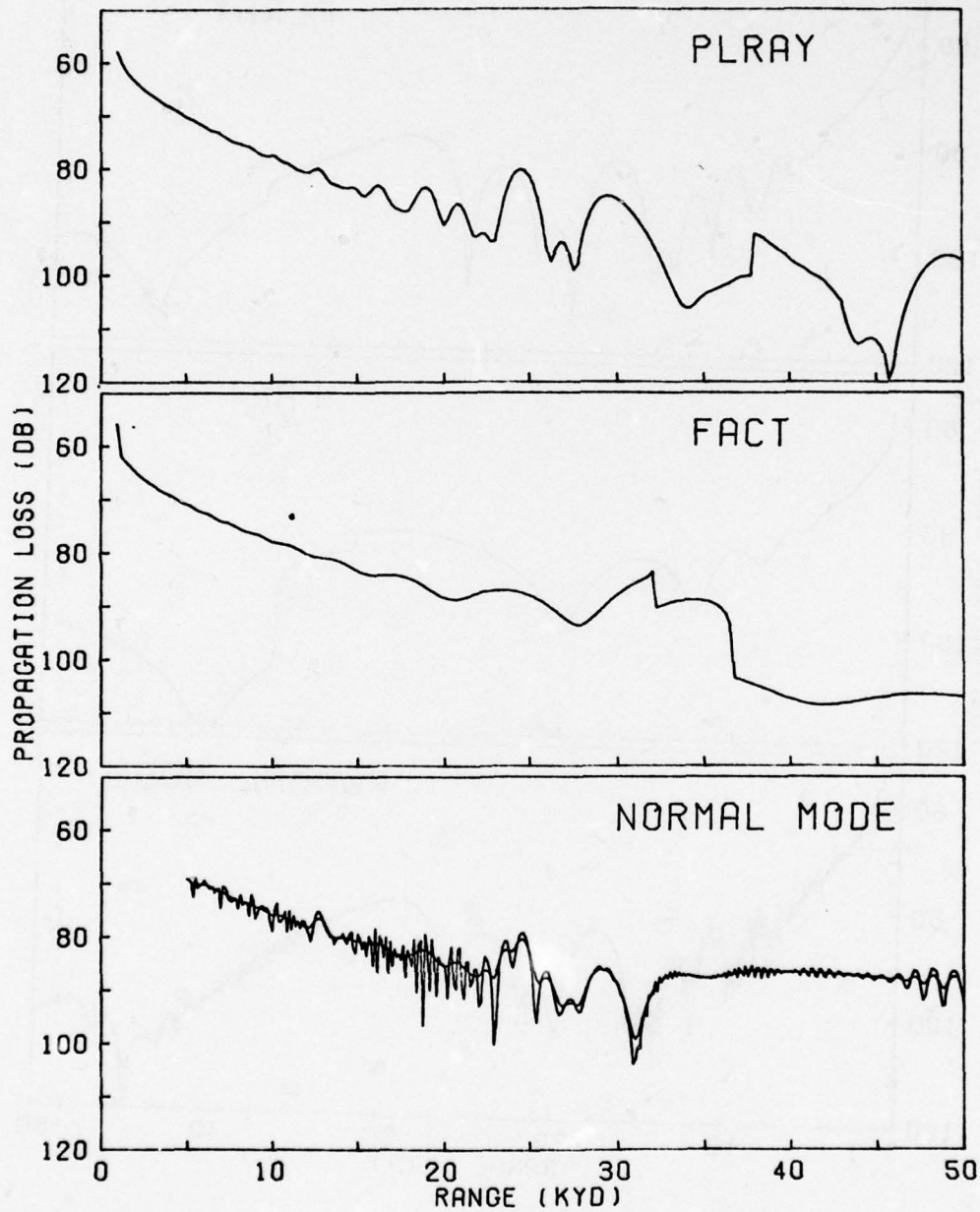


FIGURE 50 - Semicoherent Propagation Loss, Profile 8; Frequency 200 Hz, Source Depth 250 Ft, Receiver Depth 150 Ft



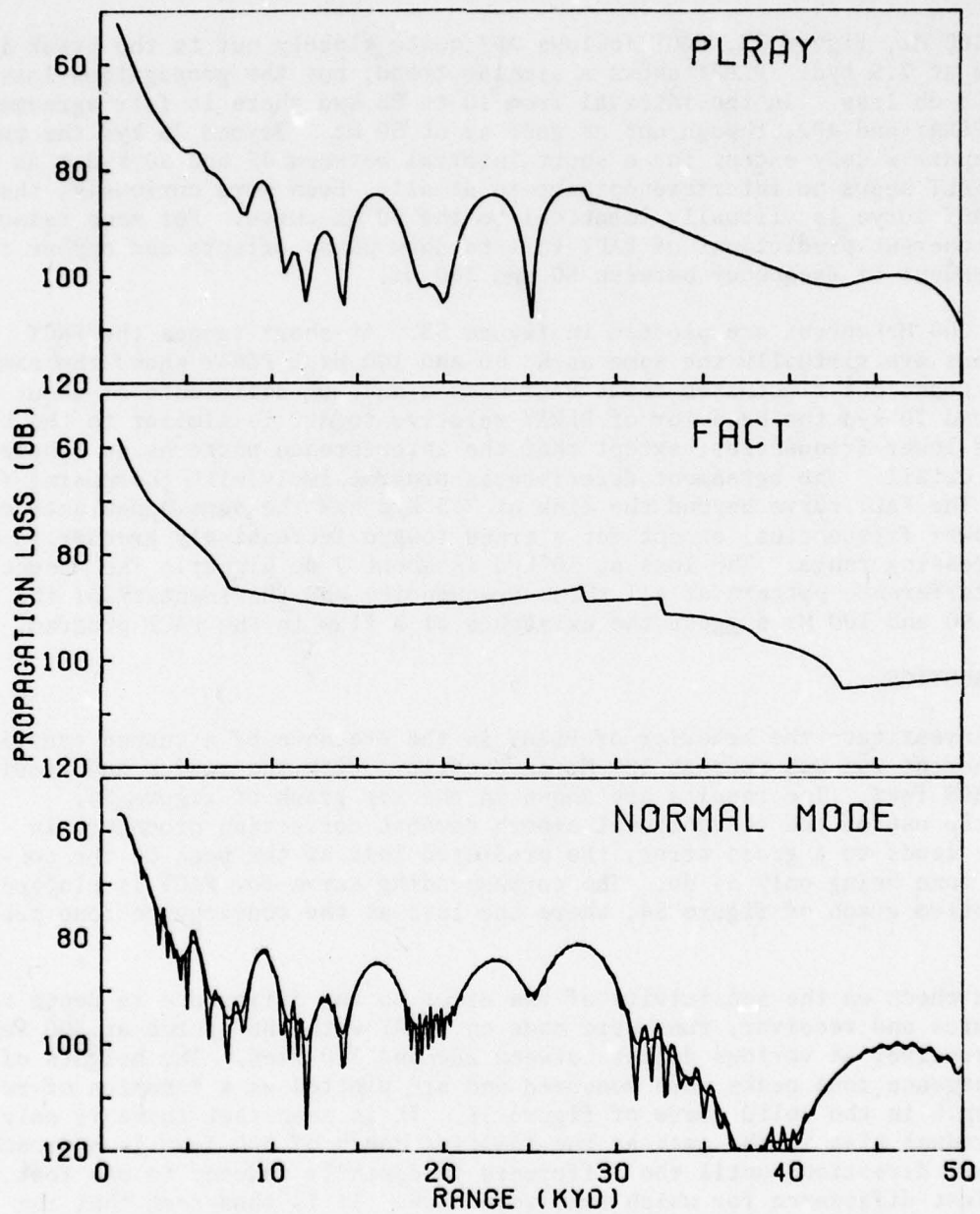


FIGURE 51 - Semicoherent Propagation Loss, Profile 8; Frequency 50 Hz,  
Source Depth 250 Ft, Receiver Depth 450 Ft

FACT beyond 7.5 kyd is exceedingly strange. It shows none of the phase oscillations characteristic of the semicoherent mode of ray summation.

At 100 Hz, figure 52, FACT follows AP2 quite closely out to the break in the slope at 7.5 kyd. PLRAY shows a similar trend, but the propagation loss is about 3 db less. In the interval from 10 to 25 kyd there is fair agreement between PLRAY and AP2, though not as good as at 50 Hz. Beyond 25 kyd the two curves depart widely except for a short interval between 45 and 50 kyd. As before, FACT shows no interference pattern at all. Even more curiously, the 100 Hz FACT curve is virtually identical to the 50 Hz curve. For some reason the semicoherent predictions of FACT fail to show phase effects and appear to be independent of frequency between 50 and 100 Hz.

The 200 Hz curves are plotted in figure 53. At short ranges the FACT predictions are virtually the same as at 50 and 100 Hz. PLRAY shows the same general trend, but fluctuates about FACT with a maximum difference of about 3 db. Beyond 10 kyd the behavior of PLRAY relative to AP2 is similar to the behavior at lower frequencies, except that the interference patterns no longer agree in detail. The agreement deteriorates progressively with increasing frequency. The FACT curve beyond the kink at 7.5 kyd has the same appearance as at the lower frequencies, except for a trend toward increasingly greater loss with increasing range. The loss at 50 kyd is about 7 db higher. The absence of an interference pattern at all three frequencies and the identity of the results at 50 and 100 Hz suggest the existence of a flaw in the FACT program.

#### CUSPED CAUSTICS

To investigate the behavior of PLRAY in the presence of a cusped caustic, a semicoherent run was made at 100 Hz on Profile 3 with the source and receiver both at 300 feet. The results are shown in the top graph of figure 54. Clearly the use of the conventional smooth caustic correction procedure in this case leads to a gross error, the predicted loss at the peak of the convergence zone being only 54 db. The corresponding curve for FACT is plotted on the bottom graph of figure 54, where the loss at the convergence zone peak is 72 db.

As a check on the sensitivity of the error to the difference in depth between source and receiver, runs were made on PLRAY with the source at 300 feet and the receiver at various depths between 280 and 320 feet. The heights of the convergence zone peaks were measured and are plotted as a function of receiver depth in the solid curve of figure 55. It is seen that there is only a very gradual rise in the peak as the limiting depth of 300 feet is approached from either direction, until the difference in depth is reduced to one foot, the smallest difference for which runs were made. It is thus seen that the region of serious error is very narrow.

Companion runs were made on FACT and AP2 at receiver depths of 280, 290, 295, 300, 305, 310, and 320 feet. The peak values of the FACT convergence zone are plotted in the dashed curve of figure 55. The corresponding peak values for AP2, after smoothing by a 5-point weighted sliding window, are plotted in the dot-dash curve. The selection of 5 points for the window is a compromise between the unsmoothed output, which contains a local spike at the maximum point, and the 9-point smoothing which introduces too much rounding of

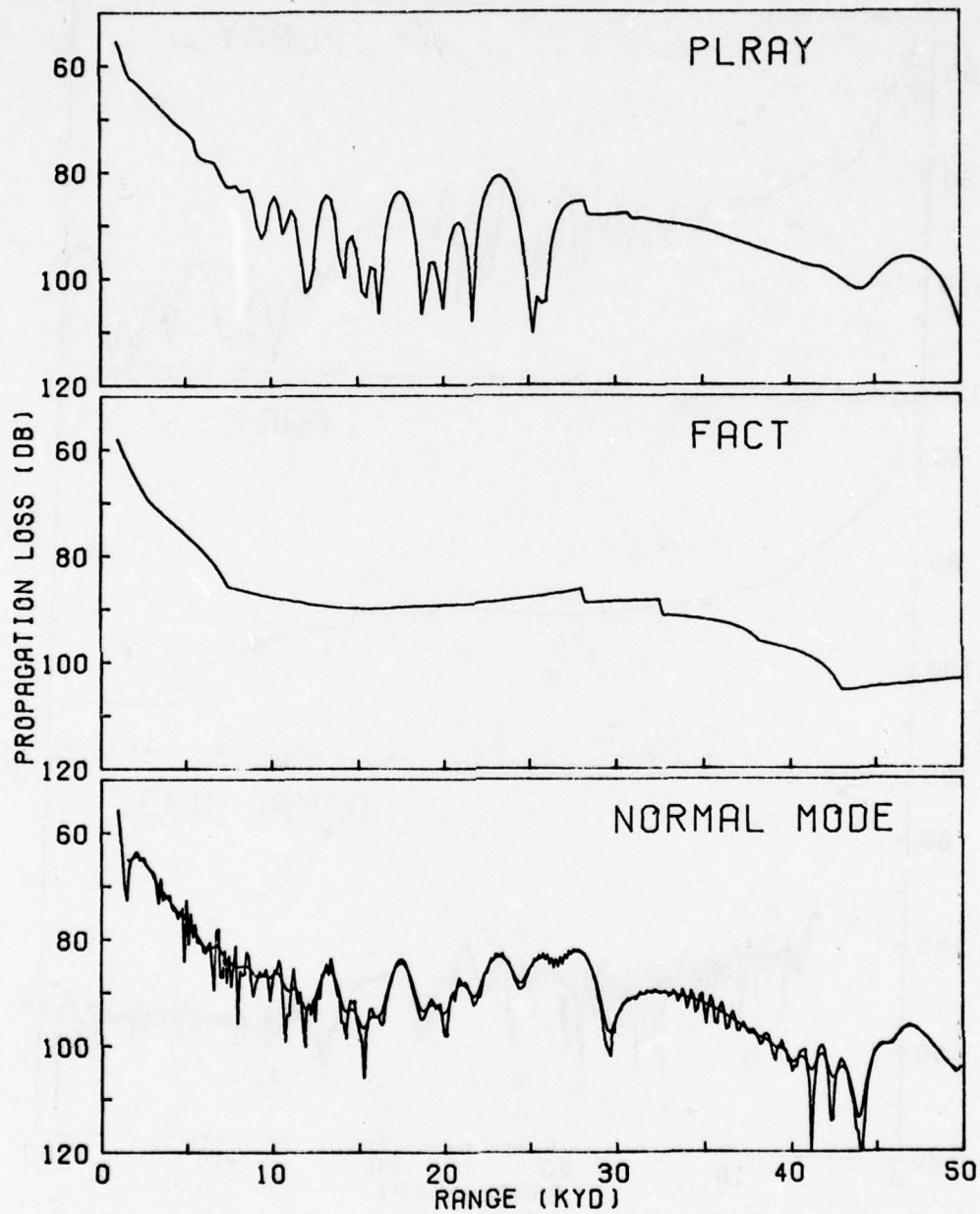


FIGURE 52 - Semicoherent Propagation Loss, Profile 8; Frequency 100 Hz,  
Source Depth 250 Ft, Receiver Depth 450 Ft



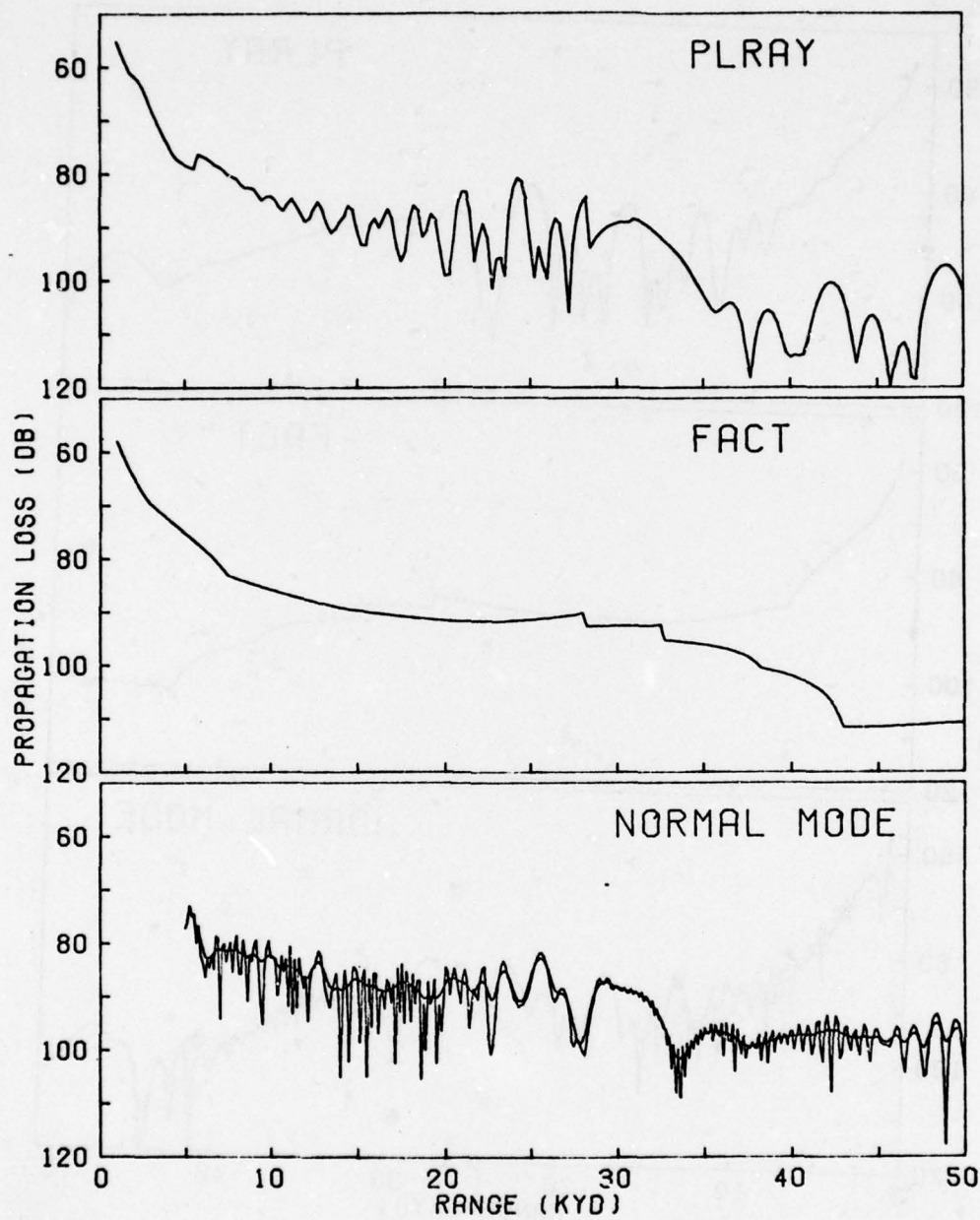


FIGURE 53 - Semicoherent Propagation Loss, Profile 8; Frequency 200 Hz, Source Depth 250 Ft, Receiver Depth 450 Ft

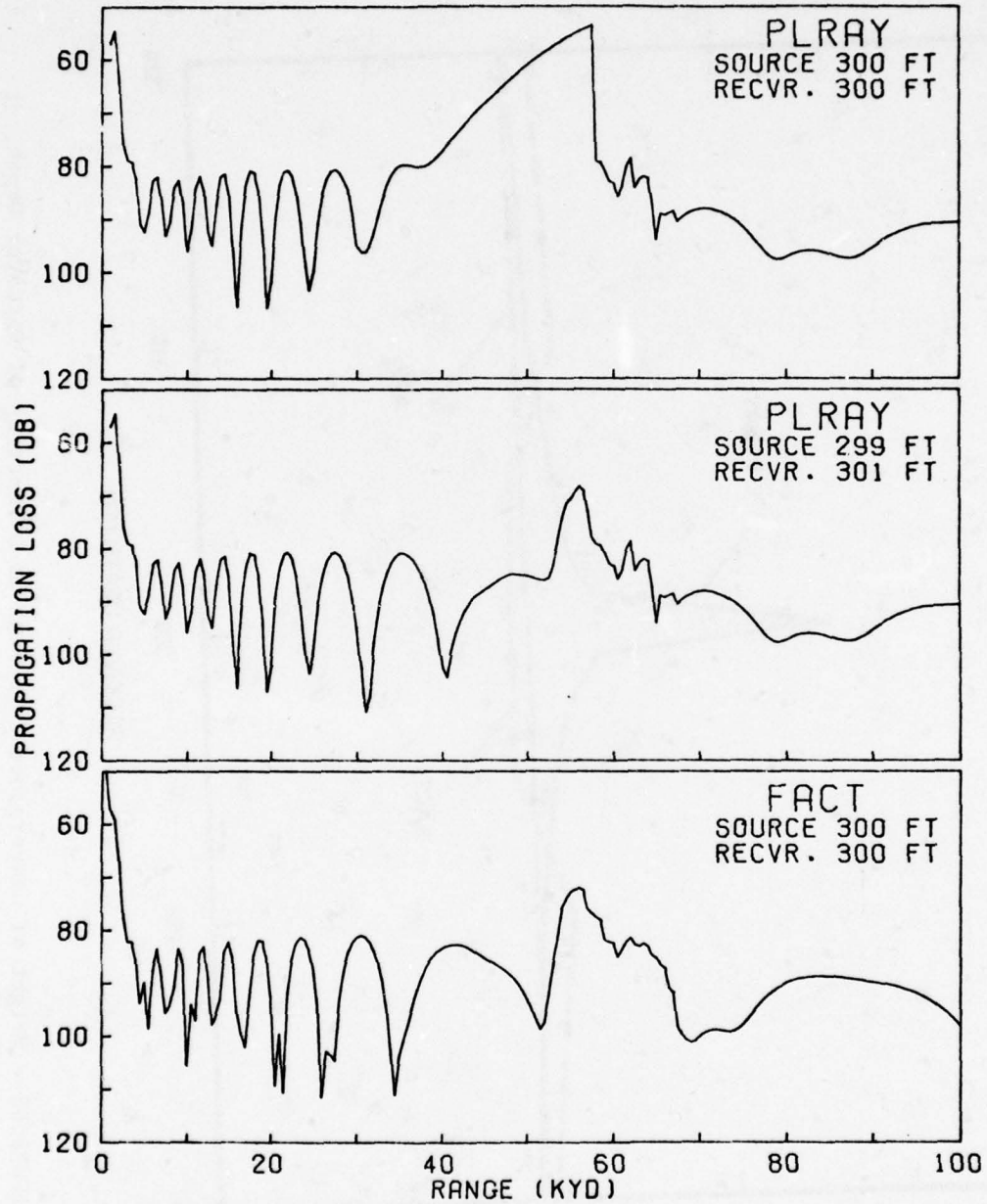


FIGURE 54 - Semicoherent Propagation Loss, Profile 3, Showing Effect of Cusped Caustic; Frequency 100 Hz

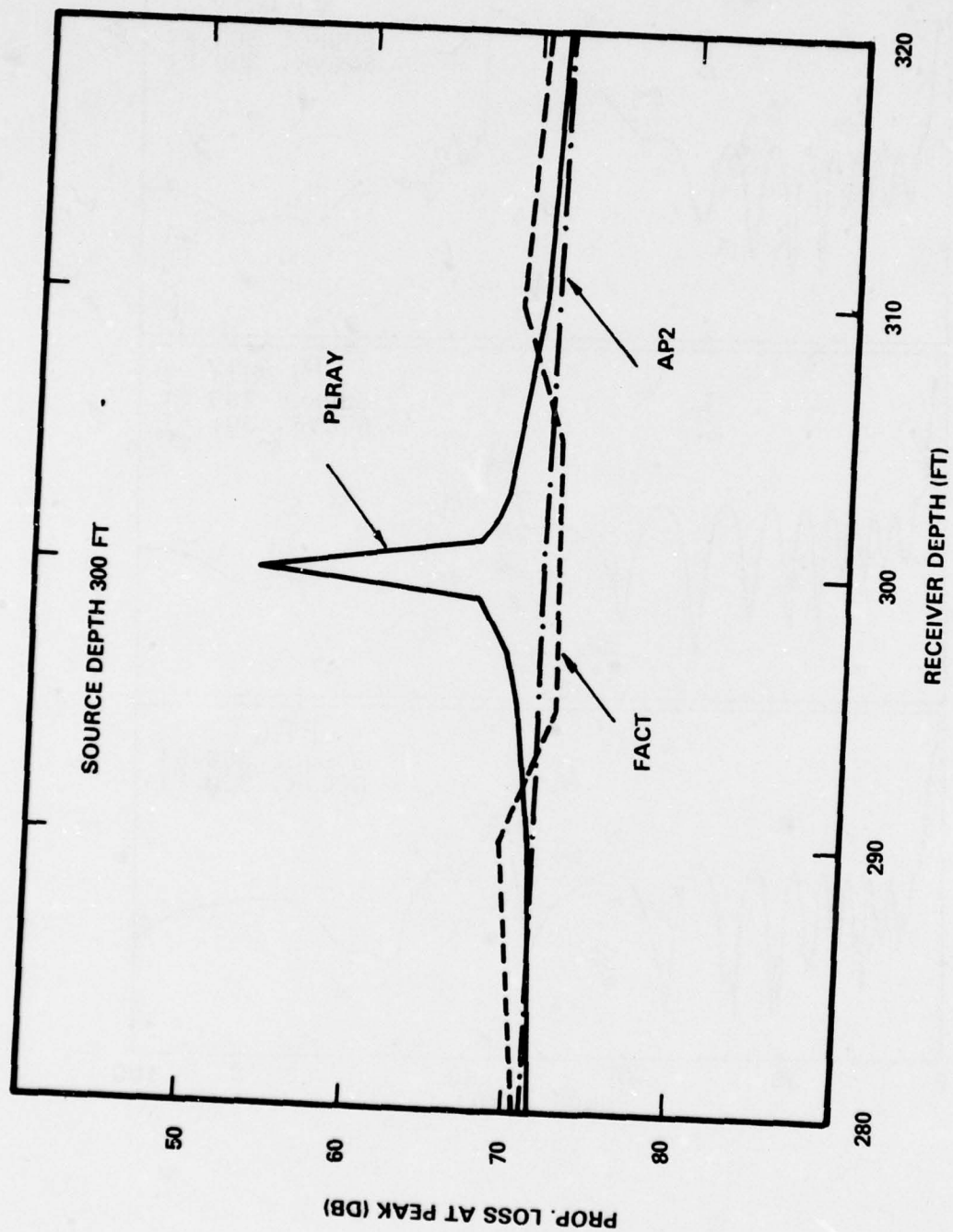


FIGURE 55 - Height of Convergence Zone Peak as a Function of Receiver Depth, Profile 3; Frequency 100 Hz



the narrow convergence zone peak. A plot of the unsmoothed data would raise the AP2 curve of figure 55 by about 1 db.

Inspection of figure 55 reveals that the normal mode curve is essentially flat over the entire plot, the maximum variation being only 0.5 db. At depths less than 290 feet and greater than 310 feet FACT exhibits the same tendency as PLRAY with even higher zone peaks. However, between 290 and 310 feet the curve drops below the AP2 curve, suggesting that the cusped caustic correction of FACT produces a slight over-correction.

To avoid the gross error resulting from the lack of a cusped caustic correction, PLRAY has been modified to insert a provision to move the source upward and the receiver downward, when necessary, to insure a depth separation of at least 2 feet. When this is done, a diagnostic is printed. The effect of the modification may be seen in the center plot of figure 54, in which the source is at 299 feet and the receiver at 301 feet. The 2-foot depth separation has reduced the convergence zone to reasonable proportions, within less than 3 db of AP2, without altering the curve perceptibly at ranges well away from the cusped caustic.

## DISCUSSION

PLRAY has been compared with FACT in 21 different cases involving 8 different velocity profiles. In most of the cases comparisons have been made for both the semicoherent and the incoherent types of ray summation. In most of the semicoherent cases the two ray program outputs have been checked against the output of the AP2 normal mode program which provides a more accurate representation of the sound field because it is an exact solution of the wave equation. In many of the runs the normal mode program was not capable of producing useful results at short ranges in the bottom-bounce region where the number of modes required was in excess of the maximum available number of 500. The portions of the AP2 propagation loss plots below the minimum reliable range have been omitted. However, in most of these cases AP2 produced useful results in the direct propagation zone at very low ranges and although not shown on the plots, these results have provided a check on the performance of PLRAY and FACT.

### INCOHERENT RUNS

It has been observed in the incoherent runs that when using the same bottom loss inputs PLRAY and FACT consistently show excellent agreement in the bottom-bounce regions. The one case (figure 31) in which a significant difference was observed was a run at a frequency of 300 Hz. The discrepancy is due to the manner in which the FNWC bottom loss curves are implemented. In the low frequency region FNWC curves are provided at frequencies of 100, 500, and 1000 Hz. At all frequencies below 100 Hz the 100 Hz curve is used in both programs. Between 100 and 500 Hz and between 500 and 1000 Hz PLRAY interpolates linearly between the appropriate pair of curves. FACT, on the other hand, applies the 100 Hz curve to all frequencies up to 150 Hz, the 500 Hz curve to all frequencies between 150 Hz and 700 Hz, and the 1000 Hz curve to

all frequencies between 700 and 1000 Hz; thus, there are discontinuous jumps in the bottom loss at 150 and 700 Hz.

The behavior of PLRAY and FACT in the direct propagation zone (the region covered by the direct and surface-reflected shallow rays) is much the same in both the incoherent and semicoherent runs and will be discussed below. With a few exceptions the same is true of the convergence zones.

#### SEMICOHERENT RUNS - BOTTOM-BOUNCE INTERFERENCE PATTERNS

In the semicoherent runs the phase interference patterns are manifested chiefly in the bottom-bounce regions. Since the semicoherence technique considers only the coherence between the rays of each individual arrival order and treats the resultant intensities of the various arrival orders incoherently, the interference patterns tend to be smoothly scalloped. The normal mode output is fully coherent and contains a fine structure which results from interference between different arrival orders. Comparison with the PLRAY and FACT outputs is facilitated by the smoothing technique which filters out most of the fine structure. It will be noted, however, that the smoothing procedure produces excessive rounding of the sharp dips at the points of destructive interference between the scallops. At such points the original unsmoothed AP2 curves provide a more realistic comparison with PLRAY and FACT.

In most of the runs the individual features of the AP2 smoothed interference pattern are clearly recognizable in both the PLRAY and FACT curves. In several of the runs the agreement is excellent. The agreement tends in general to deteriorate with increasing source and/or receiver depth, with increasing range, and with increasing frequency. The deterioration with increasing depth is undoubtedly due to the approximate nature of the coherence computation, which is based on the assumption that between the depth of interest (source or receiver) and the surface the direct and surface-reflected rays are parallel straight lines. As the source or receiver becomes deeper, the rays depart more from parallelism and more distortion is introduced by ray refraction. Similar considerations apply to the effect of increasing range. At short ranges where the angles are large, the rays are approximately straight lines. As the range increases, the rays become more nearly horizontal and refraction effects become important. These effects are aggravated by an increase in the frequency, which shortens the wavelength and increases the phase differences.

In comparing the interference patterns of the three programs it has been observed in a number of instances that although the patterns agree quite well in the levels and relative locations of the individual features, the absolute ranges do not agree. The effect appears as an expansion or contraction of the range scale. The most likely source of the range distortion was at first thought to be the difference in the methods employed in the three programs in fitting the velocity profile. FACT uses linear segments; PLRAY uses curvilinear segments which join with continuous slope; AP2 uses segments in which the square of the index of refraction (or  $1/c^2$ ) varies linearly with depth. As a check on this hypothesis runs on Profile 1 covering a portion of the bottom-bounce region were made with the old NADC Ray-Tracing Program (reference (a)) using both linear and curvilinear segments, since that program offers the option of either type of curve fit. The results were negative. The change from

curvilinear to straight-line segments produced virtually no change in the interference pattern.

A second possible source of the range distortion is the difference between PLRAY and FACT in the method of computing the coherent intensity. Where the four bottom-bounce rays of a given arrival order are involved, PLRAY uses the average range of all four rays, whereas FACT uses only the first (down-up) ray. However, a check on the range difference in the run with Profile 1 revealed that the effect was too small in magnitude. Moreover, this effect would always be in the same direction, whereas errors in both directions have been observed in the various runs. In addition, this explanation does not account for the discrepancies between PLRAY and AP2. A third possible source of error is the approximation made by FACT in replacing the actual range-angle curves with parabolas fitted to three points. It has been found that this approximation is capable of introducing both range and intensity errors. However, it can have no bearing on the behavior of PLRAY relative to AP2.

The source of the range distortion has not yet been determined. It is clearly profile-dependent and, relative to AP2, it appears to affect PLRAY and FACT in opposite directions. With profiles having appreciable surface ducts (Profiles 1, 4, and 8) there seems to be a tendency for PLRAY to show an expansion and FACT a contraction, while with the other profiles there seems to be a tendency in the other direction. Finally, it should be noted that the range scale distortion affects only the bottom-bounce region; it appears to have no effect (or at least no correlated effect) on the location of the convergence zones.

If allowance is made for the distortion of the range scales, there is fair to good--and occasionally excellent--agreement in the interference patterns between AP2 and the two ray programs, out to at least moderate ranges, in most of the runs. On the whole, neither of the programs performed significantly better than the other. There are, however, two notable exceptions. First, in the runs on Profile 8, with the source in the surface duct, FACT shows anomalous behavior at all three frequencies. In the first set of runs with the receiver in the duct the interference pattern generated by FACT differs radically from those of PLRAY and AP2. Even more anomalously, in the second set of runs, with the receiver below the duct, FACT exhibits no interference pattern at all. Moreover, FACT generated the same output at 100 Hz as at 50 Hz.

Secondly, in the two runs (figure 40 and 46) in which both source and receiver were located near the axis of a major sound channel, both PLRAY and FACT failed to show reasonable agreement with AP2. The first of these runs was based on a profile from the Iceland area. Profile 5 contains a very deep sub-surface channel extending down to 1600 feet, with its axis at 485 feet. The source was located at 300 feet, well into the channel, and the receiver was located below the channel axis at 1000 feet. In such a situation the dominant contribution to the propagation tends to come from the channel and contains many more caustics than are normally encountered when no such channel is present. It appears that neither of the programs did an adequate job of handling the caustics. However, as may be seen in figures 40 and 41, FACT performed considerably better than PLRAY. The second case of poor agreement involves Profile 7, which was taken from the Mediterranean Sea. The region of minimum sound speed in Profile 7 is very broad and flat, ranging from about



250 feet to 1600 feet and encompassing both the source at 300 feet and the receiver at 1000 feet. In addition to the caustic problem, which does not appear to have been so serious in this case, there is another factor which adversely affects the coherence computations. The sound speed at the surface is more than 80 ft/sec higher than at either the source or receiver and in the intervening region there is a very strong negative gradient. The resulting bending of the rays may be expected to introduce significant errors into the assumption of straight-line propagation on which the coherence computations are based.

The range sampling problem has been discussed in detail in connection with the runs on Profile 3 and will only be summarized here for the sake of completeness. In FACT, whenever the number of range points per cycle of the interference oscillations is too small to provide adequate sampling, the amplitude of the oscillations is reduced by application of an attenuation factor. The attenuation factor varies from the full value of 1 at 6 points per cycle to 0 at  $2\frac{2}{3}$  points per cycle. PLRAY uses a smooth curve which closely approximates the linear segments of FACT. The two programs differ, however, in the method of computing the number of points per cycle. PLRAY computes instantaneous values from an analytical formula, whereas FACT computes an average value based on the total range interval covered by all the rays of the sector. In cases where the number of points per cycle varies drastically from one end of the range interval to the other, the attenuation factors applied by FACT deviate drastically from the factors applied by PLRAY.

Comparison of the FACT output with AP2 at short ranges where the number of points per cycle is far less than 6 and yet the amplitudes of the oscillations are not appropriately attenuated, has led to the conclusion that the values of 6 and  $2\frac{2}{3}$  are too high and should be reduced. Further investigation is needed to determine the proper values.

#### CONVERGENCE ZONES

In general there is quite good agreement among the three programs on the locations of the convergence zones but much poorer agreement on the shapes of the zones and the heights of the peaks. In one or two runs (see figures 34 and 38) PLRAY gave better performance in relation to AP2 than FACT; in others (see figure 24) FACT was definitely superior. Occasionally (see figure 44) both ray programs performed reasonably well. However, in the majority of the runs neither PLRAY nor FACT agreed well enough with AP2 to make it meaningful to attempt to rate one of them as being better than the other.

There are a few runs which merit special comment. In the run on Profile 1 (figure 20) the convergence zone shown by both PLRAY and FACT is not present in the AP2 output. The appearance of the zones indicates a basic error of ray theory. Reference to figure 6 shows that the depth excess in Profile 1 is less than 100 feet. This means that the energy which forms the convergence zone is confined to an extremely narrow bundle of rays. Whereas ray theory assumes that the bundle remains intact at all ranges, the normal mode output shows that there is actually sufficient leakage by diffraction to dissipate the energy before it reaches the convergence zone range. In the runs on Profile 4 it will be noted that as the receiver depth is increased (figures 34 and 36) FACT develops a very deep valley between the two convergence zone peaks. The valley does not appear in either PLRAY or AP2. In the runs on Profile 6, figures 42

and 43, the FACT convergence zones have a very unrealistic appearance. The fact that there is fair agreement between PLRAY and AP2 in the zone suggests that FACT has run into a problem, probably involving the caustic correction.

In the runs on Profiles 2, 3, and 5, figures 22 and 23, 26 and 27, and 38 and 39, there is a noticeable difference in the FACT convergence zones between the semicoherent and incoherent cases, but little or no difference in the PLRAY zones. In the incoherent run of figure 27 the leading edge of the FACT zone occurs about one kiloyard sooner and the first peak is about 2 db higher than in the semicoherent run. The second peak has disappeared altogether. In the case of Profile 5 the intensity throughout the bulk of the semicoherent zone, figure 38, is 3 to 5 db higher than the intensity in the incoherent zone, figure 39.

#### DIRECT ZONES

The primary interest in the direct zone propagation is focused on those profiles (1, 4, and 8) which contain surface ducts of appreciable thickness. In the other profiles, with one exception, there is reasonably good agreement among the three programs. The exception is the run of figure 26 and has been discussed earlier.

The surface duct of Profile 1 is rather poor at the frequency of 105 Hz, the number of trapped modes (see equation K-13 of appendix K) being only 0.5. As a result, the intensity drops very rapidly in the first few kiloyards. As may be seen in figure 20, PLRAY and FACT show essentially the same rate of fall-off. Beyond 3 kyd, where the normal mode curve begins, there is good agreement also with AP2.

The duct of Profile 4 at 150 Hz is slightly better, the trapped mode parameter being 0.7. The direct propagation zone extends to about 7 kyd. As pointed out previously, there is fair to good agreement between PLRAY and AP2 throughout this region in the runs at all receiver depths, figures 32, 34, and 36. In the first run FACT shows a tendency to deviate slightly in the direction of smaller loss. In the second and third runs FACT deviates in the direction of higher loss, rather badly so in the second run.

The trapped mode parameter of Profile 8 has values of 0.44, 0.63, and 1.05 at frequencies of 50, 100, and 200 Hz. Although all three values lie below the threshold at which the good duct model of PLRAY applies, a value in excess of 1 results in fairly good duct propagation, as is evident in figure 50. In the runs in which the receiver was located within the duct, figures 48 through 50, PLRAY was found to agree well with AP2 at the two lower frequencies while FACT predicted a loss that was somewhat too large. At 200 Hz, both PLRAY and FACT predicted too high a loss relative to AP2, FACT being a little closer than PLRAY. The results of the runs for the case in which the receiver was below the duct were quite variable. At 50 Hz, figure 51, PLRAY and FACT agree with each other but deviate from AP2, which shows an appreciably higher loss in the direct zone. At 100 Hz, figure 52, FACT agrees with AP2 while PLRAY shows too low a loss. At 200 Hz, figure 23, no two of the curves agree very well, though all three show essentially the same trend.

It is clear that the surface duct models of both PLRAY and FACT are a major improvement over ray theory in predicting acoustic propagation in a surface duct. Both models predict approximately the correct leakage of energy out of the duct as a function of frequency. With the source and receiver both in the duct, PLRAY appears to give results which agree somewhat more closely with normal mode predictions than FACT. When the source or receiver is slightly below the bottom of the duct, the results appear to be more variable with neither model agreeing particularly well with the normal mode results. In this case, of course, the only contribution from the duct comes from the leakage of energy out of the duct. Considering the slopes of the propagation loss curves as a function of frequency it is seen that the frequency variation has far less effect when the source or receiver is below the duct than when both source and receiver are in the duct.

In the AP2 curves there is a noticeable change in the slope between 50 and 100 Hz but very little change between 100 and 200 Hz. In the PLRAY curves no consistent trend can be discerned, since the 50 and 200 Hz curves are essentially the same out to 10 kyd, whereas the 100 Hz curve shows a considerably gentler slope. The FACT curves are suspect because of the identity of the curves throughout their entire length at 50 and 100 Hz and the absence of an interference pattern in all three curves.

#### CUSPED CAUSTICS

Lacking a cusped caustic correction, PLRAY gives clearly unacceptable results when the source and receiver are at the same depth, as is evident in figure 54. The error is manifested as an erroneous caustic correction which results in an excessively wide convergence zone with an erroneously high peak intensity. However, the error is extremely sensitive to the difference in depth between the source and receiver. In the sample runs on Profile 3 a separation of only two feet reduced the level of the zone peak by 15 db to within less than 3 db of the values predicted by the normal mode program.



R E F E R E N C E S

- (a) C. L. Bartberger and T. L. Stover, The NADC Ray-Tracing Program, Naval Air Development Center Report No. NADC-SD-6833, 4 November 1968, UNCLASSIFIED.
- (b) C. W. Spofford, The FACT Model, Acoustic Environmental Support Detachment, Maury Center Report 109, November 1974, UNCLASSIFIED.
- (c) M. M. Holl, Technical Notes on Sound Propagation in the Sea, Volume 2, Meteorology International Report on Project M-153, June 1968, UNCLASSIFIED.
- (d) W. D. Wilson, Equation for the Speed of Sound in Sea Water, J. Acoust Soc Amer, Vol 32, p 1357, October 1960.
- (e) W. H. Thorp, Analytic Description of the Low-Frequency Attenuation Coefficient, J. Acoust Soc Amer, Vol 42, p 270, July 1967.
- (f) L. M. Brekhovskikh, Waves in Layered Media, Academic, New York, 1960, pp 474-492.
- (g) M. A. Pedersen and D. F. Gordon, Normal Mode and Ray Theory Applied to Underwater Acoustic Conditions of Extreme Downward Refraction, J. Acoust Soc Amer, Vol 51, pp 323-368, January 1972.
- (h) M. Abramowitz and I. A. Stegun, Handbook of Mathematical Functions, National Bureau of Standards Applied Mathematics Series No. 55, pp 446-449, U.S. Government Printing Office, 1964.
- (i) M. A. Pedersen and D. F. Gordon, Normal Mode Theory Applied to Short-Range Propagation in an Underwater Acoustic Surface Duct, J. Acoust Soc Amer, Vol 37, pp 105-118, January 1965.
- (j) C. Bartberger and L. Ackler, Normal Mode Solutions and Computer Programs for Underwater Sound Propagation, Part I - Two-Layer and Three-Layer Programs, Naval Air Development Center Report No. NADC-72001-AE, 4 April 1973, UNCLASSIFIED.
- (k) C. Bartberger and L. Ackler, Normal Mode Solutions and Computer Programs for Underwater Sound Propagation, Part II - Program for Arbitrary Velocity Profiles, Naval Air Development Center Report No. NADC-72002-AE, 4 April 1973, UNCLASSIFIED.
- (l) D. C. Stickler, Normal Mode Program With Both Discrete and Branch-Line Contributions, J. Acoust Soc Amer, Vol 57, pp 856-861, April 1975.



A P P E N D I X   A  
LISTING OF FORTRAN SOURCE DECK



PAGE 1

PROGRAM PLRAY

```

PROGRAM PLRAY (INPUT,OUTPUT,TAPE1=OUTPUT)
C - INPUT DATA DECK FOR NADC RAY PROPAGATION LOSS PROGRAM, PLRAY
C CARD 1 - CONTROL INTEGERS
C   NF = NO. OF FREQUENCIES (UP TO 6)
C   NREC = NO. OF RECEIVER DEPTHS (UP TO 8)
C   IPROF = CONTROL PARAMETER FOR ENVIRONMENTAL INPUTS
C   IPROF = -1, CURVE-FIT ONLY. NO RAY TRACE. READ CARDS 2 AND 4 ON
C   IPROF = 0, NORMAL
C   IPROF = 1, BY-PASS ENVIRONMENTAL INPUTS. OMIT CARDS 2, 3, AND 4
C   IPROF = 2, BY-PASS VP INPUTS. OMIT CARD SET 4.
C   IPROF = 3, BY-PASS SPECIAL BOTTOM INPUTS. OMIT CARD SET 3.
C   IUNIT = UNITS PARAMETER FOR BT TEMPERATURES
C   IUNIT = 0, DEG F (DEPTHS MUST BE IN FEET)
C   IUNIT = 1, DEG C (DEPTHS MUST BE IN METERS)
C   IBEAM = BEAM CONTROL PARAMETER
C   IBEAM = 0, NO BEAM PATTERNS
C   IBEAM = 1, READ AND USE BEAM PATTERNS
C   IBEAM = 2, DO NOT READ. USE PATTERNS PREVIOUSLY READ IN
C   IPLOT = PLOT CONTROL PARAMETER
C   IPLOT = 0, NO PLOT
C   IPLOT = 1, PLOT
C   IPR = CONTROL INTEGER FOR PRINTING DIAGNOSTIC DATA
C   IPR = 0, NORMAL
C   IPR = 1, LEVEL 1 PRINTING
C   IPR = 2, LEVEL 1 + LEVEL 2
C CARD 2 - ENVIRONMENTAL DATA HEADER CARD
C   ISP = SURFACE PARAMETER (SEA STATE)
C   IRP = BOTTOM PARAMETER
C   IRP = -1, INFINITE BOTTOM LOSS (100 DB)
C   IRP = 0, BOTTOM LOSS = 0
C   IRP = 1 TO 5, FNNC BOTTOM TYPES
C   IRP = 6, READ SPECIAL BOTTOM LOSS INPUTS
C   LAT = LATITUDE (DEGREES, DECIMAL NUMBER)
C   (REQUIRED ONLY WHEN SPECIFYING TEMPERATURE AND SALINITY)
C   IDR = LEFTER N OR S (USED ONLY FOR IDENTIFICATION)
C   IDBT = RUN IDENTIFICATION

```

PAGE 2

PROGRAM PLRAY

C CARD SET 3 - SPECIAL BOTTOM INPUTS. REQD ONLY WHEN IBP=6 AND IPROF =  
 C CARD 3A - NFR = NO. OF FREQUENCIES  
 C FRH(J) = FREQUENCY (HZ)  
 C CARD PAIR 3B - DB(I,6,J) = BOTTOM LOSS (DB)  
 C CARD PAIR 3C - DG(I,6,J) = GRAZING ANGLE (DEG)  
 C CARD SET 4 - VELOCITY PROFILE  
 C ZN(DB) = DEPTH (FEET OR METERS)  
 C CB(NB) = SOUND SPEED (FT/SEC OR M/SEC)  
 C T = TEMPERATURE (DEG F OR C)  
 C S = SALINITY (PPT)  
 C NOTE - UNITS MUST BE CONSISTENT, EITHER ENGLISH OR METRIC  
 C NOTE - PUNCH 1 IN COL. 41 OF LAST V.P. CARD  
 C CARD 5  
 C F(IF) = FREQUENCY (HZ)  
 C JCOH(IF) = COHERENCE PARAMETER  
 C JCOH(IF) = 0, SEMICOHERENT  
 C JCOH(IF) = 1, INCOHERENT  
 C CARD 6 - ZSO = SOURCE DEPTH (FT)  
 C ZRO(I,REC) = RECEIVER DEPTH (FT)  
 C CARD 7 - RANGES (YD)  
 C RMIN = MINIMUM RANGE  
 C DR = RANGE INCREMENT  
 C RMAX = MAXIMUM RANGE  
 C CARD SET 8 - BEAM INPUTS (OMIT UNLESS IBEAM = 1)  
 C CARD 8A - ITYPE(IF) = BEAM TYPE PARAMETER  
 C ITYPE(IF) = 0, OMNIDIRECTIONAL  
 C ITYPE(IF) = 1, TABULAR INPUTS  
 C ITYPE(IF) = 2, VLA, OMNI ELEMENTS  
 C ITYPE(IF) = 3, VLA, LIMACON ELEMENTS  
 C ITYPE(IF) = 4, SINGLE HORIZONTALLY ORIENTED LIMACON ELEMENT  
 C ITYPE(IF) = 5, SINGLE VERTICALLY ORIENTED LIMACON ELEMENT  
 C IF DIR. OF MAX VLA RESP. IS NOT SAME AS BEAM AXIS, SET ITYPE = -  
 C CARD SFT 8B (ITYPE = 1 ONLY) - PRAT(1,IF) = PRESS. RATIO REL. TO R  
 C CARD 8C (APPLICABLE TO ITYPE(IF) = 2 TO 5 ONLY)  
 C NN(IF) = TOTAL NO. ELEMENTS IN ARRAY (APPLICABLE TO VLA TYPES ON  
 C (ELEMENTS SYMMETRICALLY LOCATED RELATIVE TO CENTER)

PAGE 3

PROGRAM PLRAY

```

C      PHSTR = BEAM STEER ANGLE, POS. UP (DEG) (APPLICABLE TO VLA TYPES
C      B(IF) = LIMACON PARAMETER (APPLICABLE TO LIMACON ELEMENTS ONLY)
C      CARD 80 (APPLICABLE TO VLA TYPES ONLY)
C      X(I,IF) = DISTANCE OF ITH ELEMENT ON EITHER SIDE FROM CENTER (FT
C      N = NO. ELEMENTS ON EACH SIDE (INCLUDING CENTER IF NN(IF) IS ODD
C      CARD 8E (APPLICABLE TO VLA TYPES ONLY)
C      W(I,IF) = WEIGHT OF ITH ELEMENT ON EITHER SIDE OF CENTER
C      NOTE - AS MANY DATA SETS AS DESIRED MAY BE STACKED IN SEQUENCE.
C      INSERT ONE BLANK CARD AT END.
C      COMMON CB(50),CSP(50),GP(50),IBEAM,IBP,IDBT(4),IPR,IPOF,ISP,
C      *NB,NF,PI,RADE,RTD,ZB(50),ZP(50)
C      COMMON CA(50),CAA,CAA2,CBB,CBB2,IAA,IAD,IBB,IDF(50),IDUCT,ISD,NA,
C      *SN,ZA(50),ZAA,ZAD,ZBB,ZR,ZS
C      COMMON BMFAC(6),CL(10),CV,CV2,ILB,ILS,NL,NTH,SIGN(4),TH(50),
C      *TH1,TH2,VA(50),VBM
C      COMMON ALPHA(6),BLOSS(50,6),BOTL(6),F(6),F13(6),IBOT,ISURF,
C      *SLOSS(6)
C      COMMON DR,H(251,6),HC(15,4,6),ICAUST(4),IFMAX,J1,KA(4,6),KB(4,6),
C      *KMAX,KMN,KMNJ(4),KMXJ(4),NCYC,NJ,R(50,4),RCYC(50),RMIN,RP(50,4),
C      *RPCYC(50),RPSR(50),RPUP(50),RSR(50),RUP(50)
C      COMMON /DATA/ DB(15,6,6),DG(15,6,6),FR(6)
C      COMMON /COH/ JCOH(6)
C      DIMENSION ZR0(8),COTYP(6)
C      REAL LAT
C      DATA FR /100.,500.,1000.,2000.,3500.,8000./
C      PI=3.14159265359 $ RTD=180./PI
C      RADE=20890000. $ CFAC=3.28083333
C      HMIN=1.258925E-100 $ ZDMAX=1000.
C      MAXK=251
C      10 READ 1010,NF,NREC,IPOF,IUNIT,IBEAM,IPL0T,IPR
C      1010 FORMAT(I015)
C      IF (NF.F0.0) GO TO 999
C      PRINT 2010
C      2010 FORMAT(1H1,40X,52HNADC RAY PROPAGATION LOSS PROGRAM -- NEW MODEL,
C      *1975,/)
C      PRINT 2020,NF,NREC,IPOF,IUNIT,IREAM,IPL0T,IPR

```



PAGE 4

PROGRAM PLRAY

```

2020 FORMAT(34X,7HNF      =,I3,10X,7HNREC  =,I3,10X,7HIIPROF =,I3,10X,
*7HIUNIT =,I3,34X,7HIBEAM =,I3,10X,7HIPLUT =,I3,10X,7HIIPR  =,I3,/)
      IF(IPROF.EQ.1) GO TO 11
      READ 1020,ISP,IRP,LAT,IDR,IDBT
1020  FORMAT(215,10X,F9.0,A1,10X,4A10)
      IF(LAT.EQ.0.) LAT=45.0
11  PRINT 2030,IDBT
2030  FORMAT(36X,24HRUN IDENTIFICATION -- ,4A10,/)
      PRINT 2040,LAT,IDR,ISP,IRP
2040  FORMAT(22X,10HLATITUDE =,F6.2,9H DEGREES ,A1,10X,17HSEA STATE (ISP
*) =,I3,10X,24HBOTTOM PARAMETER (IRP) =,I3,/)
      IF(IPROF.EQ.1) GO TO 85
      IF(IPROF.EQ.3.OR.IPROF.LT.0) GO TO 13
      IF(IRP.NE.6) GO TO 13
C---READ EXTERNAL BOTTOM LOSS INPUTS
      READ 1025,NFR,(FR(J),J=1,NFR)
1025  FORMAT(15,5X,6F10.0)
      DO 12 J=1,NFR
      READ 1040,(DB(I,6,J),I=1,15)
      READ 1040,(DG(I,6,J),I=1,15)
12  CONTINUE
13  IF(IPROF.EQ.1.OR.IPROF.EQ.2) GO TO 85
      NB=1
      READ 1030,ZB(NB),CB(NB),T,S,NDCCD
1030  FORMAT(4F10.0,11)
C---TEST TO DETERMINE WHETHER INPUTS ARE SOUND SPEED OR TEMP. AND SALINI
      IF(CB(NB).EQ.0.) GO TO 20
C---TEST TO DETERMINE WHETHER INPUTS ARE ENGLISH OR METRIC
      IF(CB(NB).LT.3000.) GO TO 15
      JPR=1 $ PRINT 2050
2050  FORMAT(56X,5HDEPTH,10X,11HSOUND SPEED/56X,4H(FT),12X,8H(FT/SEC),/)
      GO TO 35
15  JPR=2 $ PRINT 2051
2051  FORMAT(38X,5HDEPTH,10X,11HSOUND SPEED,10X,5HDEPTH,10X,11HSOUND SPE
*ED/39X,3H(M),13X,7H(M/SEC),12X,4H(FT),12X,8H(FT/SEC),/)
      GO TO 35

```

PAGE 5

PROGRAM PLRAY

```

20 IF(IUNIT.NE.0) GO TO 5
   JPR=3 $ PRINT 2052
2052 FORMAT(38X,5HDEPTH,11X,11HSOUND SPEED,8X,11HTEMPERATURE,8X,8HMSALIN
      *ITY/38X,4H(FT),12X,7H(DEG F),12X,5H(PPT),/)
      GO TO 35
25 JPR=4 $ PRINT 2053
2053 FORMAT(30X,5HDEPTH,10X,11HTEMPERATURE,7X,8HMSALINITY,11X,5HDEPTH,
      *10X,11HSOUND SPEED/31X,3H(M),13X,7H(DEG C),11X,5H(PPT),12X,4H(FT),
      *12X,8H(FT/SEC),/)
      GO TO 35
30 NB=NB+1
   READ 1030,ZB(NB),CB(NB),T,S,NDCCD
35 GO TO (40,45,50,55) JPR
40 PRINT 2060,ZB(NB),CB(NB)
2060 FORMAT(44X,F18.2,F18.3)
      GO TO 60
45 ZZ=ZB(NB) $ ZB(NB)=ZB(NB)*CFAC
   CC=CB(NB) $ CB(NB)=CB(NB)*CFAC
   PRINT 2061,ZZ,CC,ZB(NB),CB(NB)
2061 FORMAT(26X,F18.2,F18.3,F18.3,F18.2,F18.3)
      GO TO 60
C---CALCULATE SOUND SPEED FROM TEMPERATURE AND SALINITY
50 ZZ=ZB(NB)/CFAC $ TT=(T-32.)/1.8
   CB(NB)=VELOC(ZZ,TT,S,LAT)
   PRINT 2062,ZB(NB),CB(NB),T,S
2062 FORMAT(27X,F18.2,3F18.3)
      GO TO 60
55 ZZ=ZB(NB) $ ZB(NB)=ZB(NB)*CFAC
   CB(NB)=VELOC(ZZ,T,S,LAT)
   PRINT 2063,ZZ,T,S,ZB(NB),CB(NB)
2063 FORMAT(20X,F18.2,2F17.3,F18.2,F18.3)
60 CB(NB)=CB(NB)/(1.-ZB(NB)/RADE) $ ZB(NB)=ZB(NB)*(1.+ZB(NB)/(2.*RADE
   *))
   IF (NDCCD.EQ.0) GO TO 30
C---FIT CURVILINEAR SEGMENTS TO VELOCITY PROFILE
   CALL CURFIT

```

PAGE 6

PROGRAM PLRAY

```

      IF(IPROF.LI.0) GO TO 10
C---LOCATE BOTTOM OF SURFACE DUCT
      CM=CB(1) $ IDUCT=1
      DO 80 IB=1,NB
      IF(ZB(IB).GT.ZDMAX) GO TO 85
      IF(CB(IB).LE.CM) GO TO 80
      CM=CB(IB)
      IF(CB(IB).GT.CB(IB-1).AND.CR(IB).GT.CB(IB+1)) IDUCT=IB
      80 CONTINUE
      85 IF(IBP.NE.6) GO TO 100
      PRINT 2070
      2070 FORMAT(/,54X,26HSPECIAL BOTTOM LOSS INPUTS,/)
      PRINT 2071,(FR(J),J=1,NFR)
      2071 FORMAT(59X,14HFREQUENCY (HZ)/4X,6F19.1)
      PRINT 2072
      2072 FORMAT(/,7X,6(6X,13HANGLE  LOSS))
      PRINT 2073
      2073 FORMAT(7X,6(6X,13H(DEG)  (DB)),/)
      DO 90 I=1,15
      90 PRINT 2074,(DG(I,6,J),DB(I,6,J),J=1,NFR)
      2074 FORMAT(7X,6(3X,2F8.2))
      100 READ 1035,(F(IF),IF=1,6),(JCOH(IF),IF=1,6)
      1035 FORMAT(6F10.0,10X,6I1)
      DO 110 IF=1,NF
      110 JCOH(IF)=IABS(JCOH(IF))
      PRINT 2080,(F(IF),JCOH(IF),IF=1,NF)
      2080 FORMAT(/,25X,19HFREQUENCIES (HZ) =,6(F11.2,2H (,11,1H))
      READ 1040,ZS0,(ZR0(I),I=1,NREC)
      1040 FORMAT(8F10.0)
      PRINT 2090,ZS0,(ZR0(I),I=1,NREC)
      2090 FORMAT(24X,19HSOURCE DEPTH (FT) =,F11.2/21X,22HRECEIVER DEPTHS (FT
*) =,8F11.2)
      READ 1040,RMIN,DR,RMAX
      KMAX=(RMAX-RMIN)/DR+1.
      IF(KMAX.GT.MAXK) KMAX=MAXK
      RMAX=RMIN+(KMAX-1)*DR

```



PAGE 7

PROGRAM PLRAY

```

      PRINT 2100,RMIN,DR,RMAX
2100 FORMAT(/,30X,11HRANGES (YD),10X,6HRMIN =,F8.1,10X,4HDR =,F8.1,10X,
      *6HRMAX =,F9.1,/)
C---READ BEAM PATTERN INPUTS
      IF (IBEAM.EQ.1) CALL BEAM(0)
      FMAX=0.
      DO 120 IF=1,NF
      F13(IF)=F(IF)**(1./3.)
      F2=1.E-6*F(IF)*F(IF)
      ALPHA(IF)=(0.1*F2/(1.+F2)+40.*F2/(4100.+F2))/1000.
      IF (F(IF).LE.FMAX) GO TO 120
      FMAX=F(IF) $ IFMAX=IF
120 CONTINUE
      CALL SURF
C---CORRECTION FOR CURVATURE OF THE EARTH
      ZS=ZS0*(1.+ZS0/(2.*RADE))
C---SOURCE AND/OR RECEIVER MAY NOT BE PLACED WITHIN 0.1 FT OF SURFACE OR
      IF (ZS.NE.0..AND.ABS(ZS-ZB(NB)).GT.0.1) GO TO 130
      PRINT 3001
3001 FORMAT(10X,4SHSOURCE MAY NOT BE PLACED AT SURFACE OR BOTTOM)
      GO TO 10
130 IF (IPR.GT.1) PRINT 4001,(ZB(I),I=1,NB)
4001 FORMAT(3H ZB,10F12.4)
      IF (IPR.GT.1) PRINT 4002,(CB(I),I=1,NB)
4002 FORMAT(3H CB,10F12.4)
      ZST=ZS
      DO 460 IREC=1,NREC
      PRINT 2180,ZS0,ZR0(IREC)
2180 FORMAT(/,10X,14HSOURCE DEPTH =,F8.1,3H FT,15X,16HRECEIVER DEPTH =,
      *F8.1,3H FT,/)
      ZS=ZST
C - CORRECTION FOR CURVATURE OF THE EARTH
      ZR=ZR0(IREC)*(1.+ZR0(IREC)/(2.*RADE))
      IF (ZR.NE.0..AND.ABS(ZR-ZB(NB)).GT.0.1) GO TO 140
      PRINT 3002,IREC
3002 FORMAT(10X,7H(IREC =,I2,50H) RECEIVER MAY NOT BE PLACED AT SURFAC

```

PAGE 8

## PROGRAM PLRAY

```

*E OR BOTTOM)
GO TO 460
140 IF (ABS(ZR-ZS).GE.2.) GO TO 150
ZAV=(ZR+ZS)/2.
ZS=ZAV-1. $ ZR=ZAV+1.
PRINT 3003
3003 FORMAT(10X,88HSOURCE DEPTH RAISED AND RECEIVER DEPTH LOWERED TO PR
*OVIDE MINIMUM SEPARATION OF TWO FEET)
150 CALL INSERT
ICASE=1
IF (ZB8.LT.ZAA) ICASE=2
IF (IPR.GT.1) PRINT 4003,(ZA(I),I=1,NA)
4003 FORMAT(3H ZA,10F12.4)
IF (IPR.GT.1) PRINT 4004,(CA(I),I=1,NA)
4004 FORMAT(3H CA,10F12.4)
CALL SECLIM
IF (IPR.NE.0) PRINT 4009,(CL(I),I=1,NL)
4009 FORMAT(3H CL,10F12.4)
DO 200 K=1,KMAX
DO 200 IF=1,NF
200 H(K,IF)=0.
PRINT 2200
2200 FORMAT(/,35X,14HFREQUENCY (HZ))
2210 PRINT 2210,(F(IF),IF=1,NF)
2210 FORMAT(19X,7F12.1)
DO 205 IF=1,NF
IF (JCOH(IF).EQ.0) COTYP(IF)=4HSCOH
IF (JCOH(IF).EQ.1) COTYP(IF)=4HICOH
IF (JCOH(IF).EQ.2) COTYP(IF)=4H COH
205 CONTINUE
PRINT 2215,(COTYP(IF),IF=1,NF)
2215 FORMAT(19X,6(8X,A4))
PRINT 2220
2220 FORMAT(11X,5HRANGE)
PRINT 2230
2230 FORMAT(11X,5H(YDS),11X,21HPROPAGATION LOSS (DB),/)

```

PAGE 9

## PROGRAM PLRAY

```

ILO=2
DO 210 IL=1,NL
  IF (ABS(CL(IL)).EQ.CA(IAD)) ILO=IL
210 CONTINUE
  ISURF=IBOT=0
C---SECTOR LOOP
DO 400 IL=1,NL
  TH2=ACOS(CAA/ABS(CL(IL)))
  IF (IL.EQ.1) GO TO 390
C---RAY COMPUTATIONS SUPPRESSED. SURFACE DUCT MODEL TO BE USED INSTEAD
  IF (IL.LE.ILO.AND.ZAA.LT.ZAD.AND.ZBB.LT.ZAD) GO TO 390
  IF (IL.GT.ILS) ISURF=1
  IF (IL.GT.ILB) IBOT=1
  MJ=2
  IF (IL.EQ.2.AND.CL(1).EQ.CAA.AND.ICASE.EQ.1) MJ=1
  IF (MJ.EQ.1) TH1=-TH2
  CALL DIVSEC(IL)
  IF (IPR.NE.0) PRINT 4005,IL,ISURF,IBOT,NTH
4005 FORMAT(/,20H IL ISURF IBOT NTH ,4I9)
  IF (IPR.NE.0) PRINT 4006,(TH(ITH),ITH=1,NTH)
4006 FORMAT(3H,TH,17X,6E18.10)
  IF (NTH.EQ.0) GO TO 390
DO 250 ITH=1,NTH
  CV=CAA/COS(TH(ITH)) $ CV2=CV*CV
  SGN=TH(ITH)/ABS(TH(ITH))
  VA(ITH)=SGN*SQRT(CV2/CAA2-1.)
250 CALL INCR(ITH)
  IF (IPR.NE.0) PRINT 4007,(VA(ITH),ITH=1,NTH)
4007 FORMAT(3H VA,17X,6E18.10)
  IF (IPR.LE.1) GO TO 255
DO 251 ITH=1,NTH
251 PRINT 4008,RSR(ITH),RUP(ITH),RCYC(ITH),RPSR(ITH),RPUP(ITH),RPCYC(I
  *TH)
4008 FORMAT(20H RSR RUP RCYC RPSAME,6E18.10)
255 CONTINUE
  NCYC=0 $ NJ=MJ $ J1=2*ICASE-3

```



PAGE 10

## PROGRAM PLRAY

```

IF(ZAA.LT.ZAD.AND.ZBB.LT.ZAD) GO TO 286
IF(IPR.GT.0) PRINT 4011,IL,NCYC
4011 FORMAT(/,8H IL NCYC,7X,2I9)
DO 280 ITH=1,NIM
C---RANGES AND RANGE DERIVATIVES FOR ZEROth ORDER (DIRECT) ARRIVALS
  R(ITH,1)=RSR(ITH) $ RP(ITH,1)=RPSR(ITH)
  IF(ITH(ITH).LT.0.) GO TO 260
  R(ITH,MJ)=RUP(ITH)+J1*RSR(ITH)
  RP(ITH,MJ)=RPUP(ITH)+J1*RPSR(ITH)
260 IF(IPR.LE.1) GO TO 280
  IF(MJ.EQ.1) GO TO 270
  PRINT 4010,R(ITH,1),R(ITH,2),RP(ITH,1),RP(ITH,2)
4010 FORMAT(20H R1 RJI RPI RPJ1 ,4E18.10)
  GO TO 280
270 PRINT 4015,R(ITH,1),RP(ITH,1)
4015 FORMAT(20H R(ITH,1) RP(ITH,1) ,2E18.10)
280 CONTINUE
  IF(MJ.EQ.2) GO TO 282
  SIGN(1)=1.
  GO TO 284
282 SIGN(1)=SN*(2*ICASE-3) $ SIGN(2)=1.
284 CALL RAYSUM(IL)
286 CONTINUE
DO 310 ITH=1,NTH
  IF(MJ.EQ.1) GO TO 290
  R(ITH,1)=-(RUP(ITH)+J1*RSR(ITH))
  RP(ITH,1)=-(RPUP(ITH)+J1*RPSR(ITH))
  R(ITH,2)=J1*RSR(ITH) $ R(ITH,3)=-R(ITH,2) $ R(ITH,4)=-R(ITH,1)
  RP(ITH,2)=J1*RPSR(ITH) $ RP(ITH,3)=-RP(ITH,2)
  RP(ITH,4)=-RP(ITH,1)
  GO TO 310
290 IF(ITH(ITH).GT.0.) GO TO 300
  R(ITH,1)=RSR(ITH)-RUP(ITH) $ RP(ITH,1)=RPSR(ITH)-RPUP(ITH)
  R(ITH,2)=RSR(ITH) $ RP(ITH,2)=RPSR(ITH)
  GO TO 310

```

PAGE 11

PROGRAM PLRAY

```

300 R(ITH,1)=-RSR(ITH) $ RP(ITH,1)=-RPSR(ITH)
   R(ITH,2)=-RSR(ITH)*RUP(ITH) $ RP(ITH,2)=-RPSR(ITH)*RPUP(ITH)
310 CONTINUE
   NJ=2*MJ $ J1=0
320 NCYC=NCYC+1
   IF(IPR.GT.0) PRINT 4011,IL,NCYC
   RM=1.E7
DO 330 ITH=1,NTH
DO 330 J=1,NJ
C  RANGES AND DERIVATIVES FOR HIGHER ORDER ARRIVALS (NCYC = ORDER)
   R(ITH,J)=R(ITH,J)*RCYC(ITH)
   RP(ITH,J)=RP(ITH,J)*RPCYC(ITH)
   IF(R(ITH,J).LT.RM) RM=R(ITH,J)
330 CONTINUE
   IF(IPR.LE.1) GO TO 335
DO 331 ITH=1,NTH
331 PRINT 4020,(R(ITH,J),J=1,NJ)
4020 FORMAT(9H R(ITH,J),11X,4E18.10)
DO 332 ITH=1,NTH
332 PRINT 4021,(RP(ITH,J),J=1,NJ)
4021 FORMAT(10H RP(ITH,J),10X,4E18.10)
335 CONTINUE
   IF(RM.LE.RMAX) GO TO 340
C---ALL RAY RANGES BEYOND MAXIMUM RECEIVER RANGE
   IF(IL.NE.NL) GO TO 390
340 IF(MJ.EQ.2) GO TO 350
   SIGN(1)=SN $ SIGN(2)=1.
   GO TO 380
350 SIGN(1)=-1. $ SIGN(2)=SN $ SIGN(3)=-SN $ SIGN(4)=1.
380 CALL RAYSUM(IL)
C---TERMINATE COMPUTATIONS WHEN MIN. LOSS IN LAST SECTOR EXCEEDS 130 DB
   IF(NCYC.EQ.999) GO TO 410
   GO TO 320
390 TH1=TH2
400 CONTINUE
410 IF(ISD.EQ.0) GO TO 430

```

PAGE 12

## PROGRAM PLRAY

```
C---IMPLEMENT SURFACE DUCT MODEL
CALL SOUCT
430 DO 450 K=1,KMAX
  RK=RMIN*(K-1)*DR
  DO 440 IF=1,NF
    C---ASSIGN ARBITRARY MINIMUM VALUE (999 DB)
    IF(H(K,IF).LT.HMIN) H(K,IF)=HMIN
  C---CONVERT INTENSITY TO PROPAGATION LOSS
  440 H(K,IF)=-10.*ALOG10(H(K,IF))
  PRINT 2240,RK,H(K,IF),IF=1,NF)
  2240 FORMAT(F16.1,4X,6F12.3)
  450 CONTINUE
  IF(IPLT.EQ.1) CALL PLPLOT
  460 CONTINUE
  GO TO 10
999 STOP
END
```



PAGE 1

## FUNCTION VELOC

```

FUNCTION VELOC(Z,T,SAL,LAT)
REAL LAT,M0,M1,M2,M3
IF(SAL)10,20
10 S=SAL $ GO TO 30
20 S=34.
30 IF(Z)50,40
40 PP=10.1325 $ C=COS(LAT/28.64789)
GR7=.980616-2.5928E-3*C+6.9E-6*C*C
GO TO 60
50 SG=(GR7+1.101E-7*(7+ZOLD))*(Z-ZOLD)
PP=PPOLD+ZOLD*SG
M0=1.-4.886E-6*PP/(1.+1.83E-5*PP)
R=TM3SP1/((M3*PP+M2)*PP+M1)*PP+M0)
PP=PPOLD+.5*(R+ZOLD)*SG
60 S2=S*S $ S3=S*S2 $ S4=S*S3
T2=T*T $ T3=T*T2 $ T4=T*T3
P=.101971*PP $ P2=P*P $ P3=P*P2 $ P4=P*P3
SIG = -9.3445863E-2 +8.1487658E-1*S -4.8249614E-4*S2
* +6.7678614E-6*S3 $ SIG2=SIG*SIG
A0 = (3.1186330E-6 +4.5317157E-3*T -5.4593903E-4*T2
* -1.9824828E-6*T3 -1.4385354E-10*T4 )/(67.26 +T )
A1 = 1.0E-3 -4.7867E-6*T +9.8185E-8*T2 -1.0843E-9*T3
A2 = 1.803E-8*T -8.164E-10*T2 +1.667E-11*T3
TM3SP1=(1.+A0) + A1*SIG + A2*SIG2
M0=1.-4.886E-6*PP/(1.+1.83E-5*PP)
T10 = -2.2072E-7 +3.673E-8*T -6.63E-10*T2 +4.0E-12*T3
T11 = 1.725E-8 -3.28E-10*T +4.0E-12*T2
T12 = -4.5E-11 +1.0E-12*T
M1 = T10 +T11*SIG +T12*SIG2
T20 = -6.68E-14 -1.24064E-12*T +2.14E-14*T2
T21 = -4.248E-13 +1.206E-14*T -2.0E-16*T2
T22 = 1.8E-15 -6.0E-17*T
M2 = T20 +T21*SIG +T22*SIG2
M3 = 1.5E-17*T
R=TM3SP1/((M3*PP+M2)*PP+M1)*PP+M0)
ZOLD=Z $ PPOLD=PP $ WOLD=W

```

PAGE 2

FUNCTION VELOC

```

VT = 4.5721*T -4.4532E-2*T2 -2.6045E-4*T3 +7.9851E-6*T4
VP = 1.60272E-1*P +1.0268E-5*P2 +3.5216E-9*P3 -3.3603E-12*P4
VS = 1.39799*(S -35.) +1.69202E-3*(S -35.)*S2
VSTP=(S-35.)*(-1.1244E-2*T+7.7711E-7*T2+7.7016E-5*P
*-1.2943E-7*P2+3.1580E-8*P*T+1.5790E-9*P*T2)
*P*(-1.8607E-4*T+7.4812E-6*T2+4.5283E-8*T3)
*+P2*(-2.5294E-7*T+1.8563E-9*T2)-1.9646E-10*P3*T
VELOC=3.28084*(1449.14+VT+VP+VS+VSTP)
END

```

PAGE 1

## SUBROUTINE CURFIT

```

      SUBROUTINE CURFIT
C---CURVE-FITTING PROCEDURE (CURFIT, PARAB, FIT, BRIDGE) IS ESSENTIALLY
C AS IN OLD NADC MODEL -- FITS CURVILINEAR SEGMENTS TO VELOCITY PROFIL
      COMMON CD(50),CSP(50),GP(50),IBEAM,IHP,IDRT(4),IPR,IPROF,ISP,
      *NR,NF,PI,RADE,RTD,YD(50),YP(50)
      COMMON C,C1,C2,CA,CAL,CA2,CA1R,CA2R,CH(100),D1,D2,FKA,KAL,KA2,
      *KALR,KA2R,L,N,TOL,Y,Y1,Y2,YA,YAL,YA2,YALR,YA2R,YB(100),YDUCT,YY(3)
      REAL KAL,KA1B,KA2,KA2R
      DIMENSION LL(100),NN(100)
      DO 1 I=1,NR
      YB(I)=YD(I)
      1 CF(I)=CD(I)
      CALL PARAB
      L=1 & N=4 & K=1
      10 IF (L+N-1).GT.NB) 170,20
      20 MM=L+N-1
      IF (YB(L),LT,YDUCT,AND,YB(MM).GT,YDUCT) 160,25
      25 YAV=.5*(YB(L)+YB(MM))
      TD=2.9-2.5*EXP(-.000112*YAV)
      G=0. & M1=L+1 & M2=L+N-2
      GU=(CB(L+1)-CB(L))/(YB(L+1)-YB(L))
      GMIN=ABS(GU)
      DO 50 I=M1,M2
      GL=GU
      GU=(CH(I+1)-CH(I))/(YB(I+1)-YB(I))
      IF (GL*GU.LE.0.) 60,30
      30 IF (ABS(GU).LT,GMIN) 40,50
      40 GMIN=ABS(GU)
      50 CONTINUE
      G=GMIN
      60 Z=FXP(9.6*(G-.35))
      TG=3.*Z/(7+1.)
      TOL=TD+TG
      CALL FIT
C - CHECK CURVE FIT
      DO 70 I=1,N & J=L+I-1

```



PAGE 2

## SUBROUTINE CURFIT

```

      CUR=SQRT(CA/(1.-FKA*(YH(J)-YA)**2))
      ARDIF=ABS(CUR-CB(J))
      IF (ARDIF.GT.TOL)160.70
70  CONTINUE
      LZ=L+N-1
      IF (YA.GT.YB(L).AND.YA.LT.YH(LZ))80.150
80  I=L+1
90  IF (FKA*(CB(I)-CB(I-1)).LT.0..AND.FKA*(CB(I)-CB(I+1)).LT.0.)110.100
100 I=I+1
      IF (I.GE.LZ)160.90
110 YY(I)=.5*(YB(L)+YA) & YY(2)=YA & YY(3)=.5*(YA+YH(L7))
      DO 140 M=1,3
      CC=SQRT(CA/(1.-FKA*(YY(M)-YA)**2))
      J=L
120 J=J+1
      IF (YB(J).GT.YY(M))130.120
130 F1=(YY(M)-YB(J-1))/(YB(J)-YH(J-1)) & F2=1.-F1
      CCL=F1*CB(J)+F2*CB(J-1)
      ARDIF=ABS(CC-CCL)
      IF (ARDIF.GT.(1.+TOL))160.140
140 CONTINUE
150 LL(K)=L & NN(K)=N
      CSP(K)=CA & GP(K)=FKA & YP(K)=YA
      N=N+1
      IF ((L+N-1).GT.NB)200.20
160 IF (N.EQ.4)170.190
170 NB=NB+2 & KX=L+3
      DO 180 LXX=KX,NB & LY=NB+KX-LXX
      YB(LX)=YB(LX-2)
      CB(LX)=CB(LX-2)
      YH(L+1)=(2.*YB(L)+YH(KX))/3.
      CH(L+1)=(2.*CH(L)+CH(KX))/3.
      YH(L+2)=(YH(L)+2.*YH(KX))/3.
      CB(L+2)=(CH(L)+2.*CH(KX))/3.
      GO TO 20
190 K=K+3 & L=L+N-2 & N=N+4 & GO TO 10

```

PAGE 3

## SUBROUTINE CURFIT

```

C - BRIDGING OF LEAST-SQUARES SEGMENTS
200 YD(1)=YB(1) $ CD(1)=SQRT(CSP(1)/(1.-GP(1)*YP(1)*YP(1)))
    CA2=CSP(1) $ KA2=GP(1) $ YA2=YP(1)
    IF(K.LT.4)255,215
215 DO 250 I=4,K,3
    LLL=LL(I) $ Y=YB(LLL)
    TOL=3.1-2.5*EXP(-.000112*Y)
    CA1=CA2 $ KA1=KA2 $ YA1=YA2
    CA2=CSP(I) $ KA2=GP(I) $ YA2=YP(I)
    DEL1=Y-YB(LLL-1) $ DEL2=YB(LLL+1)-Y
220 Y1=Y-DEL1 $ Y2=Y+DEL2
    C1=SQRT(CA1/(1.-KA1*(Y1-YA1)**2))
    IF(KA1)221,222
221 D1=CA1/(C1*C1*(Y1-YA1)*KA1)
222 C2=SQRT(CA2/(1.-KA2*(Y2-YA2)**2))
    IF(KA2)223,224
223 D2=CA2/(C2*C2*(Y2-YA2)*KA2)
224 CALL BRIDGE
    SSPD=SQRT(CA1/(1.-KA1*(Y-YA1)**2))
    IF(ABS(C-SSPD).LT.TOL)240,230
230 DEL1=DEL1/2. $ DEL2=DEL2/2. $ GO TO 220
240 YD(I-2)=Y1 $ CD(I-2)=C1
    CSP(I-2)=CA1B $ GP(I-2)=KA1B $ YP(I-2)=YA1B
    YD(I-1)=Y $ CD(I-1)=C
    CSP(I-1)=CA2B $ GP(I-1)=KA2B $ YP(I-1)=YA2B
    YD(I)=Y2
250 CD(I)=C2
255 CONTINUE
    YD(K+1)=YB(NB) $ CD(K+1)=SQRT(CSP(K)/(1.-GP(K)*(YB(NB)-YP(K))**2))
    CSP(K+1)=GP(K+1)=YP(K+1)=0.
    PRINT 9000
9000 FORMAT(4(/),45X,45HVFLOCITY PROFILE FUNCTION AFTER CURVE-FITTING, /
    *//,11X,5HSLAYER,16X,5HDEPTH,12X,11H SOUND SPEED,26X,18H SEGMENT PAKAM
    *ETFRS,/,11X,6HNU*HFR,16X,4H(FT),14X,8H(FT/SEC),14X,3HCSP,18X,2HGP,
    *18X,2HYP,/)
    NB=K+1 $ I=K+0

```

PAGE 4

## SUBROUTINE CURFIT

```

310 I=I+1 & K=K+1
    PRINT 9001,I,YD(K),CD(K),CSP(K),GP(K),YP(K)
9001 FORMAT(12X,I3,13X,F12.6,9X,F12.7,2X,3E20.10)
    IF(K.EQ.NR)400,320
320 IF(YP(K).GT.YD(K).AND.YP(K).LT.YD(K+1))330,310
330 CC=SORT(CSP(K))
    IF(CC.GT.CO(K))340,350
340 PRINT 9002,YP(K),CC
9002 FORMAT(12X,3HMAX,13X,F12.6,9X,F12.7)
    GO TO 360
350 PRINT 9003,YP(K),CC
9003 FORMAT(12X,3HMIN,13X,F12.6,9X,F12.7)
360 KK=K+1 & NR=NR+1
    DO 370 LI=KK,NR & L=NR+KK-LI
    YD(L)=YD(L-1) & CD(L)=CD(L-1)
    CSP(L)=CSP(L-1) & GP(L)=GP(L-1) & YP(L)=YP(L-1)
370 CONTINUE
    YD(K)=YP(K-1) & CD(K)=CC & GO TO 310
400 IF(NR.GT.50)410,420
410 PRINT 9004,NR
9004 FORMAT(///,36X,45HVELOCITY PROFILE AFTER CURVE-FITTING CONTAINS.
    *13,16H POINTS BUT ONLY,/,36X,64H50 ARE ALLOWED. REMOVE POINTS FRO
    *M INPUT PROFILE AND RE-SUBMIT.)
    IPROF=-1
420 RETURN
    END

```



PAGE 1

SUBROUTINE PARAB

```

SUBROUTINE PARAB
COMMON CD(50),CSP(50),GP(50),IHEAM,IBP,IDRT(4),IPR,IPROF,ISP,
*NB,NF,PI,RADE,RID,YD(50),YP(50)
COMMON C,C1,C2,CA,CA1,CA2,CA1B,CA2B,CB(100),D1,D2,FKA,KAL,KA2,
*KALR,KA2B,L,N,TOL,Y,Y1,Y2,YA,YA1,YA2,YA1R,YA2B,YB(100),YDUCT,YY(3)
REAL KAL,KALB,KA2,KA2B
IF(NB.LT.4)100,5
5 DO 10 I=4,NB
IF(YB(I-2).GT.500.)20,10
10 CONTINUE
GO TO 100
20 I=I+1
IF(I.GT.NB)100,30
30 Y1=YB(I-3) $ Y2=YB(I-2) $ Y3=YB(I-1)
C1=CB(I-3) $ C2=CB(I-2) $ C3=CB(I-1) $ C4=CB(I)
IF(C2.GT.C1.AND.C2.GE.C3.AND.C3.GT.C4)50,40
40 IF(C2.LT.C1.AND.C2.LE.C3.AND.C3.LT.C4)50,20
50 CY12=(C2-C1)/(Y2-Y1) $ CY13=(C3-C1)/(Y3-Y1)
A3=(CY13-CY12)/(Y3-Y2)
IF(ABS(A3)*Y3*Y3.LT.0.1)20,60
60 A2=CY12-A3*(Y1+Y2)
A1=C1-A2*Y1-A3*Y1*Y1
Y=-A2/(2.*A3) $ C=A1-A2*A2/(4.*A3)
NX=I-2
IF(Y.GT.Y2)70,80
70 NX=I-1
80 DO 90 K=NX,NB $ KK=NR+NX+1-K
YB(KK)=YB(KK-1)
90 CR(KK)=CR(KK-1)
F1=(Y-YB(NX-1))/(YB(NX+1)-YB(NX-1)) $ F2=1.-F1
CCL=F1*CB(NX+1)+F2*CB(NX-1)
YB(NX)=Y $ CB(NX)=.75*C+.25*CCL
I=I+2 $ NB=NB+1 $ GO TO 20
100 I=1
110 I=I+1
IF(I.EO.NB)130,120

```

PAGE 2

SUBROUTINE PARAB

120 IF (CB(I).GT.CB(I-1)).AND.CB(I).GE.CB(I+1).AND.CH(I).GT.CH(I))130,  
\*110

130 YDUCT=YH(I)

RETURN

END

PAGE 1

SUBROUTINE FIT

```

SUBROUTINE FIT
COMMON CD(50),CSP(50),GP(50),IREAM,IPR,IDBT(4),IPR,IPOF,ISP,
*NB,NF,PI,RADE,RTD,YD(50),YP(50)
COMMON C,C1,C2,CA,CAL,CA2,CA1B,CA2B,CH(100),D1,D2,FKA,KAL,KA2,
*KALB,KA2B,L,N,TOL,Y,Y1,Y2,YA,YAL,YA2,YALB,YA2B,YB(100),YDUCT,Y,Y(3)
REAL KAL,KALB,KA2,KA2B
ZM1=ZM2=ZM3=ZM4=CM2=CM2Z1=CM2Z2=0.
DO 10 II=1,N $ I=L+II-1
Z=YB(II)-YB(L)
ZM1=ZM1+Z
ZM2=ZM2+Z*Z
ZM3=ZM3+Z*Z*Z
ZM4=ZM4+Z*Z*Z*Z
CM2=CM2+1./(CH(II)*CH(II))
CM2Z1=CM2Z1+Z/(CH(II)*CH(II))
10 CM2Z2=CM2Z2+Z*Z/(CH(II)*CH(II))
DET=N*ZM2*ZM4+ZM1*ZM3*ZM2+ZM2*ZM1*ZM3-N*ZM3*ZM3-ZM1*ZM1*ZM2*ZM
*2*ZM2
F1=(CM2*ZM2*ZM4+CM2Z1*ZM3*ZM2+CM2Z2*ZM1*ZM3-CM2*ZM3*ZM3-CM2Z1*ZM1*
*ZM4-CM2Z2*ZM2*ZM2)/DET
F2=(N*CM2Z1*ZM4+ZM1*CM2Z2*ZM2+ZM2*CM2*ZM3-N*CM2Z2*ZM3-ZM1*CM2*ZM4-
*ZM2*CM2Z1*ZM2)/DET
F3=(N*ZM2*CM2Z2+ZM1*ZM3*CM2+ZM2*ZM1*CM2Z1-N*ZM3*CM2Z1-ZM1*ZM1*CM2Z
*2-7M2*ZM2*CM2)/DET
LM=L+N-1 $ ZM=YB(LM)-YB(L)
IF (ABS(F3).LT.1.E-14/(7M*ZM)) 20,30
20 IF (ABS(F2).LT.1.E-14/(7M)) 40,25
25 YBAR=.5*(YB(L)+YB(LM)) $ CBAH=.5*(CB(L)+CH(LM))
GBAR=(CB(LM)-CH(L))/7M
YA=YBAR+CBAR/(3.*GBAR)
FKA=-4.5*GBAR*GBAR/(CBAR*CBAR)
CA=1.5*CBAR*CBAR
RETURN
30 YA=YB(L)-F2/(2.*F3)
FKA=4.*F3*F3/(F2*F2-4.*F1*F3)
CA=-FKA/F3

```



PAGE 2

SURROUTINE FIT

```
RETURN
40 YA=FKA=0.
   CSAR=.5*(CR(L)+CH(LM))
   CA=CBAR*CBAR
RETURN
END
```

PAGE 1

## SURROUTINE BRIDGE

```

SURROUTINE BRIDGE
COMMON CD(50),CSP(50),GP(50),IBeam,IRP,IDRT(4),IPR,IProf,ISP,
*NB,NF,PI,RADE,RTD,YD(50),YP(50)
COMMON C,C1,C2,CA,CA1,CA2,CA1B,CA2B,CH(100),D1,D2,FKA,KAI,KA2,
*KAIR,KA2B,L,N,TOL,Y,Y1,Y2,YA,YA1,YA2,YA1B,YA2B,YB(100),YDUCT,YY(3)
REAL KAI,KA1B,KA2,KA2B
F1=CA1*KA2-CA2*KAI
F2=CA2*KAI*YA1-CA1*KA2*YA2
F3=CA1*KA2*YA2*YA2-CA2*KAI*YA1*YA1+CA2-CA1
F4=-F2/F1 $ F5=F4*F4 $ F6=F3/F1
IF (F6.GT.F5)60,10
10 F7=SQRT(F5-F6) $ YPLUS=F4+F7 $ YMINUS=F4-F7
DYPLUS=ABS(YPLUS-Y) $ DYMINUS=ABS(YMINUS-Y)
IF (DYPLUS.LT.DYMINUS)20,30
20 IF (YPLUS.GT.Y1.AND.YPLUS.LT.Y2)40,60
30 IF (YMINUS.GT.Y1.AND.YMINUS.LT.Y2)50,60
40 Y=YPLUS $ GO TO 70
50 Y=YMINUS $ GO TO 70
60 TOL=TOL+3.
70 Y1=Y1-Y $ Y2=Y2-Y
IF (KAI)80,90
80 IF (KA2)110,100
90 YA2B=Y2*(C2*C2*D2-CA1*D2-CA1*Y2)/(C2*C2*D2-2.*CA1*Y2-CA1*D2+CA1*Y1
*)
DY2=Y2-YA2B
KA2R=1./(DY2*(D2+DY2))
CA2B=C2*C2*D2*KA2H*DY2
YA1B=Y1
KA1R=CA1*KA2B*YA2B/(CA2H*Y1)
CA1R=CA1
GO TO 120
100 YA1B=Y1*(C1*C1*D1-CA2*D1-CA2*Y1)/(C1*C1*D1-2.*CA2*Y1-CA2*D1+CA2*Y2
*)
DY1=Y1-YA1B
KA1R=1./(DY1*(D1+DY1))
CA1R=C1*C1*D1*KA1H*DY1

```

PAGE 2

SUBROUTINE BRIDGE

```

YA2B=Y2
KA2B=CA2*KA1B*YA1B/(CA1B*Y2)
CA2B=CA2
GO TO 120
110 YA2B=Y2*(C1*C1*D1*Y2-C2*C2*D2*Y1+D1*D2*(C1*C1-C2*C2))/(-C1*C1*D1*Y
  *1+2.*C1*C1*D1*Y2-C2*C2*D2*Y1+D1*D2*(C1*C1-C2*C2))
  G2=1./(C2*C2*D2*(Y2-YA2B))
  CA2B=C2*C2/(1.+C2*C2*(Y2-YA2B)**2*G2)
  KA2B=G2*CA2B
  YA1B=(C1*C1*D1*Y1*YA2B)/(YA2B*(C1*C1*D1-C2*C2*D2)+C2*C2*D2*Y2)
  G1=1./(C1*C1*D1*(Y1-YA1B))
  CA1B=C1*C1/(1.+C1*C1*(Y1-YA1B)**2*G1)
  KA1B=G1*CA1B
120 YA1B=Y+YA1B $ YA2B=Y+YA2B $ Y1=Y+Y1 $ Y2=Y+Y2
  C=SQRT(CA1B/(1.-KA1B*(Y-YA1B)**2))
  RETURN
  END

```



PAGE 1

## SUBROUTINE INSERT

```

SUBROUTINE INSERT
C ---FORMS NEW V.P. TABLE (7A,CA) WITH SOURCE AND RECEIVER DEPTHS INSERTE
COMMON CB(50),CSP(50),GP(50),IBEAM,IRP,IDHT(4),IPR,IPROF,ISP,
*NB,NF,PI,RADE,RTD,7R(50),ZP(50)
COMMON CA(50),CAA,CAA2,CBB,CBB2,IAA,IAO,IRB,IRF(50),IDUCT,ISD,NA,
*SN,7A(50),ZAA,ZAD,ZBR,ZR,ZS
IF(ZS.LT.ZR) GO TO 20
ZMN=ZR $ ZMX=ZS
GO TO 30
20 ZMN=ZS $ ZMX=ZR
30 IA=IB=IDF(1)=1
  ZA(1)=ZB(1) $ CA(1)=CB(1)
C---FORM NEW V.P. INCLUDING SOURCE AND RECEIVER DEPTHS
40 IA=IA+1 $ IB=IB+1
  IF(ZR(IR)-ZMN)50,60,70
50 IDF(IA)=IB $ ZA(IA)=ZR(IB) $ CA(IA)=CR(IB)
  GO TO 40
60 IMN=IA $ CMN=CH(IB)
  GO TO 80
70 IMN=IA $ ZA(IA)=ZMN
  I=IDF(IA)=IB-1
  CMN=SQRT(CSP(I)/(1.-GP(I))*(ZMN-ZP(I))**2))
  CA(IA)=CMN $ IA=IA+1
80 IF(7MX.NE.ZMN) GO TO 85
  IMX=IMN $ CMX=CMN
  GO TO 120
85 IF(ZR(IR)-ZMX)90,100,110
90 IDF(IA)=IB $ ZA(IA)=ZR(IR) $ CA(IA)=CR(IB)
  IA=IA+1 $ IB=IB+1
  GO TO 85
100 IMX=IA $ CMX=CH(IR)
  GO TO 120
110 IMX=IA $ ZA(IA)=ZMX
  I=IDF(IA)=IB-1
  CMX=SQRT(CSP(I)/(1.-GP(I))*(ZMX-ZP(I))**2))
  CA(IA)=CMX $ IA=IA+1

```

PAGE 2

## SUBROUTINE INSERT

```

120 IDF(IA)=IH $ ZA(IA)=7P(IB) $ CA(IA)=CH(IB)
    IF(IH.GE.NH) GO TO 130
    IA=IA+1 $ IH=IH+1
    GO TO 120
130 NA=IA
    IF(7MN.EQ.ZS) GO TO 140
    IR=IMN $ CR=CMN
    IS=IMX $ CS=CMX
    GO TO 150
140 IR=IMX $ CR=CMX
    IS=IMN $ CS=CMN
C----REDEFINE SOURCE AND RECEIVER. NEW SOURCE HAS LARGER OF THE TWO SOUN
150 IF(CS.LT.CR) GO TO 160
    CAA=CS $ CBB=CR
    ZAA=ZS $ ZBB=ZR
    IAA=IS $ IBB=IR
    SN=1.
    GO TO 170
160 CAA=CR $ CBB=CS
    ZAA=ZR $ ZBB=ZS
    IAA=IR $ IBB=IS
    SN=-1.
170 CAA2=CAA*CAA $ CBB2=CBB*CBB
    ISD=0 $ ZAD=0. $ IAD=1
    IF(IDUCT.EQ.1) GO TO 999
    DO 180 IA=1,NA
    IRD=IDF(IA)
    IF(IRD.EQ.IDUCT) GO TO 200
180 CONTINUE
    GO TO 999
C----SURF. DUCT MODEL EMPLOYED IF SOURCE IS IN DUCT AND RECH. DEPTH IS LE
C 1.8 * DUCT DEPTH (OR VICE VERSA)
200 IAD=IA
    ZAD=ZA(IA) $ ZADM=1.8*7AD
    IF(7AA.GT.ZBB) GO TO 210
    IF(7AA.LT.ZAU.AND.7HR.LT.ZADM) ISD=1

```

PAGE 3

SUBROUTINE INSERT

```
GO TO 999
210 IF (Z88.LT.ZAD.AND.7AA.LT.ZADM) ISD=1
999 RETURN
END
```



PAGE 1

## SUBROUTINE SECLIM

```

SUBROUTINE SECLIM
C---SETS UP BOUNDARIES OF ANGULAR SECTORS CONTAINING DIFFERENT FAMILIES
COMMON CB(50),CSP(50),GP(50),IBEAM,IBP,IDRT(4),IPR,IPOF,ISP,
*NR,NF,PI,RADE,RTD,7R(50),ZP(50)
COMMON CA(50),CAA,CAA2,CBB,CBB2,IAA,IAD,IBB,IDF(50),IDUCT,ISD,NA,
*SN,7A(50),ZAA,ZAD,ZPR,ZR,ZS
COMMON RMFAC(6),CL(10),CV,CV2,ILR,ILS,NL,NTH,SIGN(4),TH(50),
*TH1,TH2,VA(50),VRM
DIMENSION G(50)
DO 10 IA=1,NA
IB=IDF(IA)
IF(IA.EQ.NA) IB=NR-1
G(IA)=CA(IA)*CA(IA)*GP(IA)*(ZA(IA)-ZP(IA))/CSP(IA)
10 CONTINUE
IF(IPR.GT.1) PRINT 4001,(G(IA),IA=1,NA)
4001 FORMAT(3H G,17X,6E18.10)
IL=1 $ ILT=IAA
CL(1)=CAA
IF(7BR-7AA) 20,7C,30
20 IL=IBB $ I2=IAA-1
GO TO 40
30 IL=IAA+1 $ I2=IBB
40 DO 50 IA=I1,I2
IF(CA(IA).LE.ABS(CL(1))) GO TO 50
CL(1)=-CA(IA) $ ILT=IA
50 CONTINUE
70 IUP=ILT-1 $ IDN=ILT+1
80 IF(CA(IDN).GT.CA(IUP)) GO TO 200
IF(IDN.EQ.NA) GO TO 120
IF(CA(IDN).LE.ABS(CL(1)))GO TO 100
IF(CA(IDN).GT.CA(IDN-1).AND.CA(IDN).GT.CA(IDN+1)) GO TO 90
IF(ABS(G(IDN)).GT.ABS(G(IDN-1)).AND.ABS(G(IDN)).GT.ABS(G(IDN+1)))
*GO TO 90
IF(ABS(G(IDN)).GE.ABS(G(IDN-1)).OR.ABS(G(IDN)).GE.ABS(G(IDN+1)))
*GO TO 100
90 IL=IL+1 $ CL(IL)=-CA(IDN)

```

PAGE 2

## SUBROUTINE SECLIM

```

100 IDN=IDN+1
   GO TO 80
120 IF (CA(IDN)).LE.ABS(CL(IL))) GO TO 130
   IL=IL+1 $ CL(IL)=CA(NA)
130 ILR=IL
140 IF (IUP.EQ.1) GO TO 170
   IF (CA(IUP)).LE.ABS(CL(IL))) GO TO 160
   IF (CA(IUP)).GT.CA(IUP-1).AND.CA(IUP).GT.CA(IUP+1)) GO TO 150
   IF (ABS(G(IUP)).GT.ABS(G(IUP-1)).AND.ABS(G(IUP)).GT.ABS(G(IUP+1)))
     *GO TO 150
   IF (ABS(G(IUP)).GE.ABS(G(IUP-1)).OR.ABS(G(IUP)).GE.ABS(G(IUP+1)))
     *GO TO 160
150 IL=IL+1 $ CL(IL)=-CA(IUP)
160 IUP=IUP-1
   GO TO 140
170 IF (CA(1)).LE.ABS(CL(IL))) GO TO 180
   IL=IL+1 $ CL(IL)=CA(1)
180 ILS=IL
   GO TO 350
200 IF (IUP.EQ.1) GO TO 230
   IF (CA(IUP)).LE.ABS(CL(IL))) GO TO 220
   IF (CA(IUP)).GT.CA(IUP-1).AND.CA(IUP).GT.CA(IUP+1)) GO TO 210
   IF (ABS(G(IUP)).GT.ABS(G(IUP-1)).AND.ABS(G(IUP)).GT.ABS(G(IUP+1)))
     *GO TO 210
   IF (ABS(G(IUP)).GE.ABS(G(IUP-1)).OR.ABS(G(IUP)).GE.ABS(G(IUP+1)))
     *GO TO 220
210 IL=IL+1 $ CL(IL)=-CA(IUP)
220 IUP=IUP-1
   GO TO 80
230 IF (CA(IUP)).LE.ABS(CL(IL))) GO TO 240
   IL=IL+1 $ CL(IL)=CA(1)
240 ILS=IL
260 IF (IDN.EQ.NA) GO TO 300
   IF (CA(IDN)).LE.ABS(CL(IL))) GO TO 280
   IF (CA(IDN)).GT.CA(IDN-1).AND.CA(IDN).GT.CA(IDN+1)) GO TO 270
   IF (ABS(G(IDN)).GT.ABS(G(IDN-1)).AND.ABS(G(IDN)).GT.ABS(G(IDN+1)))

```

PAGE 3

## SUBROUTINE SECLIM

```

*GO TO 270
IF(ARS(G(IDN)).GE.ARS(G(IDN-1)).OP.ARS(G(IDN)).GE.ARS(G(IDN+1)))
*GO TO 280
270 IL=IL+1 $ CL(IL)=--CA(IDN)
280 IDN=IDN+1
GO TO 260
300 IF(CA(NA).LE.ABS(CL(IL))) GO TO 310
IL=IL+1 $ CL(IL)=CA(NA)
310 ILR=IL
C---FINAL SECTOR RUNS FROM 30 TO 90 DEG.
350 NL=IL+1 $ CL(NL)=1.154700538*CAA
RETURN
END

```



PAGE 1

SUBROUTINE DIVSEC

```

SUBROUTINE DIVSEC(IL)
C---SETS UP FAMILY OF NON-UNIFORMLY SPACED RAY SOURCE ANGLES IN EACH SEC
COMMON CR(50),CSP(50),GP(50),IREAM,IRP,IDHT(4),IPR,IPROF,ISP,
*NB,NF,PI,RADE,RTD,7R(50),ZP(50)
COMMON CA(50),CAA,CAA2,CBB,CBB2,IAA,IAD,IBB,IDF(50),IDUCT,ISD,NA,
*SN,ZA(50),ZAA,ZAD,ZER,ZR,ZS
COMMON BMFAC(6),CL(10),CV,CV2,ILR,ILS,NL,NTH,SIGN(4),TH(50),
*TH1,TH2,VA(50),VRM
DIMENSION THT(30)
DATA DEL0 / .00001/, IMAX /50/
DELM=.01
IF(IL.EQ.NL) DELM=.04
C---DELO IS BLANK INTERVAL AT EACH EDGE OF SECTOR
DEL=DELO
TH(1)=TH1+DEL
IF(CL(IL).GT.0.) GO TO 10
THT(1)=TH2-DEL
IF(THT(1).GT.TH(1)) GO TO 10
NTH=0 $ GO TO 999
10 DEL=5.*DELO
DO 30 I=2,IMAX
C---RAY SPACING INCREASES IN GEOM. PROGRESSION UNTIL LIMIT DELM IS REACH
DEL=2.*DEL
IF(DEL.GT.DELM) DEL=DELM
TH(I)=TH(I-1)+DEL
C---IF CL(IL) NEGATIVE, RAY SPACING IS DECREASED AT OUTER EDGE, AS AT IN
IF(CL(IL).LT.0.) GO TO 20
IF(TH(I).GT.(TH2-DELO)) 40,30
20 THT(I)=THT(I-1)-DEL
IF(THT(I).LT.TH(I)) GO TO 50
30 CONTINUE
ILI=IL-1 $ PRINT 2001,ILI
2001 FORMAT(10X,23HT00 MANY RAYS IN SECTOR,13)
I=IMAX
40 TH(I)=TH2-DELO $ NTH=I
GO TO 999

```

NADC-77296-30

PAGE 2

SUBROUTINE DIVSEC

```
50 IF (THT(I).LT.IH(I-1)) GO TO 70
60 I1=I $ NTH=2*(I-1)
   GO TO 80
70 TH(I)=(TH(I)+THT(I))/2.
   I1=I $ NTH=2*I-1
80 IF (NTH.LE.IMAX) GO TO 90
   IL1=IL-1 $ PRINT 2001,IL1
   NTH=IMAX
90 DO 100 I=I1,NTH
   II=NTH-I+1
100 TH(I)=THT(II)
999 RETURN
END
```

PAGE 1

SUBROUTINE INCR

```

SUBROUTINE INCR(ITH)
C---COMPUTES RANGES (R) AND RANGE DERIVATIVES (RP) FOR EACH RAY
C RSP = RANGE OF DIRECT PATH FROM SOURCE TO RECEIVER
C RCYC = RANGE OF ONE COMPLETE CYCLE
C RUP = PORTION OF RCYC ABOVE RECEIVER DEPTH
COMMON CB(50),CSP(50),GP(50),IBEAM,IRP,IDBT(4),IPR,IPOF,ISP,
*NB,NF,PI,RADE,RTD,ZR(50),ZP(50)
COMMON CA(50),CAA,CAA2,CBB,CBR2,IAA,IAD,IBB,IDF(50),IDUCT,ISD,NA,
*SN,ZA(50),ZAA,ZAD,ZRR,ZR,ZS
COMMON BMFAC(6),CL(10),CV,CV2,ILB,ILS,NL,NTH,SIGN(4),TH(50),
*TH1,TH2,VA(50),VHM
COMMON ALPHA(6),BLOSS(50,6),BOTL(6),F(6),F13(6),IBOT,ISURF,
*SLOSS(6)
COMMON DR,H(251,6),HC(15,4,6),ICAUST(4),IFMAX,J1,KA(4,6),KB(4,6),
*KMAX,KMN,KMNJ(4),KMXJ(4),NCYC,NJ,R(50,4),RCYC(50),RMIN,RP(50,4),
*RPCYC(50),RPSR(50),RPUP(50),RSR(50),RUP(50)
DIMENSION DX(50),DXP(50)
CUT=CDT=0.
FAC=CAA2*VA(ITH)/CV2
IUP=I1=1 & I2=IAA-1
C---SEARCH FOR UPPER VERTEX OF RAY
DO 10 I=I1,I2
IA=IAA-I
IF(CA(IA).GE.CV) GO TO 20
10 CONTINUE
GO TO 30
20 IUP=IA & CUT=CA(IA) & CA(IA)=CV
ZUT=ZA(IA) & S=1.
IB=IDF(IA) & PROD=CSP(IA)*GP(IA)
IF(PROD.GT.0.) S=-1.
ZA(IA)=ZP(IA)+S*SQRT((1.-CSP(IA)/CV2)/GP(IA))
30 I1=IAA+1
C---SEARCH FOR LOWER VERTEX OF RAY
DO 40 IA=I1,NA
IF(CA(IA).GE.CV) GO TO 50
40 CONTINUE

```



PAGE 2

## SUBROUTINE INCR

```

      IDN=NA-1
      GO TO 60
50  IDN=IA-1 $ CDT=CA(IA) $ CA(IA)=CV
      ZDT=ZA(IA) $ S=1.
      IR=IDF(IA)-1 $ PROD=CSP(IB)*GP(IB)
      IF (PROD.GT.0.) S=-1.
      7A(IA)=ZP(IB)-S*SQRT((1.-CSP(IB)/CV2)/GP(IB))
60  IF (CV.EQ.CA(IUP)) GO TO 70
      V2=SQRT(CV2/(CA(IUP)*CA(IUP))-1.)
      GO TO 60
70  V2=0.
C---COMPUTE RANGE AND RANGE DERIV. INCREMENTS IN EACH LAYER
80  DO 130 IA=IUP,IDN
      V1=V2
      IF (CV.EQ.CA(IA+1)) GO TO 90
      V2=SQRT(CV2/(CA(IA+1)*CA(IA+1))-1.)
      GO TO 100
90  V2=0.
100  IR=IDF(IA)
      CSPT=CSP(IB) $ GPT=GP(IB) $ ZPT=ZP(IB)
      Q1=CV*SQRT(ABS(GPT/CSPT))
      Q2=CV*SQRT(ABS(GPT/(CV2-CSPT)))
      Q3=CSPT/(CV2-CSPT)
      PROD=CSPT*GPT
      IF (PROD.LT.0.) GO TO 110
      W1=Q2*(ZA(IA)-ZPT)
      IF (W1.GT.1.) W1=1.
      IF (W1.LT.-1.) W1=-1.
      W11=SQRT(1.-W1*W1)
      W2=Q2*(ZA(IA+1)-ZPT)
      IF (W2.GT.1.) W2=1.
      IF (W2.LT.-1.) W2=-1.
      W22=SQRT(1.-W2*W2)
      DX(IA)=ASIN(W2*W11-W1*W22)/(3.*Q1)
      GO TO 120
110  DX(IA)=ALOG((V2+Q1*(7A(IA+1)-ZPT))/(V1+Q1*(7A(IA)-ZPT)))/(3.*Q1)

```

PAGE 3

SUBROUTINE INCR

```

120 VV1=VV2=0.
    IF (V1.NE.0.) VV1=1./V1
    IF (V2.NE.0.) VV2=1./V2
    DXP(IA)=-FAC*(DX(IA)+Q3*((7A(IA+1)-ZPT)*VV2-(ZA(IA)-ZPT)*VV1)/3.)
130 CONTINUE
    IF (CUT.EQ.0.) GO TO 135
    ZA(IUP)=ZUT $ CA(IUP)=CUT
135 IF (COT.EQ.0.) GO TO 140
    ZA(ION+1)=ZOT $ CA(ION+1)=COT
140 IF (ZBB.LT.ZAA) GO TO 150
    S=-1. $ I1=IAA $ I2=IBB-1
    GO TO 160
150 S=1. $ I1=IBB $ I2=IAA-1
160 RSR(ITH)=RPSR(ITH)=0.
    IF (I2.LT.I1) GO TO 175
C---COMPUTE RANGE AND RANGE DERIV. INCREMENTS. SOURCE TO RECEIVER
    DO 170 IA=I1,I2
    RSR(ITH)=RSR(ITH)+DX(IA)
170 RPSR(ITH)=RPSK(ITH)+DXP(IA)
175 RUP(ITH)=RPUP(ITH)=RCYC(ITH)=RPCYC(ITH)=0.
C---COMPUTE R AND RP INCREMENTS. COMPLETE CYCLE AND PORTION ABOVE RECEIV
    DO 180 IA=IUP,ION
    RCYC(ITH)=RCYC(ITH)+2.*DX(IA)
    RPCYC(ITH)=RPCYC(ITH)+2.*DXP(IA)
    IF (IA.GE.IBB) GO TO 180
    RUP(ITH)=RUP(ITH)+2.*DX(IA)
    RPUP(ITH)=RPUP(ITH)+2.*DXP(IA)
180 CONTINUE
    IF (IRPT.EQ.0) GO TO 999
    THRO=RTD*ACOS(CA(NA)/CV)
C---COMPUTE BOTTOM LOSS
    CALL BOTTOM(THRO)
    DO 190 IF=1,NF
190 BLOSS(ITH,IF)=BOTL(IF)
999 RETURN
    END

```

PAGE 1

## SUBROUTINE RAYSUM

```

      SUBROUTINE RAYSUM(IL)
      C-----COMPUTES RAY INTENSITIES AT SPECIFIED RECEIVER RANGES
      COMMON CH(50),CSP(50),GP(50),IBEAM,IBP,IDBT(4),IPK,IPROF,ISP,
      *NB,NF,PI,RADE,RTD,7K(50),ZP(50)
      COMMON CA(50),CAA,CAAP,CBB,CEH2,IAA,IAD,IAB,IDF(50),IDUCT,ISD,NA,
      *SN,7A(50),ZAA,ZAD,ZHR,ZR,ZS
      COMMON BMFAC(6),CL(10),CV,CV2,ILP,ILS,NL,NTH,SIGN(4),IH(50),
      *TH1,TH2,VA(50),VRM
      COMMON ALPHA(6),GLOSS(50,6),HOTL(6),F(6),F13(6),IBOT,ISURF,
      *SLOSS(6)
      COMMON DR,H(251,6),HC(15,4,6),ICAUST(4),IFMAX,J1,KA(4,6),KB(4,6),
      *KMAX,KMN,KMNJ(4),KMXJ(4),NCYC,NJ,R(50,4),RCYC(50),RMIN,RP(50,4),
      *RPCYC(50),RPSR(50),RPUP(50),PSR(50),RUP(50)
      COMMON /COH/ JCOH(6)
      DIMENSION A0(4),A1(4),EMF(4,2,6),HTRM(4,2,6),ICTH(4),JA(2),
      *RPPK(4,2),VAKK(4,2)
      DATA AX,XA /1.2,4.3333/
      DATA RCOH /12000./
      RMN=1.E10 & RMX=0.
      C-----FIND MIN. AND MAX. RAY RANGES IN SECTOR
      DO 30 J=1,NJ
      PMNJ=1.E10 & RMXJ=0.
      ICAUST(J)=0
      DO 10 ITH=1,NTH
      IF(R(ITH,J).LE.RMXJ) GO TO 2
      RMXJ=R(ITH,J) & ITHMX=ITH
      2 IF(R(ITH,J).GE.RMNJ) GO TO 4
      RMNJ=R(ITH,J) & ITHMN=ITH
      4 IF(R(ITH,J).GT.RMX) RMX=R(ITH,J)
      IF(R(ITH,J).LT.RMN) RMN=R(ITH,J)
      10 CONTINUE
      C-----SEARCH FOR PRESENCE OF CAUSTIC
      IF(R(NTH,J).GT.R(1,J))GO TO 12
      RU=R(1,J) & RD=R(NTH,J)
      GO TO 14
      12 RU=P(NTH,J) & RD=R(1,J)

```



PAGE 2

## SUBROUTINE RAYSUM

```

14 DRUP=RMXJ-RU & DRON=RD-RMNJ
   IF (DRUP.LE.0.) GO TO 16
   IF (DRON.LE.0.) GO TO 20
   IF (DRUP.GT.DRDN) GO TO 20
   GO TO 18
16 IF (DRDN.LE.0.) GO TO 24
18 ICAUST(J)=1 & ICTH(J)=ITHMN
   IF (RP(ITHMN,J).GT.0.) GO TO 24
   GO TO 22
20 ICAUST(J)=-1 & ICTH(J)=ITHMX
   IF (RP(ITHMX,J).LT.0.) GO TO 24
22 ICTH(J)=ICTH(J)+1
24 RMNJ(J)=(RMNJ-RMIN)/DR+2. & KMXJ(J)=(RMXJ-RMIN)/DR+1.
   IF (KMNJ(J).LT.1) KMNJ(J)=1
   IF (KMXJ(J).GT.KMAX) KMXJ(J)=KMAX
   IF (KMXJ(J).LT.KMNJ(J)) ICAUST(J)=0
30 CONTINUE
   KMN=(RMN-RMIN)/DR+2. & KMX=(RMX-RMIN)/DR+1.
   IF (KMX.GT.KMAX) KMX=KMAX
   IF (KMN.LT.1) KMN=1
   IF (IPR.GT.1) PRINT 4001,KMN,KMX,(KMNJ(J),KMXJ(J),J=1,NJ)
4001 FORMAT(20H KMN KMX (KMNJ KMXJ),I17,I4.4(I10,I4))
   IF (IL.EQ.NL) GO TO 70
   IF (KMX.LT.KMN) GO TO 999
   DO 60 J=1,NJ
   IF (ICAUST(J).EQ.0) GO TO 60
   KTH=ICTH(J)
C----COMPUTE CAUSTIC CORRECTIONS
   CALL RCAUST(KTH,J)
60 CONTINUE
   IF (IL.NE.NL) GO TO 110
70 DO 100 J=1,NJ
   RK=R(NTH,J) & RPK=RP(NTH,J) & VAK=VA(NTH)
   IF (PK.LT.1.) GO TO 100
C----CONSTANTS IN SIMPLIFIED FORMULA FOR STEEP ANGLE PROPAGATION
   A0(J)=-RPK/(RK*RK) & A1(J)=1./RK-A0(J)*VAK

```

PAGE 3

## SUBROUTINE RAYSUM

```

100 CONTINUE
   IF(IPR.GT.1) PRINT 4010,(A0(J),J=1,NJ)
4010 FORMAT(11H RYSM A0(J),48X,4E15.8)
   IF(IPR.GT.1) PRINT 4020,(A1(J),J=1,NJ)
4020 FORMAT(11H RYSM A1(J),48X,4E15.8)
   K1=1
   GO TO 120
110 K1=KMN
120 IF(KMX.LT.K1) GO TO 999
   HLIM=0.
   DO 900 K=K1,KMX
   RK=RMIN+(K-1)*DR
   DO 130 J=1,NJ
   DO 130 JJ=1,2
   VAKK(J,JJ)=0.
   DO 130 IF=1,NF
130 HTRM(J,JJ,IF)=0.
   DO 420 J=1,NJ
   KTYPE=0
   IF(K.GT.KMXJ(J)) GO TO 420
   ILOOP=NLOOP+1
   IF(IL.NE.NL) GO TO 140
   IF(K.GE.KMNJ(J)) GO TO 190
   KTYPE=1
C---SIMPLIFIED APPROXIMATE COMPUTATION APPLICABLE TO STEEP ANGLES
   VAK=(1./RK-A1(J))/A0(J)
   RPK=-A0(J)*RK*RK
   CVK2=CAA2*(1.+VAK*VAK) $ CVK=SQRT(CVK2)
   THRD=RTD*ACOS(CA(NA)/CVK)
   CALL BOTTOM(THRD)
   GO TO 220
140 IF(K.LT.KMNJ(J)) GO TO 420
C---LOOK FOR TWO BRANCHES ON RANGE-VA CURVE
   IF(ICAUST(J)) 150,190,160
150 IF(K.GE.KA(J,IFMAX)) GO TO 420
   IF(RK.LT.P(1,J)) GO TO 170

```

PAGE 4

## SUBROUTINE RAYSUM

```

      ITHMX=ICTH(J)
      IF(RK.LT.R(NTH,J)) GO TO 190
      GO TO 180
160  IF(K.LE.KA(J,IFMAX)) GO TO 420
      IF(RK.GT.R(1,J)) GO TO 170
      ITHMX=ICTH(J)
      IF(RK.GT.R(NTH,J)) GO TO 190
      GO TO 180
170  ITHMN=ICTH(J) $ ILOOP=2
180  NLOOP=2
190  IF(ITHMX.LE.ITHMN) GO TO 365
C---INTERPOLATE BETWEEN RAYS IN EITHER SIDE OF RECEIVER RANGE
      DO 200 JTH=ITHMN,ITHMX
      ITH=JTH
      IF(ILOOP.EQ.1) ITH=ITHMX-JTH+1
      DR2=RK-R(ITH,J)
      IF(JTH.EQ.ITHMN) GO TO 200
      PROD=DR1*DR2
      IF(PROD.LT.0.) GO TO 210
200  DR1=DR2
210  IF(ILOOP.EQ.1) ITH=ITH+1
      ITH1=ITH
      RAT=(RK-R(ITH-1,J))/(R(ITH,J)-R(ITH-1,J))
      VAK=(1.-RAT)*VA(ITH-1)+RAT*VA(ITH)
      RPK=(1.-RAT)*RP(ITH-1,J)+RAT*RP(ITH,J)
      CVK2=CAA2*(1.+VAK*VAK) $ CVK=SQRT(CVK2)
220  IF(RPK.GT.0.) GO TO 230
      JJ=1
      GO TO 240
230  JJ=2
240  VAKK(J,JJ)=VAK
      VRK=SQRT(CVK2/CH2-1.)
      RPKA=AKS(RPK) $ RPKK(J,JJ)=RPKA
C---COMPUTE RAY SPREADING LOSS FACTOR
      HK=CAA*CAA2/(CVK2*CHH*VHK*HK*RPKA)
      IF(IREAM.EQ.0) GO TO 300

```



PAGE 5

## SUBROUTINE RAYSUM

```

      IF (SN.EQ.-1.) GO TO 250
      VRM=SIGN(J)*VAK
      GO TO 260

      250 VRM=SIGN(J)*VBK
      C---COMPUTE BEAM LOSS FACTORS
      260 CALL BEAM(1)
      DO 270 IF=1,NF
      270 HMF(J,JJ,IF)=BMFAC(IF)
      IF (IPR.GT.1) PRINT 4030,K,J,JJ,VHM,(HMFAC(IF),IF=1,NF)
      4030 FORMAT(26H RYSM K J JJ VHM BMFAC(IF).8X,I4,2I3,7F12.6)
      300 DO 360 IF=1,NF
      IF (ICAUST(J)) 310,330,320
      310 IF (K.GE.KA(J,IF)) GO TO 360
      GO TO 330
      320 IF (K.LE.KA(J,IF)) GO TO 360
      330 BLK=SLK=0.
      IF (IBOT.EQ.0) GO TO 350
      IF (K.TYP.EQ.1) GO TO 340
      BLK=(1.-RAT)*BLOSS(ITH1-1,IF)+RAT*BLOSS(ITH1,IF)
      GO TO 350
      340 BLK=BOTL(IF)
      350 IF (ISUPF.NE.0) SLK=SLOSS(IF)
      C---COMPUTE OVERALL ATTENUATION FACTOR
      FAC=1./10.**((NCYC*(HLK+SLK)+ALPHA(IF)*RK)/10.)
      IF (IREAM.NE.0) FAC=FAC*BMFAC(IF)*HMFAC(IF)
      C---RAY INTENSITY
      HTRM(J,JJ,IF)=HK*FAC
      IF (HTRM(J,JJ,IF).GT.HLIM) HLIM=HTRM(J,JJ,IF)
      IF (IPR.GT.1) PRINT 4050,K,J,JJ,IF,BLK,FAC,HK,HTRM(J,JJ,IF)
      4050 FORMAT(34H RYSM K J JJ IF BLK FAC HK HTRM .I4,3I3,3X,2F12.6,
      *2E15.8)
      360 CONTINUE
      365 IF (ILOOP.EQ.NLOOP) GO TO 370
      ILOOP=ILOOP+1
      ITHMN=ICTH(J) * ITHMX=INTH
      GO TO 190

```

PAGE 6

## SUBROUTINE RAYSUM

```

370 IF(ICAUST(J).EQ.0) GO TO 420
DO 410 IF=1,NF
  IF(ICAUST(J)) 380,410,390
380 IF(K.GE.KA(J,IF).OR.K.LT.KB(J,IF)) GO TO 410
  KC=K-KB(J,IF)+1
  GO TO 400
390 IF(K.LE.KA(J,IF).OR.K.GT.KB(J,IF)) GO TO 410
  KC=K-KA(J,IF)
  400 TRM=HTRM(J,1,IF)+HTRM(J,2,IF)
C---COMPARE RAY AND CAUSTIC INTENSITIES IN OVERLAP REGION
  IF(TRM.GT.HC(KC,J,IF)) GO TO 410
C---SELECT AND STOKE CAUSTIC CORRECTION INTENSITY
  H(K,IF)=H(K,IF)+HC(KC,J,IF)
  IF(IPR.NE.0) PRINT 4060,K,J,IF,KC,TRM,HC(KC,J,IF),H(K,IF)
4060 FORMAT(24H RYSM K J IF KC TRM HC H,I14,I3,3X,2I3,39X,3E15.8)
  HTRM(J,1,IF)=HTRM(J,2,IF)=0.
410 CONTINUE
420 CONTINUE
DO 450 JJ=1,2
DO 480 IF=1,NF
  ISUM=IND=ICOH=0 $ HK=TRM=0.
DO 450 J=1,NJ
  IF(HTRM(J,JJ,IF).EQ.0.) GO TO 450
  ISUM=ISUM+1 $ IND=10*IND+J
  HK=HK+HTRM(J,JJ,IF)
450 CONTINUE
  IF(ISUM.EQ.0.) GO TO 480
  IF(JCOH(IF).EQ.1.OR.ISUMF.EQ.0) GO TO 670
  GO TO (670,460,470,620) ISUM
460 IF(IND.EQ.14.OR.IND.EQ.23) 670,600
470 IF(7AA.GT.288) GO TO 530
  IF(IND.GT.123) GO TO 480
  J=3
  GO TO 490
480 IF(IND.GT.124) GO TO 500
  J=4

```

PAGE 7

## SUBROUTINE HAYSUM

```

490 IND=12
   GO TO 590
500 IF(IND.GT.134) GO TO 510
   J=1
   GO TO 520
510 J=2
520 IND=34
   GO TO 590
530 IF(IND.GT.123) GO TO 540
   J=2
   GO TO 580
540 IF(IND.GT.124) GO TO 550
   J=1
   GO TO 570
550 IF(IND.GT.134) GO TO 560
   J=4
   GO TO 580
560 J=3
570 IND=24
   GO TO 590
580 IND=13
590 TRM=HTRM(J,JJ,IF) & HK=HK-TRM
600 JA(1)=IND/10 & JA(2)=IND-10*JA(1)
   VAK=0.
   DO 610 J=1,2
   JB=JA(J)
610 VAK=VAK+VAKK(JB,JJ)/2.
   GO TO 640
620 VAK=0.
   DO 630 J=1,4
630 VAK=VAK+VAKK(J,JJ)/4.
640 CVK2=CAAP*(1.+VAK*VAK) & CVK=SQRT(CVK2)
   V0=SQRT(CVK2/(CA(1)*CA(1))-1.)
   IF(IND.F0.13.04.IND.F0.24) GO TO 650
   IF(NCVC.F0.0.AND.7AA.GT.ZFH) GO TO 650
   ZRCH=2.*ZAA/V0

```



PAGE 8

## SUBROUTINE HAYSUM

```

      IF (ZRCOH.LT.KCOH) ICOH=1
      IF (ISUM.LT.4) GO TO 660
      650 ZRCOH=2.*ZHR/V0
      IF (ZRCOH.GE.KCOH) GO TO 660
      ICOH=ICOH+2
      GO TO 680
      660 IF (ICOH.GT.0) GO TO 680
      670 TRM=TRM+HK
      GO TO 870
      680 IF (ICOH.EQ.3) GO TO 800
      IL00P=1
      IF (ISUM.EQ.4) GO TO 700
      NLO0P=1
      GO TO 750
      700 NLO0P=2
      IND=12
      IF (ICOH.EQ.2) IND=13
      720 JA(1)=IND/10 & JA(2)=IND-10*JA(1)
      VAK=HK=0.
      DO 730 J=1,2
      JH=JA(J)
      HK=HK+HTRM(JB,JJ,IF)
      730 VAK=VAK+VAKK(JB,JJ)/2.
      CVK2=CAA2*(1.+VAK*VAK) & CVK=SQRT(CVK2)
      V0=SQRT(CVK2/(CA(1)*CA(1))-1.)
      750 PHFAC=4.*PI*V0*F(IF)/CVK
      7=7AA
      IF (ICOH.EQ.2) Z=ZHH
      PHIS=PHFAC*2 & FRACTS=1.
      IF (IREAM.EQ.0) GO TO 760
      JH=JA(1) & BMF1=BMF(JB,JJ,IF)
      JH=JA(2) & BMF2=BMF(JB,JJ,IF)
      DEN=BMF1*BMF1+BMF2*BMF2
      FRACTS=2.*HMFL*BMF2/DEN
      760 IF (JCOH(IF).EQ.2) GO TO 770
      FRACTA=AH5(FRACTS) & SGN=FRACTS/FRACTA

```

PAGE 9

## SUBROUTINE RAYSUM

```

      ANPPC=CVK2*CVK*V0*RPKA/(2.*CAA2*VAK*DR*(IF)*Z)
      FRACTB=1./(1.+EXP(AX*(XA-ANPPC)))
      IF (FRACTB.LT.FRACTA) FRACTS=SGN*FRACTH
770  COFACS=1.-FRACTS*COS(PHIS)
      HKK=HK*COFACS
      TRM=TRM+HKK
      IF (IPR.GT.1) PRINT 4070,IND,ILOOP,FRACTS,PHIS,COFACS,HK,HKK
4070  FORMAT(34H IND ILOOP FRCTS PHS COFCS HK HKK,I10,I6,2F12.6,F15.6,
      *2E15.8)
      IF (ILOOP.EQ.NLOOP) GO TO 870
      IND=34
      IF (ICOH.EQ.2) IND=24
      ILOOP=ILOOP+1
      GO TO 720
800  PHFAC=4.*PI*V0*(IF)/CVK
      PHIA=PHFAC*ZAA & PHIR=PHFAC*ZBR
      ANFAC=CVK2*CVK*V0*RPKA/(2.*CAA2*VAK*DR*(IF))
      ANPPCA=ANFAC/ZAA & ANPPCH=ANFAC/ZBR
      FRACTS=1.
      IF (SN.EQ.-1.) GO TO 810
      PHIS=PHIA & ANPPC=ANPPCA
      IF (IREAM.EQ.0) GO TO 830
      RMF1=(RMF(1,JJ,IF)+RMF(3,JJ,IF))/2.
      RMF2=(RMF(2,JJ,IF)+RMF(4,JJ,IF))/2.
      GO TO 820
810  PHIS=PHIR & ANPPC=ANPPCH
      IF (IREAM.EQ.0) GO TO 830
      RMF1=(RMF(1,JJ,IF)+RMF(2,JJ,IF))/2.
      RMF2=(RMF(3,JJ,IF)+RMF(4,JJ,IF))/2.
      DEN=RMF1*RMF1+RMF2*RMF2
      FRACTS=2.*RMF1*RMF2/DEN
830  IF (JCOH(IF).EQ.2) GO TO 840
      FRACTA=ABS(FRACTS) & SGN=FRACTS/FRACTA
      FRACTB=1./(1.+EXP(AX*(XA-ANPPC)))
      IF (FRACTB.LT.FRACTA) FRACTS=SGN*FRACTH
840  COFACS=1.-FRACTS*COS(PHIS)

```

PAGE 10

SUBROUTINE RAYSUM

```

      IF(SN.EQ.-1.) GO TO 850
      PHIR=PHIR $ ANPPC=ANPPC
      GO TO 860
      850 PHIR=PHIR $ ANPPC=ANPPC
      860 FRACTR=1.
           IF(JCOH(IF).EQ.0) FRACTR=1./(1.+EXP(AX*(XA-ANPPC)))
      COFACR=1.-FRACTR*COS(PHIR)
      TRM=HK*COFACS*COFACR
      IF(IPR.GT.1) PRINT 4080,FRACTS,FRACTR,PHIS,PHIR,COFACS,COFACR,HK
      4080 FORMAT(34H FRACTS FRACTR PHS PHR CFCS CFCR HK,2F9.6,2F12.6,2F15.6,
      *E15.8)
      870 H(K,IF)=H(K,IF)+TRM
           IF(IPR.NE.0) PRINT 4100,K,JJ,ICOH,IF,ISUM,TRM,H(K,IF)
      4100 FORMAT(34H RYSM K JJ ICOH IF ISUM TRM H ,14,413.54X,2E15.8)
      880 CONTINUE
      890 CONTINUE
      900 CONTINUE
      999 RETURN
      END

```



PAGE 1

## SUBROUTINE RCAUST

```

      SUBROUTINE RCAUST(KTH,J)
      C---COMPUTES CAUSTIC CORRECTIONS
      COMMON CH(50),CSP(50),GP(50),IBEAM,IRP,IDHT(4),IPR,IPOF,ISP,
      *NR,NF,PI,RADE,RTD,7F(50),ZP(50)
      COMMON CA(50),CAA,CAA2,CBB,CBB2,IAA,IAD,IAB,IDF(50),IDUCT,ISD,NA,
      *SN,7A(50),ZAA,ZAD,ZAR,ZR,ZS
      COMMON RMFAC(6),CL(10),CV,CV2,ILR,ILS,NL,NTH,SIGN(4),TH(50),
      *TH1,TH2,VA(50),VRN
      COMMON ALPHA(6),BLOSS(50,6),BOTL(6),F(6),F13(6),IHOT,ISURF,
      *SLOSS(6)
      COMMON DR,H(251,6),HC(15,4,6),ICAUST(4),IFMAX,J1,KA(4,6),KB(4,6),
      *KMAX,KMN,KMNJ(4),KMxJ(4),NCYC,NJ,R(50,4),RCYC(50),RMIN,RP(50,4),
      *RPCYC(50),RPSR(50),RPU(50),RSR(50),RUP(50)
      DATA CCI,X1,X2,X3 /8,92368,3,5,-1.77,-2.2/
      C - CCI=(3.**((2./3.))*((2.)*(PI**((2./3.)))) FIRST FACTOR IS FT-YD CONVERSI
      C---SECOND DERIVATIVE OF RANGE WITH RESPECT TO VA
      RPP=(RP(KTH,J)-RP(KTH-1,J))/(VA(KTH)-VA(KTH-1))
      PPPA=ARS(RPP)
      ISGN=1
      IF(ICAUST(J).LT.0) ISGN=-1
      VAC=VA(KTH)-RP(KTH,J)/RPP
      DV1=VA(KTH-1)-VAC * DV2=VA(KTH)-VAC
      C---RANGE TO THE CAUSTIC
      KC=(R(KTH,J)+R(KTH-1,J))-RPP*(DV1*DV1+DV2*DV2)/2.)/2.
      IF(KTH.LE.2) GO TO 2
      C---ALTERNATE COMPUTATIONS OF SECOND DERIVATIVE
      RPPT=(RP(KTH-1,J)-RP(KTH-2,J))/(VA(KTH-1)-VA(KTH-2))
      IF((RPP*RPPPT).LT.0.) GO TO 2
      RPPTA=ARS(RPPT)
      IF(RPPTA.GE.KPPA) GO TO 2
      RPP=RPPT * RPPA=RPPTA
      ? IF(KTH.EQ.NTH) GO TO 4
      RPPT=(RP(KTH+1,J)-RP(KTH,J))/(VA(KTH+1)-VA(KTH))
      IF((RPP*RPPPT).LT.0.) GO TO 4
      RPPTA=ARS(RPPT)
      IF(RPPTA.GE.KPPA) GO TO 4

```

PAGE 2

## SUPPORTIVE YCAUST

```

RPP=RPPT $ RPPA=RPPTA
4 PAT=(VAC-VA(KTH-1))/(VA(KTH)-VA(KTH-1))
  CVC=CAA*SORT(1.+VAC*VAC) $ CVC2=CVC*CVC
  RPPC=ISGN*(RPPA/(VAC*VAC*CAA))*1./3.)
  COEF=-CC1*CAA/(CVC2*RPPTC)
  VHC=SORT(CVC2/CH2-1.)
  FAC1=CAA*CVC/13.*RC*CHH*ABS(VAC)*VHC)
  IF (IREAM.EQ.0) GO TO 15
  IF (SN.EQ.-1.) GO TO 5
  VRM=SIGN(J)*VAC
  GO TO 10
5 VRM=SIGN(J)*VHC
10 CALL BEAM(1)
  IF (IPR.GT.1) PRINT 4103,J,VRM,(HMFAC(IF),IF=1,NF)
4103 FORMAT(21H RCST J VRM HMFAC(IF).123,7F12.6)
15 DO 100 IF=1,NF
  RLK=SLK=0.
  IF (IR0T.NE.0) RLK=(1.-RAT)*HLOSS(KTH-1,IF)+RAT*HLOSS(KTH,IF)
  IF (ISUPF.NE.0) SLK=HLOSS(IF)
  COEF1=COEF*F13(IF)*F13(IF)
  COEF2=COEF*COEF*FAC1*F13(IF)
  C---RANGE LIMIT ON SHADOW SIDE OF CAUSTIC
  RC1=RC+X1/COEF1 $ K1=(RC1-RMIN)/DR+1.
  C---FIRST RANGE LIMIT ON INSONIFIED SIDE OF CAUSTIC
  RC2=RC+X2/COEF1 $ K2=(RC2-RMIN)/DR+1.
  C---SECOND RANGE LIMIT ON INSONIFIED SIDE (CONDITIONAL REGION)
  RC3=RC+X3/COEF1 $ K3=(RC3-RMIN)/DR+1.
  IF (ISGN.LT.0) GO TO 20
  K1=K1+1
  IF (K1.LT.1) K1=1
  K3T=K2+15
  IF (K3.GT.K3T) K3=K3T
  IF (K2.GT.KMXJ(J)) K2=KMXJ(J)
  IF (K3.GT.KMXJ(J)) K3=KMXJ(J)
  GO TO 30
20 K2=K2+1 $ K3=K3+1

```

PAGE 3

## SUBROUTINE RCAUST

```

K3T=K2-15
IF(K3.LT.K3T) K3=K3T
IF(K1.GT.KMAX) K1=KMAX
IF(K2.LT.KMNJ(J)) K2=KMNJ(J)
IF(K3.LT.KMNJ(J)) K3=KMNJ(J)
30 IF(ISGN*(K3-K1).GE.0) GO TO 40
   ICAUST(J)=0
   GO TO 100
40 IF(IPR.GT.1) PRINT 4102,K1,K2,K3,HCI,KC2,VAC,PPP,COEF1,COEF2
4102 FORMAT(34H K1,2,3 HCI KC2 VAC RPP COF1 COF2,2X,3I4,2X,2F12.4,
*4E15.8)
L2=ISGN*(K2-K1)+1 * L3=ISGN*(K3-K1)+1
KA(J,IF)=K2 * KB(J,IF)=K3
DO 90 L=1,L3
  K=K1+ISGN*(L-1)
  RK=PMIN+(K-1)*DR
  X=COEF1*(RK-KC)
C---HK IS INTENSITY (EXCLUSIVE OF RAY ATTENUATION). FAC IS ATTENUATION
  AII=A12(X) * HK=COEF2*AII
  FAC=1./10.**((NCYC*(RLK+SLK)+ALPHA(IF)*HK)/10.)
  IF(IREAM.NE.0) FAC=FAC*RMFAC(IF)*RMFAC(IF)
  TPM=HK*FAC
  IF(L.LE.L2) GO TO R0
  IF(ICAUST(J).LT.0) GO TO 50
  KC=K-K2
  GO TO 60
50 KC=K-K3+1
C---CONDITIONAL INTENSITIES (TO BE COMPARED WITH RAY INTENSITIES)
60 HC(KC,J,IF)=TRM
  IF(IPR.GT.1) PRINT 4110,K,IF,KC,HLK,FAC,RC,HK,TRM
4110 FORMAT(34H RCST K IF KC HLK FAC RC HK TRM ,14.6X,2I3,2F12.6,
*3E15.8)
  GO TO 90
C---UNCONDITIONAL INTENSITIES (STORED IN H ARRAY)
R0 H(K,IF)=H(K,IF)+TPM
  IF(IPR.NE.0) PRINT 4120,K,J,IF,KTH,BLK,FAC,RC,HK,TPM,H(K,IF)

```



SUBROUTINE RCAUST  
PAGE 4  
4120 FORMAT(34H WCST K J IF KT BL FAC PC HK TRM H,I4,I3,3X,2I3,2F12.6,  
#4E15.8)  
90 CONTINUE  
100 CONTINUE  
RETURN  
END

PAGE 1

## FUNCTION AI2

```

      FUNCTION AI2(X)
      C---COMPUTES SQUARE OF AIRY FUNCTION AI(X)
      DIMENSION A(4)
      DATA C1/0.355028/.C2/0.258819/.EPS/1.E-6/
      DATA A/-0.0195216, 0.31288, 3.04077,6.709/
      IF (X.GT.1.) GO TO 20
      SUM1=TERM1=1. $ SUM2=TERM2=X
      X3=X*X*X $ I=0
10    I=I+1
      TERM1=TERM1*X3/(3*I*(3*I-1))
      TERM2=TERM2*X3/(3*I*(3*I+1))
      SUM1=SUM1+TERM1 $ SUM2=SUM2+TERM2
      IF (ABS(TERM1).GT.EPS.OR.ABS(TERM2).GT.EPS) GO TO 10
      AI=C1*SUM1-C2*SUM2
      AI2=AI*AI
      GO TO 999
20    XX=X-2. $ SUM1=A(1)
      DO 30 I=2,4
30    SUM1=SUM1*XX+A(I)
      AI2=EXP(-SUM1)
999  RETURN
      END

```

PAGE 1

SUBROUTINE SURF

```

      SUBROUTINE SURF
C-----COMPUTES SURFACE REFLECTION LOSS (SAME AS IN OLD NADC PROGRAM)
      COMMON CH(50),CSP(50),GP(50),IREFAN,IRP,INDHT(4),IPR,IPOF,ISP,
      *NR,NF,PI,RADE,RTD,7R(50),ZP(50)
      COMMON CA(50),CAA,CAA2,CHB,CHB2,IAA,IAD,IHB,IDF(50),IDUCT,ISD,NA,
      *SN,7A(50),ZAA,ZAD,7RH,ZR,ZS
      COMMON RMFAC(6),CL(10),CV,CV2,ILH,ILS,NL,NTH,SIGN(4),TH(50),
      *TH1,TH2,VA(50),VRM
      COMMON ALPHA(6),RLOSS(50,6),ROT(6),F(6),F13(6),IROT,ISURF,
      *SLOSS(6)
      WH=5.*ISP*ISP/12.
      DO 20 IF=1,NF
      SP=WH*F(IF)/1000.
      IF(SP.NE.0.) GO TO 10
      SLOSS(IF)=0. $ GO TO 20
      SLOSS(IF)=13./(1.+126./(SP**1.666))
      10 CONTINUE
      20 RETURN
      END

```



SUBROUTINE BOTTOM

PAGE 1

```

      SUBROUTINE BOTTOM(THHD)
C-----COMPUTES BOTTOM LOSS FROM FENC CURVES (AS IN OLD NADC PROGRAM) ON FR
C SPECIAL INPUTS IN DATA DECK
      COMMON CB(50),CSP(50),GP(50),IBEAM,IMP,IDHT(4),IPR,IPROF,ISP,
      *NP,NF,PI,PADE,RTD,7H(50),ZP(50)
      COMMON CA(50),CAA,CAAP,CBB,CBB2,IAA,IAD,IHH,IDF(50),IDUCT,ISD,NA,
      *SN,7A(50),ZAA,ZAD,7BH,ZH,ZS
      COMMON HMFAC(6),CL(10),CV,CV2,ILR,ILS,NL,NTH,SIGN(4),TH(50),
      *TH1,TH2,VA(50),VRM
      COMMON ALPHA(6),RLOSS(50,6),HOTL(6),F(6),F13(6),IBOT,ISURF,
      *SLOSS(6)
      COMMON /DATA/ DB(15,6,6),DG(15,6,6),FR(6)
      DIMENSION BOT(2),IFR(2)
      DIMENSION B1(75),B2(75),B3(75),B4(75),B5(75),B6(75),B1(75),G2(75),
      *G3(75),G4(75),G5(75),G6(75)
      EQUIVALENCE (DB(1),B1(1)),(DB(91),B2(1)),(DB(181),B3(1)),(DB(271),
      *B4(1)),(DB(361),B5(1)),(DB(451),B6(1)),(DG(1),G1(1)),(DG(91),
      *G2(1)),(DG(181),G3(1)),(DG(271),G4(1)),(DG(361),G5(1)),(DG(451),
      *G6(1))

```

The FENC bottom loss curves have been intentionally  
 deleted here in order that this publication be available  
 for Public Release.

PAGE 2

SUBROUTINE BOTTOM

```

DATA(G1=19.0,35.0,40.0,52.0,11(90.0),19.0,25.0,35.0,45.0,55.0,
110(90.0),11.0,20.0,25.0,35.0,45.0,55.0,9(90.0),11.0,20.0,30.0,
240.0,55.0,10(90.0),5.0,7.0,8.0,17.0,18.0,19.0,20.0,21.0,22.0,
36(90.0))
DATA(G2=18.2,30.0,40.0,50.0,55.0,10(90.0),17.0,20.0,30.0,40.0,
150.0,55.0,9(90.0),13.0,20.0,35.0,45.0,53.0,10(90.0),7.0,11.0,20.0,
225.0,30.0,34.0,9(90.0),2.0,3.0,5.0,15.0,20.0,22.0,9(90.0))
DATA(G3=19.0,25.0,35.0,51.0,11(90.0),18.0,25.0,35.0,45.0,55.0,
110(90.0),14.0,20.0,30.0,40.0,50.0,53.0,9(90.0),4.0,10.5,20.0,22.0,
223.0,26.0,9(90.0),2.0,3.0,10.0,15.0,17.0,20.0,23.0,5(90.0))
DATA(G4=18.0,23.0,30.0,40.0,55.0,10(90.0),16.8,20.0,25.0,30.0,
135.0,45.0,55.0,8(90.0),13.0,25.0,30.0,35.0,42.0,45.0,50.0,6(90.0),
29.0,12.0,13.0,20.0,22.0,23.0,27.0,8(90.0),2.0,3.0,5.0,10.0,14.0,
317.0,18.0,20.0,23.0,6(90.0))
DATA(G5=2.0,3.0,10.0,15.0,20.0,30.0,35.0,40.0,7(90.0),2.0,3.0,
112.0,20.0,25.0,32.0,37.0,42.0,7(90.0),2.0,3.0,6.0,7.0,8.0,12.0,
213.0,17.5,23.0,27.5,32.0,4(90.0),2.0,3.0,7.0,10.0,13.0,15.0,20.0,
324.0,7(90.0),2.0,3.0,5.0,10.0,12.0,13.0,15.0,20.0,23.0,28.0,
45(90.0))
DATA(G6=7.0,8.0,11.0,13.0,14.0,15.0,20.0,25.0,27.0,28.0,5(90.0),
17.0,8.0,10.0,15.0,18.0,20.0,25.0,30.0,7(90.0),7.0,8.0,15.0,20.0,
223.0,25.0,27.0,4(90.0),7.0,8.0,10.0,15.0,18.0,20.0,22.0,23.0,28.0,
36(90.0),2.0,3.0,5.0,10.0,15.0,18.0,23.0,7(90.0))
IF(IRD)300,320,5
5 DO 240 IF=1,NF
FF=F(IF)
IFR(2)=0
IF(FF-FR(1))70,70,10
10 IF(FF-FR(2))60,90,20
20 IF(FF-FR(3))80,110,30
30 IF(FF-FR(4))100,130,40
40 IF(FF-FR(5))120,150,50
50 IF(FF-FR(6))140,160,160

```

PAGE 3

## SUBROUTINE HOTTOM

```

60 IFR(2)=2
   F2=(FF-FK(1))/(FW(2)-FR(1))
70 IFR(1)=1
   GO TO 170
80 IFR(2)=3
   F2=(FF-FK(2))/(FR(3)-FR(2))
90 IFR(1)=2
   GO TO 170
100 IFR(2)=4
   F2=(FF-FK(3))/(FR(4)-FR(3))
110 IFR(1)=3
   GO TO 170
120 IFR(2)=5
   F2=(FF-FK(4))/(FR(5)-FR(4))
130 IFR(1)=4
   GO TO 170
140 IFR(2)=6
   F2=(FF-FK(5))/(FR(6)-FR(5))
150 IFR(1)=5
   GO TO 170
160 IFR(1)=6
170 DO 220 IJK=1,2
   IF (IFR(IJK)) 180,230,180
180 J=IFR(IJK)
   I=1
   IF (THRD-DG(I,IBP,J)) 200,200,190
190 I=I+1
   IF (THRD-DG(I,IBP,J)) 210,200,190
200 ROT(IJK)=DB(I,IBP,J)
   GO TO 220
210 IM=I-1
   O2=(THRD-DG(IM,IBP,J))/(DG(I,IBP,J)-DG(IM,IBP,J))
   ROT(IJK)=(1.-O2)*DB(IM,IBP,J)+O2*DB(I,IBP,J)
220 CONTINUE
   ROTL(IF)=(1.0-F2)*ROT(1)+F2*ROT(2)
   GO TO 240

```



PAGE 4

SUBROUTINE BOTTOM

```

230 BOTL(IF)=BOT(1)
240 CONTINUE
    GO TO 999
300 DO 310 IF=1,NF
310 BOTL(IF)=100.
    GO TO 999
320 DO 330 IF=1,NF
330 BOTL(IF)=0.
999 RETURN
    END
    
```

PAGE 1

SUBROUTINE SDOCT

```

      SUBROUTINE SDOCT
      C---SIMPLIFIED SURFACE DUCT MODEL, DERIVED FROM NORMAL MODE COMPUTATIONS
      C - REVISED MODEL, INCLUDING BOTH POOR AND GOOD DUCTS -- JAN. 1975
      COMMON CB(50),CSP(50),GP(50),IHEAM,IHP,IDHT(4),IPR,IPROF,ISP,
      *NR,NF,PI,RADE,RTD,ZP(50),ZP(50)
      COMMON CA(50),CAA,CAA2,CBH,CH2,IAA,IAD,IAB,IDF(50),IDUCT,ISD,NA,
      *SN,YA(50),ZAA,ZAD,ZPR,ZP,ZS
      COMMON HMFAC(6),CL(10),CV,CV2,ILR,ILS,NL,NTH,SIGN(4),IH(50),
      *TH1,TH2,VA(50),VRM
      COMMON ALPHA(6),BLOSS(50,6),BOTL(6),F(6),F13(6),IHOT,ISURF,
      *SLOSS(6)
      COMMON DR,H(251,6),HC(15,4,6),ICAUST(4),IFMAX,J1,KA(4,6),KB(4,6),
      *KMAX,KMN,KMNJ(4),KMXXJ(4),NCYC,NJ,R(50,4),RCYC(50),RMIN,RP(50,4),
      *RPCYC(50),RPSR(50),RPUP(50),RSR(50),RUP(50)
      COMMON /SDCT/ EN,FR,THETA,ZA,V0
      DIMENSION BMF2(6)
      DATA A10,A11,A2,A30,A31,A32/3.7,0.1586,-3.237,0.7965,2.78,-10.422/
      DATA B1,B2,B3 /1.5,-6.0,0.92/
      DATA C1,C2 /32.0,13.0/
      DATA HM/1.E-13/
      IF(IREAM.EQ.0) GO TO 6
      CAD2=CA(IAD)*CA(IAD)
      CAC2=CAA2
      IF(SN.EQ.-1.) CAC2=CRH2
      VRM=SQRT(CAD2/CAC2-1.)
      CALL BEAM(1)
      IF(IPR.GT.1) PRINT 4000,VRM,(HMFAC(IF),IF=1,NF)
      4000 FORMAT(5H SDCT,BX,13HVHM RMFAC(IF),18X,7F12.6)
      DO 2 IF=1,NF
      2 RMF2(IF)=BMFAC(IF)*HMFAC(IF)
      VRM=-VRM
      CALL BEAM(1)
      IF(IPR.GT.1) PRINT 4000,VRM,(HMFAC(IF),IF=1,NF)
      DO 4 IF=1,NF
      4 HMF2(IF)=(HMF2(IF)+HMFAC(IF)*HMFAC(IF))/2.
      6 IND=0

```

PAGE 2

## SUBROUTINE SDUCT

```

ZA=7AD
ZAI=7AD/100. $ ZAP2=7AI*SQRT(ZAI)
FMIN=200./ZAI*.2.4
DO 250 IF=1,NF
  FR=F(IF) $ FF=FR/100.
  C---TEST TO DETERMINE WHETHER DUCT IS TOO POOR TO MOTHER WITH
  IF (FR.LT.FMIN) GO TO 250
  EN=0.25+0.067462*FF*.7A32
  A1=A10/ZAI**A11 $ A3=A30*EXP((A31+A32*EN)*EN)
  C---ALPHA IS ATTENUATION COEFFICIENT DUE TO DIFFRACTION LEAKAGE
  ALPHA=EXP(A1+A2*EN+A3)/1000.
  IF (ISP-3) 10,20,30
  10 W=0.00444 $ GO TO 40
  20 W=0.00666 $ GO TO 40
  30 W=0.00888
  C---ALPHA3 IS ATTENUATION COEFFICIENT DUE TO SURFACE ROUGHNESS (FACT MODE
  40 ALPHA3=W*SQRT(FR/(1000.*7A))
  ALP1=ALP1+ALP3+ALPHA*(IF)
  V0=5000.*(1./SQRT(1.-0.0692/FR**(.2./3.))-1.)
  IF (FN.GT.1.5) GO TO 110
  C---POOR DUCT MODEL
  US=DEPFN(ZAA) $ THETS=THETA
  UR=DEPFN(ZBR) $ THETR=THETA
  U=US*UR
  FAC1=1667.*U*U/FR
  DO 100 K=1,KMAX
  RK=AMIN+(K-1)*DR
  FAC2=1.
  HK=FAC1/RK
  IF (HK.GT.2500.) FAC2=10.**((HK-2500.)/5000.)
  HKK=2./(FAC2*HK*HK)
  IF (THETS.GT.1.57) GO TO 60
  STH=SIN(THETS) $ HKK=HKK*STH*STH
  60 IF (THETR.GT.1.57) GO TO 70
  STH=SIN(THETR) $ HKK=HKK*STH*STH
  C---HKK - NORMAL MODE INTENSITY. HKK - SPHERICAL SPREADING

```



PAGE 3

## SUBROUTINE SDOCT

```

70 IF (HKK.GT.HK) HK=HKK
   FAC=1./10.**((ALP1*HK/10.))
   IF (IBEAM.NE.0) FAC=FAC*RMF2(IF)
   TRM=HK*FAC
   IF (TRM.LT.HM) GO TO 250
   H(K,IF)=H(K,IF)+TRM
   IF (IPR.NE.0) PRINT 4001,K,IF,ALP1,FAC,U,HK,TM,H(K,IF)
4001 FORMAT(34H SDOCT K IF ALP1 FAC U HK TPM H,I4,I9,3X,2F12.6,
   *4E15.8)
100 CONTINUE
   GO TO 250
110 IF (IND.EQ.1) GO TO 150
C---GOOD DUCT MODEL
IND=1
EXS=EXP(B2*(ZAA/ZA-H3))
EXR=EXP(B2*(ZBB/ZA-H3))
FXA=EXP
IF (7AA.GT.ZBB) EXA=EXS
ALPH2=B1/(1000.*(1.+EXA))
ALP2=ALPH2+ALPH3+ALPHA(IF)
CS=(C1+EXS*C2)/(1.+EXS)
CR=(C1+EXR*C2)/(1.+EXR)
C=CR+CS
COFF=0.10472*V0*SQRT(V0)
FAC=1.-0.016*ZAA/V0
IF (FAC.LT.0.) FAC=0.
FAC1=COFF*(1.-FAC*SQRT(FAC))
FAC=1.-0.016*ZBB/V0
IF (FAC.LT.0.) FAC=0.
FAC2=COFF*(1.-FAC*SQRT(FAC))
150 DO 200 K=1,KMAX
   PK=4*MIN+(K-1)*DR
   HK=1./((PK*10.**((ALP1*HK+C)/10.)))
   HKK=2./((HKK*10.**((ALP2*HK/10.)))
C---HK - CYLINDRICAL SPREADING . HKK - SPHERICAL SPREADING
   IF (HKK.GT.HK) HK=HKK

```

PAGE 4

## SUBROUTINE SDOCT

```

FAC=1.
THETA=FAC1*FF
IF (THETA.GT.1.57) GO TO 160
STH=SIN(THETA) & FAC=STH*STH
160 THETA=FAC2*FF
IF (THETA.GT.1.57) GO TO 170
STH=SIN(THETA) & FAC=FAC*STH*STH
170 IF (IHEAM.NE.0) FAC=FAC*HMF2(IF)
TRM=FAC*HK
IF (TRM.LT.HM) GO TO 250
H(K,IF)=H(K,IF)+TRM
IF (IPR.NE.0) PRINT 4002,K,IF,ALP1,ALP2,FAC,HK,TRM,H(K,IF)
4002 FORMAT(34H SDOCT K IF ALP1 ALP2 FAC HK TRM H,14,I9,3X,2F12.6,
&F15.8)
200 CONTINUE
250 CONTINUE
999 RETURN
END

```

PAGE 1

FUNCTION DEPFN

```

FUNCTION DEPFN(Z)
C---COMPUTES DEPTH FUNCTIONS FOR POOR DUCT MODEL
C --- REVISED MODEL, JUNE 1974
COMMON /SUCT/ EN,F,THETA,ZA,V0
DATA B10,B11,B12,B13,B14,B2 /2.9,0.885,-0.087,4.328,0.18,-5.5/
DATA C10,C11,C12,C13,C14 / 0.04,0.039,-0.006,0.075,0.01/
DATA C20,C21,C22 /1.415,-0.31,0.795/
DATA C30,C31,C32,C33 /0.1808,0.3996,0.594,0.193/
DATA D10,D11,D12,D13 /0.244,-2.04,8.42,3.58/
DATA D20,D21,D22 /-0.444,3.42,3.49/
DATA E /0.10472/
ZAA=ZA/100. $ FF=F/100.
IF(ZAA.GT.4.) GO TO 10
R1=R10+(B11+B12*7AA)*7AA
GO TO 20
10 B1=B13+B14*ZAA
20 V1=EXP(B1+B2*EN)
V=V0+V1 $ V32=V*SQRT(V)
ZTP=62.5*V
IF(FF.GT.2.5) GO TO 30
C1=C10+(C11+C12*FF)*FF
GO TO 40
30 C1=C13+C14*FF
40 IF(FF.GT.2.) GO TO 50
C2=C20+C21*FF $ C3=C30+C31*FF
GO TO 60
50 C2=C22 $ C3=C32+C33*FF
60 UFAC=C1+EXP(-(C2+C3*7AA))
Z1=0.8*ZA $ Z11=0.9*ZTP
IF(Z11.LT.Z1) Z1=Z11
77=7
IF(7.GT.11) Z7=Z1
V7=1.-77/ZTP
V712=SQRT(V7) $ V714=SQRT(V712) $ V732=V7*V712
IF(V714.LT.0.82) V714=0.82
THETA=E*FF*V32*(1.-V732)

```



PAGE 2

```
FUNCTION DEPFN
  U=IFAC*SIN(THETA)/V714
  IF (7.LE.Z1) GO TO 100
  Z2=1.2*7A $ Z2=7
  IF (7.GT.Z2) Z2=Z2
  D1=D10+D11*EN+D12*EXP(-D13*EN)
  U=U*EXP(D1*(Z2-Z1)/7A)
  IF (7.LE.Z2) GO TO 100
  D2=D20+D21*EXP(-D22*EN)
  U=U*EXP(D2*(Z-Z2)/7A)
100 DEPFN=U
  RETURN
END
```

PAGE 1

SUBROUTINE REAM

```

      SUBROUTINE REAM(L)
      COMMON CH(50),CSP(50),GP(50),IBEAM,IRP,IOHT(4),IPR,IPOF,ISP,JCOH,
      *NR,NF,PI,RADE,RTD,7H(50),ZP(50)
      COMMON CA(50),CAA,CAAP,CBB,CBP,IAA,IAD,IAR,IDF(50),IDUCT,ISO,NA,
      *SN,7A(50),ZAA,ZAD,7PH,ZH,ZS
      COMMON BMFAC(6),CL(10),CV,CV2,ILR,ILS,NL,NTH,SIGN(4),TH(50),
      *TH1,TH2,VA(50),VHM
      COMMON ALPHA(6),BLOSS(50,6),BOTL(6),F(6),F13(6),IBOT,ISURF,
      *SLOSS(6)
      DIMENSION BM(100,6),HMC(5),RML(5),NRF(6),THC(5),THETA(100),
      *SINE(100,6)
      IF(L.GT.0) GO TO 100
      C---READ AND PRINT BEAM PATTERN INPUTS
      READ 1010,(NRF(IF),IF=1,NF)
      1010 FORMAT(6I5)
      DO 50 IF=1,NF
      N=NRF(IF)
      READ 1020,(THETA(I),I=1,N)
      READ 1020,(BM(I,IF),I=1,N)
      1020 FORMAT(8F10.0)
      PRINT 2010,F(IF)
      2010 FORMAT(/,50X,26HBEAM PATTERN FOR FREQUENCY,F7.1,3H HZ,/)
      PRINT 2020
      2020 FORMAT(5(5X,21HANGLE PRESS. LOSS))
      PRINT 2030
      2030 FORMAT(5(5X,21H(DEG) RATIO (DB)))
      NLINE=(N+4)/5
      DO 20 ILINE=1,NLINE
      NCOL=1+(N-ILINE)/NLINE
      DO 10 ICOL=1,NCOL
      I=ILINE+(ICOL-1)*NLINE
      THC(ICOL)=THETA(I)*HMC(ICOL)=BM(I,IF)
      10 RML(ICOL)=-10.*ALOG10(HM(I,IF)*BM(I,IF))
      20 PRINT 2040,(THC(ICOL),HMC(ICOL),RML(ICOL),ICOL=1,NCOL)
      2040 FORMAT(5(F10.1,F9.5,F7.2))
      DO 30 I=1,N

```

PAGE 2

SUBROUTINE BEAM

```

      THET=THETA(I)
      THET=THET/RTD * SIN(I,IF)=SIN(THET)
      30 CONTINUE
      50 CONTINUE
      RETURN
C---COMPUTE BEAM LOSS FACTORS BY LINEAR INTERPOLATION
      100 SBM=VHM/SQRT(1.+VHM*VHM)
      00 150 IF=1,NF
      N=NR(I,IF)
      DO 110 I=1,N
      IF(SINE(I,IF)-SBM) 110,120,130
      110 CONTINUE
      120 BMFAC(IF)=BM(I,IF)
      RETURN
      130 RAT=(SBM-SINE(I-1,IF))/(SINE(I,IF)-SINE(I-1,IF))
      BMFAC(IF)=(1.-RAT)*BM(I-1,IF)+RAT*BM(I,IF)
      150 CONTINUE
      RETURN
      END

```



PAGE 1

SUBROUTINE PLPLOT

```

SUBROUTINE PLPLOT
COMMON CB(50),CSP(50),GP(50),IBEAM,IBP,IDRT(4),IPR,I PROF,ISP,
*NR,NF,PI,RADE,RTD,ZR(50),ZP(50)
COMMON CA(50),CAA,CAA2,CBB,CHH2,IAA,IAD,IHB,IDF(50),IDUCT,ISD,NA,
*SN,ZA(50),ZAA,ZAD,ZHR,ZR,ZS
COMMON RMFAC(6),CL(10),CV,CV2,ILR,ILS,NL,NTH,SIGN(4),TH(50),
*TH1,TH2,VA(50),VHM
COMMON ALPHA(6),BLOSS(50,6),ROTL(6),F(6),F13(6),IBOT,ISURF,
*SLOSS(6)
COMMON DR,H(251,6),HC(15,4,6),ICAUST(4),IFMAX,J1,KA(4,6),KB(4,6),
*KMAX,KMN,KMNJ(4),KMXXJ(4),NCYC,NJ,R(50,4),RCYC(50),RMIN,RP(50,4),
*RPCYC(50),RPSR(50),RPIIP(50),RPSR(50),RUP(50)
COMMON /COH/ JCOH(6)
DIMENSION DXDR(13),X(251),HH(251),LAB(2),KAB(3),T(2),TT(2),TTT(3),
1C(1),CC(2),CCC(1)
EQUIVALENCE (X(1),HC(1,1,1)),(HH(1),RP(1,1))
DATA DXDR/100.,200.,250.,500.,1000.,2000.,2500.,5000.,10000.,20000
*.,25000.,50000.,100000./
DATA KAR/10HPROPAGATIO,10HN LOSS (DB,1H)/
DATA LAB/10HRANGE (KYD,1H)/
DATA T/10HFREQUENCY .7H(HZ) = /
DATA TT/10HSOURCE DEP,10HTH (FT) = /
DATA TTT/10HRECEIVER D,10HEPTH (FT) ,2H= /
DATA C/10HINCOHERENT/
DATA CC/ 10HSEMI-COHER,3HENT/
DATA CCC/8HCOHERENT/
RAT=ZS/RADE
ZSS=ZS*(1.-RAT*(1.-RAT)/2.)
RAT=ZR/RADE
ZRR=ZR*(1.-RAT*(1.-RAT)/2.)
PMAX=RMIN+(KMAX-1)*DR
DELR=(PMAX-RMIN)/10.
DO 10 I=1,13
IF(OXDR(I),GE,DELR) GO TO 20
10 CONTINUE
PRINT 3000

```

PAGE 2

## SUBROUTINE PLPLOT

```

3000 FORMAT(10X,21H RANGE SCALE TOO LARGE)
      GO TO 999
20 DELR=DXDP(I)
   DS=DELR/1000.
   LX=RMIN/DELR $ XO=LX
   SMIN=LX*DELR/1000.
   DO 100 IF=1,NF
     DO 30 K=1,KMAX
       HH(K)=(H(K,IF)-50.)/10.
       IF(HH(K).GT.7.) HH(K)=7.
30   X(K)=(RMIN+(K-1)*DR)/DELR-XO
       CALL INITIAL(1,100,11,0)
       CALL PLOT(0,0,0,-3)
       CALL AXIS(0,0,0,0,KAB,-21,7,0,0,50,0,10,0,0)
       CALL AXIS(7,0,0,0,LAR,-11,10,0,90,0,SMIN,DS,0)
       CALL SYMBOL(0,5,3,25,0,21,IDHT,90,0,4,0)
       CALL SYMBOL(.75,5,0,14,1,90,0,16)
       CALL NUMBER(.75,7,25,0,14,F(IF),90,0,2)
       CALL SYMBOL(1,0,5,0,14,11,90,0,20)
       CALL NUMBER(1,0,7,45,0,14,ZSS,90,0,2)
       CALL SYMBOL(1,25,5,0,14,11,90,0,22)
       CALL NUMBER(1,25,7,8,0,14,ZRR,90,0,2)
       IF(JCOH(IF).EQ.1) GO TO 200
       IF(JCOH(IF).EQ.0) GO TO 210
       IF(JCOH(IF).EQ.2) GO TO 220
200   CALL SYMBOL(1,50,5,0,14,C,90,0,10)
       GO TO 230
210   CALL SYMBOL(1,50,5,0,14,CC,90,0,13)
       GO TO 230
220   CALL SYMBOL(1,50,5,0,14,CCC,90,0,8)
230   CONTINUE
       CALL LINE(HH,X,KMAX,0,1)
       CALL RSTR(2)
100   CONTINUE
999   CONTINUE
      RETURN

```

NADC-77296-30

PAGE 3

SUBROUTINE PLPLOT

END



NADC-77296-30

APPENDIX B

GLOSSARY OF PRINCIPAL FORTRAN SYMBOLS

## BLANK COMMON

| <u>Symbol</u> | <u>Defined</u>            | <u>Definition</u>  |
|---------------|---------------------------|--|
| ALPHA(IF)     | PLRAY                     | Attenuation coefficient of water (dB/kyd)                              |
| BLOSS(ITH,IF) | INCR                      | Bottom reflection loss (dB)  |
| BMFAC(IF)     | BEAM                      | Beam loss factor (pressure ratio relative to beam axis)                |
| BOTL(IF)      | BOTTOM                    | Bottom reflection loss (dB)  |
| CA(IA)        | INSERT                    | Sound speed, augmented velocity profile (ft/sec)                       |
| CAA           | INSERT                    | Sound speed at ray source (ft/sec)                                     |
| CB(IB)        | PLRAY                     | Sound speed, original velocity profile (ft/sec or m/sec)               |
| CBB           | INSERT                    | Sound speed at ray receiver (ft/sec)                                   |
| CL(IL)        | SECLIM                    | Sound speed at sector boundary (ft/sec)                                |
| CSP(IB)       | CURFIT                    | Parameter of V.P. profile segment                                      |
| CV            | PLRAY                     | Ray vertex velocity (ft/sec)   |
| DR            | PLRAY                     | Range increment (yd)   |
| F(IF)         | PLRAY                     | Frequency (Hz)   |
| F13(IF)       | PLRAY                     | Cube root of frequency   |
| GP(IB)        | CURFIT                    | Parameter of V.P. profile segment                                      |
| H(K,IF)       | RAYSUM<br>RCAUST<br>SDUCT | Resultant multipath intensity (converted to propagation loss in PLRAY) |
| HC(KC,J,IF)   | RCAUST                    | Temporary intensity array  |
| IAA           | INSERT                    | Index of ray source depth, augmented V.P.                              |
| IAD           | INSERT                    | Index of bottom of surface duct, augmented V.P.                        |
| IBB           | INSERT                    | Index of ray receiver depth, augmented V.P.                            |
| IBEAM         | PLRAY                     | Beam control parameter   |
| IBOT          | PLRAY                     | Flag indicating whether ray hits bottom                                |
| IBP           | PLRAY                     | Bottom type parameter  |
| ICAUST(J)     | RAYSUM                    | Caustic type (min. range, max. range, none)                            |
| IDBT(4)       | PLRAY                     | Title of Run   |
| IDF(IA)       | INSERT                    | Identification function relating IA to IB                              |
| IDUCT         | PLRAY                     | Index of bottom of surface duct (original V.P.)                        |
| IFMAX         | PLRAY                     | Index of largest frequency   |
| ILB           | SECLIM                    | Value of IL in first sector in which rays hit bottom                   |
| ILS           | SECLIM                    | Value of IL in first sector in which rays hit surface                  |



|            |        |   |
|------------|--------|---|
| IPR        | PLRAY  | Diagnostic print control parameter                      |
| I PROF     | PLRAY  | Environmental input control parameter                   |
| ISD        | INSERT | Flag determining implementation of surface duct model   |
| ISP        | PLRAY  | Surface parameter (sea state)                           |
| ISURF      | PLRAY  | Flag indicating whether ray hits surface                |
| KA(J,IF)   | RCAUST | Equivalent to K2 (RCAUST)                               |
| KB(J,IF)   | RCAUST | Equivalent to K3 (RCAUST)                               |
| KMAX       | PLRAY  | Index of maximum receiver range                         |
| KMN        | RAYSUM | Index of minimum range of all NJ ray types              |
| KMNJ(J)    | RAYSUM | Index of minimum range of Jth ray type                  |
| KMXJ(J)    | RAYSUM | Index of maximum range of Jth ray type                  |
| NA         | INSERT | No. points in augmented velocity profile                |
| NB         | PLRAY  | No. points in original velocity profile                 |
| NCYC       | PLRAY  | Arrival order number                                    |
| NF         | PLRAY  | No. frequencies   |
| NJ         | PLRAY  | No. multipath ray types                                 |
| NL         | SECLIM | No. sectors (less one)                                  |
| NTH        | DIVSEC | No. rays computed in a sector                           |
| R(ITH,J)   | PLRAY  | Ray range (yd)  |
| RADE       | PLRAY  | Radius of earth (ft)                                    |
| RCYC(ITH)  | INCR   | Ray cycle range (yd)                                    |
| RMIN       | PLRAY  | Minimum receiver range (yd)                             |
| RP(ITH,J)  | PLRAY  | Range derivative (yd)                                   |
| RPCYC(ITH) | INCR   | Derivative of RCYC(ITH) (yd)                            |
| RPSR(ITH)  | INCR   | Derivative of RSR(ITH) (yd)                             |
| RPUP(ITH)  | INCR   | Derivative of RUP(ITH) (yd)                             |
| RSR(ITH)   | INCR   | Range, source to receiver (yd)                          |
| RTD        | PLRAY  | Conversion factor, radians to degrees                   |
| RUP(ITH)   | INCR   | Range of portion of ray cycle above receiver depth (yd) |
| SIGN(J)    | PLRAY  | Algebraic sign of ray angle at true source              |
| SLOSS(IF)  | SURF   | Surface reflection loss (dB)                            |
| SN         | INSERT | Flag indicating whether true source is at ZAA or ZBB    |
| TH(ITH)    | DIVSEC | Ray source angle (rad)                                  |
| TH1        | PLRAY  | Ray source angle at inner boundary of sector (rad)      |

|         |                           |  |
|---------|---------------------------|--|
| TH2     | PLRAY                     | Ray source angle at outer boundary of sector (rad)     |
| VA(ITH) | PLRAY                     | Tangent of ray source angle                            |
| VBM     | RAYSUM<br>RCAUST<br>SDUCT | Tangent of source angle at beam location (true source) |
| ZA(IA)  | INSERT                    | Depth, augmented velocity profile (ft)                 |
| ZAA     | INSERT                    | Depth of ray source (ft)                               |
| ZAD     | INSERT                    | Bottom of surface duct (ft)                            |
| ZB(IB)  | PLRAY                     | Depth, original velocity profile (ft or m)             |
| ZBB     | INSERT                    | Depth of ray receiver (ft)                             |
| ZP(IB)  | CURFIT                    | Parameter of V.P. profile segment                      |
| ZR      | PLRAY                     | True receiver depth (ft)                               |
| ZS      | PLRAY                     | True source depth (ft)                                 |

COMMON /DATA/

| <u>Symbol</u> | <u>Definition</u>                            |
|---------------|--|
| DB(I,IBP,J)   | Bottom loss from input curves (dB)           |
| DG(I,IBP,J)   | Bottom grazing angle from input curves (deg) |
| FR(J)         | Bottom loss frequency (Hz)                   |

COMMON /COH/

| <u>Symbol</u> | <u>Definition</u>           |
|---------------|-----------------------------|
| JCOH(IF)      | Coherence control parameter |

COMMON /SDCT/

| <u>Symbol</u> | <u>Definition</u>  |
|---------------|--|
| EN            | No. "trapped" modes in surface duct (not an integer)   |
| FR            | Frequency (Hz)   |
| THETA         | Phase angle in depth function (rad)  |
| VO            | Difference between phase velocity of perfectly trapped first mode and sound speed at surface |
| ZA            | Depth of bottom of surface duct (ft)   |

INDEX VARIABLES

| <u>Symbol</u> | <u>Application</u>         |
|---------------|----------------------------|
| IA            | Augmented velocity profile |

|     |   |
|-----|---|
| IB  | Original velocity profile                                       |
| IF  | Frequency   |
| IL  | Sector  |
| ITH | Ray in sector   |
| J   | Multipath ray type  |
| K   | Range   |
| KC  | Range relative to smallest range of caustic correction interval |

## PLRAY

| <u>Symbol</u> | <u>Definition</u>   |
|---------------|---|
| CFAC          | Conversion factor (ft/m)  |
| FMAX          | Largest specified frequencies (Hz)  |
| HMIN          | Intensity corresponding to 999 dB propagation loss                                    |
| ICASE         | Flag indicating whether source is above or below receiver                             |
| IPLOT         | Houston plot control parameter  |
| J1            | Used in initiating ray ranges   |
| MAXK          | Maximum permissible no. range points (251)  |
| MJ            | Flag (does first sector extend continuously from negative to positive source angles?) |
| NDCD          | End code, terminating reading of V.P. cards   |
| NFR           | No. frequencies of input bottom loss curves   |
| NREC          | No. receiver depths   |
| RK            | Receiver range (yd)   |
| RMAX          | Maximum receiver range (yd)   |
| S             | Salinity  |
| SGN           | Algebraic sign of ray source angle  |
| T             | BT temperature ( $^{\circ}\text{F}$ or $^{\circ}\text{C}$ )                           |
| ZDMAX         | Max. duct depth for which surface duct model is implemented (1000 ft)                 |
| ZRO(I)        | True receiver depth (ft)  |
| ZSO           | True source depth (ft)  |

## INSERT

| <u>Symbol</u> | <u>Definition</u>                           |
|---------------|---|
| CR            | Sound speed at true receiver depth (ft/sec) |
| CS            | Sound speed at true source depth (ft/sec)   |



## SECLIM

| <u>Symbol</u> | <u>Definition</u>                         |
|---------------|---|
| G(IA)         | Sound speed gradient (sec <sup>-1</sup> ) |

## DIVSEC

| <u>Symbol</u> | <u>Definition</u>  |
|---------------|--|
| DEL           | Ray source angle increment (rad)   |
| DELO          | Dead interval at sector boundaries (rad)   |
| IMAX          | Maximum allowable no. rays in sector (50)  |
| THT(I)        | Temporary array of source angles in outer portion of sector, symmetrically located with respect to TH(I) (rad) |

## INCR

| <u>Symbol</u> | <u>Definition</u>   |
|---------------|---|
| CDT           | Temporary storage of CA(IA) at bottom of layer containing lower ray vertex (ft/sec) |
| CUT           | Temporary storage of CA(IA) at top of layer containing upper ray vertex (ft/sec)    |
| DX(IA)        | Increment of range in layer IA (yd)   |
| DXP(IA)       | Derivative of DX with respect to VA (yd)  |
| IDN           | Index of layer containing lower ray vertex  |
| IUP           | Index of layer containing upper ray vertex  |
| Q1,Q2,Q3      | Constant factors in formulas for DX and DXP   |
| S             | Algebraic sign required to compute ray vertex depth from vertex velocity            |
| THBD          | Grazing angle at bottom (deg)   |
| VV1,VV2       | Reciprocals of V1 and V2 respectively   |
| V1,V2         | Tangent of ray angle at top/bottom of layer   |
| ZDT           | Temporary storage of ZA(IA) at bottom of layer containing lower ray vertex (ft)     |
| ZUT           | Temporary storage of ZA(IA) at top of layer containing upper ray vertex (ft)        |

## RAYSUM

| <u>Symbol</u> | <u>Definition</u>  |
|---------------|--|
| ANFAC         | Constant factor in formula for ANPPC                             |
| ANPPC         | No. range points per cycle of ray interference pattern           |
| ANPPCA        | Value of ANPPC at ray source end                                 |
| ANPPCB        | Value of ANPPC at ray receiver end                               |
| A0(J),A1(J)   | Parameters in intensity computations for steep angle propagation |
| BLK           | Bottom loss, interpolated to Kth range point                     |
| BMF(J,JJ,IF)  | Beam pressure ratio (equivalent to BMFAC(IF))                    |

|               |  |
|---------------|--|
| COFACR        | Coherence factor at receiver end of ray  |
| COFACS        | Coherence factor at source end of ray  |
| CVK           | Vertex velocity, interpolated to range RK  |
| FAC           | Attenuation factor, including water, surface, bottom, and beam losses  |
| FRACTA        | Absolute value of FRACTS   |
| FRACTB        | Coherence attenuation factor computed from formula involving no. of range points per cycle   |
| FRACTR        | Coherence attenuation factor at true receiver end (applicable when coherence occurs at both ends)                                  |
| FRACTS        | Coherence attenuation factor (including effect of beam pattern)  |
| HK            | Intensity of range RK, exclusive of coherence factor   |
| HTRM(J,JJ,IF) | Temporary intensity array  |
| ICOH          | Coherence flag, indicating whether coherence occurs at neither end (0), ray source end (1), ray receiver end (2), or both ends (3) |
| ICTH(J)       | Values of index ITH such that caustic lies between ITH-1 and ITH   |
| IND           | Parameter indicating which of multipath rays propagate to range RK   |
| ISUM          | No. of multipath rays which propagate to range RK  |
| ITHMN         | Minimum value of ITH in ray interpolation loop   |
| ITHMX         | Maximum value of ITH in ray interpolation loop   |
| JA(J)         | Identifier indicating which of the multipath ray types are applicable in coherence computations                                    |
| JJ            | Index identifying the branches of range-VA curve   |
| KMX           | Largest value of K among all NJ multipath ray types in sector  |
| KTH           | Same as ICTH(J)  |
| KTYP          | Flag indicating whether special formula is to be used for intensity computation  |
| PHFAC         | Constant factor in formula for phase angle in interference pattern   |
| PHIA          | Phase angle between interfering rays at ray source end (rad)   |
| PHIB          | Phase angle between interfering rays at ray receiver end (rad)   |
| PHIR          | Phase angle between interfering rays at true receiver end (rad)  |
| PHIS          | Phase angle between interfering rays (rad)   |
| RCOH          | Nominal limiting value of horizontal separation of interfering rays at source or receiver depth (ft)                               |
| RK            | Receiver range at index K (yd)   |
| RMN           | Minimum range among all NJ multipath ray types in sector (yd)  |
| RMNJ          | Minimum range of Jth multipath ray type in sector (yd)   |
| RMX           | Maximum range among all NJ multipath ray types in sector (yd)  |

|            |   |
|------------|---|
| RMXJ       | Maximum range of Jth multipath ray type in sector (yd)                            |
| RPK        | Interpolated value of range derivative RP at range RK                             |
| RPKK(J,JJ) | Array of absolute values of RPK   |
| SGN        | Indicates algebraic sign of product of the beam functions of two interfering rays |
| SLK        | Surface loss (dB)   |
| THBD       | Grazing angle at bottom (deg)   |
| TRM        | Intensity in final form for insertion into H(K,IF) array                          |
| VAK        | Interpolated value of VA at range RK  |
| VAXK(J,JJ) | Array of values of VAK  |
| VBK        | Tangent of angle at receiver depth of interpolated ray to RK                      |
| VO         | Tangent of angle at surface of interpolated ray to range RK                       |
| ZRCOH      | Horizontal separation of two interfering rays at receiver depth (ft)              |
| ZSCOH      | Horizontal separation of two interfering rays at source depth (ft)                |

## RCAUST

| <u>Symbol</u> | <u>Definition</u>  |
|---------------|--|
| AII           | Square of Airy function, $Ai(x)$   |
| CCL           | Constant factor $2 \cdot (3\pi)^{2/3}$   |
| COEF1         | Coefficient relating argument of Airy function to horizontal distance from caustic   |
| COEF2         | Coefficient relating intensity to AII  |
| CVC           | Vertex velocity of interpolated ray to caustic (ft/sec)  |
| FAC           | Attenuation factor, including water, bottom, surface, and beam losses  |
| HK            | Intensity  |
| ISGN          | Algebraic sign of RPK  |
| K1            | Limiting value of K on shadow side of caustic  |
| K2            | First limiting value of K on insonified side of caustic (caustic correction applies unconditionally between K1 and K2)         |
| K3            | Second limiting value of K on insonified side of caustic (caustic correction is compared with ray intensity between K2 and K3) |
| K3T           | Cut-off value of K3  |
| L             | Range index beginning with 1 at $K = K1$ and increasing to $ K3 - K1  + 1$ at $K = K3$   |
| L2,L3         | Values of L at $K = K2$ and $K = K3$   |
| RC            | Range to caustic (yd)  |
| RC1           | Limiting range on shadow side of caustic (yd)  |



|      |  |
|------|--|
| RC2  | First limiting range on insonified side of caustic (yd)    |
| RC3  | Second limiting range on insonified side of caustic (yd)   |
| RK   | Receiver range at index K (yd)                             |
| RPP  | Second derivative of R with respect to VA (yd)             |
| RPPT | Alternate value of RPP computed from adjacent pair of rays |
| TRM  | Intensity  |
| VAC  | Tangent of source angle of interpolated ray to caustic     |
| VBC  | Tangent of receiver angle of interpolated ray to caustic   |
| X    | Argument of Airy Function                                  |
| X1   | Limiting value of X on shadow side                         |
| X2   | First limiting value of X on insonified side               |
| X3   | Second limiting value of X on insonified side              |

## SDUCT

| <u>Symbol</u> | <u>Definition</u>   |
|---------------|---|
| ALPH1         | Leakage attenuation coefficient in cylindrical spreading formula (dB/yd)              |
| ALPH2         | Attenuation coefficient in spherical spreading formula, good duct model (dB/yd)       |
| ALPH3         | Attenuation coefficient due to surface roughness (dB/yd)                              |
| ALP1          | Overall attenuation coefficient, cylindrical spreading formula (dB/yd)                |
| ALP2          | Overall attenuation coefficient, spherical spreading formula, good duct model (dB/yd) |
| CR            | Constant loss term associated with receiver depth (dB)                                |
| CS            | Constant loss term associated with source depth (dB)                                  |
| FF            | Frequency (Hz)/100  |
| FNIN          | Minimum frequency for which surface duct computations are made (Hz)                   |
| HK            | Intensity (exclusive of attenuation) in cylindrical spreading formula                 |
| HKK           | Intensity (exclusive of attenuation) in spherical spreading formula                   |
| HM            | Minimum intensity at which surface duct computations are terminated                   |
| IND           | Flag to avoid repeated computation of constants                                       |
| RK            | Range at index K (yd)   |
| THETR         | Phase angle in receiver depth function (rad)  |
| THETS         | Phase angle in source depth function (rad)  |
| U             | Product of US and UR  |
| UR            | Receiver depth function   |

US                    Source depth function  
 ZA1                  Depth of surface duct (ft/100)

## BEAM

| <u>Symbol</u> | <u>Definition</u>  |
|---------------|--|
| BM(I,IF)      | Beam loss factor (pressure ratio relative to beam axis) for the Ith grazing angle and IFth frequency |
| NBF(IF)       | Number of points required to specify IFth beam pattern   |
| SINE(I,IF)    | Sine of THETA(I) for IFth frequency  |
| THETA(I)      | Grazing angle at true source (deg)   |

AD-A062 019

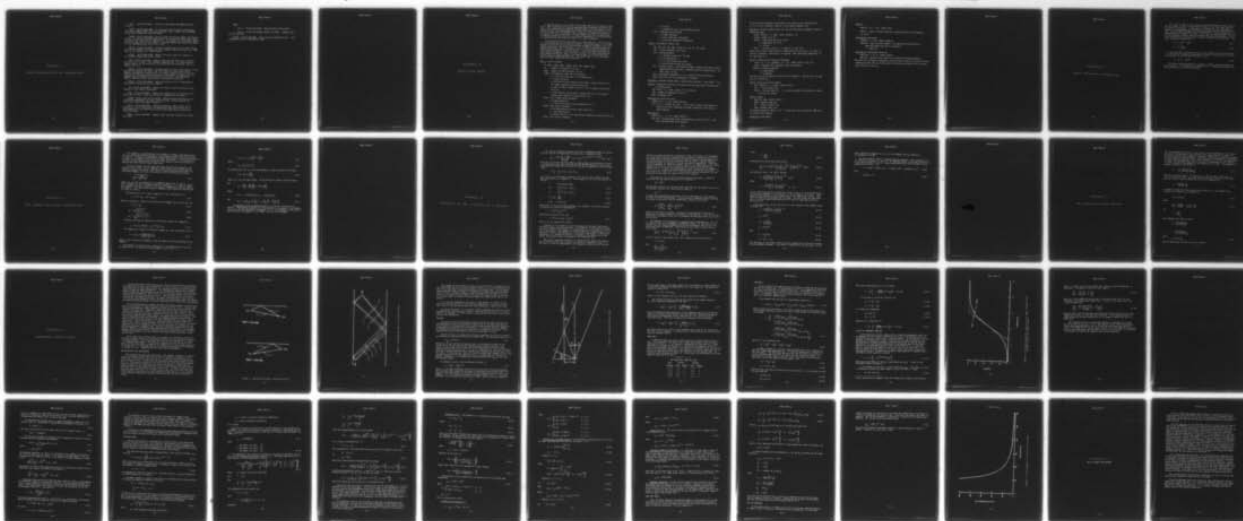
NAVAL AIR DEVELOPMENT CENTER WARMINSTER PA SENSORS A--ETC F/6 20/1  
PLRAY - A RAY PROPAGATION LOSS PROGRAM.(U)  
OCT 78 C L BARTBERGER

NADC-77296-30

UNCLASSIFIED

NL

3 OF 3  
AD  
A062 019



END  
DATE  
FILMED  
3-79  
DDC



# APPENDIX C

## BRIEF DESCRIPTION OF SUBROUTINES

VELOC. Called from PLRAY. Calculates sound speed from temperature and salinity.

CURFIT. Called from PLRAY. Fits the input velocity profile points with curvilinear segments which join with continuous slope. PARAB, FIT, and BRIDGE are auxiliary subroutines called by CURFIT.

INSERT. Called from PLRAY. Inserts source and receiver depths into velocity profile. Of these two depths INSERT selects the one with the larger sound speed to serve as the source for ray computations. If a surface duct is present, INSERT checks the source and receiver depths to determine whether the surface duct model is to be implemented and, if so, sets a flag.

SECLIM. Called from PLRAY. Divides the angular space of ray source angles into sectors bounded by limiting rays which separate rays of one type (e.g., RSR) from rays of another (e.g., bottom bounce).

DIVSEC. Called from PLRAY. Computes the source angles of a family of non-uniformly spaced rays in each sector.

INCR. Called from PLRAY. Computes range and range derivative increments for each ray in a sector. The increments computed are: (1) source depth to receiver depth, (2) the portion of a ray cycle above receiver depth, and (3) a complete ray cycle.

RAYSUM. Called from PLRAY. Processes rays of a sector, one sector at a time. Searches for presence of caustics and calls RCAUST for each caustic found. Computes individual ray intensities at all ranges covered by rays of the sector (exclusive of the rays covered by the caustic corrections). Computes the incoherent sum of multipath ray intensities at each range. When applicable, computes coherence factors and resultant semicoherent intensities.

RCAUST. Called from RAYSUM. Computes intensities over a predetermined range interval on either side of a caustic.

A12. Called from RCAUST. Computes the square of the Airy function  $Ai(x)$ , required for the caustic corrections.

SURF. Called from PLRAY. Computes the surface loss as a function of frequency and sea state. (Does not include any dependence on ray angle.)

BOTTOM. Called from INCR and RAYSUM. Computes bottom reflection loss as a function of frequency, ray angle, and bottom type. Contains bottom loss curves for 5 FNWC bottom types internally.

SDUCT. Called from PLRAY. Computes intensities from a special set of formulas in lieu of conventional ray computations when either source or receiver depth is in the surface duct and the other depth does not exceed 1.8 times duct depth.

DEPTH. Called from SDUCT. Computes depth functions required for surface duct model.

BEAM.

Part 1. Called from PLRAY. Reads and prints beam inputs.

Part 2. Called from RAYSUM, RCAUST, and SDUCT. Computes beam pattern functions.

PLPLOT. Called from PLRAY. Plot routine for Houston plotter. Plots propagation loss as a function of range.





# APPENDIX D

## INPUT DATA DECK

A complete data set for a normal run of PLRAY consists of 8 cards (or card sets), some of which may be omitted, depending upon the options selected by the user. After completing the computations specified by the first data set, the program returns to the beginning and reads the first card of a new data set. If this is a blank card, the program stops. However, if a complete new data set is supplied, it will be processed. As many complete data sets as desired may be stacked together and they will be processed sequentially. A blank card must be inserted at the end of the last data set to stop the program.

The instructions which follow apply to a single data set. The first input is a card containing a set of control integers. The second input is a card containing the title of the run and environmental parameters relating to the ocean surface and bottom. The third input is a set of cards containing externally supplied bottom loss data. The fourth input is a set of cards containing the sound velocity profile. The fifth input is a card containing the frequencies and coherence parameters. The sixth input is one or two cards containing the source depth and receiver depths. The seventh input is a card on which the desired receiver ranges are specified. The eighth input is a set of cards on which the source beam patterns are specified.

#### Card 1, control integers

NF, NREC, IPROF, IUNIT, IBEAM, IPLOT, IPR Format (10I5)

NF = number of frequencies, up to 6

NREC = number of receiver depths, up to 8

IPROF = environmental input control parameter

= -1, VP curve-fitting only; no ray computations

= 0, normal operation

= 1, omit both VP and external bottom inputs; bypass Card Sets 2-4; use inputs supplied in previous data set

= 2, omit VP inputs; bypass Card Set 4; use VP supplied in previous data set

= 3, omit external bottom inputs; bypass Card Set 3; use external bottom inputs supplied in previous data set.

IUNIT = unit system control parameter

= 0, normal operation

= 1, required only when reading temperatures in °C

IBEAM = beam control parameter

= 0, no beam patterns involved; bypass Card set 8

= 1, read beam patterns

= 2, bypass Card Set 8; use beam patterns supplied in previous data set

IPLOT = plot control parameter



= 0, no plot  
 = 1, propagation loss plot on Houston plotter  
 IPR = diagnostic print control  
 - 0, normal operation  
 = 1, print diagnostic information  
 = 2, print more diagnostic information

Card 2, environmental header card

ISP, IBP, LAT, IDR, IDBT Format 215, 10X, A1, 10X, 4A10)  
 ISP = surface parameter (sea state)  
 IBP = bottom parameter  
 = -1, infinite bottom loss (100 dB)  
 = 0, zero bottom loss  
 = 1 to 5, FNWC bottom loss curves  
 = 6, read external bottom loss curves  
 LAT = latitude (deg), a real (decimal) number. Required only when reading temperatures and salinities; otherwise only for identification. Default value, 45 deg.  
 IDR = hemisphere designation, N or S; used only for identification  
 IDBT = run title, up to 40 alphanumeric characters

Card Set 3, external bottom inputs, required only when IBP = 6 and IPRF = 0 or 2

Card 3a, frequencies of bottom loss curves; must be specified in monotonically increasing order

NFR, FR(J), J = 1, NFR) Format (15, 5X, 6F10.0)  
 NFR = number of frequencies, up to 6  
 FR(J) = frequency (Hz)

Card Pair 3b, bottom loss data

(DB(I,6,J) I = 1, 15) Format (8F10.0)  
 DB (I, 6, J) = bottom loss (dB). If less than 15 points are required to specify the curve, remaining 10-column fields may be left blank; 2 cards required

Card Pair 3c

(DG(I,6,J), I = 1, 15) Format (8F10.0)  
 DG(I,6,J) = grazing angle (deg) corresponding to loss DB (I,6,J). Last value specified must be 90 degrees.

If more than one frequency is specified, stack cards in the following order:  
3b, 3c for first frequency, then 3b, 3c for second frequency, etc.

Card Set 4, velocity profile deck, one card for each point, arranged in order of increasing depth.

ZB(IB), CB(IB), T, S, NDCD Format (4F100.0, 11)

ZB(IB) = depth (ft or m)

CB(IB) = sound speed (ft/sec or m/sec)

T = temperature ( $^{\circ}$ F or  $^{\circ}$ C)

S = salinity

NDCD = end code; punch a 1 in column 41 of last card

Inputs may be either sound speeds or temperatures and salinities. Use same set of units throughout, either metric or English. When specifying temperatures in  $^{\circ}$ C, IUNIT must be 1.

Card 5, frequencies and coherence parameters.

(F(IF), IF = 1,6), (JCOH(IF), IF = 1,6) Format (6F10.0, 10X, 6I1)

F(IF) = frequency (Hz); monotonic order not required

JCOH(IF) = coherence parameter

- 0, semicoherent

= 1, incoherent

The same value of IF applies to both F(IF) and JCOH(IF). Only NF values of each need to be specified.

Card 6, source and receiver depths

(ZS0, (ZRO(I), I = 1, NREC) Format (8F10.0

ZS0 = source depth (ft)

ZRO(I) = receiver depth (ft). If 8 receiver depths are specified, a second card will be needed.

Card 7, ranges

RMIN, DR, RMAX Format (8F10.0)

RMIN = minimum range (yd)

DR = range increment (yd)

RMAX = maximum range (yd)

The maximum number of ranges is 251. If more than 251 are specified, RMAX will be automatically adjusted.

Card Set 8, beam inputs

Card 8a

(NBF(IF), IF = 1, NF) Format (615)

NBF(IF) = number of points required to specify beam for IFth frequency,  
up to 100

Card Set 8b, beam angles

(THETA(I), I = 1,N) Format (10F8.0)

THETA(I) = angle, positive upward. The angles must be specified in  
increasing order from -90 to +90 degrees

N = NBF (IF)

Card Set 8c, beam pattern functions

(BM(I,IF), I = 1, N) Format (10F8.0)

BM(I,IF) = pressure ratio relative to direction of maximum response.

When more than one beam is specified, place Card Sets 8b and 8c for the first beam immediately after Card 8a; follow these with Card Sets 8b and 8c for the second beam, then the third, etc.



Case 30

(NAD 1983) 1R - 1.00 (NAD 1983)

(NAD 1983) - number of points required to specify line for this treatment

up to 100

(NAD 1983) 1R - 1.00 (NAD 1983)

(NAD 1983) 1 - 1.00 (NAD 1983)

(NAD 1983) - number of points required to specify line for this treatment

(NAD 1983) - number of points required to specify line for this treatment

up to 100

(NAD 1983) 1R - 1.00 (NAD 1983)

(NAD 1983) 1 - 1.00 (NAD 1983)

(NAD 1983) - number of points required to specify line for this treatment

(NAD 1983) - number of points required to specify line for this treatment

(NAD 1983) - number of points required to specify line for this treatment

(NAD 1983) - number of points required to specify line for this treatment

APPENDIX E

EARTH CURVATURE CORRECTION

Let  $z_u$  and  $c_u$  refer to the original (uncorrected) depth and sound speed in the real ocean,  $z_c$  and  $c_c$  to the corrected values in the flat ocean, and  $R$  to the radius of the earth. As described in reference (a), the transformation consists of straightening out the annular ring containing the ocean into a flat slab in such a way that angles are locally preserved. The ocean surface is unwrapped without changing its length. Other lines of constant depth, which are arcs of concentric circles, must be stretched while being straightened. At the same time they must be spread apart in order to preserve local directions. The exact correction formulas are

$$z_c = -R \ln(1 - z_u/R) \quad (E-1)$$

$$c_c = \frac{c_u}{1 - z_u/R} \quad (E-2)$$

Since the radius of the earth is very large compared with the ocean depth, it is convenient to expand the logarithm in a series, and sufficiently accurate to throw away all but the first two terms. Thus,

$$z_c = z_u (1 + z_u/2R) \quad (E-3)$$

The earth curvature correction as applied in PLRAY, consists of equations (E-3) and (E-2). In reference (a), equation (E-2) is further approximated, but that approximation is really unnecessary.



APPENDIX F

STEEP ANGLE APPROXIMATION

The fact that rays propagate in approximately straight-line paths at steep angles permits the use of an approximation which avoids the necessity of computing actual ray paths and thereby saves a significant amount of computation. At very steep angles, where the ray paths are very close to straight lines, the horizontal range is inversely proportional to the tangent of the ray angle. At angles beyond about 30 degrees or so, the range can be approximated with sufficient accuracy by a formula of the form

$$r = 1/(a_0 v_a + a_1) \quad (F-1)$$

where  $a_0$  and  $a_1$  are constants and  $v_a$  is the tangent of the ray source angle. As applied in SUBROUTINE RAYSUM,  $r$  is the independently specified receiver range, and equation (F-1) is solved for  $v_a$  in order to compute the range derivative  $r'$ . Thus,

$$v_a = (1/r - a_1)/a_0 \quad (F-2)$$

and

$$r' = \frac{\partial r}{\partial v_a} = -a_0 r^2 \quad (F-3)$$

To provide smooth transition into the region of shallower angles where exact ray formulas are used, the constants  $a_0$  and  $a_1$  are evaluated from the steepest ray computed, which in PLRAY is the 30-degree ray. Solving equations (F-1) and (F-3) for  $a_0$  and  $a_1$  yields

$$a_0 = -r'_{30}/r_{30} \quad (F-4)$$

$$a_1 = 1/r_{30} - a_0 v_{30} \quad (F-5)$$

where the subscript 30 refers to the 30-degree ray.

The above approximation is one of the excellent novel features of the FACT model.

APPENDIX G

RAY RANGES AND RANGE DERIVATIVES



This appendix is concerned with the increments in range  $\Delta r$  and range derivative  $\Delta r'$  associated with the passage of a ray through a single layer of the velocity profile. In PLRAY the independent variable with respect to which the derivative is taken is the tangent of the ray source angle, denoted by  $v_a$ . As indicated in the text, the ray source may be either the true source or the true receiver, depending upon which has the larger sound speed.

The basic formulas for the range and range derivative are derived in reference (a), pp. 32-39. In this appendix we shall apply them to PLRAY with appropriate changes in notation. The relation between sound speed and depth in a curvilinear segment (eq. (64) of reference (a)) will be written in the form

$$c = \sqrt{\frac{c_p^2}{1 - g_p(z - z_p)^2}} \quad (G-1)$$

where  $c_p^2$ ,  $g_p$ , and  $z_p$  correspond to the FORTRAN symbols CSP, GP, and ZP. In a Type I segment all three of these parameters are positive; in a Type II segment  $g_p$  is negative and  $c_p^2$  is positive; in a Type III segment  $g_p$  is positive and  $c_p^2$  is negative. ( $c_p$  itself, which would be imaginary, has no physical significance in a Type III curve.)

The formula for  $\Delta r$  in a Type I segment (eq. (73), reference (a)) is

$$r = (\sin^{-1} w_\ell - \sin^{-1} w_u) / q_1 \quad (G-2)$$

where the subscript  $\ell$  refers to the bottom of the segment and  $u$  to the top, and

$$w = q_2 (z - z_p) \quad (G-3)$$

$$q_1 = c_v \sqrt{|g_p / c_p^2|} \quad (G-4a)$$

$$q_2 = c_v \sqrt{|g_p / (c_v^2 - c_p^2)|} \quad (G-4b)$$

Equation (G-2) may be rewritten in a form more suitable for computation

$$r = \sin^{-1}(w_\ell \sqrt{1 - w_u^2} - w_u \sqrt{1 - w_\ell^2}) / q_1 \quad (G-5)$$

The formula for a Type II or Type III segment (eq. (82) of reference (a)) is

$$r = (1/q_1) \ln \frac{q_1(z_\ell - z_p) + v_\ell}{q_1(z_u - z_p) + v_u} \quad (G-6)$$

where  $v_u$  and  $v_\ell$  denote the tangents of the ray angle at the top and bottom of the segment.

The formula for the derivative, applicable to all segment types is eq. (75) of reference (a). In terms of the ray tangents  $v_u$  and  $v_\ell$ , it is

$$\Delta u = \Delta r + q_3 \left( \frac{z_\ell - z_p}{v_\ell} - \frac{z_u - z_p}{v_u} \right) \quad (G-7)$$

where

$$q_3 = c_p^2 / (c_v^2 - c_p^2) \quad (G-8)$$

The definition of  $\Delta u$ , eq. (32) of reference (a), may be written in the form

$$\Delta u = -\cot \theta_a \frac{\partial \Delta r}{\partial \theta_a} \quad (G-9)$$

where  $\theta_a$  is the ray source angle. The derivative is taken at constant depth.

But

$$\Delta r' = \frac{\partial \Delta r}{\partial v_a} = \frac{\partial \Delta r}{\partial \theta_a} \frac{d\theta_a}{dv_a} = \cos^2 \theta_a \frac{\partial \Delta r}{\partial \theta_a}$$

Hence

$$\Delta r' = -\Delta u \cos^2 \theta_a \tan \theta_a = -(c_a^2 v_a \Delta u / c_v^2) \quad (G-10)$$

And

$$\Delta r' = -(c_a^2 v_a / c_v^2) \left[ \Delta r + q_3 \left( \frac{z_\ell - z_p}{v_\ell} - \frac{z_u - z_p}{v_u} \right) \right] \quad (G-11)$$

In SUBROUTINE INCR the FORTRAN symbols for  $\Delta r$  and  $\Delta r'$  are DX(IA) and DXP(IA). The boundary designated with the subscript  $\ell$  corresponds to the FORTRAN index IA+1, and the subscript u corresponds to IA. The subscript a, referring to the ray source, corresponds to the symbol A (or AA) in the FORTRAN.





APPENDIX H

INTENSITY IN THE VICINITY OF A CAUSTIC

The caustic correction formulas contained in SUBROUTINE RCAUSE are derived from eq. (83.43) of Brekhovskikh (reference (f)), reproduced below:

$$\psi_N^+ = 2^{11/6} \left( \frac{\xi}{r \beta_0 \beta} \right)^{1/2} \left| w'''(\xi_0) \right|^{-1/3} e^{i [\pi/4 + w(\xi_0)]} v(x) \quad (H-1)$$

where  $\psi_N^+$  is the wave function, which is proportional to the acoustic pressure,  $w$  is the phase of the wave, obtained from the WKB approximation, and  $\xi$  is the horizontal wave number which, by Snell's law, may be expressed in the following forms:

$$\xi = \frac{\omega}{c_v} = \frac{\omega}{c_a} \cos \theta_a = \frac{\omega}{c_b} \cos \theta_b \quad (H-2)$$

In eq. (H-2)  $\omega$  is the angular frequency ( $2\pi f$ ) and the other symbols have the same significance as in appendix I. Other symbols in eq. (H-1) are defined as follows:

$r$  = horizontal range

$$\beta_0 = \frac{\omega}{c_a} \sin \theta_a = \omega v_a / c_v \quad (H-3)$$

$$\beta = \frac{\omega}{c_b} \sin \theta_b = \omega v_b / c_v \quad (H-4)$$

$$w'''(\xi) = \frac{\partial^2 r}{\partial \xi^2} \quad (H-5)$$

$$v(x) = \sqrt{\pi} \text{Ai}(x) \quad (H-6)$$

where  $\text{Ai}(x)$  is one of the Airy functions. The argument  $x$  of the Airy function is given by eq. (38.52) of Brekhovskikh

$$x = 2^{1/3} w'(\xi_0)^{-1/3}$$

which may be written in the form

$$x = 2^{1/3} (r_c - r) / w'''(\xi_0)^{1/3} \quad (H-7)$$

where  $r_c$  is the range to the caustic.

Equation (H-1) is based on a series expansion of the phase  $w(\xi)$  along a horizontal line at the receiver depth. All parameters in this equation except  $v(x)$  are evaluated at the caustic. In particular,  $\xi_0$  is the value of  $\xi$  for the ray to the caustic. The argument of the Airy function is proportional to the horizontal distance from the caustic. The field at the caustic is obtained by inserting  $x = 0$ . Positive values of  $x$  correspond to the shadow side of the caustic and negative values correspond to the insonified side.

The caustic correction intensity is unconditionally computed and used in lieu of the uncorrected ray intensity for values of  $x$  between 3.5 and -1.77. The limit 3.5 lies far enough down on the exponential decay curve of the Airy

function to yield intensities of negligible value. The value -1.77 corresponds to a point beyond the first maximum on the oscillatory (insonified) side such that under ideal conditions the intensity would be equal to the incoherent sum of the intensities of the two rays which form the caustic, thereby assuring continuity between the regions of the ray and caustic computations. When real-world environments are inserted in PLRAY, however, the conditions for the series expansion on which eq. (H-1) is based are never ideal, and a discontinuity usually occurs. To avoid the discontinuity, caustic intensities are computed out to  $x = -2.2$ , a point well down toward the first zero of the Ai function. In the interval of  $x$  from -1.77 to -2.2, both caustic and ray intensities are computed and at each range the larger of the two is selected.

To convert eq. (H-1) into the desired intensity for PLRAY, it should be noted that the rms acoustic pressure at the receiver is

$$p_b = |\psi_N^+|$$

The constant factor in  $\psi_N^+$  has been chosen such that the rms acoustic pressure at the reference distance of 1 yard from the source is

$$p_a = 1$$

In normal mode solutions the intensity ratio is considered to be the square of the ratio of these two pressures. In ray solutions a geometric factor involving  $\cos \theta_a$  and  $\cos \theta_b$  enters into the formulation, leading to the result

$$H = \frac{p_b^2 / \rho c_b}{p_a^2 / \rho c_a} = \frac{c_a p_b^2}{c_b p_a^2} = \frac{c_a}{c_b} \left| \psi_N^+ \right|^2 \quad (\text{H-8})$$

where  $\rho$  is the density of water. A discussion of the ambiguity of these two definitions is given by Pedersen and Gordon in reference (g). Since the current derivation is intended for use in a ray program, the definition given in eq. (H-8) will be used.

The remainder of this appendix is concerned with transforming eq. (H-1) to the form in which it is programmed in SUBROUTINE RCAUST. At the outset it will be noted that the complex exponential factor may be dropped, since we are concerned only with its magnitude. Substitution of eqs. (H-2) to (H-6) into eq. (H-1) yields

$$\left| \psi_N^+ \right|^2 = 2^{11/6} \sqrt{\pi} \left( \frac{c_v}{\omega r v_a v_b} \right)^{1/2} \left( \frac{\partial^2 r}{\partial \xi^2} \right)^{-1/3} \text{Ai}(x) \quad (\text{H-9})$$

It may be shown by application of eq. (H-2), together with the definition

$$v_a = \tan \theta_a$$

that

$$\frac{\partial^2 r}{\partial \xi^2} \frac{c_v^6}{\omega^2 v_a^2 c_a^4} r'' \quad (\text{H-10})$$



where

$$r'' = \frac{\partial^2 r}{\partial v_a^2} \quad (H-11)$$

Substitution of (H-10) into (H-9) yields

$$|\psi_N^+| = 2\pi^{2/3} f^{1/6} \left( \frac{c_a^2}{r v_a v_b c_v^3} \right)^{1/2} \left( \frac{v_a^2 c_a}{r''} \right)^{1/3} Ai(x) \quad (H-12)$$

The intensity ratio, eq. (H-8), becomes

$$H = \frac{4\pi^{4/3} f^{1/3} c_a^3}{r c_b c v^3 v_a v_b} \left( \frac{v_a^2 c_a}{r''} \right)^{2/3} Ai^2(x) \quad (H-13)$$

where

$$x = - \frac{2\pi^{2/3} f^{2/3} c_a}{c_v^2} \left( \frac{v_a^2 c_a}{r''} \right)^{1/3} (r - r_c) \quad (H-14)$$

In eqs. (H-13) and (H-14) all quantities except  $x$  and  $r$  are to be evaluated for the ray which propagates to the caustic;  $r_c$  is the range to the caustic. These equations are correct in their present form if all lengths are in yards. However, in PLRAY all sound speeds are in ft/sec. For this reason the right-hand side of eq. (H-13) must be multiplied by  $3^{1/3}$  and the right-hand side of eq. (H-14) by  $3^{2/3}$ .

To reexpress eqs. (H-13) and (H-14) in a form similar to the FORTRAN coding in RCAUST, let

$$C = \frac{2(3\pi)^{2/3} c_a}{c v^2} \left( \frac{v_a^2 c_a}{r''} \right)^{1/3} \quad (H-15)$$

$$C_1 = f^{2/3} C \quad (H-16)$$

$$F_1 = \frac{c_a c_v}{3 r c_b v_a v_b} \quad (H-17)$$

$$C_2 = C^2 F_1 f^{1/3} \quad (H-18)$$

Then

$$H = C_2 Ai^2(x) \quad (H-18)$$

$$x = C_1 (r - r_c) \quad (H-19)$$

The similarity of the symbols should facilitate comparison of the above formulas with the FORTRAN statements. The reader is reminded that the subscript  $a$  in the

above equation corresponds to A or AA in the FORTRAN, and the subscript b corresponds to B or BB.

The Airy function ( $Ai(x)$ ) is computed from the standard series (reference (h)) for values of  $x$  between -2.2 and 1.0. The FUNCTION AI2(X) is the square of  $Ai(x)$ . In the interval from 1.0 to 3.5 a simple approximation has been developed for the computation of  $Ai^2(x)$ . Let

$$y = 6.709 + 3.04077 (x-2) + 0.31288 (x-2)^2 - 0.0195216 (x-2)^3 \quad (H-20)$$

Then

$$Ai^2(x) = e^{-y} \quad (H-21)$$

above equation corresponds to A or AA in the PARTIAL, and the subscript  
corresponds to B or BB.

The first function  $f_1(x)$  is computed from the standard normal distribution  
for values of  $x$  between -3.5 and 3.5. The function  $f_1(x)$  is the square of  $f(x)$   
in the interval from 1.0 to 3.5 a single approximation has been developed for the  
computation of  $f_1(x)$ .

$$f_1(x) = 0.709 + 0.0007(x-2) + 0.000001(x-2)^2 + 0.00000001(x-2)^3$$

Then

$$f_2(x) = f_1(x) + f_1(x)^2$$

6-11



APPENDIX I

RAY SPREADING LOSS FACTOR

The The spreading loss factor is the ratio of the ray intensity at the receiver location to the intensity at the reference point one yard from the source, neglecting all losses except geometric spreading. PLRAY uses the same basic formula as the old NADC Ray-Tracing Program. The purpose of this appendix is to transform the old expression contained in eq. (38) of reference (a) into the form appearing in PLRAY. The spreading loss factor, which will be designated by the symbol  $H$ , is the reciprocal of the argument of the logarithm in eq. (38). With appropriate changes in notation, the factor is

$$H = \left| \frac{s_1^2 \cos^2 \theta_s}{r u \sin \theta_s \sin \theta_R} \right| \quad (I-1)$$

where  $\theta_s$  is the ray angle at the source,  $\theta_R$  is the ray angle at the receiver,  $r$  is the horizontal range,  $s_1$  is the length of one yard, expressed in the same units as  $r$  and  $u$ , and  $u$  is defined by eq. (32) of reference (a).

$$u = - \frac{\cos \theta_s}{\sin \theta_s} \frac{\partial r}{\partial \theta_s} \quad (I-2)$$

In PLRAY the range derivative is taken with respect to  $v_a$ , the tangent of  $\theta_a$  instead of  $\theta_a$  itself ( $\theta_s$  in reference  $\ell$ ).

$$v_a = |\tan \theta_a| \quad (I-3)$$

Hence

$$\frac{\partial r}{\partial \theta_a} = \frac{\partial r}{\partial v_a} \frac{dv_a}{d\theta_a} = \frac{1}{\cos^2 \theta_a} \frac{\alpha}{\alpha v_a} \quad (I-4)$$

Let

$$r' = \left| \frac{\partial r}{\partial v_a} \right|$$

The spreading loss factor is then

$$H = \left| \frac{s_1^2 \cos^3 \theta_a}{r r' \sin \theta_b} \right|$$

$$= \frac{s_1^2 \cos^3 \theta_a}{r r' v_b \cos \theta_b}$$

where

$$v_b = |\tan \theta_b| \quad (I-5)$$

and the superscript  $b$  refers to the ray receiver.

Finally, applying Snell's law,

$$\frac{c_a}{\cos \theta_a} = \frac{c_b}{\cos \theta_b} = c_v$$

where  $c_a$  and  $c_b$  are the sound speeds at the ray source and ray receiver depths and  $c_v$  is the ray vertex velocity, we obtain

$$H = \frac{s_1^2 c_a^3}{c_v^2 c_b v_b r r'} \quad (I-6)$$

Equation (I-6) is in the form in which it is programmed in SUBROUTINE RAYSUM. Since  $r$  and  $r'$  are in yards,  $s_1$  has the value unity. The FORTRAN equivalents of the symbols in eq. (I-6) are:

CAA =  $c_a$   
 CBB =  $c_b$   
 CVK2 =  $c_v^2$   
 VBK =  $v_b$   
 RK =  $r$   
 RPK =  $r'$





# APPENDIX J

## COHERENCE COMPUTATIONS

Like the FACT model, PLRAY provides the option of semicoherent ray summation. The significance of the term "semicoherent" is that coherence is confined to the individual rays of each arrival order; the resultant intensities of the different arrival orders are added incoherently. The semicoherent approach has a certain amount of physical reasonableness in that the various rays within a given arrival order normally propagate by paths which lie close together and are very different from the ray paths of other arrival orders. Another good feature is that the semicoherent ray summation preserves the smooth, broad features of the interference pattern which frequently can be correlated with experimental data, but ignores the rapid fluctuations which in the real world have only a statistical significance.

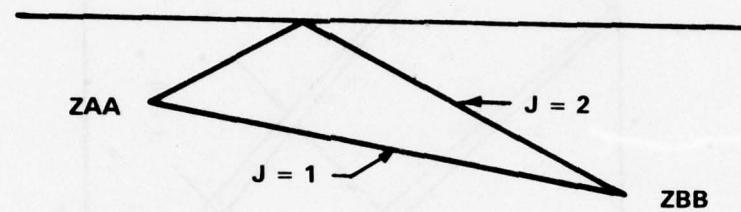
The most accurate way to compute the phase difference between two interfering rays is to calculate the absolute phases from the ray travel times. However, both FACT and PLRAY employ a simple approximate method which does not require the calculation of travel time. Coherence is computed only for those rays which are capable of striking the surface. Consider a pair of rays whose paths to the receiver differ only by one surface reflection at the source end. The rays leave the source at approximately equal angles, one upward and the other downward. The surface-reflected ray may be visualized as propagating downward from an image source located above the surface of the water symmetrically with respect to the real source. If the source depth is a relatively small fraction of the total depth of the ocean, the two ray paths, over most of their trajectories, are nearly identical and, in the immediate vicinity of the source may be considered as approximately parallel straight lines. The phase difference between the two rays may be computed to a sufficient approximation from the difference in path length, together with the phase reversal resulting from the surface reflection. Similar considerations apply to the case in which the surface reflection occurs at the receiver end.

If the source (or receiver) depth is increased, the separation between the two paths becomes greater, and the coherence between the two rays may be expected to become degraded. In FACT and PLRAY the effect of the degradation is treated in a somewhat crude manner. The horizontal separation of the two rays at the source (or receiver) depth is computed and compared with a pre-selected threshold of 12,000 feet. If the separation does not exceed the threshold, full coherence is assumed to exist. Otherwise the rays are treated incoherently.

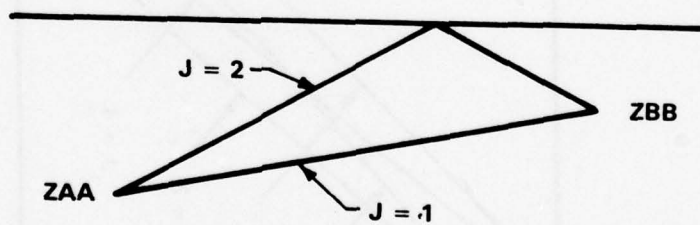
#### MULTIPATH RAY TYPE DESIGNATIONS

The multipath ray types are identified in the computer program by the index J. In the zero order arrivals there are two rays as indicated in figure J1. The direct ray is identified as the first ray ( $J = 1$ ) and the surface-reflected ray as the second ( $J = 2$ ). In the first and subsequent order arrivals there are four rays. As illustrated in figure J2 for the case of the first order bottom-bounce arrivals, the first ray experiences no surface reflections at either end, the second reflects at the source end (ZAA) only, the third reflects at the receiver end (ZBB) only, and the fourth reflects at both ends. It should be pointed out that the special case ( $MJ = 1$ ), in which there is only one ray in the zero order arrival and two rays in the first and subsequent order arrivals, is not involved in the coherence computations because in that case the rays do not strike the surface.





ICASE = 1 ( $ZAA < ZBB$ )



ICASE = 2 ( $ZAA > ZBB$ )

FIGURE J1 - Multipath Ray Types, Zero Order Arrivals.

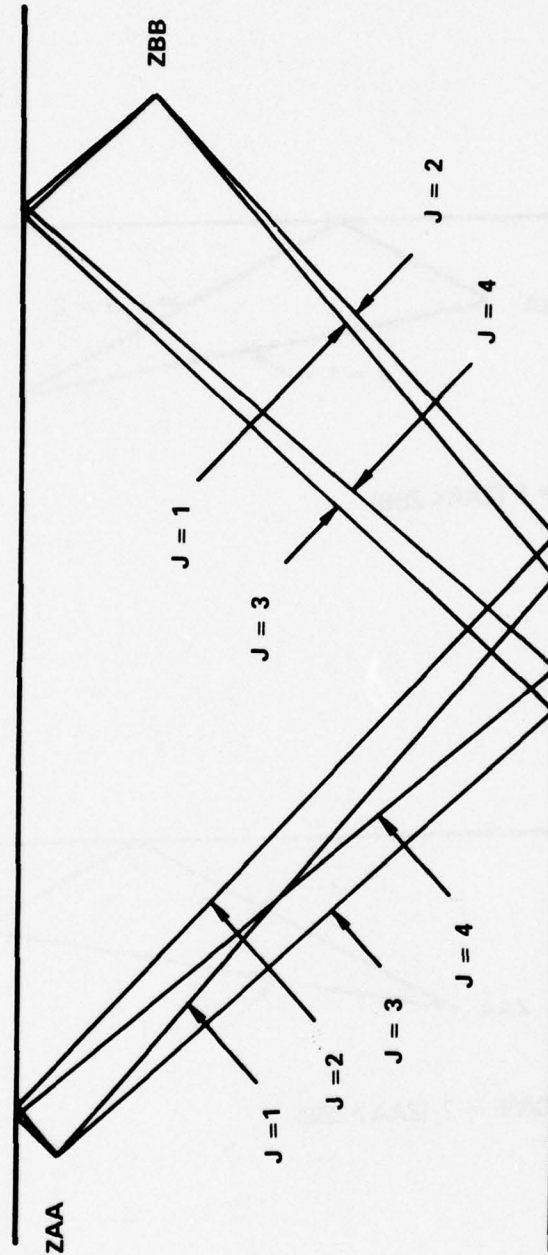


FIGURE J2 - Multipath Ray Types, First Order Arrivals.

Even though the total number of rays in an arrival order is normally two for the zeroth order and four for the subsequent orders, it is not necessarily true that all of these rays are actually present in any given sector. For any given source depth the range to which ray 1 propagates is always less than the ranges of rays 2 and 3, and these ranges in turn are always less than that of ray 4. Hence, at the inner and outer edges of the spread of ranges covered by the rays of a sector, there is usually an interval where one or more of the rays is not present.

It is also not necessarily true that all rays present in a given arrival order are actually involved in the coherence computations. The reason is that one or more of the rays may already have been included in a caustic correction.

In view of the above, it is necessary, before computing the coherence factors, to identify the individual rays involved. Obviously if only one ray is present, there is no coherence. In what follows we shall consider the cases of two, three, and four rays separately.

#### TWO RAYS

Let  $I_a$  and  $I_b$  be the individual intensities of the two rays, exclusive of the beam pattern, where the subscripts a and b refer to the particular pair of rays involved. Let  $g_a$  and  $g_b$  be the respective beam pattern functions expressed as pressure ratios relative to the beam axis. It is assumed that the symmetry of the beam is such that  $g_a$  and  $g_b$  are positive or negative real numbers. If no beam pattern has been specified,  $g_a$  and  $g_b$  are both equal to unity.

The first step is to examine the horizontal separation of the rays to determine whether the coherence calculation is applicable. The horizontal separation is

$$r_{\text{sep}} = 2z/\tan \theta_0 \quad (\text{J-1})$$

where  $\theta_0$  is the ray angle at the surface and  $z$  is the depth of either the ray source ZAA or the ray receiver ZBB, depending upon the rays involved. ZAA applies to zero order arrivals when ZAA is less than ZBB and to higher order arrivals when the rays are 1 and 2 or 3 and 4. ZBB applies to zero order arrivals when ZAA is greater than ZBB and to higher order arrivals when the rays are 1 and 3 or 2 and 4. If the rays are 1 and 4 or 2 and 3, neither pair contains a direct and surface-reflected ray at the same end, and it is assumed that no coherence is present. Otherwise, it is assumed that coherence occurs when  $r_{\text{sep}}$  is less than the threshold value.

If coherence occurs, the instantaneous pressure is

$$p = \sqrt{I_a} g_a - \sqrt{I_b} g_b e^{i\phi} \quad (\text{J-2})$$

where  $\phi$  is the phase difference between the two rays due to the path difference and the minus sign accounts for the phase reversal due to the surface reflection. Figure J3 shows the geometry of the parallel-line approximation from which  $\phi$  is computed. S is the source (or receiver) located at depth  $z$  and S' is its image. The direct ray is SA and the reflected ray is SCD. Since the actual segment SC



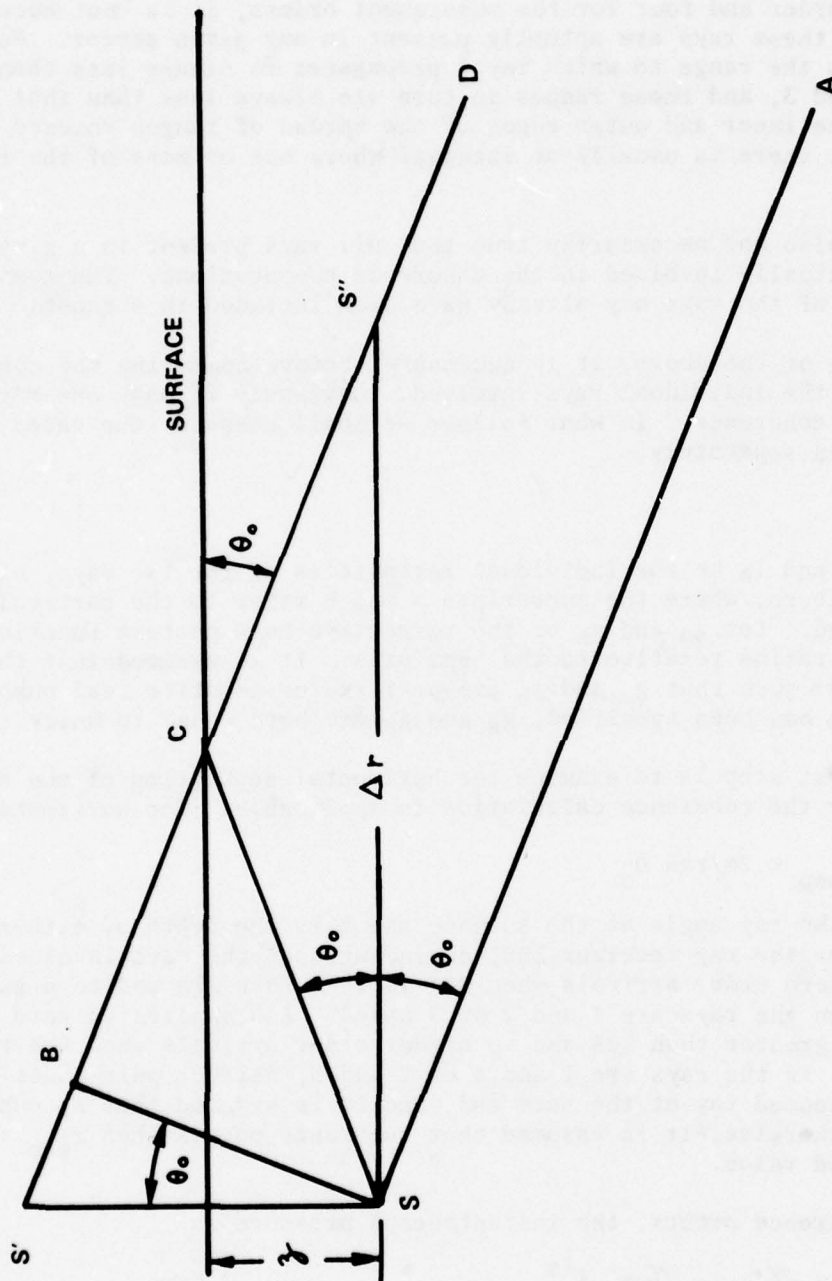


FIGURE J3 - Approximate Coherence Model.

has the same length as the image segment S'C, the difference in path length S'B is obtained by dropping the perpendicular SB on the image ray. The phase difference is found to be

$$\phi = 4 \pi f z \sin \theta_o / c_o \quad (J-3)$$

where  $f$  is the frequency and  $c_o$  is the sound speed at the surface.

The coherent intensity is given by the square of the complex pressure, eq. (J-2), and may be expressed in the form

$$I = (I_a g_a^2 + I_b g_b^2) \left( 1 - \frac{2 \sqrt{I_a I_b} g_a g_b}{I_a g_a^2 + I_b g_b^2} \cos \phi \right) \quad (J-4)$$

Since the omnidirectional intensities of the component rays of a given arrival order do not usually differ greatly, we shall make the simplifying assumption that inside the parentheses of the second factor of eq. (J-4) they may be considered equal. With this assumption the resultant intensity becomes

$$I = (I_a g_a^2 + I_b g_b^2) \left( 1 - \frac{2 g_a g_b}{g_a^2 + g_b^2} \cos \phi \right) \quad (J-5)$$

The first factor in eq. (J-5) is the incoherent sum of the two ray intensities. The effect of the coherence is accounted for by the second factor, which we shall term the coherence factor.

### THREE RAYS

In PLRAY the three ray case is broken down into a single ray and a pair of rays. The intensity of the single ray is added incoherently to the resultant intensity of the pair. In all possible combinations of three rays it is found that there is one pair of rays which is a candidate for coherence at the ray source end and another pair which is a candidate for coherence at the ray receiver end. If the ray source depth ZAA is less than the ray receiver depth ZBB, the coherence is calculated at the source end; otherwise, at the receiver end. The selection rules are given in table J-1. The ray pair is then treated in the same manner as the case of two rays.

T A B L E J - 1  
RAY SELECTION, THREE-RAY CASE

| Rays  | ZAA < ZBB |        | ZAA > ZBB |        |
|-------|-----------|--------|-----------|--------|
|       | Pair      | Single | Pair      | Single |
| 1,2,3 | 1,2       | 3      | 1,3       | 2      |
| 1,2,4 | 1,2       | 4      | 2,4       | 1      |
| 1,3,4 | 3,4       | 1      | 1,3       | 4      |
| 2,3,4 | 3,4       | 2      | 2,4       | 3      |

## FOUR RAYS

Tests are made of the applicability of coherence at both the ray source end and the ray receiver end. If the coherence is not to be computed at either end, all four ray intensities are summed incoherently. If coherence occurs at the ray source end only, rays 1 and 2 and rays 3 and 4 are treated as two separate pairs. If coherence occurs at the receiver end only, rays 1 and 3 and rays 2 and 4 are treated as separate pairs.

In the general four ray case the instantaneous pressure is

$$p = \sqrt{I_1} g_1 - \sqrt{I_2} g_2 e^{i\phi_A} - \sqrt{I_3} g_3 e^{i\phi_B} + \sqrt{I_4} g_4 e^{i(\phi_A + \phi_B)} \quad (J-6)$$

where  $\phi_A$  and  $\phi_B$  are given by eq. (J-3) with  $z$  equal to ZAA and ZBB respectively. The resultant intensity, which is the square of the modulus of  $p$ , may be written in the form

$$I = I_I \left[ 1 - \frac{2(\sqrt{I_1 I_2} g_1 g_2 + \sqrt{I_3 I_4} g_3 g_4)}{I_I} \cos \phi_A \right. \\ \left. - \frac{2(\sqrt{I_1 I_3} g_1 g_3 + \sqrt{I_2 I_4} g_2 g_4)}{I_I} \cos \phi_B \right. \\ \left. + \frac{2(\sqrt{I_2 I_3} g_2 g_3 + \sqrt{I_1 I_4} g_1 g_4)}{I_I} \cos \phi_A \cos \phi_B \right. \\ \left. + \frac{2(\sqrt{I_2 I_3} g_2 g_3 + \sqrt{I_1 I_4} g_1 g_4)}{I_I} \sin \phi_A \sin \phi_B \right] \quad (J-7)$$

where  $I_I$  is the incoherent sum

$$I_I = I_1 g_1^2 + I_2 g_2^2 + I_3 g_3^2 + I_4 g_4^2 \quad (J-8)$$

In order to reduce eq. (J-7) to a more tractable form, it is necessary to make some simplifying approximations. In PLRAY the beam pattern is applied to the true source. The true source may be either the ray source or the ray receiver, depending upon which the two depths has the larger sound speed. If the beam is at the ray source, then rays 1 and 3 have negative source angles, while rays 2 and 4 have positive source angles. Let

$$g_+ = \frac{1}{2} (g_2 + g_4) \quad (J-9a)$$

$$g_- = \frac{1}{2} (g_1 + g_3) \quad (J-9b)$$

Since all four rays have very nearly the same trajectory, it is reasonable to make the approximations

$$g_2 \sim g_4 \sim g_+ \quad (J-10a)$$

$$g_1 \sim g_3 \sim g_- \quad (J-10b)$$



With these approximations eq. (J-7) becomes

$$I = I_I \left( 1 - \frac{2g_+g_-}{g_+^2 + g_-^2} \cos \phi_A \right) (1 - \cos \phi_B) \quad (J-11)$$

If the beam is at the ray receiver, let

$$g_+ = \frac{1}{2} (g_3 + g_4) \quad (J-12a)$$

$$g_- = \frac{1}{2} (g_1 + g_2) \quad (J-12b)$$

If we make the assumptions

$$g_3 \sim g_4 \sim g_+ \quad (J-13a)$$

$$g_1 \sim g_2 \sim g_- \quad (J-13b)$$

Equation (J-7) simplifies to

$$I = I_I \left( 1 - \frac{2g_+g_-}{g_+^2 + g_-^2} \cos \phi_B \right) (1 - \cos \phi_A) \quad (J-14)$$

#### EFFECT OF INADEQUATE SAMPLING

If the specified receiver range points at which the propagation loss is to be computed are too far apart relative to the cycles of oscillation of the ray interference pattern, there exists a sampling problem. If the sampling is to be adequate, there should be at least a half dozen or so range points per cycle.\* The problem of inadequate sampling is handled arbitrarily by cutting down the amplitude of the interference oscillations by multiplying each of the cosine functions by an attenuation factor  $F$  which varies from 0 to 1. In the FACT model  $F$  is zero when the number of points per cycle is less than 8/3; it is 1 when the number of points per cycle is greater than 6 and varies linearly for intermediate values. In PLRAY the piecewise linear function is replaced with a continuous inverse hyperbolic function

$$F = 1 / \left[ 1 + e^{1.2(4.333 - n_{ppc})} \right] \quad (J-15)$$

where  $n_{ppc}$  is the number of receiver range points per cycle. A plot of this function is shown in figure J4.

It now remains to develop a suitable formula for  $n_{ppc}$ . The number of cycles is obtained by dividing the phase angle  $\phi$  in eq. (J-3) by  $2\pi$ . Thus,

$$n_c = 2fz \sin \phi_0 / c_0 \quad (J-16)$$

---

\*Recent experience has suggested that this number may be higher than necessary.

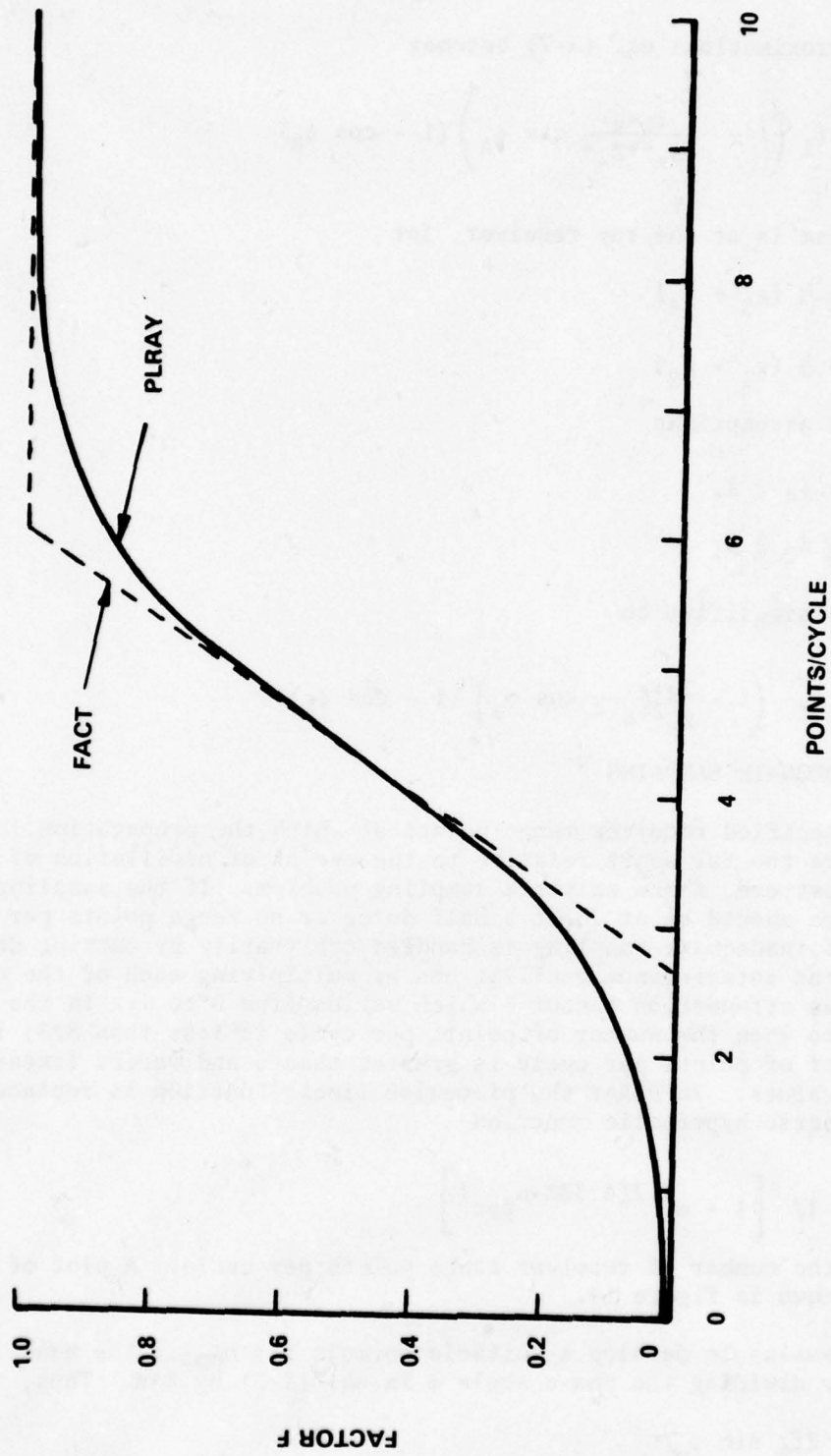


FIGURE J4 - Attenuation Factor as a Function of the Number of Range Points Per Cycle of Ray Interference Pattern.

where  $z$  is either the ray source depth ZAA or the ray receiver depth ZBB, as applicable. The number of cycles per unit range is

$$\frac{dn_c}{dr} = \frac{dn_c}{dv_a} \frac{dv_a}{dr} = \frac{1}{r'} \frac{dn_c}{dv_a} \quad (J-17)$$

where  $v_a$  is the tangent of the ray angle at the ray source, and  $r'$  is the derivative of the range with respect to  $v_a$ . From eq. (J-16) and Snell's law it may be shown that

$$\frac{dn_c}{dv_a} = \frac{2fz \sin \theta_a \cos \theta_a^2 \theta_o}{c_o \sin \theta_o} = \frac{2fzv_a c_a^2}{v_o c_v^3} \quad (J-18)$$

where  $\theta_a$  and  $c_a$  are the ray angle and sound speed at the ray source,  $v_o$  is the tangent of  $\theta_o$ , and  $c_v$  is the ray vertex velocity. If the range increment between successive receiver locations is  $\Delta r$ , the number of points per cycle is found to be

The attenuation factor  $F$  is applied directly as a multiplier of  $\cos \phi_B$  eq. (J-11) and  $\cos \phi_A$  in eq. (J-14). When applied to the terms involving the coefficient  $2g_a g_b / (g_a^2 + g_b^2)$  in eq. (J-5) and the coefficient  $2g_+ g_- / (g_+^2 + g_-^2)$  in eqs. (J-11) and J-14), the attenuation factor  $F$  is tested against the absolute value of the coefficient, and the smaller of the two is selected. If the factor  $F$  is chosen, it is given the algebraic sign of the coefficient.





A P P E N D I X   K

S U R F A C E   D U C T   M O D E L

The surface duct model incorporated in PLRAY is divided into two parts, a poor duct model and a good duct model. The poor duct model is applicable to those combinations of frequency and duct depth for which the propagation is dominated (except at very short ranges) by a single normal mode. The good duct model applies to cases where significant contributions at all ranges of interest are made by several normal modes. The criterion for determining when to use one model or the other is based on a parameter which we have termed the number of trapped modes. Before describing the two models, it will be advantageous to develop the concept and derive the formula for the number of trapped modes.

#### NUMBER OF TRAPPED MODES

The surface duct model is derived from the same two-layer bottomless ocean as forms the basis of the Pedersen-Gordon normal mode program (reference (i)) and of a similar locally generated NAVAIRDEVGEN normal mode program. The first layer is the surface duct, whose thickness is  $z_a$ . The sound speed and gradient at the surface are  $c_0$  and  $\gamma_1$ . The second speed varies with depth according to the

$$\frac{1}{c(z)^2} = \frac{1}{c_0^2} \left( 1 - \frac{2\gamma_1 z}{c_0} \right) \quad (K-1)$$

The sound speed  $c_a$  at the bottom of the duct is found by substituting  $z_a$  into eq. (K-1). The sound speed in the second layer varies in a similar manner, the gradient  $\gamma_2$  being negative.

The mode depth functions are solutions of the depth equation

$$\frac{d^2 u}{dz^2} + \left( \frac{\omega^2}{c(z)^2} - k^2 \right) u = 0 \quad (K-2)$$

where  $k$  is a parameter which takes on a set of discrete values (eigenvalues) corresponding to the normal modes. With the substitution

$$Z(z) = \frac{1}{q} \left( k^2 - \frac{\omega^2}{c_0^2} \right) + qz \quad (K-3)$$

where

$$q = (2\omega^2 \gamma_1)^{1/3} / c_0 \quad (K-4)$$

equation (K-2) transforms to Stokes' equation

$$\frac{d^2 u}{dZ^2} - Zu = 0$$

whose solution is a linear combination of the Airy function  $Ai(Z)$  and  $Bi(Z)$ ,

$$u(Z) = A Ai(Z) + B Bi(Z)$$

If it is assumed (as an approximation) that the duct is thick enough that  $u(Z)$  decays to a negligible value at the bottom ( $Z = Z_a$ ), then the coefficient  $B$  vanishes and  $u(Z)$  consists only of the  $Ai$  function.

To determine the discrete modes, we apply the boundary condition at the surface,  $u(0) = 0$ , (equivalent to neglecting the impedance of the air), or

$$Ai [Z(0)] = 0 \quad (K-5)$$

The exact solution for the first mode, which will of interest later, is

$$Z(0) = -2.3381074 \quad (K-6)$$

At this point we shall be concerned with an approximate analytic solution obtained from the asymptotic approximation

$$Ai(Z) \sim \frac{1}{\sqrt{\pi} (-Z)^{1/4}} \sin(\zeta + \pi/4) \quad (K-7)$$

where

$$\zeta = \frac{2}{3} (-Z)^{3/2} \quad (K-8)$$

The boundary condition, eq. (K-5), is satisfied if the argument of the sine in eq. (K-7) has the value  $n\pi$ , where  $n$  is an integer--the mode number. Upon substitution of the formula (K-3) for  $Z$ , the condition of mode resonance is found to be

$$\frac{c_0^3}{3\omega^2 \gamma_1} \left( \frac{\omega^2}{c_0^2} - k^2 \right)^{3/2} = (n - 1/4)\pi \quad (K-9)$$

Expressing  $k$  in terms of the mode phase velocity  $c_v$  (the vertex velocity of the equivalent ray) permits the further transformation

$$\frac{c_0^3 \omega}{3\gamma_1} \left( \frac{1}{c_0^2} - \frac{1}{c_v^2} \right)^{3/2} = (n - 1/4)\pi \quad (K-10)$$

Equations (K-9) and (K-10) define discrete values of  $k$  and  $c_v$ , corresponding to the discrete modes of a normal mode solution. For the present purpose, however, a useful measure of the quality of the duct can be obtained by setting  $c_v$  equal to the sound speed at the bottom of the duct and solving eq. (K-10) for a nonintegral value of  $n$ . The result is

$$n = \frac{1}{4} + \frac{2^{5/2} \gamma_1^{1/2}}{3c_0^{3/2}} f z_a^{3/2} \quad (K-11)$$

Inserting representative values  $\gamma_1 = 0.016 \text{ sec}^{-1}$ ,  $c_0 = 5000 \text{ ft/sec}$ , and expressing the frequency and duct depth in terms of the reduced variables

$$f' = f/100 \quad \text{and} \quad z_a' = z_a/100 \quad (K-12)$$

we obtain

$$n = 0.25 + 0.067462 f' z_a'^{3/2} \quad (K-13)$$



The parameter  $n$  may be loosely termed the number of "trapped" modes. Actually, of course, none of the modes are truly trapped. There is a continuous transition region between the lower order modes (if any) which are tightly trapped and the higher order modes which are very leaky. The value of  $n$  given above lies somewhere near the middle of the transition and as such is a reasonable measure of the number of modes which contribute significantly to the resultant intensity.

Runs made on the NAVAIRDEVGEN surface duct normal mode program have indicated that a value of 1.5 for the number of trapped modes constitutes a reasonable dividing line between the poor duct region and the good duct region.

#### POOR DUCT MODEL

The poor duct model is a semi-empirical simplification of the normal mode solution for the first mode. The formula for the pressure can be recognized as having the form of the normal mode solution. Several of the key parameters have been evaluated as functions of frequency and duct depth by empirical curve-fitting to the results of runs on the NAVAIRDEVGEN normal mode program.

The mode wave function, which is proportional to the acoustic pressure, has the form

$$\phi(r, z_S, z_R) = \sqrt{\frac{2\pi}{kr}} u(z_S) u(z_R) e^{i(\pi/4 - kr)} \quad (K-14)$$

where  $u(z_S)$  and  $u(z_R)$  are functions of the source and receiver depths  $z_S$  and  $z_R$ . To account for the mode attenuation due to leakage of energy out of the duct, the wave number  $k$  is made a complex number

$$k = \omega/c_v - i\alpha_1' \quad (K-15)$$

For propagation within the surface duct, the phase velocity  $c_v$  may be replaced by  $c_0$  without undue loss of accuracy.

The mode intensity is equal to the square of the modulus of the wave function. In forming the modulus it should be noted that

$$|k| \sim \omega^2/c_0^2 + \alpha_1'^2 \sim \omega/c_0$$

$$\left| e^{i(\pi/4 - kr)} \right| = e^{-\alpha_1' r}$$

It should also be noted that the mode is attenuated by absorption of energy in the water  $\alpha_w r$  and scattering at the surface  $\alpha_s r$  in addition to the diffraction leakage  $\alpha_1 r$  mentioned above. Inserting these extra terms and converting the attenuation coefficients from nepers/yard to db/yard, we obtain for the intensity

$$H_1 = \frac{c_0^2 u^2(z_S) u^2(z_R)}{fr} 10^{-0.1 (\alpha_1 + \alpha_s + \alpha_w) r} \quad (K-16)$$

where

$\alpha_1$  = mode leakage attenuation coefficient,

$\alpha_s$  = surface scattering attenuation coefficient,

$\alpha_w$  = water attenuation coefficient

all in db/yd.

The water attenuation coefficient is needed elsewhere in the program and is in COMMON. The surface scattering attenuation coefficient is taken from the FACT model. Allowing for the difference in the units of  $r$  between FACT and PLRAY, the formula for  $\alpha_s$  is

$$\alpha_s = W \sqrt{f/1000} z_a \quad (K-17)$$

where

$$W = \begin{cases} 0.00444, & \text{sea state } 3 \\ 0.00666, & \text{sea state } = 3 \\ 0.00888, & \text{sea state } 3 \end{cases} \quad (K-18)$$

The remainder of this section is devoted to evaluation of the depth function  $u(z)$  and the leakage attenuation coefficient  $\alpha_1$ . The depth function  $u(z)$  is a modification of the WKB approximate formula

$$u(z) = \frac{\text{const.}}{\left(\frac{\omega^2}{c^2} - \frac{\omega^2}{c_v^2}\right)^{1/4}} \sin \left\{ \frac{c_0^3}{3 \omega^2 \gamma_1} \left[ \left( \frac{\omega^2}{c^2} - \frac{\omega^2}{c_v^2} \right)^{3/2} - \left( \frac{\omega^2}{c_0^2} - \frac{\omega^2}{c_v^2} \right)^{3/2} \right] \right\} \quad (K-19)$$

where  $c_v$  = phase velocity of first mode

and  $c = c(z)$

Now,

$$\frac{1}{c^2} - \frac{1}{c_v^2} = \frac{(c_v + c)(c_v - c)}{c_v^2 c^2}$$

For propagation in the surface duct,

$$c_v \approx c \approx c_0$$

and

$$c = \frac{c_0}{\sqrt{1 - 2\gamma_1}} \approx c_0 + \gamma_1 z$$

Therefore

$$\frac{1}{c^2} - \frac{1}{c_v^2} \approx \frac{2(c_v - c_0 - \gamma_1 z)}{c_0^3}$$

$$\frac{1}{c_0^2} - \frac{1}{c_v^2} \approx \frac{2(c_v - c_0)}{c_0^3}$$

With these approximations eq. (K-19) becomes

$$u(z) = - \frac{\text{const.}}{(c_v - c_0 - \gamma_1 z)^{1/4}} \left( \frac{c_0^3}{2\omega^2} \right)^{1/4} \sin \left\{ \left( \frac{2}{c_0} \right)^{3/2} \frac{\omega}{3\gamma_1} \left[ (c_v - c_0)^{3/2} - (c_v - c_0 - \gamma_1 z)^{3/2} \right] \right\} \quad (\text{K-20})$$

For a further transformation, let

$$\Delta c = c_v - c_0 \quad (\text{K-21})$$

The turning point of the mode depth function occurs at the depth  $z_T$  such that

$$\Delta c - \gamma_1 z_T = 0$$

or

$$z_T = \Delta c / \gamma_1 \quad (\text{K-22})$$

With these substitutions the depth function becomes

$$u(z) = - \frac{\text{const.}}{(1 - z/z_T)^{1/4}} \left( \frac{c_0^3}{2\omega^2 \Delta c} \right)^{1/4} \sin \left\{ \frac{2^{5/2} \pi}{3\gamma_1 c_0^{3/2}} f \Delta c^{3/2} \left[ 1 - (1 - z/z_T)^{3/2} \right] \right\} \quad (\text{K-23})$$

Inserting the numerical values  $\gamma_1 = 0.016 \text{ sec}^{-1}$  and  $c_0 = 5000 \text{ ft/sec}$  and the reduced variables  $f'$  and  $z_a'$  (eq. (K-12)), we obtain

$$u(z) = \frac{A}{(1 - z/z_T)^{1/4}} \sin \left\{ 0.10472 f' \Delta c^{3/2} \left[ 1 - (1 - z/z_T)^{3/2} \right] \right\} \quad (\text{K-24})$$

where the coefficient A includes all the constant factors.

Equation (K-24) was used as a starting point for the development of a suitable function for the poor duct model. To serve as a guide in the development, a set of runs were made on the NAVAIRDEVGEN surface duct normal mode program for a variety of frequencies and duct depths. The previously stated values were assumed for  $c_0$  and  $\gamma_1$ . The value assumed for  $\gamma_2$  was  $-0.1 \text{ sec}^{-1}$ . Runs were made for a set of source depths within the duct and for a set of receiver depths extending to  $1.8 z_a$ . Computations were made not only of propagation loss, but also of the mode depth functions.

The parameters A and  $\Delta c$  were evaluated as functions of frequency and duct depth by comparison with the normal mode depth functions, using suitable curve-fitting techniques. In addition, eq. (K-24) was modified in the vicinity of the turning point (where the WKB approximation diverges to infinity) and at depths below the turning point.



Evaluation of  $\Delta c$ . The parameter  $\Delta c$  is expressed as the sum of two terms

$$\Delta c = \Delta c_0 + \Delta c_1 \quad (K-25)$$

where

$$\Delta c_0 = c_{v\infty} - c_0 \quad (K-26)$$

$$\Delta c_1 = c_v - c_{v\infty} \quad (K-27)$$

and  $c_{v\infty}$  is the phase velocity which would exist if the mode were completely trapped (no leakage). We may evaluate  $\Delta c_0$  from theoretical considerations. From eq. (K-5) the condition of resonance for the first mode is

$$c_0^2 \left( \frac{\pi f}{Y_1} \right)^{2/3} \left( \frac{1}{c_0^2} - \frac{1}{c_{v\infty}^2} \right) = Z_0 \quad (K-28)$$

where

$$Z_0 = -Z(0) = 2.3381074$$

Equation (K-28) solves to

$$\Delta c_0 = c_0 \left( \frac{1}{\sqrt{1 - \left( \frac{Y_1}{\pi} \right)^{2/3} \frac{Z_0}{f^{2/3}}}} - 1 \right) \quad (K-29)$$

which, upon insertion of the appropriate values, becomes

$$\Delta c_0 = 5000 \left( \frac{1}{\sqrt{1 - 0.0692/f^{2/3}}} - 1 \right) \quad (K-30)$$

The parameter  $\Delta c_1$  was evaluated by an empirical fit to the normal mode eigenvalues.

$$\Delta c_1 = e^{(a_{11} - a_{12}n)} \quad (K-31)$$

where

$$a_{11} = \begin{cases} 2.9 + 0.885 z_a' - 0.087 z_a'^2 & z_a' < 4 \\ 4.328 + 0.18 z_a' & z_a' \geq 4 \end{cases}$$

$$a_{12} = 5.5$$

and  $n$  is given by eq. (K-13).

Evaluation of coefficient A.

$$A = a_{21} + e^{-(a_{22} + a_{23} z_a')}$$



where

$$a_{21} = \begin{cases} 0.04 + 0.39 f' - 0.006 f'^2, & f' < 2.5 \\ 0.075 + 0.01 f', & f' \geq 2.5 \end{cases}$$

$$a_{22} = \begin{cases} 1.415 - 0.31 f', & f' < 2.0 \\ 0.795 & f' \geq 2.0 \end{cases}$$

$$a_{23} = \begin{cases} 0.1808 + 0.3996 f', & f' < 2.0 \\ 0.594 + 0.193 f', & f' \geq 2.0 \end{cases}$$

Formulas for the Depth Function. Three different modifications of eq. (K-24) are used, depending upon the value of the depth  $z$ . Let

$$z_1 = \text{smaller of } \begin{cases} 0.8 z_a \\ 0.9 z_T \end{cases} \quad (\text{K-33})$$

$$z_2 = 1.2 z_a \quad (\text{K-34})$$

Region 1,  $z \leq z_1$

$$u(z) = \frac{A}{D} \sin \phi(z) \quad (\text{K-35})$$

where

$$D = \text{larger of } \begin{cases} (1 - z/z_T)^{1/4} \\ 0.82 \end{cases}$$

$$\phi(z) = 0.10472 f' \Delta c^{3/2} \left[ 1 - (1 - z/z_T)^{3/2} \right] \quad (\text{K-36})$$

Region 2,  $z_1 < z \leq z_2$

$$\text{Let } u_1 = u(z_1) \quad (\text{K-37})$$

$$\text{Then } u(z) = u_1 e^{a_{31}(z - z_1)/z_a} \quad (\text{K-38})$$

where

$$a_{31} = 0.244 - 2.0 n + 4.842 e^{-3.58 n}$$

Region 3,  $z_2 < z \leq 1.8 z_a$

$$\text{Let } u_2 = u(z_2) \quad (\text{K-39})$$

Then

$$u(z) = u_2 e^{a_{32}(z - z_2)/z_a} \quad (K-40)$$

where

$$a_{32} = -0.444 + 3.42 e^{-3.49 n}$$

Evaluation of  $\alpha_1$ . The result of the curve-fitting for the leakage attenuation coefficient  $\alpha_1$  is

$$\alpha_1 = e^{(a_{41} + a_{42})/1000} \quad (K-41)$$

where

$$a_{41} = 3.7 / z_a^{0.1586}$$

$$a_{42} = -3.237 n + 0.7965 e^{2.78 n} - 10.422 n^2$$

Alternate Formula for Poor Duct. The definition of a poor duct in terms of the contribution of a single mode tends to break down at short ranges, where higher order modes become important. These modes have little or no effect at the longer ranges because they are highly attenuated. From a ray point of view we are concerned with the region of spherical spreading and the transition to cylindrical spreading. A reasonable approximation to the intensity in this region is provided by the following formula

$$H_2 = \frac{2}{r^2} \sin^2 \phi(z_S) \sin^2 \phi(z_R) \cdot 10^{-0.1(\alpha_1 + \alpha_s + \alpha_w)r} \quad (K-42)$$

where  $\phi(z)$  is the phase angle of eq. (K-36). Equation (K-42) is applied at ranges less than 2500 yd. At ranges beyond 2500 yd, it is multiplied by the factor

$$10^{-(r - 2500)/5000} \quad (K-43)$$

Resultant Intensity. At each receiver range the two intensities  $H_1$  and  $H_2$  are compared and the larger of the two is selected. Because of the tendency toward high mode attenuation ( $\alpha_1$ ) in the cylindrical spreading formula (K-16), the attenuation factor (K-43) is included in the spherical spreading formula (K-42) to prevent  $H_2$  from becoming dominant at the longer ranges. When the range reaches a value such that the intensity is less than  $10^{-13}$ , no further computations are made in the surface duct.

#### GOOD DUCT MODEL

Since no simple theoretical formulation appears to be feasible for the case where many modes are involved, the good duct model was formulated by empirical curve-fitting to a pair of formulas, one based on cylindrical spreading and the other on spherical spreading. The two formulas are

$$H_1 = \frac{1}{r} \cdot 10^{-0.1[(\alpha_1 + \alpha_s + \alpha_w)r + K_S + K_R]} \sin^2 \phi_s \sin^2 \phi_R \quad (K-44)$$

$$H_2 = \frac{2}{r^2} \cdot 10^{-0.1(\alpha_2 + \alpha_s + \alpha_w)r} \sin^2 \phi_s \sin^2 \phi_R \quad (K-45)$$

where  $\alpha_1$ ,  $\alpha_s$ , and  $\alpha_w$  are the same as in the poor duct model and

$$\phi_s = 0.10472 f' \Delta c_0^{3/2} \left[ 1 - (1 - z_s/z_{T0})^{3/2} \right]$$

$$\phi_R = 0.10472 f' \Delta c_0^{3/2} \left[ 1 - (1 - z_R/z_{T0})^{3/2} \right]$$

subject to the limitation that neither of these angles may exceed  $\pi/2$  radians, and

$$z_{T0} = \Delta c_0 / \gamma_1$$

To obtain formulas for the parameters  $\alpha_2$ ,  $K_S$ , and  $K_R$ , we define the auxiliary relations

$$x(z) = e^{-6.0 (z/z_a - 0.92)}$$

$$x_S = x(z_S)$$

$$x_R = x(z_R)$$

$$x_M = \text{smaller of } x_S \text{ and } x_R$$

Then

$$\alpha_2 = \frac{1.5}{1000 (1 + x_M)}$$

$$K(z) = \frac{32 + 13 x(z)}{1 + x(z)}$$

$$K_S = K(z_S)$$

$$K_R = K(z_R)$$

As in the case of the poor duct,  $H_1$  and  $H_2$  are compared at each receiver range and the larger of the two is selected. Computations in the duct are terminated when the intensity drops below the minimum value of  $10^{-13}$ .

#### CUT-OFF FREQUENCY

If the surface duct is so leaky that it fails to trap any significant amount of energy, there is no point in bothering with the computations. In the PLRAY



surface duct model the criterion for bypassing duct computations is expressed in terms of a minimum cut-off frequency  $f_{\min}$ , below which the surface duct model is bypassed. The cut-off frequency is expressed as a function of the reduced duct depth  $z_a'$  (eq. (K-12)) by the following formula

$$f_{\min} = 200/z_a'^{2.4} \text{ (Hz)} \quad (\text{K-46})$$

The above relationship corresponds roughly to a mode attenuation of about 15 dB/kyd. Figure K1 is a plot of eq. (K-46).



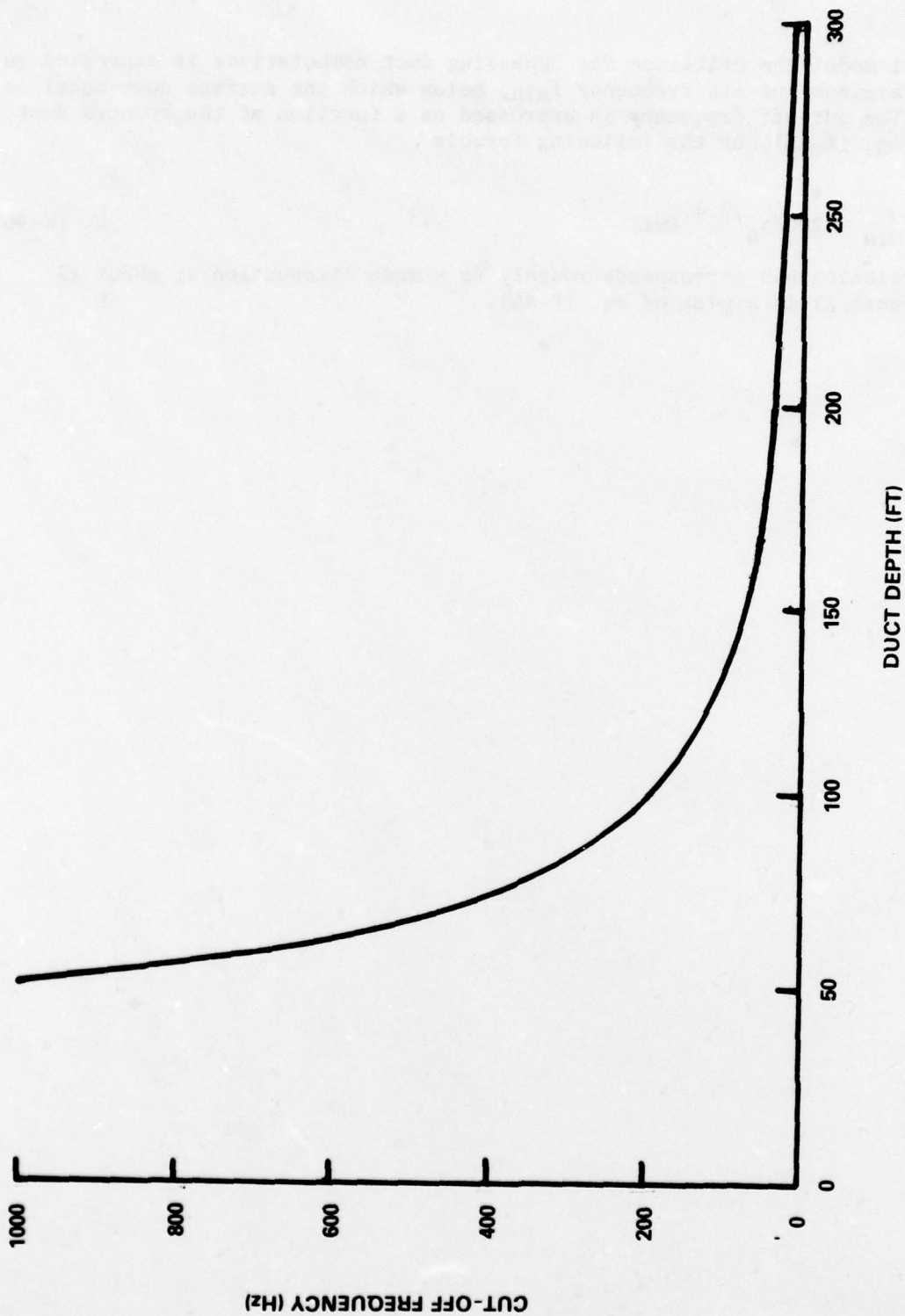


FIGURE K1 - Cut-off Frequency as a Function of Duct Depth.

APPENDIX L  
THE AP2 NORMAL MODE PROGRAM

AP2 is a normal mode program which accepts an arbitrarily specified velocity profile in the same form as PLRAY and FACT. The bottom may be specified either in the form of a set of up to ten homogeneous fluid type layers or in the form of the same type of empirical bottom loss curves as are used in PLRAY and FACT.

The basic approach to the normal mode solution is essentially the same as that of the NAVAIRDEVCON Two-Layer and Three-Layer Programs, reference (j). The integration in the complex plane is based on the same branch cut, with the result that the solution is obtained in the form of the sum of an infinite number of discrete modes and a branch line integral whose value under most practical operating conditions is negligible. As in reference (j), the input velocity profile is fitted with segments in which the square of the index of refraction varies linearly with depth, so that the solution of the depth equation is obtained in terms of Airy functions. However, instead of attempting a complete algebraic formulation of the type employed in reference (j), which obviously becomes impractical with more than three layers, the solution is obtained by an iterative procedure similar to that of the old Program for Arbitrary Velocity Profiles, reference (k). The approach bears considerable similarity to that of the discrete mode portion of D. C. Stickler's normal mode program, reference (l). The multi-layered and empirical bottoms are treated in essentially the same manner as in reference (j).

AP2 is dimensioned for 500 modes. To avoid unnecessary computation and to make space available for higher order modes above the 500th, AP2 contains an automatic procedure for bypassing those lower order modes whose excitation is too weak to contribute significantly to the resultant intensity. The procedure applies to those modes whose phase velocities are sufficiently smaller than the sound speeds at the source depth and all specified receiver depths to produce the required amplitude attenuation beyond the mode turning point. The mode computations are automatically terminated at the first mode whose phase velocity exceeds a value equal to 10 times the sound speed at the bottom of the water or after the 500th mode has been computed, whichever occurs first.

When checked against the programs of references (j) and (k), AP2 has been found to give identical outputs for the same inputs.

Within the 500-mode limitation AP2 has the same versatility as ray programs such as PLRAY and FACT. It is completely automatic and does not contain any special inputs which require the user to have a knowledge of normal mode theory or of program idiosyncrasies. It is planned to document AP2 with a formal report at the earliest opportunity.

# D I S T R I B U T I O N   L I S T   ( C o n t i n u e d )

|   | <u>No. of Copies</u> |
|---|----------------------|
| ARL, Penna State Univ . . . . .   | 1                    |
| ARL, Univ of Texas. . . . .   | 1                    |
| Woods Hole Oceano Inst. . . . .   | 1                    |
| Scripps Inst of Oceano, MPL, San Diego. . . . .   | 1                    |
| Science Applications, Inc, 8400 Westpark Drive, McLean,<br>VA 22101 (Mr. C. W. Spofford) . . . . .        | 1                    |
| General Electric Co, 3198 Chestnut St, Phila, PA 19104. . . . .   | 1                    |
| Magnavox Govt & Indus Electronics Co, 1313 Production Rd,<br>Ft Wayne, IN 46808. . . . .                  | 1                    |
| Hazeltine Corp, Greenlawn, NY 11740 . . . . .   | 1                    |
| Sanders Associates, Inc, 95 Canal St, Nashua, NH 03060. . . . .   | 1                    |
| Raytheon Co, 1847 W. Main Road, Portsmouth, RI 02871. . . . .   | 1                    |
| Defence Research Establishment, Atlantic, Forces Mail Office,<br>Italifax, N.S., Canada. . . . .          | 1                    |
| Defence Research Establishment, Pacific, Forces Mail Office,<br>Victoria, B.C., Canada VOS 1B0. . . . .   | 1                    |
| Admiralty Underwater Weapons Establishment, Portland, Dorset,<br>England, UK . . . . .                    | 1                    |
| Admiralty Research Laboratory, Teddington, England, UK. . . . .   | 1                    |
| Royal Aircraft Establishment, Farnborough, Hants, England, UK. .  | 1                    |
| Royal Australian Naval Research Laboratory, Edgehill Road,<br>Sydney, New South Wales, Australia. . . . . | 1                    |
| Weapons Research Establishment, Salisbury, Adelaide, South<br>Australia . . . . .                         | 1                    |
| Defence Scientific Establishment, HMNZ Dockyard, Auckland 9,<br>New Zealand . . . . .                     | 1                    |
| DDC . . . . .   | 12                   |



# D I S T R I B U T I O N   L I S T

REPORT NO. NADC-77296-30

AIRTASK NO. A5335330/001D/8W04800000

Work Unit No. W0480

|   | <u>No. of Copies</u> |
|---|----------------------|
| CNM, ASW-01T (Mr. R. Delaney) . . . . .             | 1                    |
| CNM, ASW-10 . . . . .                               | 1                    |
| CNM, ASW-13 . . . . .                               | 1                    |
| COMOPTEVFOR . . . . .                               | 1                    |
| ONR, Code 102-OS. . . . .                           | 1                    |
| NAVAIRSYSCOM, AIR-954 . . . . .                     | 3                    |
| (2 for retention)                                   |                      |
| (1 for AIR-370)                                     |                      |
| NAVAIRTESTCEN, WST Div. . . . .                     | 1                    |
| NAVOCEANO . . . . .                                 | 2                    |
| (1 for retention)                                   |                      |
| (1 for Mr. W. Geddes, Code 3144)                    |                      |
| NAVPGSCOL . . . . .                                 | 1                    |
| NAVSEASYSYSCOM, Code 06H1 . . . . .                 | 1                    |
| NAVSURFWPCEN . . . . .                              | 2                    |
| (1 for retention)                                   |                      |
| (1 for Mr. M. Stripling, Code WU-22)                |                      |
| NAVWPNCEN . . . . .                                 | 1                    |
| NORDA . . . . .                                     | 2                    |
| (1 for retention)                                   |                      |
| (1 for Mr. A. Anderson, Code 320)                   |                      |
| NOSC. . . . .                                       | 4                    |
| (1 for retention)                                   |                      |
| (1 for Mr. M. A. Pedersen, Code 714)                |                      |
| (1 for Mr. W. H. Watson, Code 714)                  |                      |
| (1 for Mr. R. W. McGirr, Code 714)                  |                      |
| NRL . . . . .                                       | 5                    |
| (1 for Mr. B. G. Hurdle, Code 8100.1)               |                      |
| (1 for Mr. L. P. LaLumiere, Code 8106)              |                      |
| (1 for Mr. C. R. Rollins, Code 8109)                |                      |
| (1 for Mr. R. M. Fitzgerald, Code 8120)             |                      |
| (1 for Mr. J. Cybulski, Code 8160)                  |                      |
| NSRDC . . . . .                                     | 1                    |
| NUSC, New London. . . . .                           | 4                    |
| (1 for retention)                                   |                      |
| (1 for Mr. F. R. DiNapoli, Code 3122)               |                      |
| (1 for Mr. H. Weinberg, Code 314)                   |                      |
| (1 for Mr. G. Leibiger, Code 222)                   |                      |
| NUSC, Newport (Mr. R. Bernard, Code 3524) . . . . . | 1                    |
| APL, Johns Hopkins Univ . . . . .                   | 1                    |
| APL, Univ of Wash . . . . .                         | 1                    |

CONTINUED ON INSIDE OF COVER